

UMCES

UNIVERSITY OF MARYLAND CENTER for ENVIRONMENTAL SCIENCE

CHESAPEAKE BAY

WATER QUALITY MONITORING PROGRAM

ECOSYSTEM PROCESSES COMPONENT (EPC)

LEVEL ONE REPORT #30 (INTERPRETIVE)

A Program Supported by the Department of Natural Resources
State of Maryland

December 2013

Maryland Department of Natural Resources

**MARYLAND CHESAPEAKE BAY WATER QUALITY
MONITORING PROGRAM**

ECOSYSTEMS PROCESSES COMPONENT (EPC)

**LEVEL ONE REPORT No. 30
INTERPRETIVE REPORT
(July 1984 – December 2012)**

Final Report

PREPARED FOR:

Maryland Department of Natural Resources
Tidewater Ecosystems Assessment
580 Taylor Avenue, D-2
Annapolis, MD 20401

December, 2013

W.R. Boynton	Co-Principal Investigator
L. A. Wainger	Co-Principal Investigator
C.A. O'Leary	Advanced Faculty Research Assistant
C.L.S. Hodgkins	Advanced Faculty Research Assistant
A.R. Bayard	Advanced Faculty Research Assistant
M.A.C. Ceballos	Laboratory Research Technician

University of Maryland Center for Environmental Science
Chesapeake Biological Laboratory (CBL)
PO Box 38, 146 Williams Street
Solomons, MD 20688

Table of Contents

	Page No.
List of Figures	ii
List of Tables	iv
Executive Summary	E-1
Introduction and Objectives	1-1
Comparative Analysis of Nutrient Loads and Water Quality Conditions in Selected Tributaries of Chesapeake Bay	2-1
Linking ConMon and Dataflow© for Spatial Dissolved Oxygen Criteria Assessment	3-1
Role of Late Winter-Spring Wind Influencing Summer Hypoxia in Chesapeake Bay	4-1
Multi-decade responses of a tidal creek system to nutrient load reductions: Mattawoman Creek, Maryland USA	5-1

Table of Contents

List of Figures

	Page No.
1-1	A simplified schematic diagram indicating degradation and restoration trajectories of an estuarine ecosystem. 1-4
2-1	A scatter plot of TN load versus chlorophyll- <i>a</i> concentration developed for Mattawoman creek and a few other shallow Chesapeake Bay tributaries. 2-3
2-2	A map of Chesapeake Bay showing the location of tributary estuaries included in this analysis. The green dots indicate the general location of Chesapeake Bay Water Quality Monitoring Station data used in this analysis. 2-4
2-3	Time-series plots of average annual nutrient loads to tributary estuaries of Chesapeake Bay. 2-10 - 2-19
2-4	Bar graphs showing 20 year average nutrient loads to the tributary estuaries considered in this analysis. 2-20
2-5	Scatter plot of TP versus TN loads using the 20 year average loads (a) and individual annual loads for the tributary systems used in this analysis 2-22
2-6	Bar graphs (20 year mean and standard deviation) and frequency histograms summarizing a variety of water quality conditions measured in surface waters of the tributary estuaries considered in this analysis. 2-25 - 2-32
2-7	Scatter plots of 20 year average TN load versus 20 year average DIN concentration (a) and 20 year average TP load versus 20 year average DIP concentration (b) in tributary estuaries examined in this analysis. 2-34
2-8	Scatter plots of TN load (both point and diffuse) versus surface water chlorophyll- <i>a</i> concentration from all 19 tributary systems considered in this analysis (a) and the same scatter plot with several systems removed. 2-38
2-9	Results of two multiple regression models with both using 20 year averaged data from 19 tributary estuaries. 2-39
2-10	Time series plot of surface water chlorophyll concentrations collected from three sites in the Back River estuary during summer, 1997. 2-41
3-1	A conceptual model of our approach to linking ConMon and Dataflow© data sets for evaluation of short-term (instantaneous) dissolved oxygen criteria. 3-3
3-2	Locations of all MD ConMon sites for all years of deployment through 2010. 3-4
3-3	Surface dissolved oxygen (mg/L) data at Sycamore Point ConMon station from July 1 2005 to July 10 2005 showing large fluctuations in DO concentrations over a short time period (10 days). 3-5
3-4	Surface dissolved oxygen (mg/L) data at Sycamore Point ConMon station from January 1 2005 to December 31 2009 showing seasonal-scale DO fluctuations. 3-5
3-5	Box and Whisker Plot of DO amplitude by month from Sycamore Point station in the Corsica from 2003-2005. 3-6
3-6	Examples of diel DO ConMon data plotted (black dots) with a trigonometric time series fit (blue line). 3-9
3-7	Time series boxplots of DO amplitude from (A) Sycamore Point (Corsica River) 2005-2008 and (B) CBL (Patuxent River) 2003-2005 and (C) Fenwick (Potomac) 2004-2008. 3-10
3-8	An autocorrelation function plot from the Sycamore Point ConMon station data (left) and final GLS model (right) selected. 3-11
3-9	GLS model residuals after seasonal correction. 3-12
3-10	The results of the GLS model created from Sycamore Point (Corsica River) data from January 2005 to December 2008. 3-13
3-11	The DO amplitude prediction output of the GLS model from Chesapeake Bay tributaries. 3-15
3-12	The difference between predicted DO amplitude and observed DO amplitude for each observation at (A) Chesapeake Biological Lab, (B) Pin Oak, (C) Piney Point, (D) Fenwick, (E) Blossom Point, (F) Benedict, (G) Sycamore Point in mg/L. 3-16
3-13	A Dataflow© cruise track on 2 June 2008 in the Corsica River. 3-18
3-14	Daily expected DO curves in the Corsica River. 3-19
3-15	Map of the Corsica River on (A) 1 May 2008, (B) 2 June 2008, (C) 16 July 2008, (D) 4 August 2008 and (E) 8 September 2008 with interpolated daily DO minimum values (mg/L) from the Dataflow© data across the entire tributary. 3-21

Table of Contents

List of Figures	Page No.	
3-16	Comparison between (A) Dataflow© measured DO on 16 July 2008, (B) calculated DO minimum on 16 July 2008, (C) Dataflow© measured DO on 4 August 2008 and (D) calculated DO minimum on 4 August 2008.	3-23
4-1	(a) The Chesapeake Bay Program water quality monitoring stations (●) in the mainstem of Chesapeake Bay and (b) the mid-bay section of the bay (square markers indicate the mid-bay stations along the deep channel).	4-4
4-2	The most frequently observed dissolved oxygen (DO) patterns during 1985-2007 using self-organizing map (SOM) based on the data acquired from the Chesapeake Bay Program water quality database (http://www.chesapeakebay.net/data/).	4-7
4-3	Mean summer (June-August) hypoxic volume and maximum density stratification (N_{\max}^2) in the mid-bay region (see Fig. 4-1b) during 1985-2007. Each time series is normalized by subtracting its mean value and dividing the difference by its standard deviation.	4-8
4-4	Results from application of several multiple linear regression models.	4-10
4-5	Relationship between the observed and predicted summer hypoxic volume (km^3) using a multiple linear regression model from Fig. 4-4d with two independent variables: mean winter-spring (January-May) freshwater flow (River, $\text{m}^3 \text{s}^{-1}$) from the Susquehanna River and late winter-spring (February-April) northeasterly-southwesterly wind velocity (Wind, m s^{-1}) from the Naval Air Station Patuxent River (see Fig. 4-1b).	4-13
4-6	Panels (a), (c), and (e) are the spatial patterns of the first three modes from an empirical orthogonal function (EOF) analysis that is based on sea-level pressure (SLP) anomalies during the late winter-spring (February-April) in the eastern United States (1985-2007).	4-15
4-7	Comparison of wind speed (m s^{-1}) and direction (degrees) for the years 2000 and 2003 during February-April. Panels (a) and (b) are histograms for wind speed and panels (c) and (d) are wind rose plots indicating wind direction where wind is coming from.	4-16
4-8	Differences in the late winter-spring (February-April) residual currents between the years 2000 and 2003 at (a) the bottom and (b) the surface. The solid line in the panel (a) indicates the mid-bay cross-section shown in Fig. 4-9.	4-17
4-9	Differences in the late winter-spring (February-April) residual currents between the years 2000 and 2003 at the mid-bay cross-section indicated in Fig. 4-8a.	4-18
5-1	A map of Mattawoman Creek and watershed showing locations of stream network, water quality sampling sites, location of USGS flow gage and the cross-section of the creek mouth (dashed line) where net nutrient fluxes were estimated.	5-3
5-2	A time-series of TN, TP and water flows based on data collected at the USGS gauge on Mattawoman Creek (USGS 016558000; Fig. 5-1).	5-9
5-3	Scatter plot of annual TP versus TN loads for a variety of estuarine and coastal marine ecosystem (small gray circles; see Boynton <i>et al.</i> 1995 for references for these sites).	5-11
5-4	A time-series of monthly and annual net DIN and DIP exchanges between Mattawoman Creek and the Potomac River estuary for the period 1991 – 2001.	5-13
5-5	Annual average time-series data for water quality variables measured in surface waters at two sites in Mattawoman Creek (MAT 0078 and MAT0016) and one site in the adjacent Potomac River (TF2.4) for the period 1986 – 2010.	5-15
5-6	Mean monthly (Apr-Oct) estimates of community gross primary production (P_g ; $\text{g O}_2 \text{ m}^{-3} \text{ day}^{-1}$) for the period 2004-2010.	5-18
5-7	Annual summary of SAV coverage (ha), water clarity (Secchi Disk depth) and algal biomass (chlorophyll- <i>a</i> concentration) for the period 1986-2010 in Mattawoman Creek.	5-19
5-8	Scatter plots of average annual chlorophyll- <i>a</i> concentration versus SAV coverage for Mattawoman Creek.	5-20
5-9	A schematic diagram of a nutrient budget (TN) model developed for Mattawoman Creek for the 2005-2010 time period.	5-21
5-10	A scatter plot of winter-spring TN load versus chlorophyll- <i>a</i> concentration developed for Mattawoman creek and other shallow Chesapeake Bay tributaries.	5-24
5-11	A scatter plot of chlorophyll- <i>a</i> versus Secchi disk depth developed for Mattawoman Creek and two other shallow Chesapeake Bay systems.	5-25

Table of Contents

List of Tables	Page No.	
2-1	A list of estuary names and station codes used in this analysis. Station codes are used by the Chesapeake Bay Program Water Quality Monitoring Program	2-3
2-2	A listing of Chesapeake Bay tributary mouth locations. Shore locations on both sides of the estuary mouth are indicated with common names and by latitude and longitude.	2-7
2-3	A summary of estuary and drainage basin metrics estimates using various GIS techniques. ND indicates no data available. Asterisk (*) indicates the normal tidal prism based flushing time was modified by a water return factor.	2-8
2-4	Results of Pearson Correlation Coefficient analysis (r) relating surface water chlorophyll- a concentration to a variety of variables.	2-36
3-1	Total number of observations from Sycamore Point 2003-2005 ConMon data that were considered for inclusion in model.	3-9
3-2	Analysis of Variance for Stage 2 DO Amplitude Model.	3-13
3-3	Coefficients for final DO Amplitude Model.	3-14
3-4	Root mean square error of validation runs	3-17
3-5	Percent area coverage of each DO criteria in the Corsica River after data interpolation for daily DO minimum value.	3-22
3-6	Descriptions of each type of model tested to predict DO amplitude.	3-30
4-1	Summary of correlation coefficients (r) between mean summer (June-August) hypoxic volume (km^3), winter-spring (January-May) freshwater discharge ($\text{m}^3 \text{s}^{-1}$) and total nitrogen (TN) loading (kg day^{-1}) from the Susquehanna River, near-bottom chlorophyll- a concentration (Chl_a , $\mu\text{g L}^{-1}$) in the mid-bay region during the spring bloom period (February-April), summer maximum density stratification (N_{max}^2 , $\text{rad}^2 \text{sec}^{-2}$) in the mid-bay, and summer zonal (east-west) and meridional (north-south) wind velocity (m s^{-1}). Significant relationships ($p < 0.05$) are indicated in bold numbers.	4-9
4-2	Correlation coefficient (r) between mean summer (June-August) hypoxic volume (km^3) and late winter-spring (February-April) zonal (easterly-westerly) wind velocity (m s^{-1} ; no rotation, 0 degrees).	4-11
5-1	A summary of land use / land cover in the Mattawoman Creek watershed for three time periods (1973, 2002 and 2010).	5-4
5-2	A summary of the types of data used in this analysis, sampling locations, period of data record, measurement frequency, analytical methods used and data sources.	5-5
5-3	Multiple estimates of annual diffuse source total nitrogen (TN) and total phosphorus (TP) loads to Mattawoman Creek.	5-10
5-4	A selection of community gross primary production rates from very enriched and less enriched Chesapeake Bay tributary sites.	5-17

Executive Summary 2013

- The analytical work conducted by the Ecosystem Processes Component (EPC) of the Chesapeake Bay Water Quality Monitoring Program during FY 2013 included five distinct efforts and these included the following:
 1. Organized, characterized, and analyzed water quality data from 19 tributary estuaries of the Bay system with a special emphasis on developing linkages between nitrogen (N) and phosphorus (P) sources (both point and non-point) and estuarine water quality
 2. Created, as a “proof of concept effort”, a methodology for utilizing both ConMon and Dataflow information for evaluating short term dissolved oxygen (DO) criteria attainment or non-attainment at the spatial scale of whole tributaries of the Bay system
 3. Completed work on a “case study” where a strong management action sharply decreased nutrient loading rates to a Bay tributary (Mattawoman Creek). Ecological responses to this action were documented and analyzed as part of a larger effort by the Tidal Water Monitoring and Analysis Workgroup (TMAW) to better understand responses of tidal systems to restoration actions.
 4. Completed work on a statistical model of summer season and whole Bay hypoxia. This model uses readily available data for predicting the volume of hypoxia in the Bay on an annual basis. Predictions have now been made for several years and results utilized in Bay websites.
 5. The PI (WRB) of the EPC program has continued as chair of the TMAW group. TMAW continued work on DO criteria issues during FY 2013 and much of the EPC effort is directly relevant to TMAW challenges.

Major conclusions from these efforts are listed below

- **Comparative Analyses Linking Nutrient Inputs to Estuarine Water Quality:** We assembled a data set for 19 tributary estuaries of the Bay. The data set included estimates of N and P loads (both point and diffuse), 14 physical characteristics of these 19 estuaries and selected water quality conditions, with emphasis on dissolved nutrients, water clarity and chlorophyll-*a* concentrations. The first and last of these data sets were assembled for a 20 year period (1986-2005). Loading rates of N and P varied widely in these small tributary systems ranging from very high, even by world standards (Back River), to quite low (West and Rhode Rivers). In addition, in several systems management actions were evident with decreased nutrient loading rates, mainly due to WWTP up-grades (Back River and Mattawoman Creek). The N:P load ratio was very high in many of these systems and this may reflect both the higher mobility of N in diffuse source loads and the more complete removal of P rather than N at WWTP. There were significant relationships between TN and TP loads (multi-year averages) and DIN and DIP concentrations in these estuaries with the N relationship stronger (and linear) than the P relationships. The relationship between nutrient loads (N and P) and chlorophyll-*a* was more complex. Virtually all tributaries with low areal N and P loads exhibited relatively

low chlorophyll- *a* concentration and concentration of chlorophyll-*a* was proportional to N loads. In the few cases where N and P loads were very high (e.g., Back River) chlorophyll-*a* concentration was also very high. Linear multiple regression modeling was applied to the long-term average data set (20 year average) and strong relationships between chlorophyll- *a* and variables such as N concentrations and water clarity emerged. We did not have the resources to thoroughly examine the annual data set but expect similar and possibly stronger relationships to emerge because the data set being modeled is much larger. All of these comparative analyses suggest a diverse array of small tributary systems that vary substantially regarding water quality status. This result suggests that load reductions and efforts to improve water clarity need to be tailored to each system. Additional analysis of this rich data set is certainly warranted for both scientific understanding of small tributary system dynamics and for fine-tuning management programs.

- **ConMon – Dataflow Integration for DO Criteria Analysis:** We proposed a method for linking Dataflow© and ConMon data for short-term, surface water DO criteria assessment. A statistical model of surface water DO dynamics based on ConMon data was developed. The results of this model were then used to calculate daily DO minimum across a tributary. This information was used to assess areal DO criteria compliance. Model results indicated that it is vital to consider the short-term time scale DO criteria across both space and time concurrently. Large fluctuations in DO occurred within a 24-hour time period and DO dynamics varied across the length of the tributary. The overall result was a “proof of concept” model that allowed for a more detailed characterization of the shallow water DO conditions. This model produces a technique that can be used by the Bay program for DO criteria at fine temporal and spatial scales in the surface waters of the Chesapeake Bay. Broader applications of this model include instantaneous DO criteria assessment, utilizing this model in combination with aerial remote sensing, and developing DO amplitude as an indicator of an impaired water body.
- **Chesapeake Bay Mainstem Summer Hypoxia Predictions:** We examined the processes influencing summer hypoxia in the mainstem portion of Chesapeake Bay. This work was largely funded by a NOAA grant but EPC staff and the PI (WRB) of the EPC program and chair of TWAW was centrally involved with this effort. Given the focus of TMAW on DO issues this work has been viewed as an extension of normal EPC efforts during the past funding period. The summer hypoxia analysis was based on the Chesapeake Bay Monitoring Program data collected between 1985 and 2007. Analyses indicate bottom water DO starts to be depleted in the upper mesohaline area during late spring, and hypoxia expands down-estuary by early summer. The seasonal hypoxia in the bay is related to multiple variables, (e.g., river discharge, nutrient loading, stratification, phytoplankton biomass, and wind condition), but most of these are intercorrelated. The winter-spring Susquehanna River flow contributes to not only spring-summer buoyancy effects on estuarine circulation dynamics but also nutrient loading from the land promoting phytoplankton growth. We also found that summer hypoxia is significantly correlated with the late winter-spring (February-April) northeasterly-southwesterly (NE-SW) wind. Based on winter-spring (January-May) conditions, a predictive tool was developed to forecast summer (June-August) hypoxia using the river discharge and NE-

SW wind. Late winter-spring wind pattern may affect the transport of spring bloom biomass to the western shoal or the deep channel of the bay which either alleviates or increases the summer hypoxic volume in the mid-bay region, respectively. Simulation model results also suggest that larger amounts of organic matter could be transported into the deep channel under conditions of frequent winter-spring northeasterly winds and less transport during years with frequent winter-spring southwesterly winds. This tool is relatively easy to use and data for implementation are available several months before hypoxia develops in the Bay thereby providing the opportunity for an early season forecast.

- **Case Study of Estuarine Restoration in Mattawoman Creek:** We also developed a peer-reviewed publication based on continuing EPC work that used diverse monitoring and modeling data for Mattawoman Creek to examine responses of this tidal freshwater tributary of the Potomac River estuary to a sharp reduction in point-source nutrient loading rate. Oligotrophication of these systems is not well understood; questions concerning recovery pathways, threshold responses and lag times remain to be clarified and eventually generalized for application to other systems. Prior to load reductions Mattawoman Creek was eutrophic with poor water clarity (secchi depth <0.5 m), no submerged aquatic vegetation (SAV) and large algal stocks (50-100 $\mu\text{g L}^{-1}$ chlorophyll-*a*). A substantial modification to a waste water treatment plant (WWTP) reduced annual average nitrogen (N) loads from 30 $\text{g N m}^{-2} \text{yr}^{-1}$ to 12 $\text{g N m}^{-2} \text{yr}^{-1}$ and phosphorus (P) loads from 3.7 $\text{g P m}^{-2} \text{yr}^{-1}$ to 1.6 $\text{g P m}^{-2} \text{yr}^{-1}$. Load reductions for both N and P were initiated in 1991 and completed by 1995. There was no trend in diffuse N and P loads between 1985 and 2010. Following nutrient load reduction, $\text{NO}_2 + \text{NO}_3$ and chlorophyll-*a* decreased and secchi depth and SAV coverage and density increased with initial response lag times of one, four, three and one year, respectively. A preliminary N budget was developed and indicated the following: diffuse sources now dominate N inputs, estimates of long-term burial and denitrification were not large enough to balance the budget, sediment recycling of NH_4 was the single largest term in the budget, SAV uptake of N from sediments and water provided a modest seasonal-scale N sink and the creek system acts as an N sink for imported Potomac River nitrogen. Finally, using a comparative approach (utilizing data from other shallow, low salinity Chesapeake Bay ecosystems) strong relationships were found between N loading and algal biomass and between algal biomass and water clarity, two key water quality variables used as indices of restoration in Chesapeake Bay. One of the chief conclusions of this work is that strong management actions produce ecosystem responses consistent with the conceptual model of eutrophication and oligotrophication that is the basis for the Bay restoration program. In addition, at this site, delays in responses to management actions were relatively short (<5 years).

Chapter 1

Introduction and Objectives

W.R. Boynton, L.A. Wainger, C.L.S. Hodgkins C. O’Leary and A.R. Bayard

1-1	BACKGROUND	1
1-2	OBJECTIVES OF THE WATER QUALITY MONITORING PROGRAM	3
1-3	REFERENCES	7

1-1 Background and the Ecosystem Processes Component of the Biomonitoring Program

The first phase of the Chesapeake Bay Program was undertaken during a period of four years (1984 - 1987) and had as its goal the characterization of the existing state of the bay, including spatial and seasonal variation, which were keys to the identification of problem areas. During this phase of the program, the Ecosystems Processes Component (EPC) measured sediment-water oxygen and nutrient exchange rates and determined the rates at which organic and inorganic particulate materials reached deep waters and bay sediments. Sediment-water exchanges and depositional processes are major features of estuarine nutrient cycles and play an important role in determining water quality and habitat conditions. The results of EPC monitoring have been summarized in a series of interpretive reports (Boynton *et al.*, annually from 1984 through 2011; and Bailey *et al.*, 2008). The results of this characterization effort have confirmed the importance of deposition and sediment processes in determining water quality and habitat conditions. Furthermore, it is also now clear that these processes are responsive to changes in nutrient loading rates (Boynton and Kemp 2008). Much of these data played a key role in formulating, calibrating and verifying Chesapeake Bay water quality models and these data are continuing to be used as the “gold standard” against which the sediment model is further tested and refined (e.g., Brady *et al.*, 2012; Testa *et al.*, 2013). We have also created a web-accessible and complete Chesapeake Bay sediment flux data base that is available to all interested parties (www.gonzo.cbl.umces.edu).

The second phase of the program effort, completed during 1988 through 1990, identified interrelationships and trends in key processes monitored during the initial phase of the program. The EPC was able to identify trends in sediment-water exchanges and deposition rates. Important factors regulating these processes have also been identified and related to water quality conditions (Kemp and Boynton 1992; Boynton *et al.*, 1991; Cowan and Boynton 1996; Boynton and Kemp 2008).

In 1991 the program entered its third phase. During this phase the long-term 40% nutrient reduction strategy for the bay was re-evaluated. In this phase of the process, the monitoring program was used to assess the appropriateness of targeted nutrient load reductions as well as provide indications of water quality patterns that will result from such management actions. The preliminary re-evaluation report (Progress Report of the Bay-wide Nutrient Reduction Reevaluation, 1992) included the following conclusions: nonpoint sources of nutrients contributed approximately 77%

of the nitrogen and 66% of the phosphorus entering the bay; agricultural sources were dominant followed by forest and urban sources; the "controllable" fraction of nutrient loads was about 47% for nitrogen and 70% for phosphorus; point source reductions were ahead of schedule and diffuse source reductions were close to projected reductions; further efforts were needed to reduce diffuse sources; significant reductions in phosphorus concentrations and slight increases in nitrogen concentrations have been observed in some areas of the bay; areas of low dissolved oxygen have been quantified and living resource water quality goals established; simulation model projections indicated significant reductions in low dissolved oxygen conditions associated with a 40% reduction of controllable nutrient loads. These results have recently been re-evaluated, modified and new goals established since 1991.

During the latter part of 1997 the Chesapeake Bay Program entered another phase of re-evaluation. Since the last evaluation, programs had collected and analyzed additional information, nutrient reduction strategies had been implemented and, in some areas, habitat improvements had been accomplished. The overall goal of the 1997 re-evaluation was the assessment of the progress of the program and the implementation of necessary modifications to the difficult process of restoring water quality, habitats and living resources in Chesapeake Bay. During this portion of the program, EPC was further modified to include 1) development of intensive spatial water quality mapping; 2) intensive examination of SAV habitat conditions in major regions of the Chesapeake Bay and development of a high frequency shallow water monitoring protocol (ConMon) that has been extensively implemented in many regions of the Bay and tributary rivers.

During the past several years (2008-2012) the EPC of the Biomonitoring Program has further evolved to focus on data analysis of water quality issues. Specifically, the EPC has accomplished the following: 1) rescued a rare, high quality, near-continuous and long-term water quality data set collected in the mesohaline portion of the Patuxent estuary from 1963-1969 and made this data set generally available; 2) examined multiple sites using dataflow results for a better understanding of the spatial features of water quality and factors, both local and remote, influencing these water quality distributions; 3) used ConMon data sets to assess DO criteria attainment and duration of low DO events in near-shore areas using a variety of computational approaches; and 4) developed an algorithm for computing community-scale primary production and respiration using ConMon data for purposes of developing another metric of water quality and relating these fundamental ecosystem processes to important controlling factors such as nutrient loading rates. The specific goals of the 2012 EPC Program are provided later in this chapter.

The Chesapeake Bay Water Quality Monitoring Program was initiated to provide guidelines for restoration, protection and future use of the mainstem estuary and its tributaries and to provide evaluations of implemented management actions directed towards alleviating some critical pollution problems. A description of the complete monitoring program is provided in the following documents:

Magnien *et al.* (1987),

Chesapeake Bay program web page:

<http://www.chesapeakebay.net/about/programs/monitoring>

DNR web page: <http://www.dnr.state.md.us/bay/monitoring/eco/index.html>

In addition to the EPC program portion, the monitoring program also has components that measure:

1. Freshwater, nutrient and other pollutant input rates.
2. Chemical, biological and physical properties of the water column.
3. Phytoplankton community characteristics (this program has been much reduced since 2009).
4. Benthic community characteristics (abundances, biomass and indices of health).
5. SAV distribution and density

1-2 Nutrient Effects and Conceptual Model of Water Quality Processes in Chesapeake Bay Systems

During the past three decades much has been learned about the effects of both natural and anthropogenic nutrient inputs (e.g., nitrogen, phosphorus, silica) on such important estuarine features as phytoplankton production, algal biomass, seagrass abundance and distribution and oxygen conditions in deep waters (Nixon 1981, 1988; Boynton *et al.*, 1982; Kemp *et al.*, 1983; D'Elia *et al.*, 1983; Garber *et al.*, 1989; Malone 1992; Kemp and Boynton 1992; Boynton and Kemp 2008). While our understanding is not complete, important pathways regulating these processes have been identified and related to water quality issues. Of particular importance here, it has been determined that 1) algal primary production and biomass levels in many estuaries (including Chesapeake Bay) are responsive to nutrient loading rates, 2) high rates of algal production and algal blooms are sustained through summer and fall periods by recycling of essential nutrients that enter the system during the high flow periods of the year, 3) the “nutrient memory” of estuarine systems is relatively short (one to several years for nitrogen and longer for phosphorus), and 4) submerged aquatic vegetation (SAV) communities are responsive to water quality conditions, especially light availability, that is modulated both by water column turbidity regimes and epiphytic fouling on SAV leaf surfaces.

Nutrients and organic matter enter the bay from a variety of sources, including sewage treatment plant effluents, fluvial inputs, local non-point drainage and direct rainfall on bay waters. Dissolved nutrients are rapidly incorporated into particulate matter via biological, chemical and physical mechanisms. A portion of this newly produced organic matter sinks to the bottom, decomposes and thereby contributes to the development of hypoxic or anoxic conditions and loss of habitat for important infaunal, shellfish and demersal fish communities. Eutrophic (nutrient enriched) conditions favor the growth of a diverse assemblage of estuarine bacteria who play a major role in consuming dissolved oxygen and the subsequent development of hypoxic and anoxic conditions. The regenerative and large short-term nutrient storage capacities of estuarine sediments ensure a large return flux of nutrients from sediments to the water column that can sustain continued high rates of phytoplanktonic growth and biomass accumulation. Continued growth and accumulation supports high rates of deposition of organics to deep waters, creating and sustaining hypoxic and anoxic conditions typically associated with eutrophication of estuarine systems. To a considerable extent, it is the magnitude of these processes that determines water quality conditions in many zones of the bay. Ultimately, these processes are driven by inputs of organic matter and nutrients from both natural and anthropogenic sources. If water quality management programs are instituted and loadings of organic matter and nutrients decrease, changes in the magnitude of these processes are expected and will serve as a guide in determining the effectiveness of strategies aimed at

improving bay water quality and habitat conditions. The schematic diagram in Figure 1-1 summarizes this conceptual eutrophication model where increased nitrogen (N) and phosphorus (P) loads result in a water quality degradation trajectory and reduced N and P loads lead to a restoration trajectory. There is ample empirical evidence for the importance of N and P load variation. For example, water quality and habitat conditions change dramatically between wet and dry years, with the former having degradation trajectory characteristics and the latter, restoration trajectory characteristics (Boynton and Kemp 2000; Hagy *et al.*, 2004; Kemp *et al.*, 2005). However, the exact temporal sequence of restoration may range from simple and rapid reversals to complex and lengthy processes (Kemp and Goldman 2008).

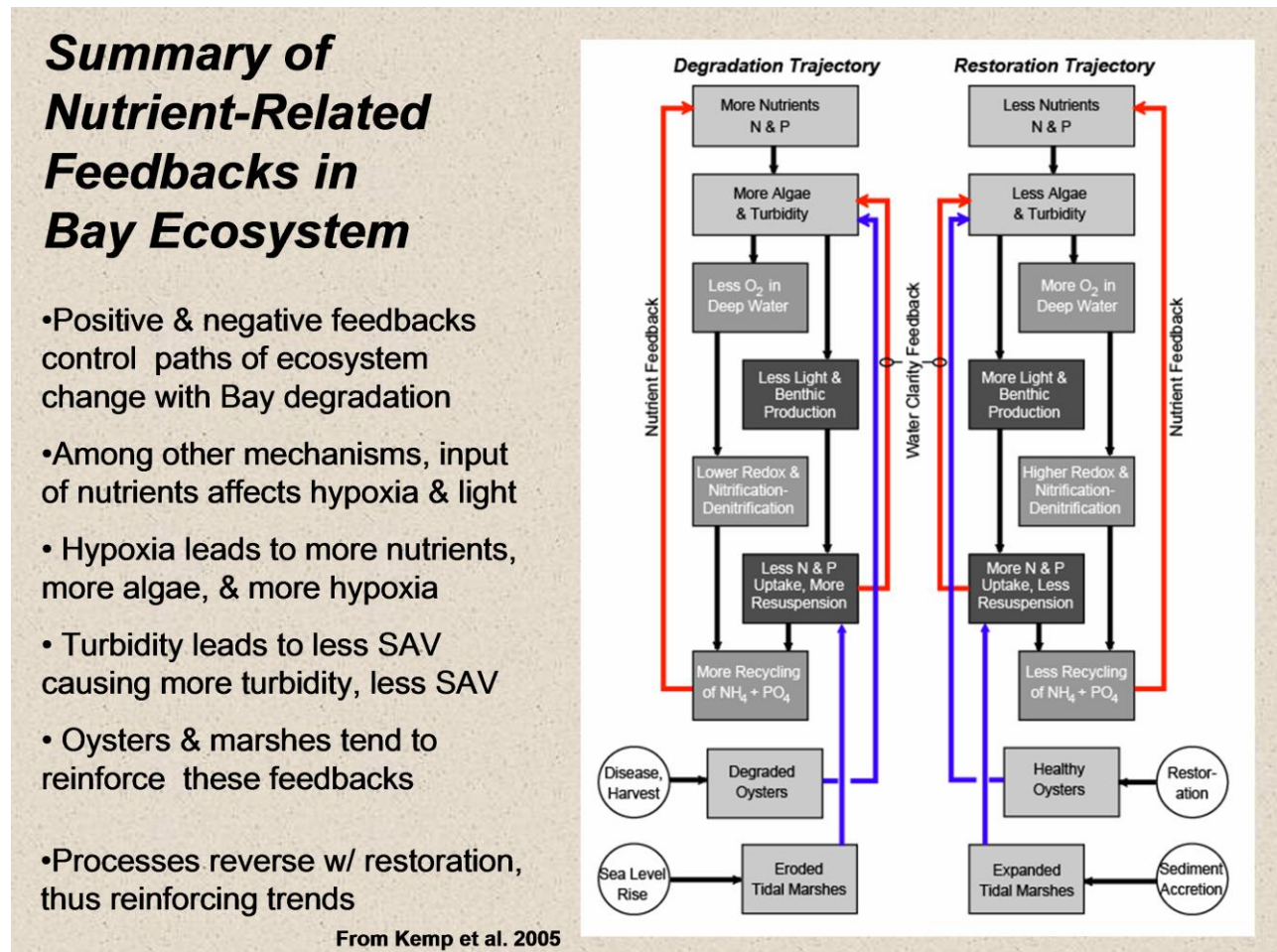


Figure 1-1. A simplified schematic diagram indicating degradation and restoration trajectories of an estuarine ecosystem. Lightly shaded boxes in the diagram indicate past and present components of the EPC program in the Patuxent River and Tangier Sound. (Adapted from Kemp *et al.*, 2005).

Within the context of this conceptual model, monitoring program data analysis has focused on SAV and other near-shore contemporary and historical habitat and water quality conditions to evaluate water quality criteria attainment. Recent efforts address management needs to understand the relative importance of local or regional drivers in controlling water quality and how quickly the biotic system may respond to changes in nutrient or sediment inputs from the watershed.

1-3 Objectives of the Water Quality Monitoring Program

The EPC has undergone multiple and significant program modification since its inception in 1984 but its overall objectives have remained consistent with those of other Monitoring Program Components. The specific objectives of the 2012 EPC program were as follows:

1. Comparative Synthesis of Estuarine Responsiveness to Nutrient Loading

The primary goal of this synthesis involved using small tributary nutrient loading data with water quality monitoring data to develop estuarine status and responsiveness indicators using statistical models. The relationships derived by statistical modeling will serve to identify which subareas of the Bay are likely to be most and least impacted by nutrient loads and which areas might be most responsive to management actions. We will use nutrient loading (from USGS sites and output from the CBP landscape model), estuarine physical factors (estuarine water flushing times) and water quality parameters (from ConMon and Biomonitoring data) to predict outcomes such as algal biomass (indexed with chlorophyll-*a* concentration) and other water quality features. This comparative analysis will provide a useful guide to expected outcomes from nutrient load changes.

2. Linking ConMon and Dataflow© for Spatial DO Criteria Assessment (Proof of Concept)

The ConMon monitoring program provides detailed time series of water quality information that can be applied to water quality assessments at many tributary sites in Maryland. These data offer some of the best information for understanding daily to interannual dynamics of DO and other conditions (e.g., water clarity, turbidity and chlorophyll-*a*) relevant to sustaining aquatic organisms. While there are a good number of ConMon sites, it is difficult to judge the spatial extent from the fixed ConMon site than can be included in any attainment or non-attainment measurement. In simple terms, it is critical to know what parcel of water can be assessed by each ConMon meter. These extents may vary with season, local influence or non-local conditions.

Dataflow© (high speed spatial mapping) provides spatially-detailed data on the magnitude and fine-scale variability of water quality variables, which can be used to better understand the dynamics and drivers of water quality by location. However, these data lack temporal resolution. For this program goal we linked Dataflow© and ConMon data for DO criteria assessment. This activity is a proof of concept effort coupling the strongest features of Dataflow© and ConMon technologies.

3. Additions to DNR Web Page

During FY2013 we transferred to MD-DNR an Excel-based computation scheme and instructions for use for estimating community production and respiration, both basic ecosystem properties and both responsive to nutrient load modifications. MD-DNR will work toward adapting this tool for use on the DNR web site when time and staff availability permit.

4. TMAW Involvement

One of our team (WRB) is chair of the TMAW committee working with support from Peter Tango and Liza Hernandez. This effort will continue and will more closely tie EPC activities to those of criteria assessment.

5. Coordination

Activities in the EPC program are coordinated with other components of the Maryland Chesapeake Bay Water Quality Monitoring Program. Members of the EPC team frequently attend Biomonitoring and related meetings and frequently coordinate and share data with other monitoring program components.

6. Additional EPC Program Products

The EPC is also informally linked to other research programs focused on understand Bay ecology, water quality and habitat conditions. As a results of these interactions during the last funding period two additional analyses have been developed and have been accepted for publication. Both are very relevant to EPC goals and have been included in this report. The first (Lee *et al.*, 2013) focused on development and testing of a statistical model to forecast summer season hypoxia in the mainstem Chesapeake Bay. This model can be used by management agencies to provide a forecast for DO conditions several months prior to development of low DO conditions. The second (Boynton *et al.*, 2013) product is a manuscript based on previous EPC work concerning restoration of water and habitat quality in Mattawoman Creek, a tributary of the upper Potomac River estuary. The TMAW group has been working on producing a series of case studies concerning management “success stories” in the Bay region and this product will be useful in that effort.

1-4 References

Boynton *et al.*, 1984 – 2011 EPC Interpretive Reports:

Boynton, W.R., W.M. Kemp, L. Lubbers, K.V. Wood and C.W. Keefe. 1984. Ecosystem Processes Component Level I Data Report No. 1. Chesapeake Biological Laboratory (CBL), University of Maryland System, Solomons, MD 20688-0038. Ref. No.[UMCEES]CBL 84-109.

Boynton, W.R., W.M. Kemp and J.M. Barnes. 1985. Ecosystem Processes Component Level I Data Report No. 2. Chesapeake Biological Laboratory (CBL), University of Maryland System, Solomons, MD 20688-0038. Ref. No.[UMCEES]CBL 85-121.

Boynton, W.R., W.M. Kemp, J.H. Garber and J.M. Barnes. 1986. Ecosystem Processes Component Level 1 Interpretive Report No. 3. Chesapeake Biological Laboratory (CBL), University of Maryland System, Solomons, MD 20688-0038. Ref. No.[UMCEES]CBL 86-56b.

Boynton, W.R., W.M. Kemp, J.H. Garber, J.M. Barnes, L.L. Robertson and J.L. Watts. 1987. Ecosystem Processes Component Level 1 Interpretive Report No. 4. Chesapeake Biological Laboratory (CBL), University of Maryland System, Solomons, MD 20688-0038. Ref. No.[UMCEES]CBL 88-06.

Boynton, W.R., W.M. Kemp, J.H. Garber, J.M. Barnes, L.L. Robertson and J.L. Watts. 1988. Ecosystem Processes Component Level 1 Interpretive Report No. 5. Chesapeake Biological Laboratory (CBL), University of Maryland System, Solomons, MD 20688-0038. Ref. No.[UMCEES]CBL 88-69.

Boynton, W.R., J.H. Garber, W.M. Kemp, J.M. Barnes, J.L. Watts, S. Stammerjohn and L.L. Matteson. 1989. Ecosystem Processes Component Level 1 Interpretive Report No. 6. Chesapeake Biological Laboratory (CBL), University of Maryland System, Solomons, MD 20688-0038. Ref. No.[UMCEES]CBL 89-080.

Boynton, W.R., J.H. Garber, W.M. Kemp, J.M. Barnes, L.L. Matteson, J.L. Watts, S. Stammerjohn and F.M. Rohland. 1990. Ecosystem Processes Component Level 1 Interpretive Report No. 7. Chesapeake Biological Laboratory (CBL), University of Maryland System, Solomons, MD 20688-0038. Ref. No.[UMCEES]CBL 90-062.

Boynton, W.R., W.M. Kemp, J.M. Barnes, L.L. Matteson, J.L. Watts, S. Stammerjohn, D.A. Jasinski and F.M. Rohland. 1991. Ecosystem Processes Component Level 1 Interpretive Report No. 8. Chesapeake Biological Laboratory (CBL), University of Maryland System, Solomons, MD 20688-0038. Ref. No.[UMCEES]CBL 91-110.

Boynton, W.R., W.M. Kemp, J.M. Barnes, L.L. Matteson, J.L. Watts, S. Stammerjohn, D.A. Jasinski and F.M. Rohland. 1992. Ecosystem Processes Component Level 1 Interpretive Report No. 9. Chesapeake Biological Laboratory (CBL), University of Maryland System, Solomons, MD 20688-0038. Ref. No.[UMCEES]CBL 92-042.

Boynton, W.R., W.M. Kemp, J.M. Barnes, L.L. Matteson, F.M. Rohland, D.A. Jasinski and H.L. Kimble. 1993. Ecosystem Processes Component Level 1 Interpretive Report No. 10. Chesapeake Biological Laboratory (CBL), University of Maryland System, Solomons, MD 20688-0038. Ref. No.[UMCEES]CBL 93-030a.

Boynton, W.R., W.M. Kemp, J.M. Barnes, L.L. Matteson, F.M. Rohland, D.A. Jasinski and H.L. Kimble. 1994. Ecosystem Processes Component Level 1 Interpretive Report No. 11. Chesapeake Biological Laboratory (CBL), University of Maryland System, Solomons, MD 20688-0038. Ref. No.[UMCEES]CBL 94-031a.

Boynton, W.R., W.M. Kemp, J.M. Barnes, L.L. Matteson, F.M. Rohland, L.L. Magdeburger and B.J. Weaver. 1995. Ecosystem Processes Component Level 1 Interpretive Report No 12. Chesapeake Biological Laboratory (CBL), University of Maryland System, Solomons, MD 20688-0038. Ref. No.[UMCEES]CBL 95-039.

Boynton, W.R., W.M. Kemp, J.M. Barnes, L.L. Matteson, F.M. Rohland, D.A. Jasinski, J.D. Hagy III, L.L. Magdeburger and B.J. Weaver. 1996. Ecosystem Processes Component Level 1 Interpretive Report No. 13. Chesapeake Biological Laboratory (CBL), University of Maryland System, Solomons, MD 20688-0038. Ref. No. [UMCEES]CBL 96-040a.

Boynton, W.R., J.M. Barnes, F.M. Rohland, L.L. Matteson, L.L. Magdeburger, J.D. Hagy III, J.M. Frank, B.F. Sweeney, M.M. Weir and R.M. Stankelis. 1997. Ecosystem Processes Component Level 1 Interpretive Report No. 14. Chesapeake Biological Laboratory (CBL), University of Maryland System, Solomons, MD 20688-0038. Ref. No. [UMCEES]CBL 97-009a.

Boynton, W.R., R.M. Stankelis, E.H. Burger, F.M. Rohland, J.D. Hagy III, J.M. Frank, L.L. Matteson and M.M. Weir. 1998. Ecosystem Processes Component Level 1 Interpretive Report No. 15. Chesapeake Biological Laboratory (CBL), University of Maryland System, Solomons, MD 20688-0038. Ref. No. [UMCES]CBL 98-073a.

Boynton, W.R., R.M. Stankelis, J.D. Hagy III, F.M. Rohland, and J.M. Frank. 1999. Ecosystem Processes Component Level 1 Interpretive Report No. 16. Chesapeake Biological Laboratory (CBL), University of Maryland System, Solomons, MD 20688-0038. Ref. No. [UMCES]CBL 99-0070a.

Boynton, W.R., R.M. Stankelis, J.D. Hagy, F.M. Rohland, and J.M. Frank. 2000. Ecosystem Processes Component Level 1 Interpretive Report No. 17. Chesapeake Biological Laboratory (CBL), University of Maryland System, Solomons, MD 20688-0038. Ref. No. [UMCES]CBL 00-0174.

Boynton, W.R., R.M. Stankelis, F.M. Rohland, J.M. Frank and J.M. Lawrence. 2001. Ecosystem Processes Component Level 1 Interpretive Report No. 18. Chesapeake Biological Laboratory (CBL), University of Maryland System, Solomons, MD 20688-0038. Ref. No. [UMCES]CBL 01-0088.

Boynton, W.R., R.M. Stankelis, F.M. Rohland, J.M. Frank, J.M. Lawrence and B.W. Bean. 2002. Ecosystem Processes Component Level 1 Interpretive Report No. 19. Chesapeake Biological Laboratory (CBL), University of Maryland System, Solomons, MD 20688-0038. Ref. No. [UMCES]CBL 02-0125a.

Boynton, W.R. and F.M. Rohland (eds.); R.M. Stankelis, E.K. Machelor Bailey, P.W. Smail and M.A.C. Ceballos. 2003. Ecosystem Processes Component (EPC). Level 1 Interpretive Report No. 20. Chesapeake Biological Laboratory (CBL), Univ. of Maryland Center for Environmental Science, Solomons, MD 20688-0038. Ref. No. [UMCES]CBL 03-303. [UMCES Technical Series No. TS-419-03-CBL].

Boynton, W.R., R.M. Stankelis, P.W. Smail and E.K. Bailey. 2004. Ecosystem Processes Component (EPC). Maryland Chesapeake Bay Water Quality Monitoring Program, Level 1 report No. 21. Jul. 1984 - Dec. 2003. Ref. No. [UMCES] CBL 04-086. [UMCES Technical Series No. TS-447-04-CBL].

Boynton, W.R., R.M. Stankelis, P.W. Smail, E.K. Bailey and H.L. Soulen. 2005. Ecosystem Processes Component (EPC). Maryland Chesapeake Bay Water Quality Monitoring Program, Level 1 report No. 22. Jul. 1984 - Dec. 2004. Ref. No. [UMCES] CBL 05-067. [UMCES Technical Series No. TS-492-05-CBL].

Boynton, W.R., P.W. Smail, E.M. Bailey and S.M. Moesel. 2006. Ecosystem Processes Component (EPC). Maryland Chesapeake Bay Water Quality Monitoring Program, Level 1 report No. 23. Jul. 1984 - Dec. 2005. Ref. No. [UMCES] CBL 06-108. [UMCES Technical Series No. TS-253-06-CBL].

Boynton, W.R., E.M. Bailey, S.M. Moesel, L.A. Moore, J.K. Rayburn, L.A. Wainger and K.V. Wood. 2007. Ecosystem Processes Component (EPC). Maryland Chesapeake Bay Water Quality Monitoring Program, Level 1 report No. 24. Jul. 1984 - Dec. 2006. Ref. No. [UMCES] CBL 07-112. [UMCES Technical Series No. TS-536-07-CBL].

Bailey, E.M., M.A.C. Ceballos and W.R. Boynton. 2008. Ecosystem Processes Component (EPC). Maryland Chesapeake Bay Water Quality Monitoring Program, Level 1 report No. 25. Jul. 1984 - Dec. 2007. Ref. No. [UMCES] CBL 08-080. [UMCES Technical Series No. TS-565-08-CBL].

Boynton, W.R., L.A. Wainger, E.M. Bailey and M.A.C. Ceballos. 2009. Ecosystem Processes Component (EPC). Maryland Chesapeake Bay Water Quality Monitoring Program, Level 1 report No. 26. Jul. 1984 - Dec. 2008. Ref. No. [UMCES] CBL 09-082. [UMCES Technical Series No. TS-583-09-CBL].

Boynton, W.R., L.A. Wainger, E.M. Bailey, A.F. Drohan and A.R. Bayard. 2010. Ecosystem Processes Component (EPC). Maryland Chesapeake Bay Water Quality Monitoring Program, Level 1 report No. 26. Jul. 1984 - Dec. 2009. Ref. No. [UMCES] CBL 10-098. [UMCES Technical Series No. TS-606-10-CBL].

Boynton, W.R., L.A. Wainger, E.M. Bailey, A.R. Bayard, C.L. Sperling and M.A.C. Ceballos. 2011. Ecosystem Processes Component (EPC). Maryland Chesapeake Bay Water Quality Monitoring Program, Level 1 report No. 28. Jul. 1984 – Dec. 2010. Ref. No. [UMCES] CBL 11-024. [UMCES Technical Series No. TS-620-11-CBL].

Boynton, W.R., L.A. Wainger, E.M. Bailey, A.R. Bayard, C.L.S.Hodgkins and M.A.C. Ceballos. 2012. Ecosystem Processes Component (EPC). Maryland Chesapeake Bay Water Quality Monitoring Program, Level 1 report No. 29. Jul. 1984 – Dec. 2011. Ref. No. [UMCES] CBL 12-020. [UMCES Technical Series No. TS-637-12-CBL].

Chapter 1 Text References:

Brady, D.C., J.M. Testa, D.M. Di Toro, W.R. Boynton, and W.M. Kemp. 2012. Sediment flux modeling: Calibration and application for coastal systems. *Estuarine, Coastal and Shelf Science*.

Boynton, W. R., W. M. Kemp, and C. W. Keefe. 1982. A comparative analysis of nutrients and other factors influencing estuarine phytoplankton production, p. 69-90. In: V.S. Kennedy (ed.) *Estuarine Comparisons*. Academic Press, New York.

Boynton, W.R. and W.M. Kemp. 2000. Influence of river flow and nutrient loading on selected ecosystem processes: a synthesis of Chesapeake Bay data. pp. 269-298 *In: J. Hobbie Ed. A Blueprint for Estuarine Synthesis*. Beckman Center, University of California at Irvine, CA. [UMCES Contribution No. 3224-CBL].

Boynton, W.R. and Kemp, W.M. 2008. Estuaries, pp. 809-856. In: Capone, D.G., Bronk, D.A., Mulholland, M.R., and Carpenter, E.J. (Eds.), *Nitrogen in the Marine Environment 2nd Edition*. Elsevier Inc., Burlington, Massachusetts.

Cowan, J.L.W. and Boynton, W.R., 1996. Sediment-water oxygen and nutrient exchanges along the longitudinal axis of Chesapeake Bay: Seasonal patterns, controlling factors, and ecological significance. *Estuaries* 19(3): 562-580.

D'Elia, C.F., D.M. Nelson, and W.R. Boynton. 1983. Chesapeake Bay nutrient and plankton dynamics: III. The annual cycle of dissolved silicon. *Geochim. Cosmochim. Acta* 47:1945-1955.

Garber, J.H., W.R. Boynton, J.M. Barnes., L.L. Matteson., L.L. Robertson., A.D. Ward and J.L. Watts. 1989. Ecosystem Processes Component and Benthic Exchange and Sediment Transformations. Final Data Report. Maryland Department of the Environment. Maryland Chesapeake Bay Water Quality Monitoring Program. Chesapeake Biological Laboratory (CBL), University of Maryland System, Solomons, MD 20688-0038. Ref. No.[UMCEES]CBL 89-075.

Hagy, J. D., W. R. Boynton, C. W. Keefe and K. V. Wood. 2004. Hypoxia in Chesapeake Bay, 1950-2001: Long-term change in relation to nutrient loading and river flow. *Estuaries* 27(4): 634-658.

Kemp, W.M., W.R. Boynton, J.C. Stevenson, R.W. Twilley and J.C. Means. 1983. The decline of submerged vascular plants in Chesapeake Bay: summary of results concerning possible causes. *Mar. Tech. Soc. J.* 17(2):78-89.

Kemp, W.M. and W.R. Boynton. 1992. Benthic-Pelagic Interactions: Nutrient and Oxygen Dynamics. In: D.E. Smith, M. Leffler and G. Mackiernan [Eds.], *Oxygen Dynamics in the Chesapeake Bay: A synthesis of Recent Research*. Maryland Sea Grant Book, College Park, MD, p. 149-221.

Kemp, W. M., W. R. Boynton, J. E. Adolf, D. F. Boesch, W. C. Boicourt, G. Brush, J. C. Cornwell, T. R. Fisher, P. M. Glibert, J. D. Hagy, L. W. Harding, E. D. Houde, D. G. Kimmel, W. D. Miller, R. I. E. Newell, M. R. Roman, E. M. Smith, and J. C. Stevenson. 2005. Eutrophication of Chesapeake Bay: Historical trends and ecological interactions. *Mar. Ecol. Prog. Ser.* 303: 1-29.

Kemp, W. M. and E. B. Goldman. 2008. Thresholds in the recovery of eutrophic coastal ecosystems: a synthesis of research and implications for management. Maryland Sea Grant Publication Number UM-SG-TS-2008-01. 46 pp.

Magnien R.E., R.M. Summers, M.S. Haire, W.R. Boynton, D.C. Brownlee, A.F. Holland, F. Jacobs, W.M. Kemp, K.G. Sellner, G.D. Foster and D.A. Wright. 1987. Monitoring for management actions. First Biennial Report. The Maryland Office of Environmental Programs, Chesapeake Bay, Water Quality Monitoring Program, Baltimore, MD.

Malone, T.C. 1992. Effects of Water Column Processes on Dissolved Oxygen Nutrients, Phytoplankton and Zooplankton. In: D.E. Smith, M. Leffler and G. Mackiernan [Eds.], *Oxygen Dynamics in the Chesapeake Bay: A synthesis of Recent Research*. Maryland Sea Grant Book, College Park, MD, p. 149-221.

Nixon, S.W. 1981. Remineralization and nutrient cycling in coastal marine ecosystems, p. 111-138. In: B.J. Neilson and L.E. Cronin [Eds.], *Estuaries and Nutrients*. Humana Press, Clifton, NJ.

Nixon, S.W. 1988. Physical energy inputs and comparative ecology of lake and marine ecosystems. *Limnol. Oceanogr.* 33 (4, part 2), 1005-1025.

Progress Report of the Baywide Nutrient Reduction Reevaluation, Chesapeake Bay Program. 1992. U.S. Environmental Protection Agency for the Chesapeake Bay Program [CSC.LR18.12/91].

Testa, J.M., D.C. Brady, D.M. Di Toro, W.R. Boynton, and W.M. Kemp. 2013. Sediment flux modeling: Nitrogen, phosphorus and silica cycles. *Estuarine, Coastal and Shelf Science*. Submitted.

Chapter 2

Comparative Analysis of Nutrient Loads and Water Quality Conditions in Selected Tributaries of Chesapeake Bay

C. L. S. Hodgkins, W.R. Boynton, C. O'Leary, L.A. Wainger, and A.R. Bayard

2-1 INTRODUCTION AND BACKGROUND	1
2-2 STUDY AREA DESCRIPTIONS	3
2-3 DATA SOURCES, DATA MANIPULATIONS AND ANALYTICAL APPROACHES	5
2-4 SUMMARY OF NUTRIENT LOAD CHARACTERISTICS	9
2-5 WATER QUALITY CHARACTERISTICS	22
2-5.1 TEMPERATURE	23
2-5.2 SALINITY	23
2-5.3 DISSOLVED NUTRIENT CONCENTRATIONS	23
2-5.4 WATER CLARITY	24
2-5.5 CHLOROPHYLL-A CONCENTRATION	24
2-6 RELATIONSHIPS BETWEEN NUTRIENT LOADS AND WATER QUALITY CONDITIONS	33
2-6.1 NUTRIENT LOADS AND IN-SITU NUTRIENT CONCENTRATIONS	33
2-6.2 NUTRIENT LOADS AND CHLOROPHYLL-A CONCENTRATIONS	34
2-7 FUTURE WORK AND OTHER RELATED ISSUES	40
2-8 REFERENCES	42

2-1 Introduction and Background

A new focus for EPC this year has been on examining linkages between terrestrial point and diffuse nutrient loads (N and P) and estuarine water quality conditions. Developing such linkages is, of course, a central theme of the Bay modeling component but here we attempt to develop such relationships using a simpler approach and an approach that is far more accessible to a wide audience. We have used a comparative ecology approach wherein estuaries with divergent

conditions (e.g., low and high nutrient loads; large or small connections to the Bay; short or long water residence times) are combined in one analysis to increase the signal to noise ratio as we examine the data for relationships between loads and water quality conditions (see Kemp and Boynton 2012 for details concerning this approach).

The water quality data set for the Bay now includes a time series beginning in 1985 and going through to the present. The data set for modeled diffuse loads begins in 1986 and goes through 2005; these modeled estimates are critical in this analysis because there are no directly measured loads for most of the small tributaries of the Bay region. Thus, to have consistent land and tidal water data we have used data from 1986-2005 in this work. We also selected 19 tributary estuaries for this analysis using several criteria including the following: 1) at least one long-term water quality monitoring site was located in the tributary; 2) the tributary was relatively shallow and not prone to strong and persistent stratification. The resulting 19 included tributaries having significant point sources and others with just diffuse sources. Overall, nutrient loading rates ranged from low to very high.

We are seeking to modify the approaches used by limnologists (with great success) for predicting the likely response of a great variety of lakes to nutrient load modifications (e.g., Vollenweider 1976). In fact, work to date on Chesapeake Bay tributaries such as the Corsica River and Mattawoman Creek have yielded strong nutrient load – algal biomass relationships without use of complex statistical models (Figure 2-1). In the current work we have added a considerable number of sites to these earlier analyses and we have also added many years of observations. As was the case for limnological analyses, we also considered other variables that might have an influence on nutrient load – water quality relationships, including such features as water residence time (or flushing time), system depth, water clarity conditions, and ratios of system shoreline length to mouth width.

The specific goals of this work were as follows: 1) create a time-series data set (20 years) for a selection of small Chesapeake Bay tributary estuaries (19); 2) include estimates of annual and decadal point and non-point nutrient (N and P) input rates; 3) characterize in-situ concentrations of dissolved inorganic and total nutrients (N and P), water clarity, temperature, salinity and chlorophyll-*a* for the above time-scales and sites; 4) develop additional metrics (average water depth, maximum depth, mouth length, shoreline length, basin size and water flushing time) characterizing these 19 estuaries. All of these metrics could influence load-estuarine response relationships; and 5) explore these data for relationships between nutrient loads and estuarine nutrient concentrations and chlorophyll-*a* concentrations.

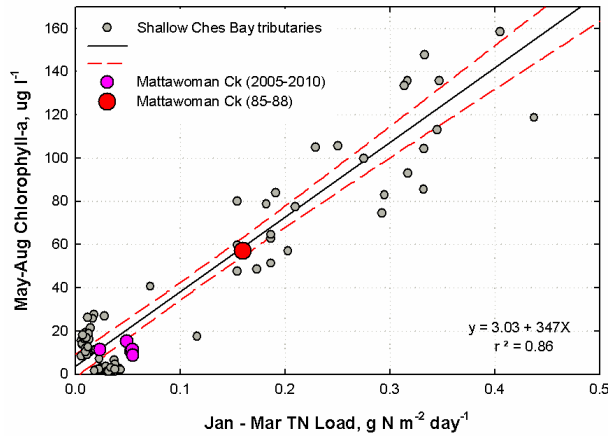


Figure 2-1. A scatter plot of TN load versus chlorophyll-*a* concentration developed for Mattawoman Creek and a few other shallow Chesapeake Bay tributaries. The large decrease in nitrogen loading to Mattawoman Creek was accompanied by a similar and large reduction in chlorophyll-*a* concentration. Data for the other Chesapeake Bay systems was from Boynton *et al.* (2009).

2-2 Study Area Descriptions

A total of 20 estuaries (Figure 2-2) were selected for the analyses done in this chapter; however for simplicity we combined the West and Rhode rivers into one estuary, bringing the number of estuaries analyzed to 19. When available we chose mesohaline stations from the tributary monitoring program. When tributary monitoring stations were not available, ConMon and/or DataFlow calibration stations were selected (Table 2-1).

Table 2-1. A list of estuary names and station codes used in this analysis. Station codes are used by the Chesapeake Bay Program Water Quality Monitoring Program

Estuary	Stations Used
Tidal Fresh	
Bohemia River	ET2.2
Bush River	WT1.1
Gunpowder River	WT2.1
Mattawoman	MAT0016
Northeast River	ET1.1
Piscataway Ck	XFB1986
Oligohaline	
Back River	WT4.1
Middle River	WT3.1
Patapsco River	WT5.1
Sassafras River	ET3.1
Mesohaline	
Choptank River	ET5.2
Corsica River	XHH3851, XHH4822, XHH5046
Magothy River	WT6.1
Patuxent River	RET1.1
Rappahannock River, VA	RET3.2
Severn River	WT7.1
South River	WT8.1
WestRhode	WT8.3, WT8.2
Wicomico River	ET7.1

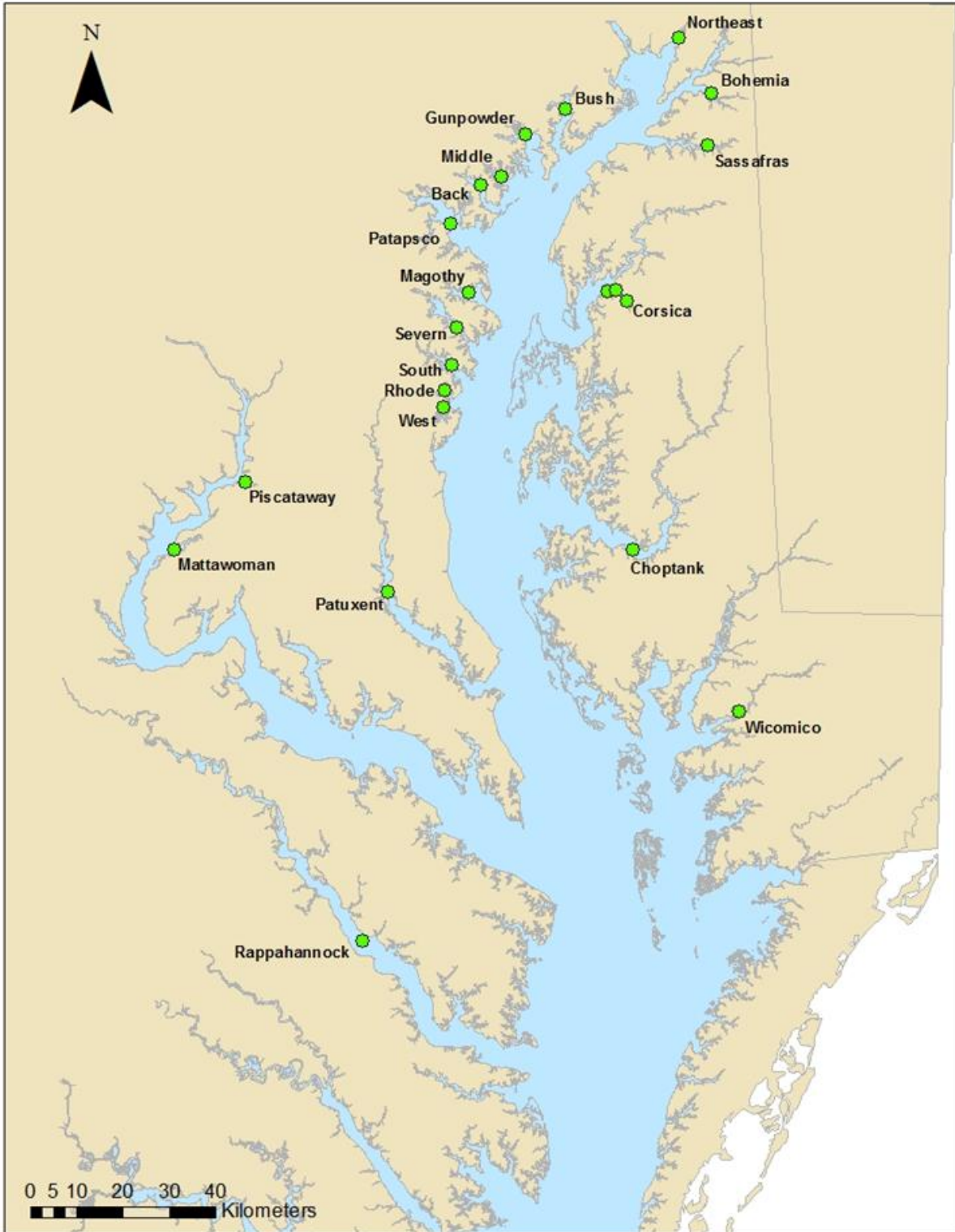


Figure 2-2. A map of Chesapeake Bay showing the location of tributary estuaries included in this analysis. The green dots indicate the general location of Chesapeake Bay Water Quality Monitoring Station data used in this analysis.

2-3 Data Sources, Data Manipulations and Analytical Approaches

Point source and diffuse nutrient loadings data were received from the Chesapeake Bay Program land use model for each estuary based on GIS shapefiles that met our watershed delineations. Water quality data were obtained from the Chesapeake Bay Program CIMS database. Given that the land use model is currently temporally limited to data up through 2005, we chose to download and analyze data from 1986 through 2005. For each estuary the following parameters were downloaded: chlorophyll-*a*, NH₄, PO₄, NO₂₃, salinity, Secchi disk depth, and water temperature. Data were stored in separate excel files by estuary. For each estuary and water quality parameter we calculated annual averages, summer (June, July, August) averages, and a long term average and standard deviation. These computations were made using values at all sampled depths by the monitoring program.

Computations performed on the nutrient loading data were similar to those of the water quality parameters. We calculated annual averages, winter-spring (January-April) averages and a long-term average. Areal loads (gm⁻²day⁻¹) were then calculated using GIS derived surface area values.

A variety of estuarine metrics were analyzed for this chapter (Table 2-3). Basin areas were computed using area values from the watershed shapefiles. We used the river-segments produced for the Chesapeake Bay Program's (USEPA, 2010) Phase 5.3 Watershed Model (USEPA, 2010) to define the watershed boundaries for these analyses. The term "river-segment" refers the area of land that immediately drains to a river reach. Estuary mouth lengths (Table 2-2) were used to define the estuary boundaries (USGS NHD, 2009). Estuary mouth and smooth shoreline lengths were defined using the editor tool in ArcGIS 10.0 (2012). The zonal statistics tool available in ESRI's ArcGIS 10.0 (2012) spatial analyst toolbox was used to generate: estuary volume, average depth, and maximum depth for each estuary boundary. These calculations were based on bathymetric DEM data at 30m raster cell resolution (NOAA, 1998). Surface area and mouth length were summarized using the calculate geometry option within ArcGIS 10.0 (2012) for each estuary boundary.

Tidal prism flushing time was calculated based on the methods provided by Wazniak *et al.* (2009). This method estimates the flushing time of small estuaries, based on assumption that the intertidal volume of the estuary and the existing water in the estuary mix completely. Estuarine physical characteristics (surface area, volume, and depth) are also factored into this calculation (Wazniak *et al.*, 2009). We did not attempt tidal prism flushing estimated for the Wicomico, Choptank, Patuxent, and Rappahannock because these are larger and more stratified systems; the tidal prism approach is not appropriate for systems with these characteristics,

Using linear and multiple regressions, we examined nutrient loading indicators (i.e., chlorophyll-*a* and nutrient concentrations) for their responses to nutrient loadings.

A Pearson's correlation coefficient was calculated between variables of interest and chlorophyll-*a* for 20 year average data from 19 different tributaries. The significance levels were calculated for 1% and 5%. Those variables that were significant at the 5% level and a few select estuary metrics (based on prior estuarine knowledge) were selected to create two multiple regression

models using stepwise selection: one with a descriptive function of chlorophyll-*a* levels and one with a predictive function of chlorophyll-*a* levels. The predictive model was chosen using those variables that contributed to chlorophyll-*a* variability while maintaining model parsimony and the lowest Akaike information criterion (AIC value). The AIC provides an estimate of information lost when a model is used to represent a process from the data and is a trade-off between the complexity of the model and the goodness of fit of the model. The descriptive model of chlorophyll-*a* included only those that were significant in the model at the 5% level.

Table 2-2. A listing of Chesapeake Bay tributary mouth locations. Shore locations on both sides of the estuary mouth are indicated with common names and by latitude and longitude.

Location of Mouth

Estuary	Start	End
Back	Rocky Pt. -76.400800 39.249077	Cuckold Pt. -76.397525 39.236324
Bohemia	Town Pt. -75.923764 39.485877	Pt. on west side of Veaxy Cove -75.939568 39.475476
Bush	Point between Sandy Pt. and Lego Pt. -76.256584 39.339398	Point on South shore of creek North of Abbey Pt. -76.232252 39.351868
Choptank	Black Walnut Pt. -76.339005 38.670115	Cook Pt -76.288712 38.629972
Corsica	Spaniard Pt. -76.145174 39.091902	Holton Pt. -76.149952 39.078896
Gunpowder	Carrol Pt. -76.331471 39.317144	Rickett Pt. -76.296199 39.303619
Magothy	Mountain Pt. -76.433308 39.059024	Point between Deep Creek and Little Magothy River -76.439296 39.052943
Mattawoman	Due south to small point on south shore -77.220231 38.554721	Deep Pt -77.209691 38.566596
Middle	Bobby Pt. -76.384124 39.286393	Pt. below Galloway Creek -76.383548 39.298227
Northeast	Carpenter Pt. -76.002505 39.540888	Red Pt. -75.980135 39.529613
Patapsco	Point east of mouth of Shallow Creek -76.428218 39.203623	Bodkin Pt -76.434181 39.131467
Patuxent	Cove north of Little Kingston Creek -76.495029 38.324216	Pt. Patience -76.483783 38.328544
Piscataway	Directly across from Mockley Pt. -77.044522 38.701979	Mockley Pt. -77.036610 38.710829
Rappahannock	Windmill Pt. -76.280898 37.612785	Stingray Pt. -76.301996 37.562343
Sassafras	Howell Pt. -76.100362 39.372363	Grove Pt. -76.040081 39.389795
Severn	Green Holly Pt -76.452671 38.975953	Mouth of Lake Ogleton -76.455628 38.946140
South	Thomas Pt. -76.466450 38.907887	Saunders Pt. -76.489587 38.888578
WestRhode	Saunders Pt. -76.489930 38.887162	North shore of Jack Creek -76.494016 38.849065
Wicomico	Nanticoke Pt. -75.894019 38.228229	Long Pt. -75.889919 38.203595

Table 2-3. A summary of estuary and drainage basin metrics estimates using various GIS techniques. ND indicates no data available. Asterisk (*) indicates the normal tidal prism based flushing time was modified by a water return factor.

Estuary	Basin Area m ² x10 ⁶	Estuary Volume m ³ x10 ⁶	Estuary Surface Area m ² x10 ⁶	Basin Area: Estuary Area	Basin Area: Estuary Volume	Estuary Average Depth m	Estuary Maximum Depth m	max depth: avg depth	Estuary Mouth Length m	Smooth Shoreline Length m	Smooth Shoreline: Mouth	Shoreline Length m	Shoreline: Mouth	Tidal Prism Flushing Time (Tf) days
Middle	33	33	9	4	1	2	3	2	1315	37601	29	69108	53	3
WestRhode	66	29	15	5	2	2	4	2	4243	34110	8	77063	18	1
Magothy	94	64	19	5	1	3	10	3	851	30651	36	83684	98	6
Corsica	97	10	4	22	10	2	5	3	1501	22458	15	37532	25	4*
Bohemia	131	15	10	13	9	2	7	5	1783	35793	20	56087	31	2
Back	144	25	16	9	6	2	8	5	1443	32878	23	45988	32	3
South	148	57	19	8	3	3	9	3	2936	48513	17	102875	35	6
Piscataway	176	3	3	53	67	1	2	3	1199	10963	9	10826	9	1
Severn	177	109	25	7	2	4	17	4	3319	49876	15	124283	37	10
Northeast	184	24	15	13	8	2	7	4	2294	20503	9	24316	11	1
Sassafras	217	82	30	7	3	3	17	6	5541	51045	9	127704	23	6
Mattawoman	245	9	6	39	27	1	8	6	1607	29572	18	34014	21	4
Bush	336	48	28	12	7	2	11	6	2513	46909	19	66885	27	3
Wicomico	561	52	29	19	11	2	12	7	2757	51021	19	148550	54	ND
Gunpowder	1181	63	38	31	19	2	6	4	3392	50842	15	85809	25	2
Patapsco	1518	451	92	17	3	5	20	4	8026	97541	12	257208	32	6
Choptank	1951	1027	272	7	2	4	26	7	6246	176557	28	860716	138	ND
Patuxent	2343	404	93	25	6	4	40	9	1094	140940	129	342262	313	ND
Rappahannock	6918	1560	367	19	4	4	24	6	5899	275006	47	1038361	176	ND

2-4 Summary of Nutrient Load Characteristics

Nutrient (N and P) loads to the Bay and Bay tributaries are central features of management actions and are, of course, a central feature of Bay ecology. For example, a great deal of attention and effort has been directed towards estimating loads at the fall-line of the major tributary rivers (USGS river input web page) and refining those load estimates (Hirsch *et al.*, 2010). A multi-decade time series is now available from those sites and has been repeatedly examined for various trends. However, nutrient loads and ecosystem responses to loads have not been so intensively examined for the many small tributary rivers of the Bay. In addition, there are virtually no direct measurements of loads to these systems available and we must rely on landscape model results for load estimates (Shenk and Linker, In Press). Direct measurements of point source loads are available for all of the major point sources (mainly Waste Water Treatment Plant discharges).

In this work we have assembled point and non-point (diffuse) total nitrogen (TN), total phosphorus (TP), dissolved inorganic nitrogen (DIN = $\text{NO}_{23} + \text{NH}_4$) and dissolved inorganic phosphorus (DIP = PO_4) loads for seasonal (winter-spring), annual and as an average for the 20 year time series of available load data. Loads reported here do not include direct atmospheric deposition of N or P to the surface waters of these systems (atmospheric deposition to the watersheds are accounted for in the diffuse load estimates) and we were not able to make any quantitative adjustments to loads coming from the mainstem Bay. In some cases loads from the Bay to tributaries may be significant (Boynton *et al.*, 2008) but an accounting of these exchanges is not available for the tributaries included in this work.

Annual average loads (TN, TP, DIN, DIP) for the 20 year time series were organized using landscape model results and point source data (Figure 2-3a-s). In this selection of relatively small Chesapeake Bay tributaries N and P loads ranged from very high (Bush, Patapsco, Piscataway and Back Rivers) to quite low (West and Rhode, Middle and South Rivers) when the loads were expressed on an areal basis (loads prorated over the surface area of each estuary and expressed as $\text{g N or P m}^{-2} \text{ yr}^{-1}$). In addition, there were some remarkable temporal trends evident in these load data. For example, the Back, Piscataway, Patapsco, Mattawoman and Magothy Rivers all showed decreasing loads of N or both N and P and much of these load reductions appeared to be associated with WWTP upgrades (Fig. 2-3 a, b, c, g, n). Others, including the Bush, Northeast, Rappahannock, Choptank, South, Middle, and Rhode and West Rivers, showed increasing loads of N, P or both nutrients (Fig. 2-3 d, j, m, p, q, r, s). Finally, at all sites there was considerable inter-annual variability to estimated N and P loads. However, at most sites the most variable load was TP followed by TN. Inter-annual variability was noticeably less for both DIN and DIP loads. At virtually all sites the largest TN and TP loads were associated with the wet years, particularly 1989, 1996 and 2003. There was about a factor of 40 and 22 differences between the highest (Back River) and lowest (Rhode and West Rivers) TN and TP loading rates among the 19 systems considered. The range of TN and TP loading rates observed in this selection of Chesapeake Bay tributaries is almost as large as the range in loading reported by Boynton *et al.* (2008) for a much larger global selection of estuaries.

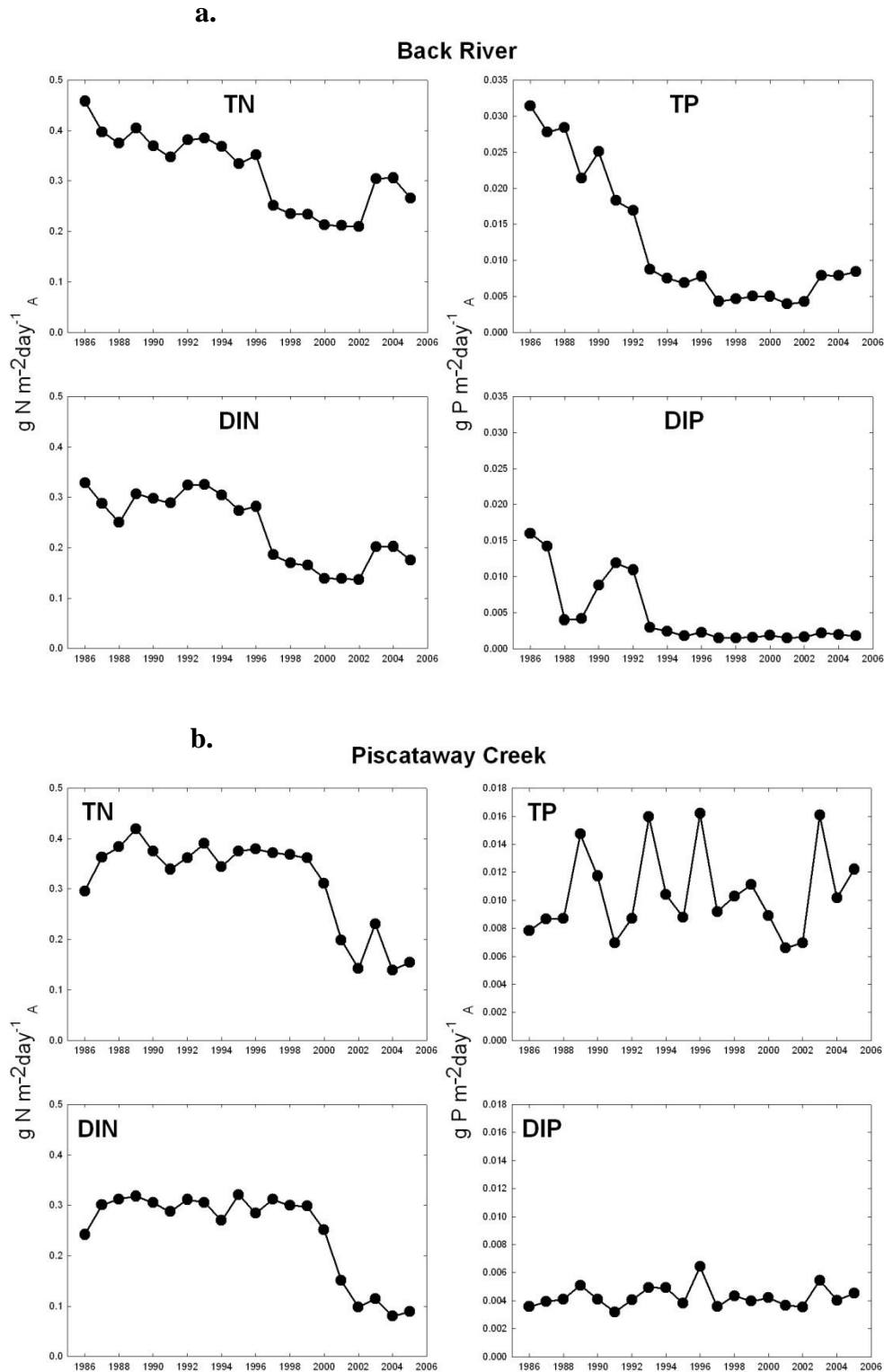
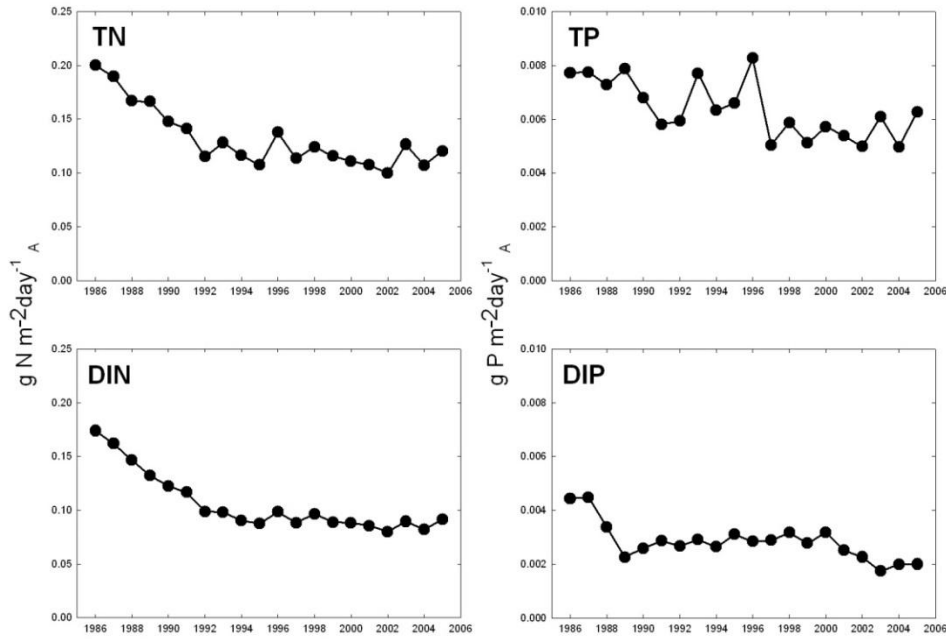


Figure 2-3. a-s. Time-series plots of average annual nutrient loads to tributary estuaries of Chesapeake Bay. Annual loads are expressed as $g N m^{-2} day^{-1}$ and can be converted to annual loads by multiplying values by 365. These loads include both point and diffuse sources but do not include direct deposition of N or P to the surface waters of these systems. Net nutrient exchanges with Chesapeake Bay and these systems is also not included (data for this not available).

c.

Patapsco River



d.

Bush River

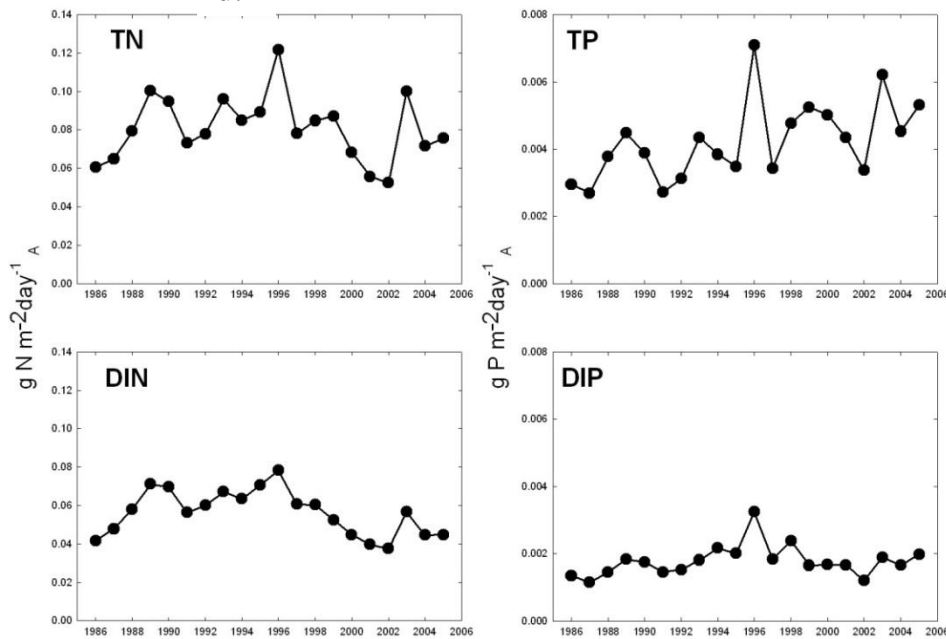
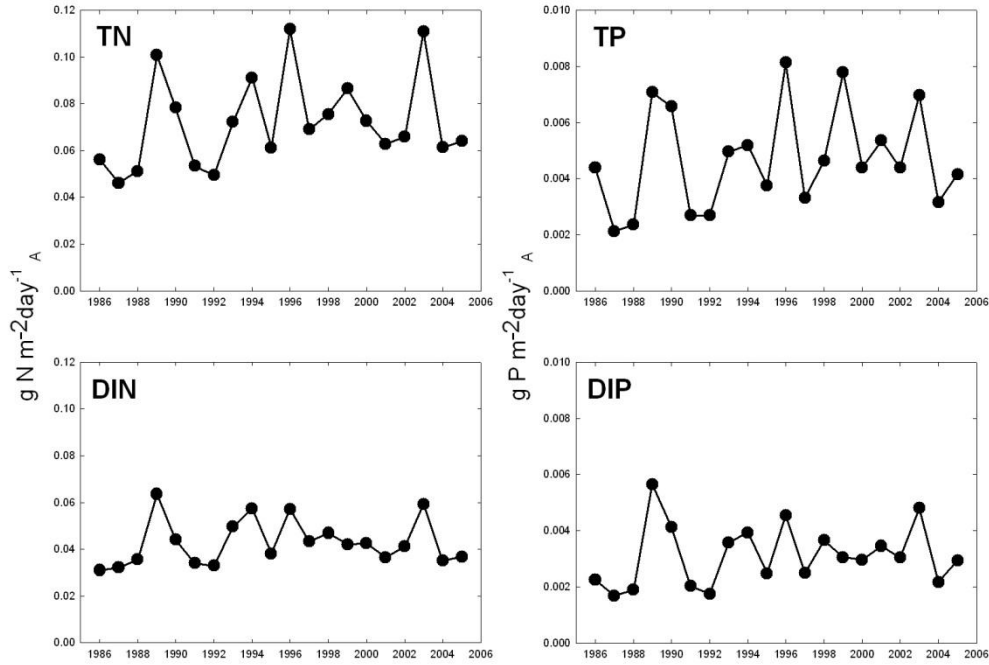


Figure 2-3 a-s. Time-series plots of average annual nutrient loads to tributary estuaries of Chesapeake Bay. Annual loads are expressed as $g N m^{-2} day^{-1}$ and can be converted to annual loads by multiplying values by 365. These loads include both point and diffuse sources but do not include direct deposition of N or P to the surface waters of these systems. Net nutrient exchanges with Chesapeake Bay and these systems is also not included (data for this not available).

e.

Corsica River



f.

Wicomico River

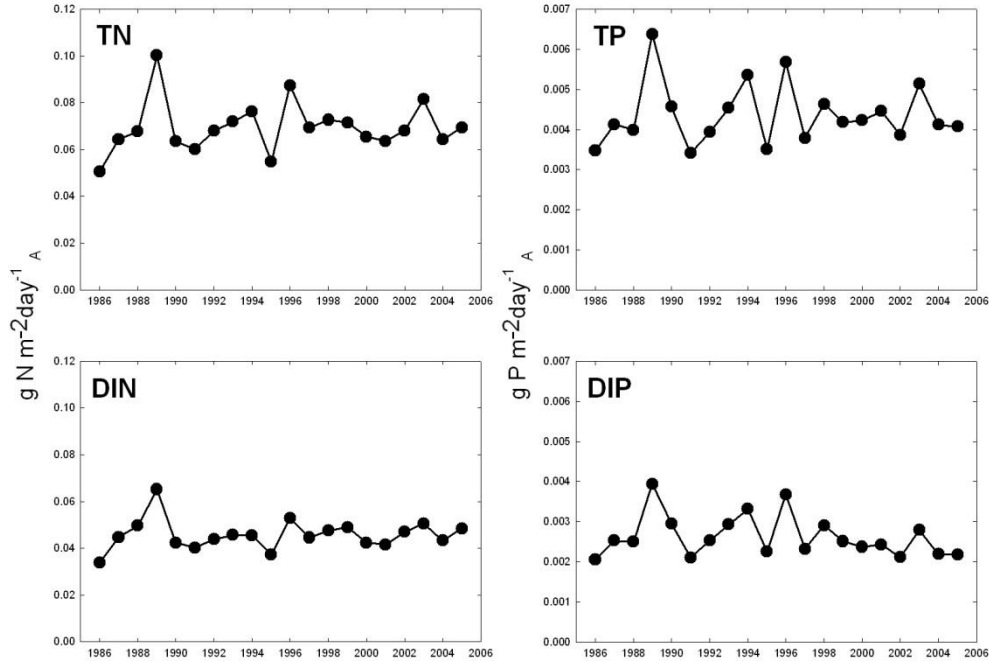


Figure 2-3 a-s. Time-series plots of average annual nutrient loads to tributary estuaries of Chesapeake Bay. Annual loads are expressed as $g N m^{-2} day^{-1}$ and can be converted to annual loads by multiplying values by 365. These loads include both point and diffuse sources but do not include direct deposition of N or P to the surface waters of these systems. Net nutrient exchanges with Chesapeake Bay and these systems is also not included (data for this not available).

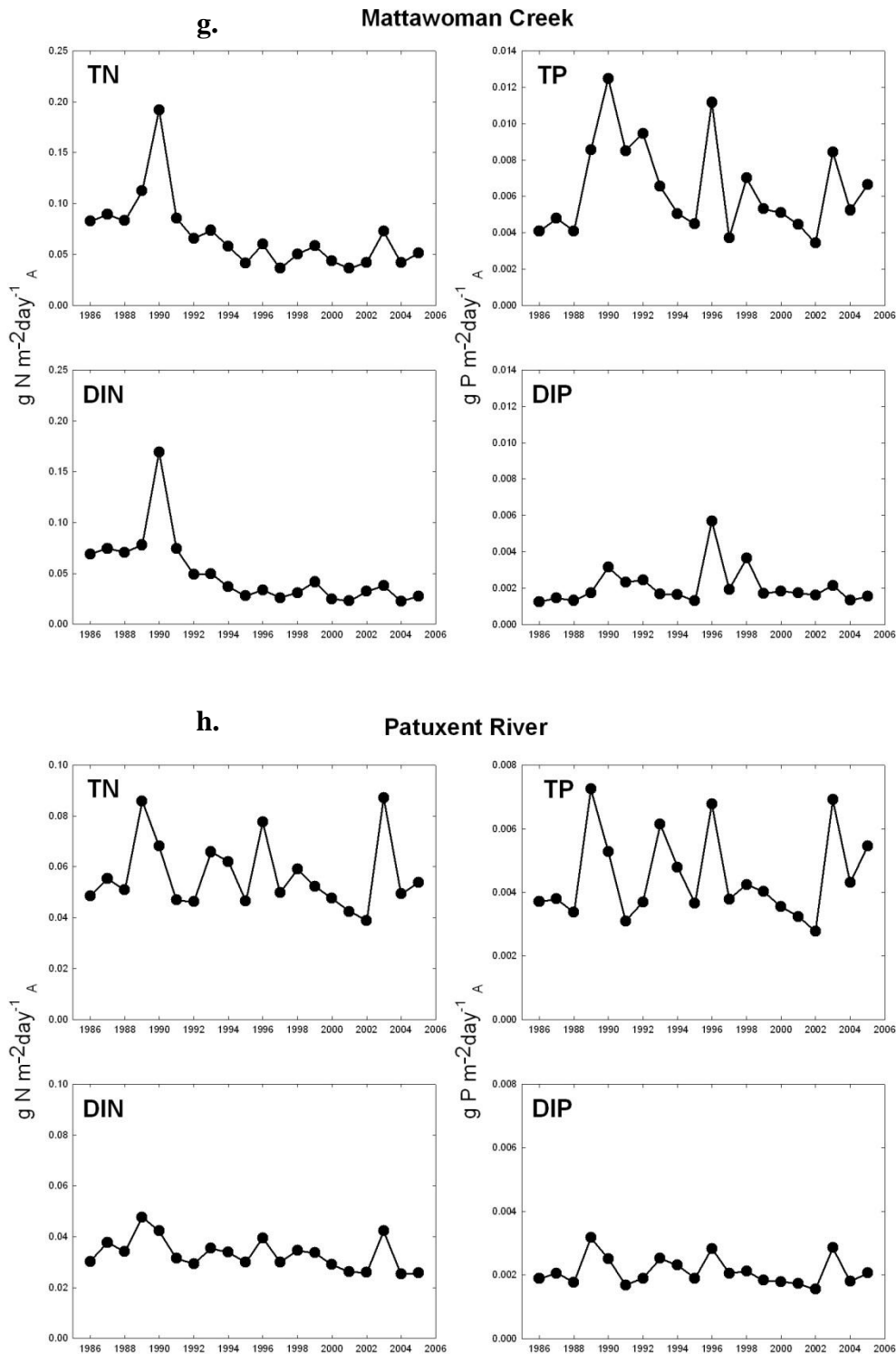


Figure 2-3 a-s. Time-series plots of average annual nutrient loads to tributary estuaries of Chesapeake Bay. Annual loads are expressed as $g\ N\ m^{-2}\ day^{-1}$ and can be converted to annual loads by multiplying values by 365. These loads include both point and diffuse sources but do not include direct deposition of N or P to the surface waters of these systems. Net nutrient exchanges with Chesapeake Bay and these systems is also not included (data for this not available).

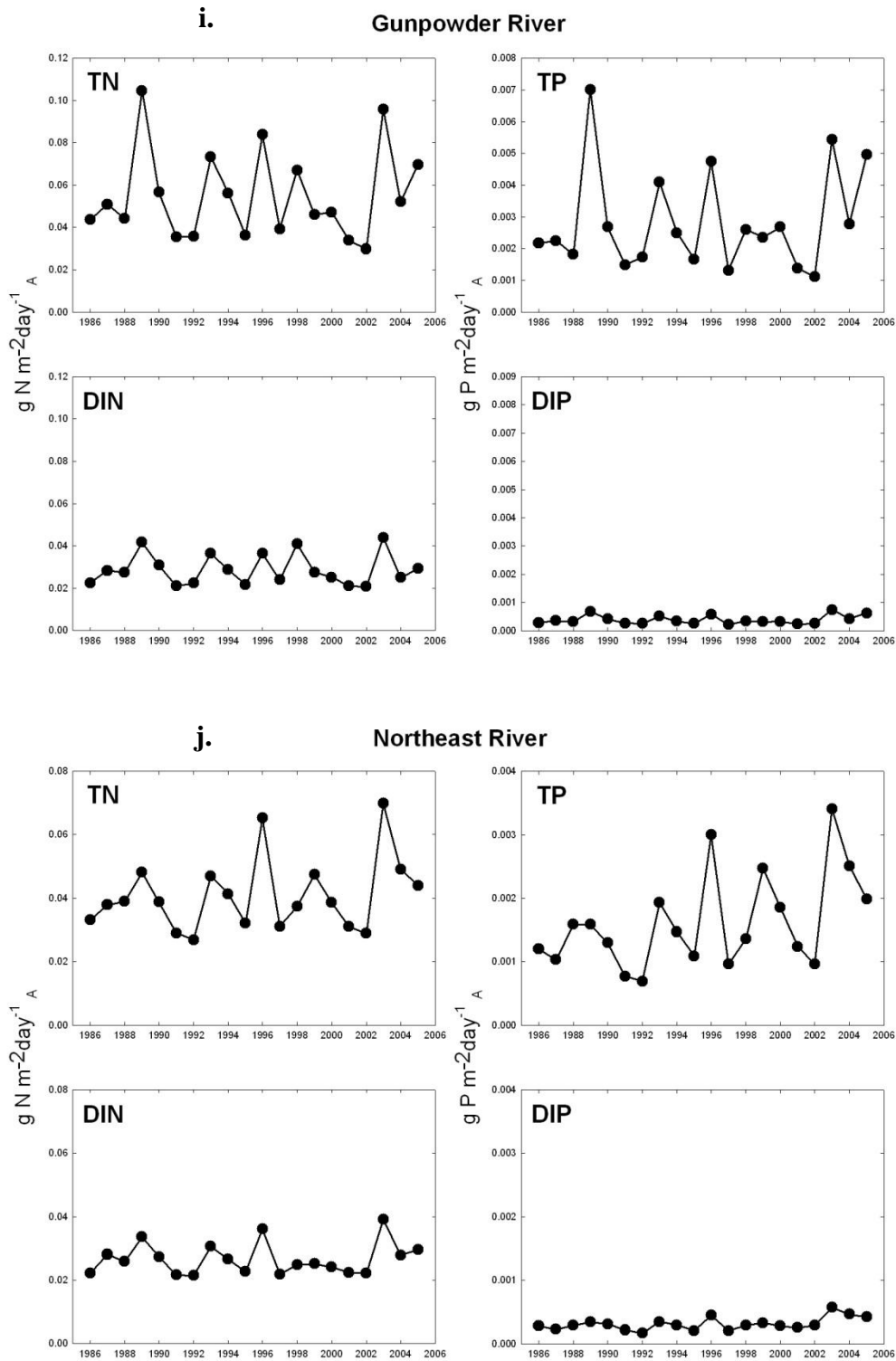


Figure 2-3 a-s. Time-series plots of average annual nutrient loads to tributary estuaries of Chesapeake Bay. Annual loads are expressed as $g\ N\ m^{-2}\ day^{-1}$ and can be converted to annual loads by multiplying values by 365. These loads include both point and diffuse sources but do not include direct deposition of N or P to the surface waters of these systems. Net nutrient exchanges with Chesapeake Bay and these systems is also not included (data for this not available).

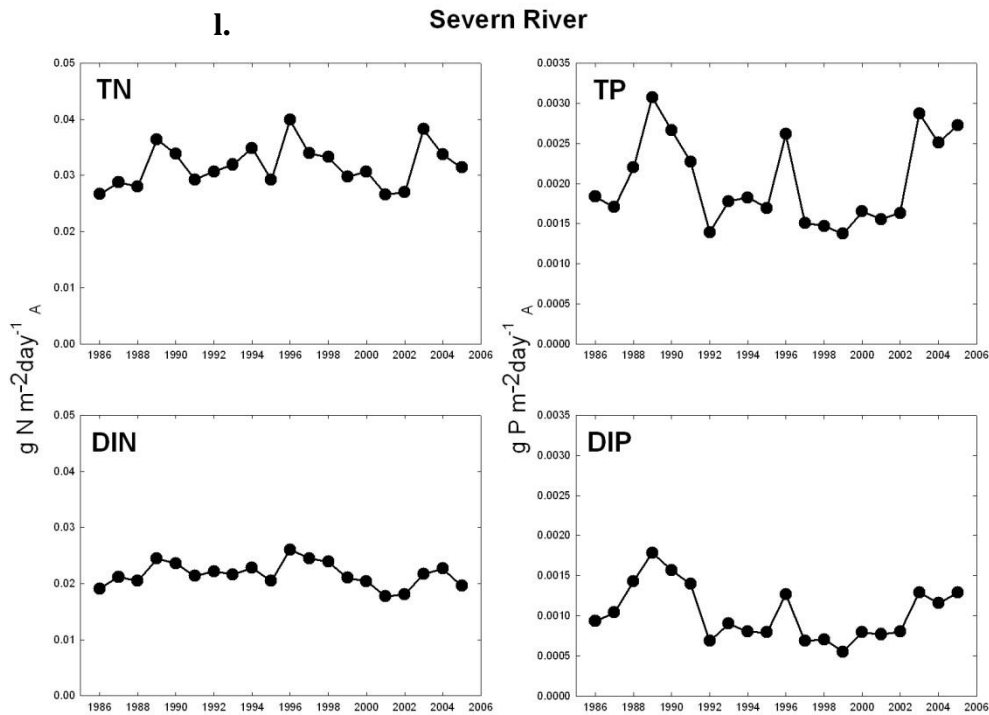
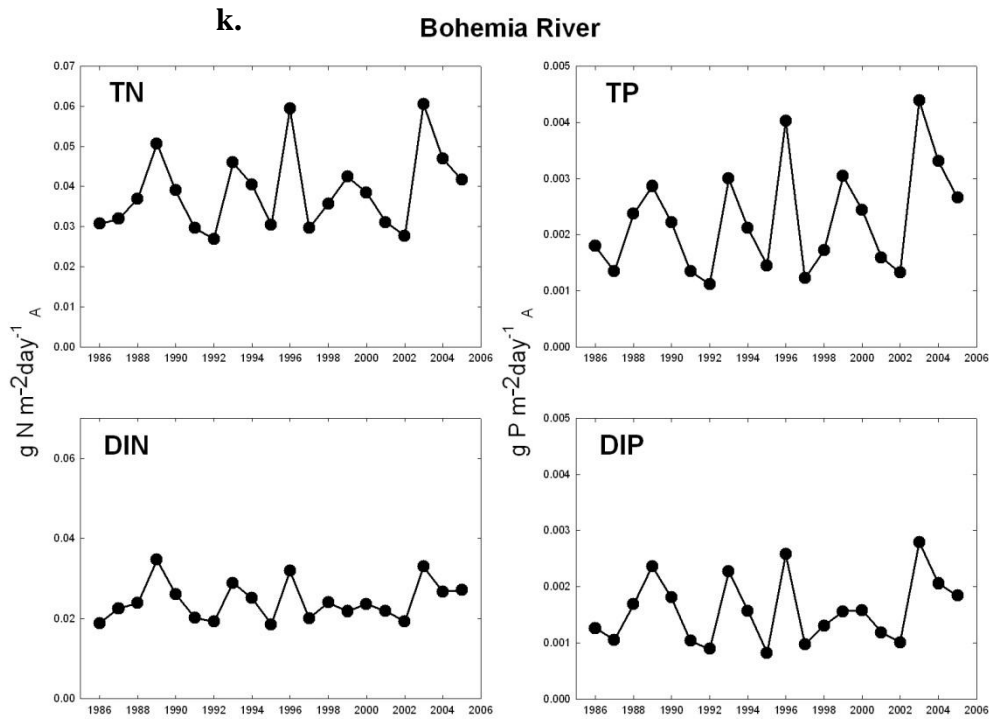


Figure 2-3 a-s. Time-series plots of average annual nutrient loads to tributary estuaries of Chesapeake Bay. Annual loads are expressed as $\text{g N m}^{-2} \text{day}^{-1}$ and can be converted to annual loads by multiplying values by 365. These loads include both point and diffuse sources but do not include direct deposition of N or P to the surface waters of these systems. Net nutrient exchanges with Chesapeake Bay and these systems is also not included (data for this not available).

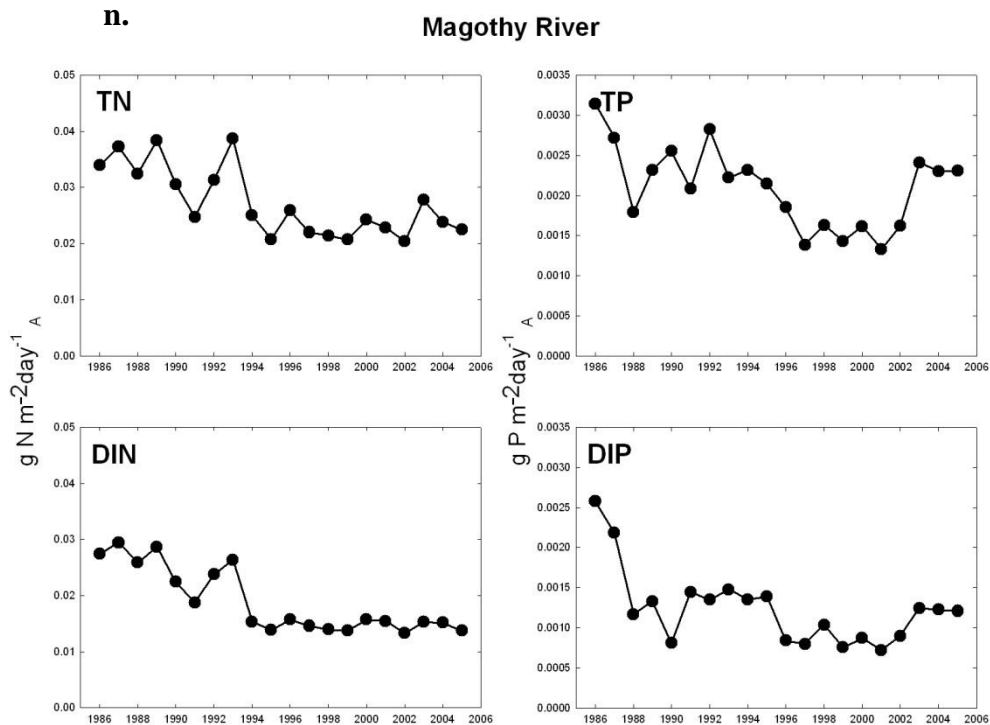
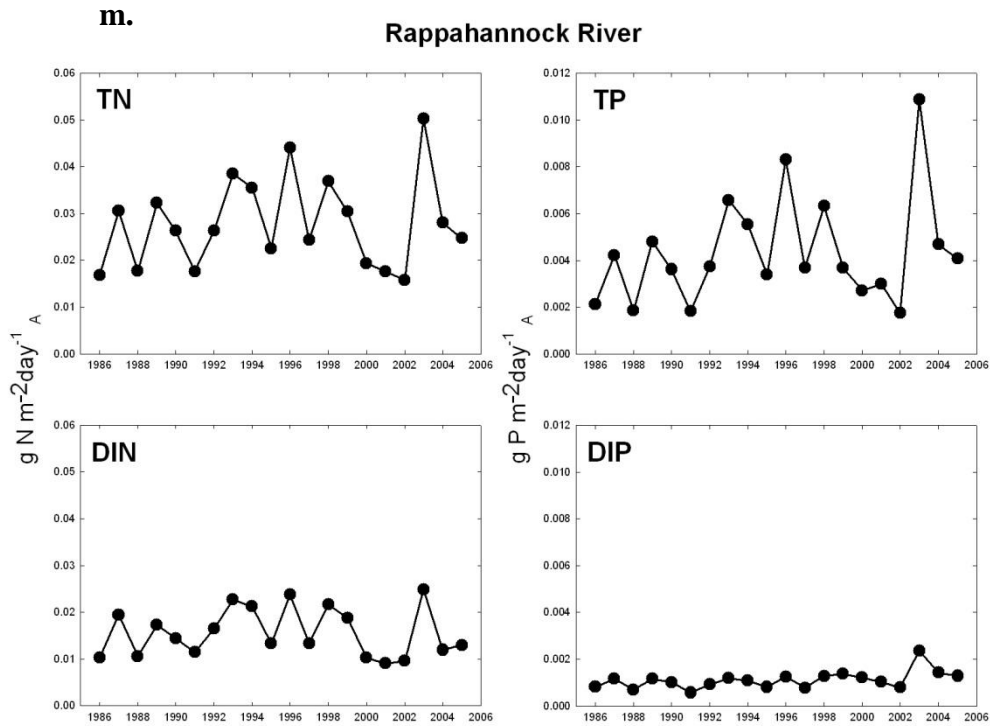


Figure 2-3 a-s. Time-series plots of average annual nutrient loads to tributary estuaries of Chesapeake Bay. Annual loads are expressed as $\text{g N m}^{-2} \text{day}^{-1}$ and can be converted to annual loads by multiplying values by 365. These loads include both point and diffuse sources but do not include direct deposition of N or P to the surface waters of these systems. Net nutrient exchanges with Chesapeake Bay and these systems is also not included (data for this not available).

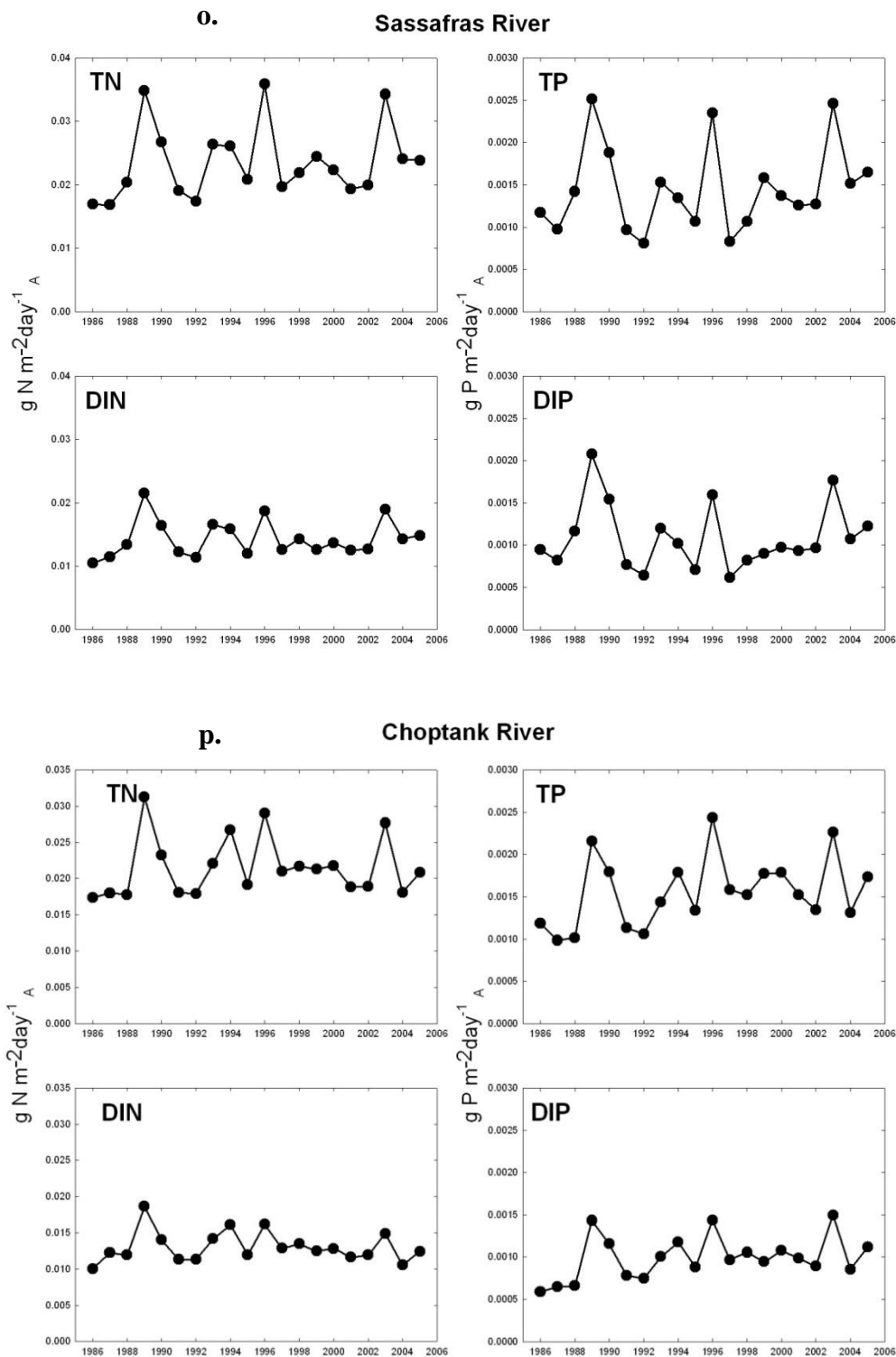


Figure 2-3 a-s. Time-series plots of average annual nutrient loads to tributary estuaries of Chesapeake Bay. Annual loads are expressed as $g\ N\ m^{-2}\ day^{-1}$ and can be converted to annual loads by multiplying values by 365. These loads include both point and diffuse sources but do not include direct deposition of N or P to the surface waters of these systems. Net nutrient exchanges with Chesapeake Bay and these systems is also not included (data for this not available).

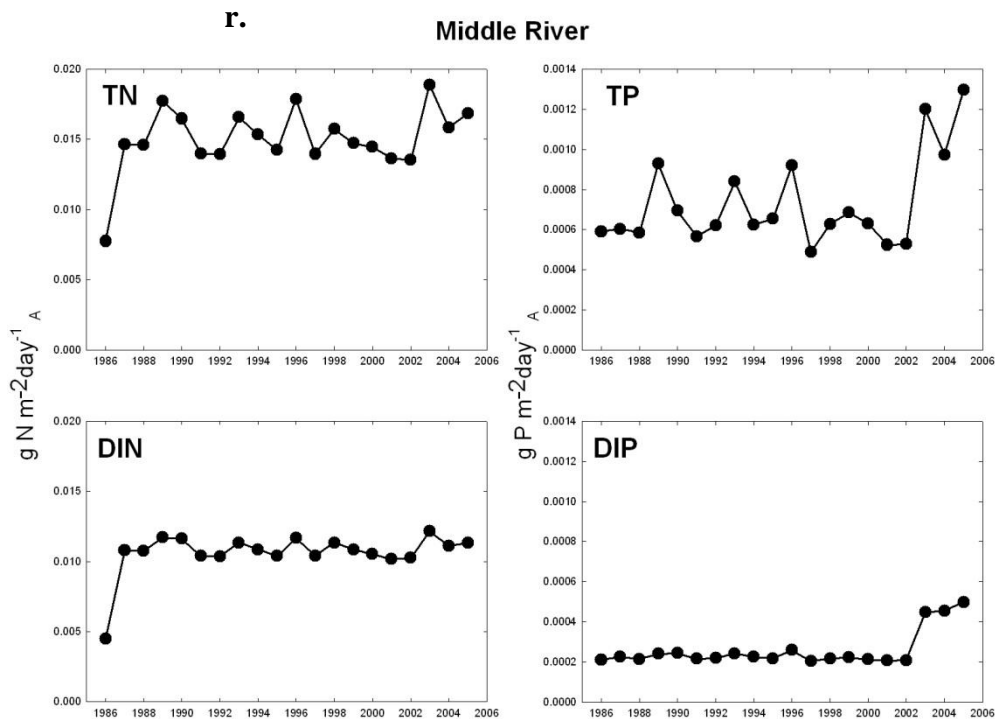
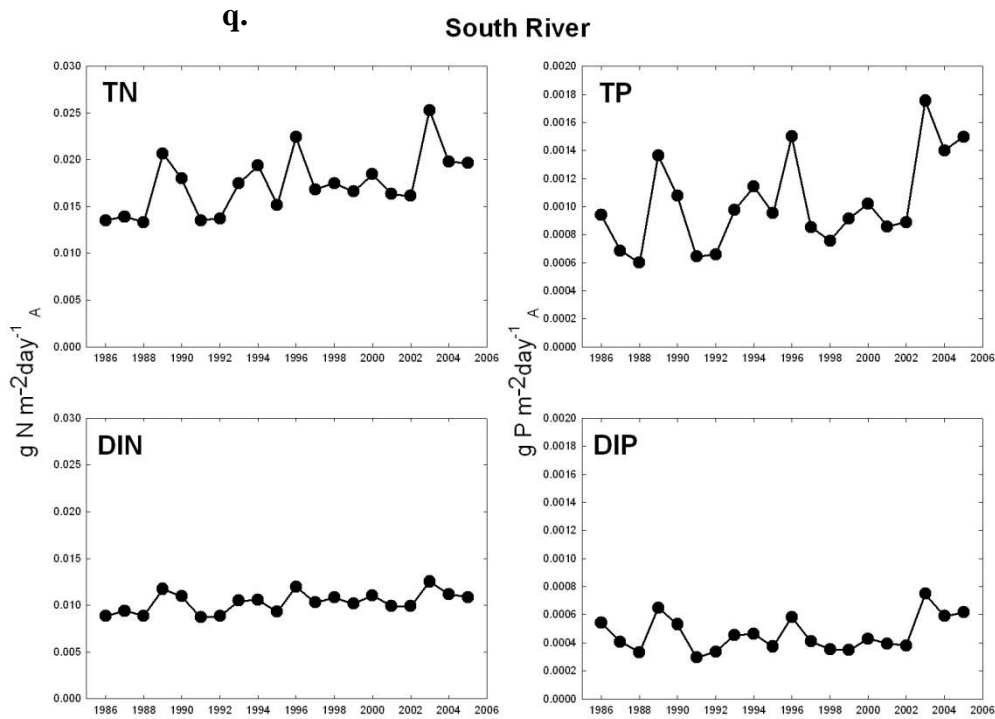


Figure 2-3 a-s. Time-series plots of average annual nutrient loads to tributary estuaries of Chesapeake Bay. Annual loads are expressed as $\text{g N m}^{-2} \text{day}^{-1}$ and can be converted to annual loads by multiplying values by 365. These loads include both point and diffuse sources but do not include direct deposition of N or P to the surface waters of these systems. Net nutrient exchanges with Chesapeake Bay and these systems is also not included (data for this not available).

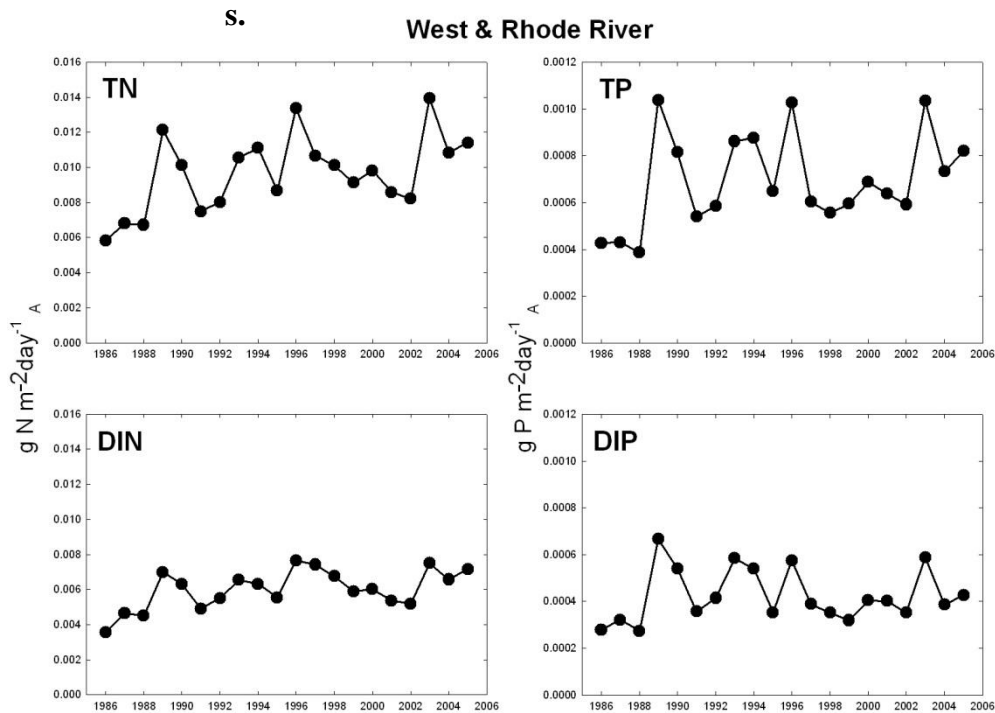


Figure 2-3 a-s. Time-series plots of average annual nutrient loads to tributary estuaries of Chesapeake Bay. Annual loads are expressed as $\text{g N m}^{-2} \text{ day}^{-1}$ and can be converted to annual loads by multiplying values by 365. These loads include both point and diffuse sources but do not include direct deposition of N or P to the surface waters of these systems. Net nutrient exchanges with Chesapeake Bay and these systems is also not included (data for this not available).

We have also computed 20 year average loads of TN and TP for all these systems (Fig. 2-4 a-b). In this case, it is clear that there are a few very heavily loaded systems (Back, Piscataway, and Patapsco) for TN and several additional sites (Bush, Corsica, Wicomico, Mattawoman, Patuxent and Gunpowder) for TP. In addition, the most heavily loaded systems are those with substantial point source loads in most, but not all cases, and loads of TN and TP in those systems are currently being reduced via upgrades to WWTP operations. Finally, water quality conditions are not always directly proportional to nutrient loading rates. Other factors come into play making this relationship more complex. For example, loads of N and P to Boston Harbor were very large (Boynton and Kemp 2008) but water quality conditions were not as degraded as they are in many of the tributaries of the Bay even though those tributaries have lower N and P loading rates. In this and other instances (e.g., Narragansett Bay) the far faster flushing times of these other systems reduces the water quality impact of large nutrient loads. Nevertheless, very poor water quality conditions are rarely associated with low N and P loading rates and poor water quality conditions are often, but not always, associated with large N and P loads. In the analyses reported later in this chapter we make an effort to account for factors such as water clarity, water residence time and estuarine morphology that play a role in the effectiveness of N and P loads on estuarine water quality.

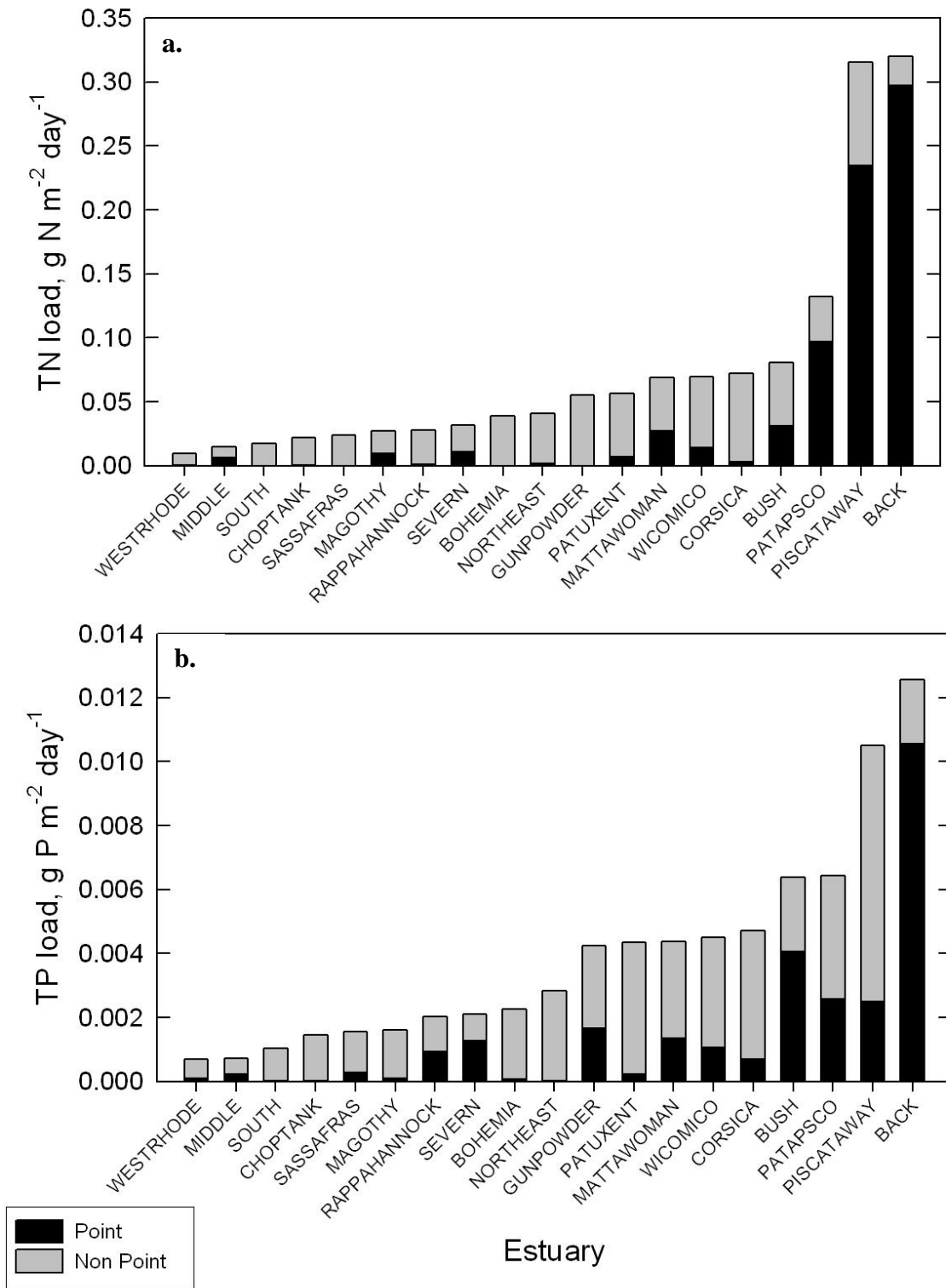


Figure 2-4 a-b Bar graphs showing 20 year average nutrient loads to the tributary estuaries considered in this analysis. Point and diffuse (also referred to as Non-Point) loads are indicated. Definitions of loads are as in Figure 2-3.

Finally, we also examined the relative amounts of N and P entering these 19 tributary systems using both 20 year average loads and annual average N and P loads for the 20 year time-series (Fig. 2-5 a-b). The Redfield Ratio is also indicated in these figures as a dashed line (computed on a weight rather than a mole basis). The relevance of showing the Redfield Ratio line is that it serves as an indication of the relative abundance of N and P relative to phytoplanktonic needs. High N:P ratios in loads indicate that P would be depleted before N assuming that any nutrient becomes limiting and the opposite for low N:P load ratios. In almost all cases, N:P ratios were either slightly above the Redfield Ratio or greatly in excess of this ratio. Tributaries with relatively low areal N and P loads generally had the lowest N:P load ratios while those tributaries with much higher areal N and P loads (e.g., Back, Piscataway and Patapsco Rivers) had high to very high N:P load ratios. In some cases (e.g., Patuxent and Back Rivers) where in the past point sources were important parts of the nutrient loads, P removal at WWTPs pre-dated N removal and this contributed to very high N:P load ratios. These N:P load ratios that exceed the Redfield Ratio, often by a large margin, would suggest importance for P-limitation of phytoplankton communities. However, both mesocosm studies (D'Elia *et al.*, 2003) and bioassay work (Fisher *et al.*, 1999) in the Bay and tributaries indicate that the nutrient limitation situation is more complex with P being limiting during winter in the freshwater and low salinity portions of the Bay and N being limiting during late spring through fall in most regions of the Bay. These studies played a central role in the Bay Program adopting a duel (both N and P) nutrient reduction strategy.

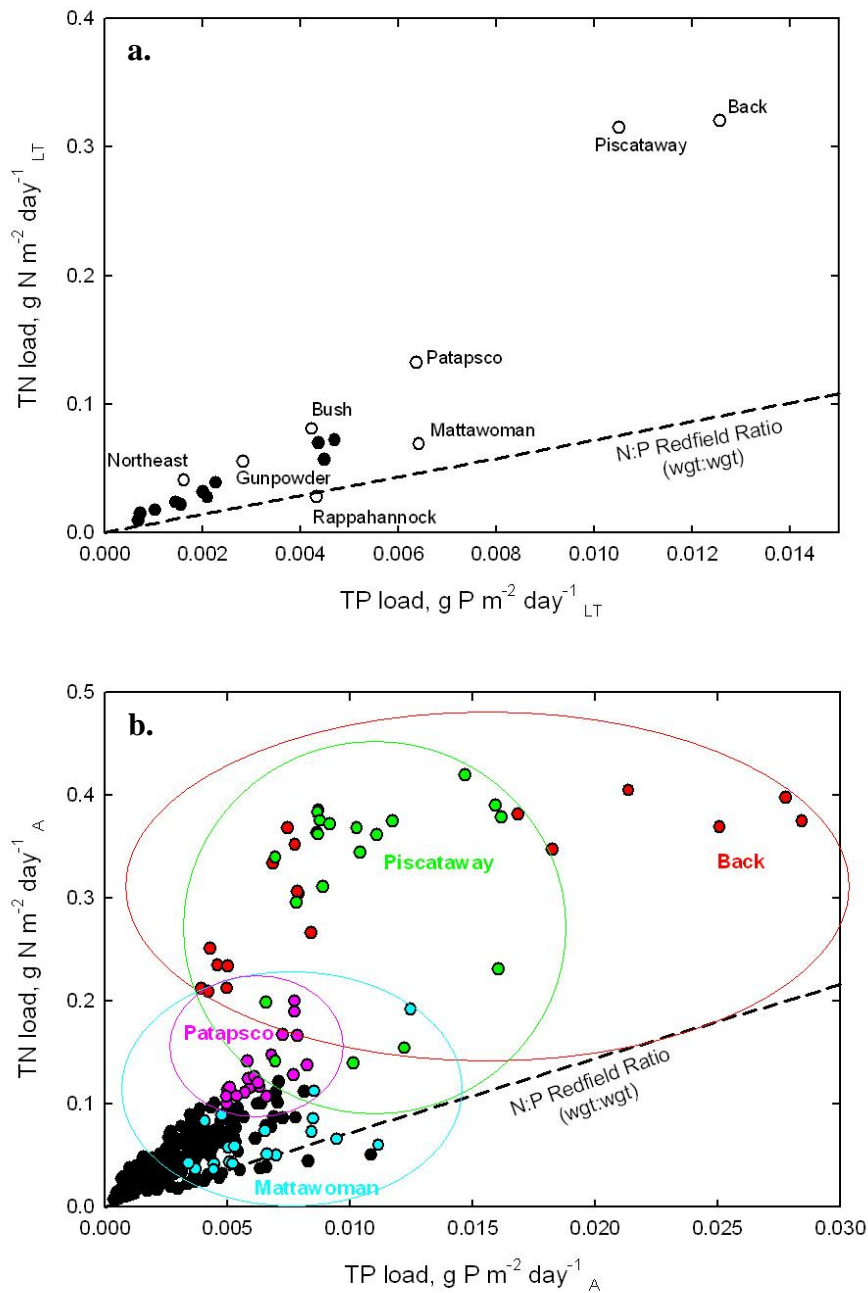


Figure 2-5 a-b. Scatter plot of TP versus TN loads using the 20 year average loads (a) and individual annual loads (b) for the tributary systems used in this analysis. The dashed line represents the Redfield Ratio (weight:weight in this case; balanced ratio = 7.2). Definitions of loads are as in Figure 2-3. Note scale changes on the x and y axes.

2-5 Water Quality Characteristics

Water quality data were also organized in 20 year averages for each of the 19 sites. These long-term averages and frequency histograms of water quality data are shown in Figure 2-6 a-h. The

purpose of organizing these data is to use these for developing linkages between external loads of N and P and in-situ water quality conditions.

2-5.1 Temperature

Based on a 20 year average there were only small differences in surface water temperature (Fig. 2-6a). Twelve of the 19 sites had average temperatures between 16-18 C and only two (Corsica and Piscataway) had average temperatures in excess of 18 C. It is not clear why these two systems exhibited higher temperatures; other small and shallow tributaries (e.g., West/Rhode, Sassafra and others) had lower average temperature regimes.

2-5.2 Salinity

As expected, there was a very large range in long-term average salinity conditions (Fig. 2-6b). Ten of the systems had salinities associated with mesohaline conditions, six with lower salinities associated with oligohaline conditions and 3 had salinities typical of tidal freshwater conditions. However, there are also indications (e.g., standard deviations in Fig. 2-6b) that some of these systems “switch” salinity classifications associated with particularly wet or dry years. It is safe to assume that large salinity changes exerted strong influences on such system characteristics as phytoplankton community composition and biogeochemical processes associated with nutrient recycling.

2-5.3 Dissolved Nutrient Concentrations

Concentrations of three key dissolved nutrients were included in this analysis (NO_{23} , NH_4 and PO_4) and long-term concentrations for these nutrients for all 19 sites are shown in Figure 2-6c (all on log scales). There was over an order of magnitude difference in NO_{23} concentrations among the 19 sites ranging from about 0.1 to 2 mg N L⁻¹. Compared with NO_{23} concentrations observed in a wider selection of estuaries from other locations NO_{23} concentrations in this suite of Chesapeake Bay tributaries were all either high or very high (Boynton and Kemp 2008). Long-term average concentrations at all sites were above what is commonly considered to be rate-limiting concentrations (~0.035 mg L⁻¹; Parsons *et al.*, 1984; Sarthou *et al.*, 2005); during summer periods at some sites NO_{23} concentrations did decrease to rate-limiting concentrations.

Long-term average concentrations of NH_4 were generally an order of magnitude lower than those of NO_{23} at the 19 sites examined (Fig. 2-6d). Most sites had concentrations between 0.05 -0.10 mg N L⁻¹ which are above what are considered to be rate-limiting concentrations.

Long-term average concentrations of PO_4 ranged from 0.01 to 0.05 mg L⁻¹ and were typical values for estuarine ecosystems (Boynton and Kemp 2008). Long-term average differences in PO_4 concentration were less than those observed for either NO_{23} or NH_4 (Fig. 2-6e). It is interesting to note that those few systems exhibiting enhanced long-term average PO_4 concentrations all had significant point source nutrient inputs.

As indicated earlier for nutrient inputs, there was also a very large range in long-term average in-situ dissolved nutrient N:P ($\text{NO}_{23} + \text{NH}_4/\text{PO}_4$) ratios (Fig 6f). Long-term ratios ranged from about 12 to almost 200 among the 19 systems examined. Only one system (Patuxent) had in-situ N:P ratios less than the Redfield Ratio; all the rest had elevated ratios (8 sites) or very elevated ratios (10 sites). Because PO_4 concentrations did not vary a great deal between sites (e.g., long-term average concentrations were about 0.01 mgP L^{-1} at 14 of the 19 sites) most of the variation in the N:P ratio was driven by differences in DIN concentrations among sites. In addition, 9 of the 10 sites with the highest long-term average N:P ratios were in the tidal freshwater or oligohaline salinity zones. In these areas of the Bay (frequently close to riverine nutrient sources) DIN concentrations are typically elevated ($>1 \text{ mgN L}^{-1}$) and contribute to the high N:P ratios observed.

2-5.4 Water Clarity

Long-term average water clarity conditions (represented by Secchi disk depths) are shown for the 19 sites in Figure 2-6g. Average depths ranged from about 0.35 m (Back River) to slightly greater than 1 m (Severn, Magothy, South and Choptank Rivers). Fifteen of the 19 sites had long-term average Secchi disk depths less than 1 m. In general, all of these systems have limited water clarity, some more than others. To put these Secchi disk values in perspective, we can use water clarity requirements for mesohaline Submerged Aquatic Vegetation (SAV) and their light requirements. In general about 30% of surface radiation needs to reach the bottom for robust SAV growth. If that is the case and average water depth in the near-shore zones of these tributaries is about 1.5 m, a Secchi disk value of about 1.1 m is needed to assure 30% of surface light reaches the bottom. Only 3 of the 19 systems examined had Secchi disk depths in excess of this value and this supports the general conclusion that these are currently very turbid systems.

2-5.5 Chlorophyll-*a* Concentration

There was a very large range in long-term average chlorophyll-*a* concentrations among the 19 sites examined (Fig. 2- 6h). Only 4 sites (Choptank, Wicomico, Rappahannock, and Piscataway) had long-term concentrations less than $15 \mu\text{g L}^{-1}$ while 9 sites had concentrations between 15 and $30 \mu\text{g L}^{-1}$. Six sites had very high chlorophyll-*a* concentrations exceeding $30 \mu\text{g L}^{-1}$ during the 20 year evaluation period (Bohemia, Bush, Northeast, Sassafrass, Corsica and Back Rivers). It is interesting to note that all of the sites having sustained high chlorophyll-*a* concentrations are located in the upper Bay region and all are either tidal freshwater or oligohaline sites.

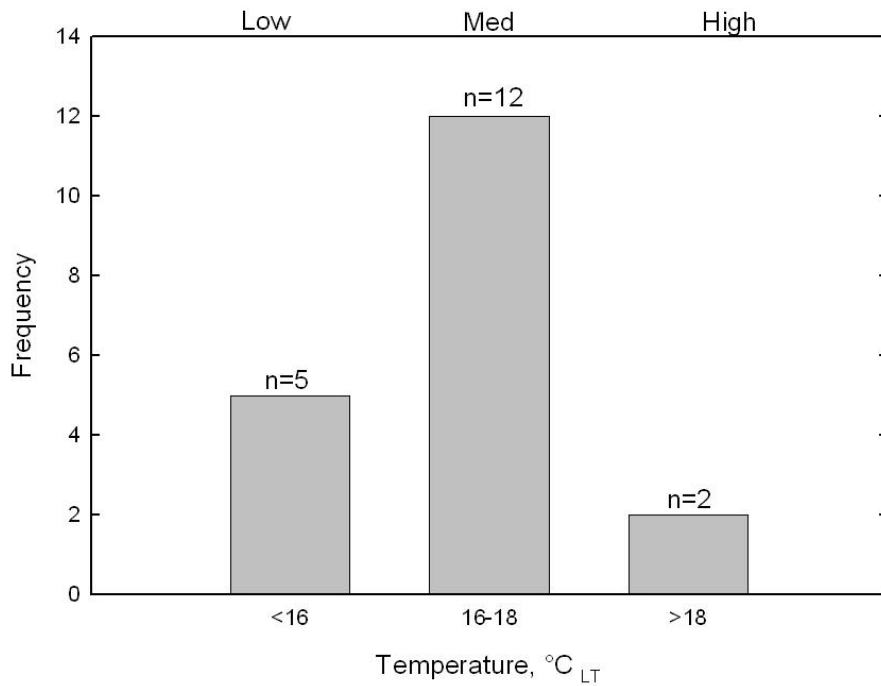
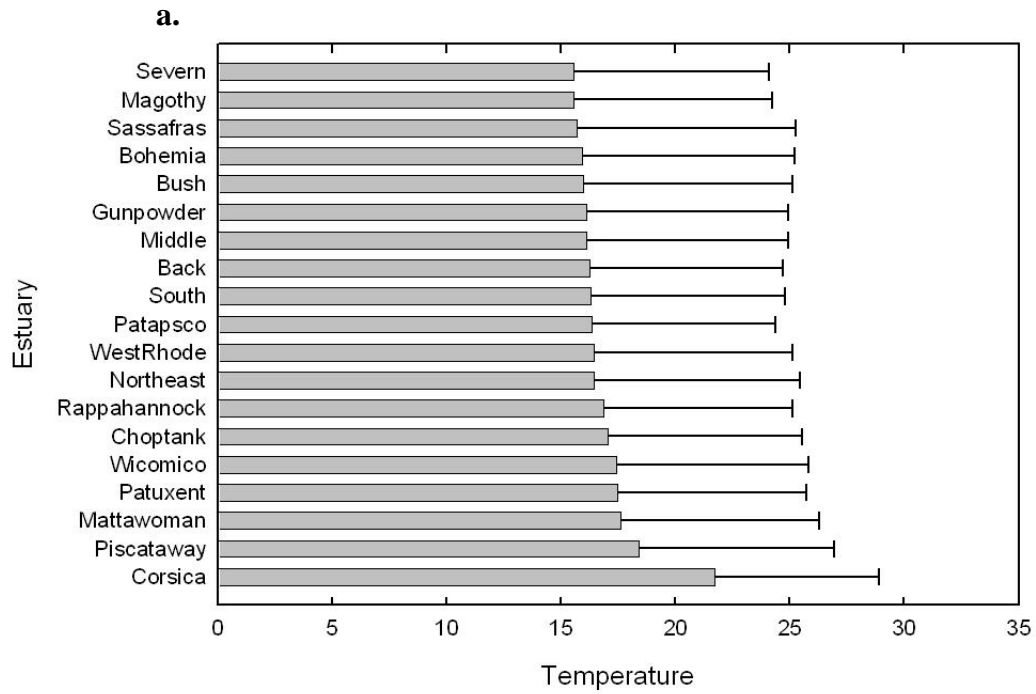
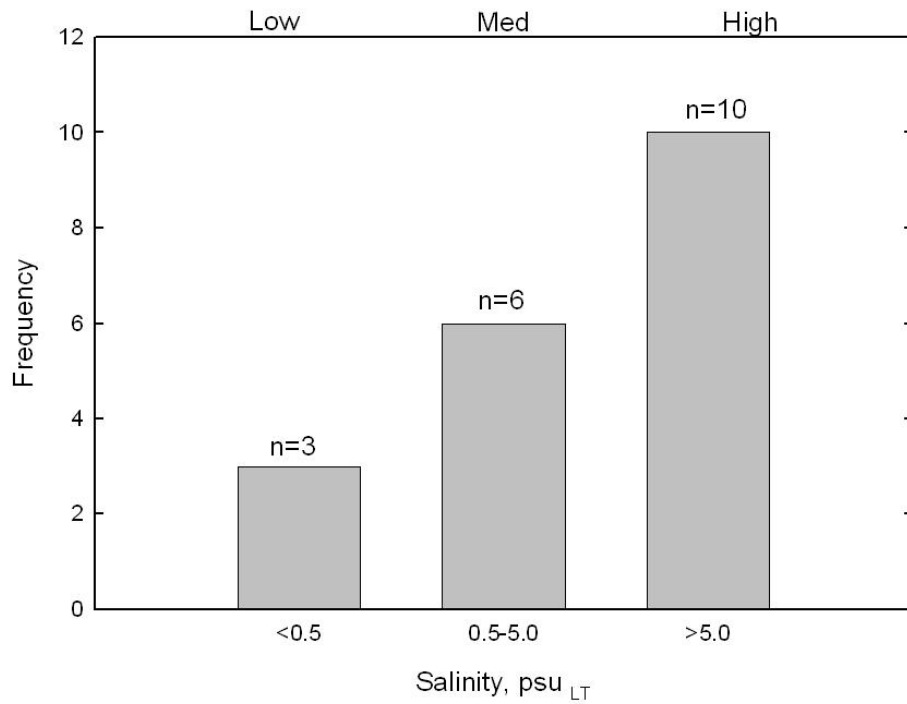
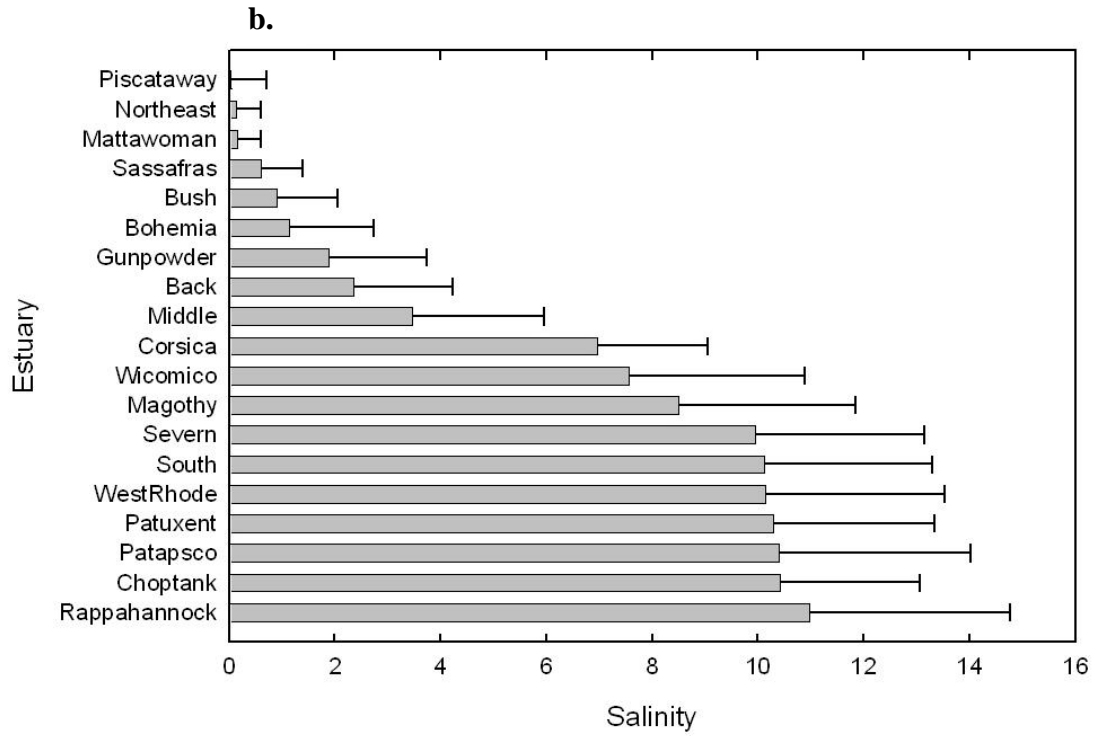
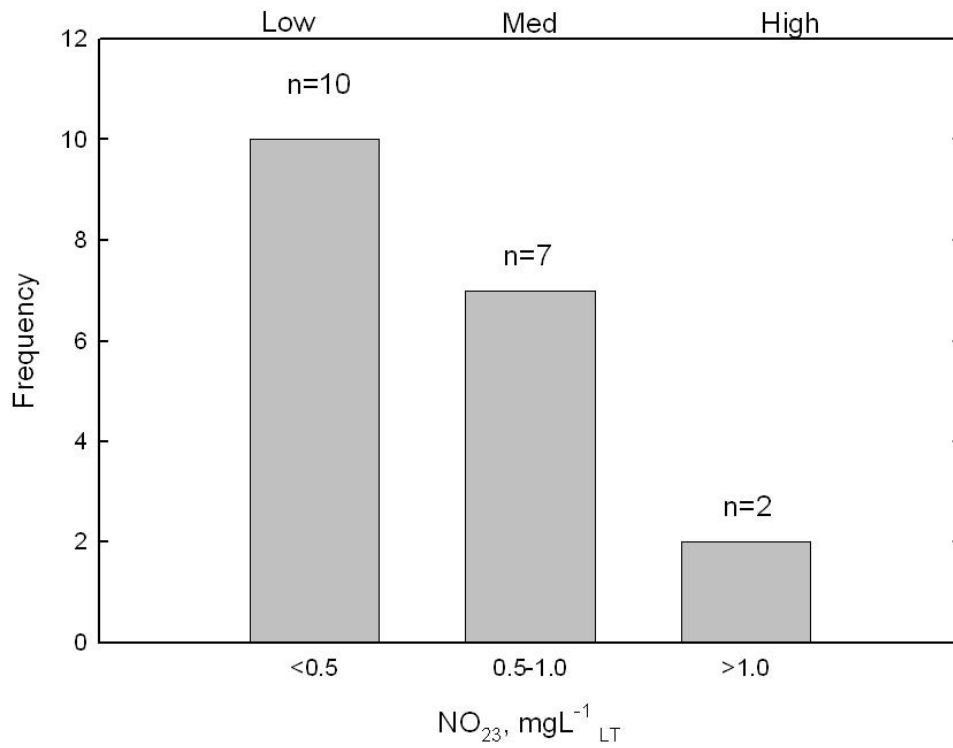
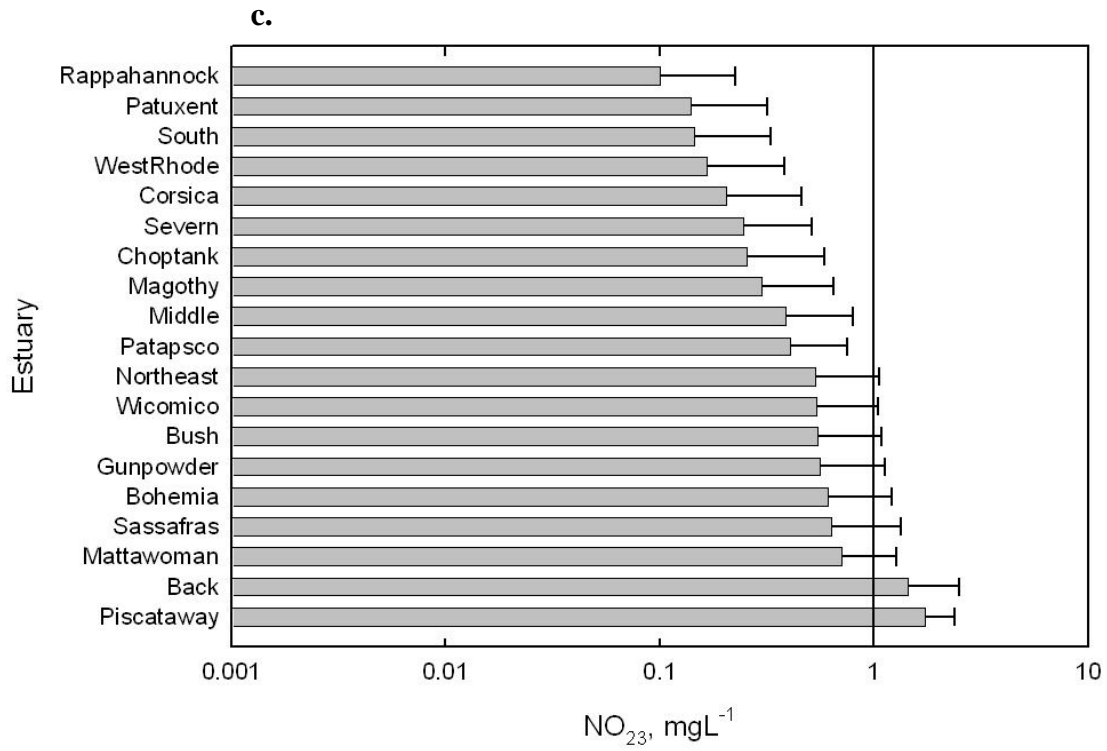
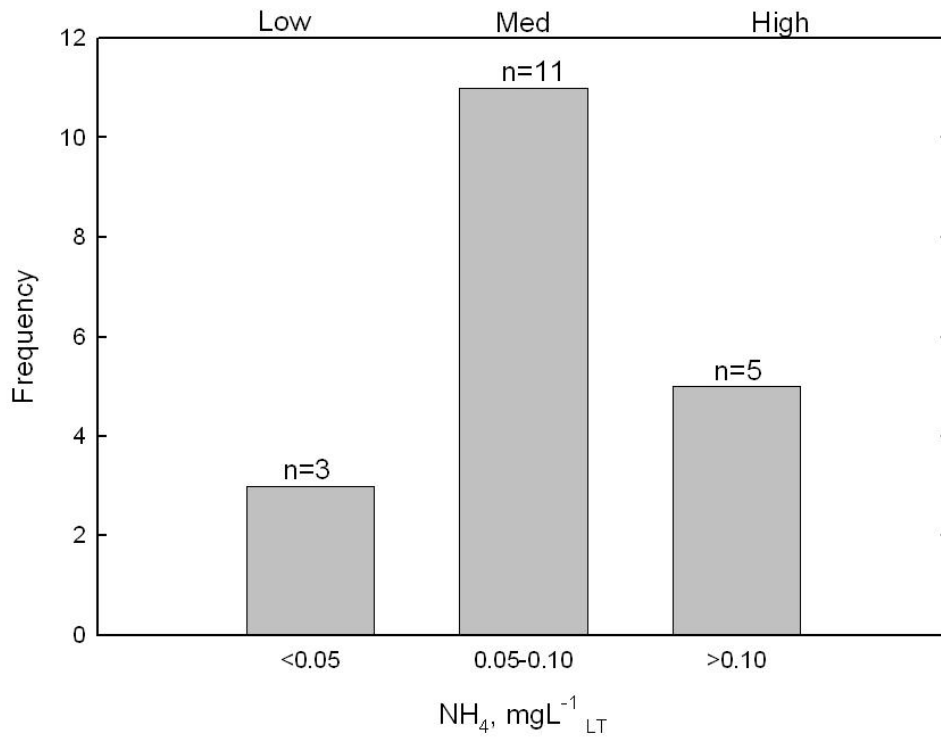
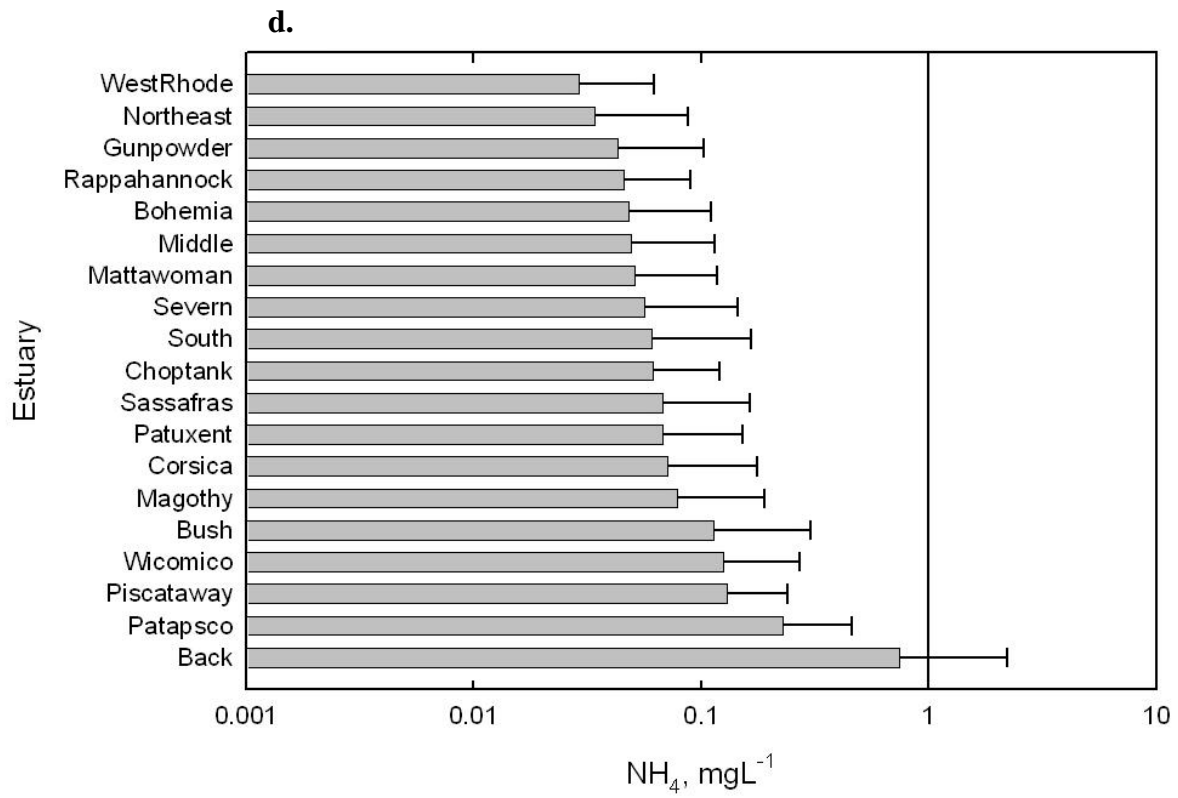
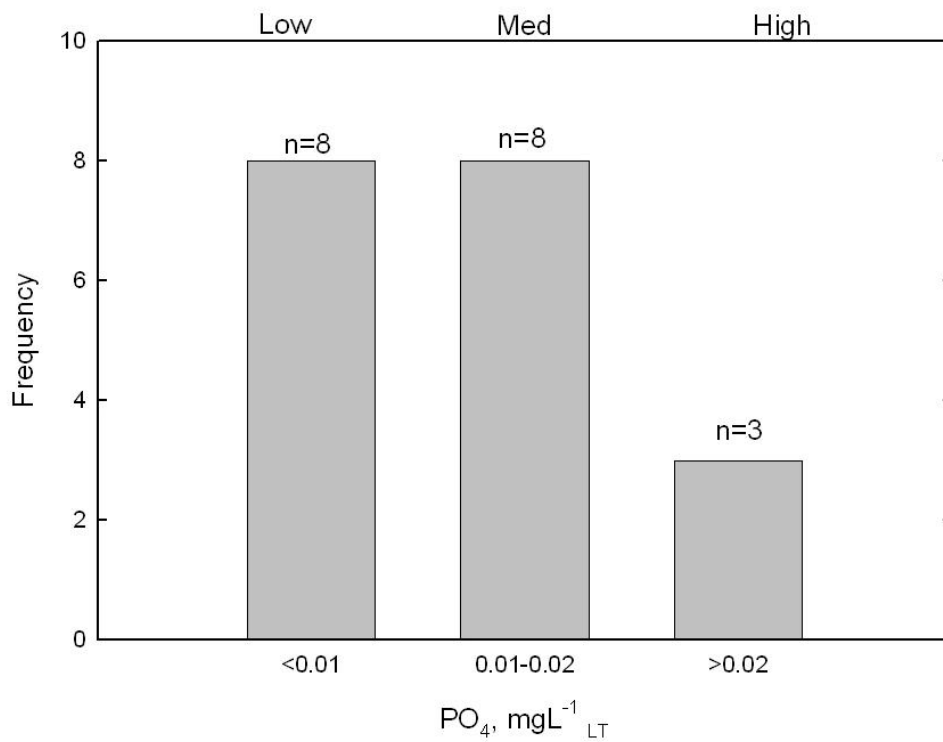
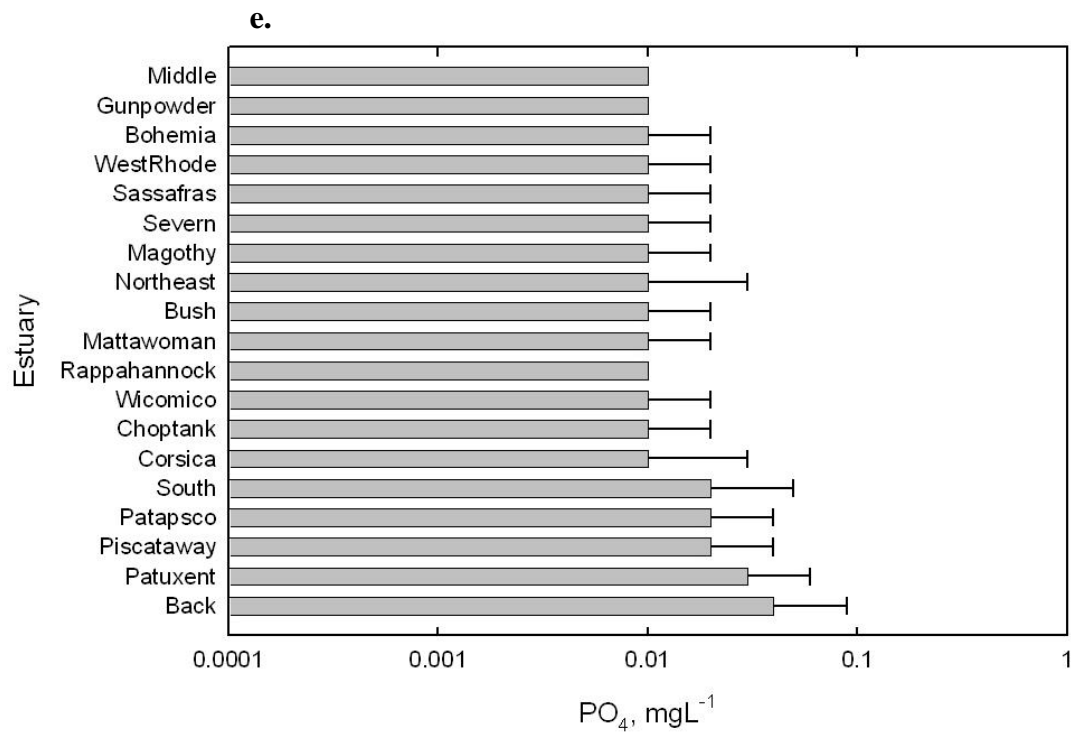


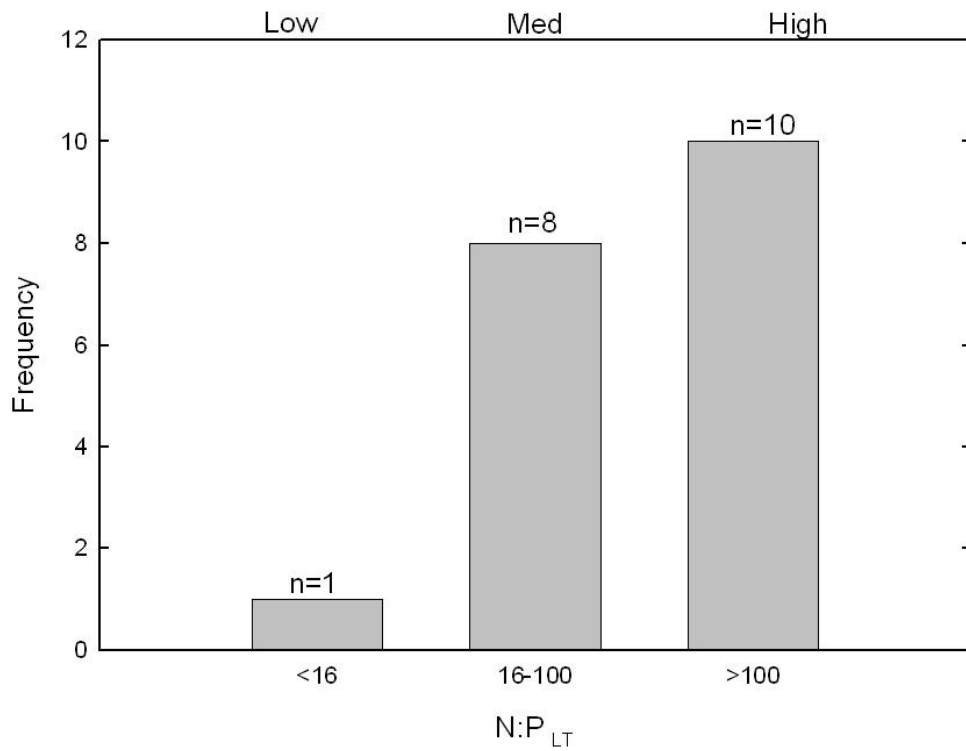
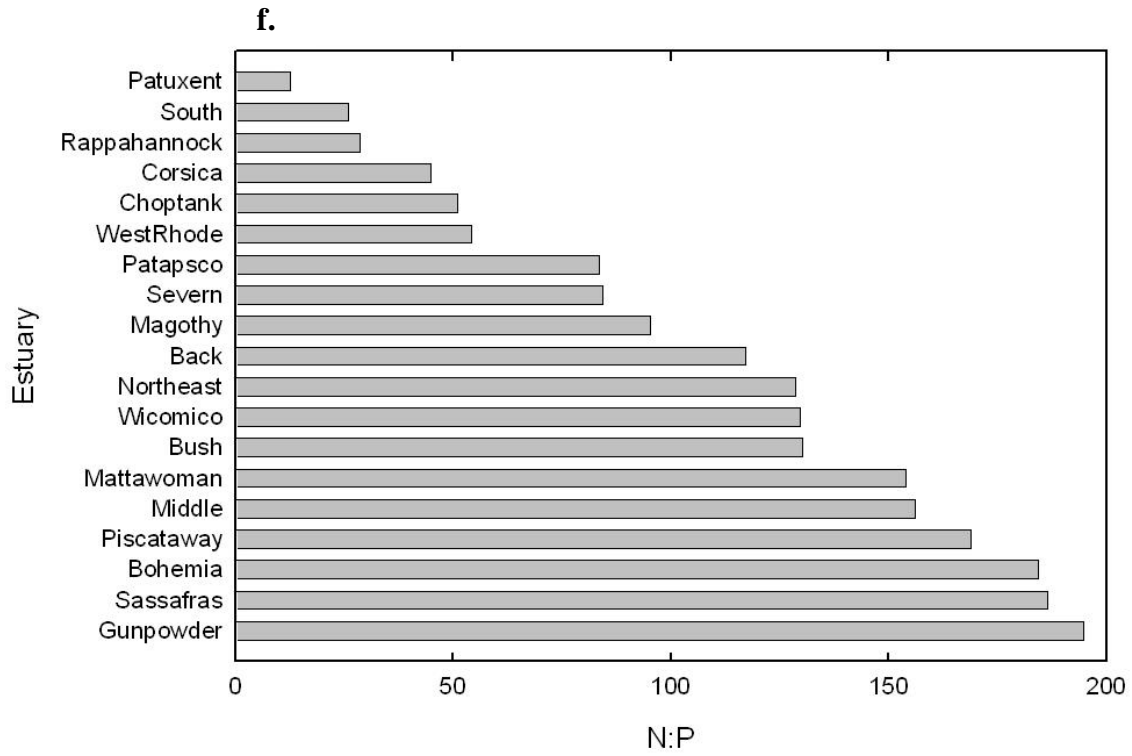
Figure 2-6 a-h. Bar graphs (20 year mean and standard deviation) and frequency histograms summarizing a variety of water quality conditions measured in surface waters of the tributary estuaries considered in this analysis. Note that nutrient histograms are log scaled.

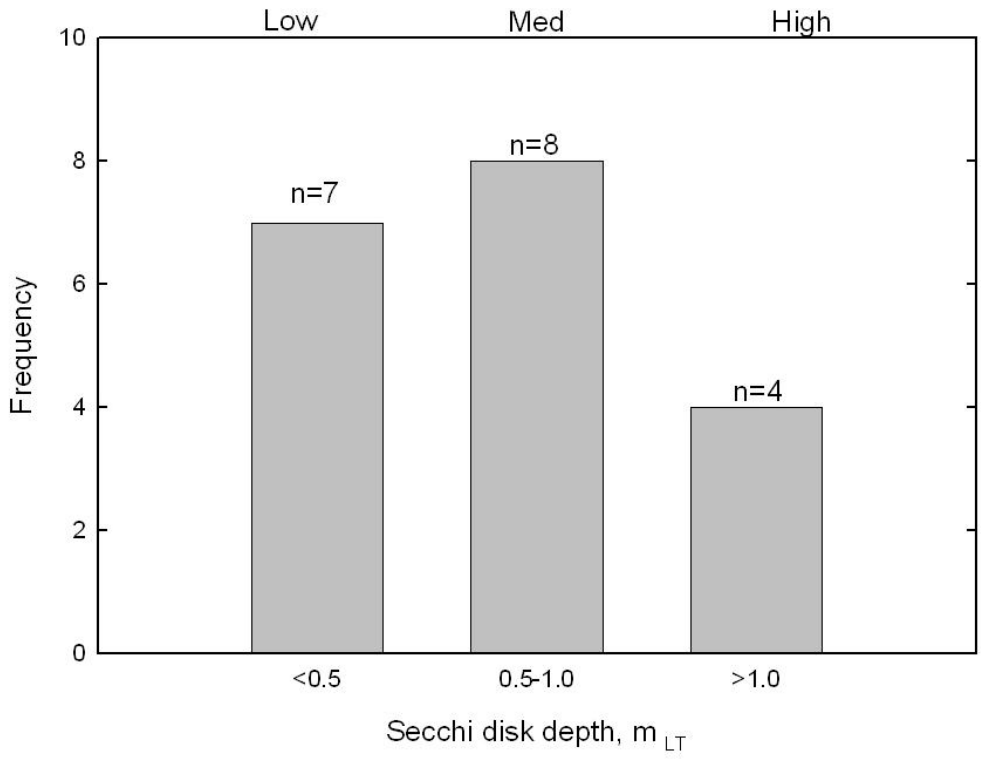
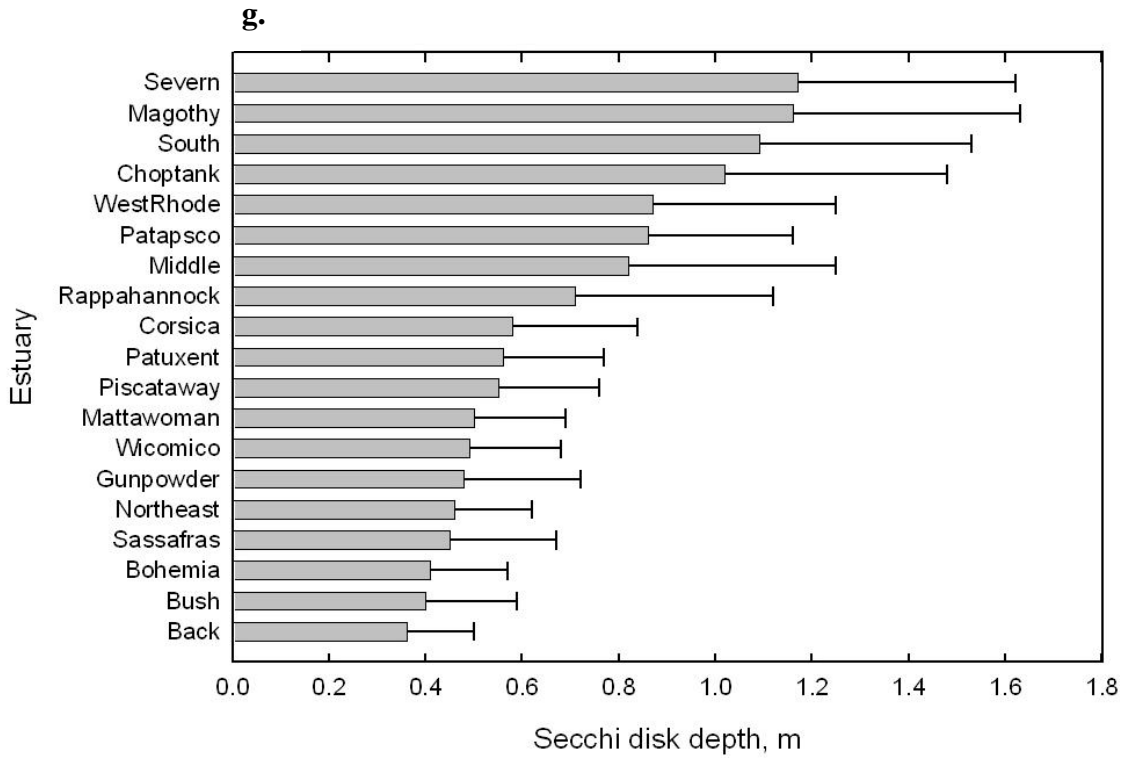


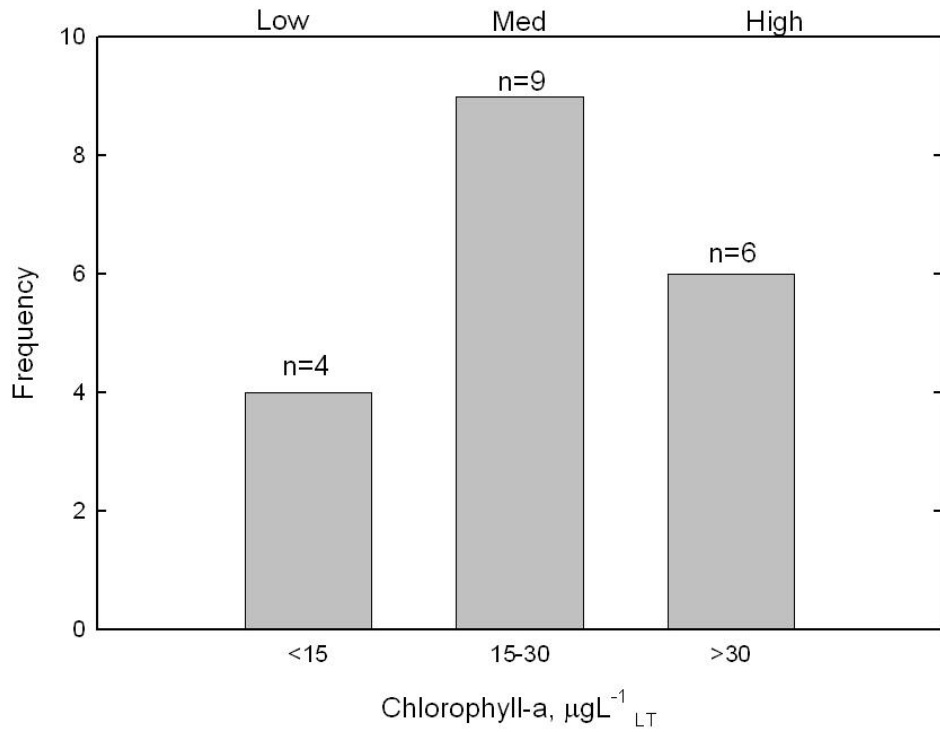
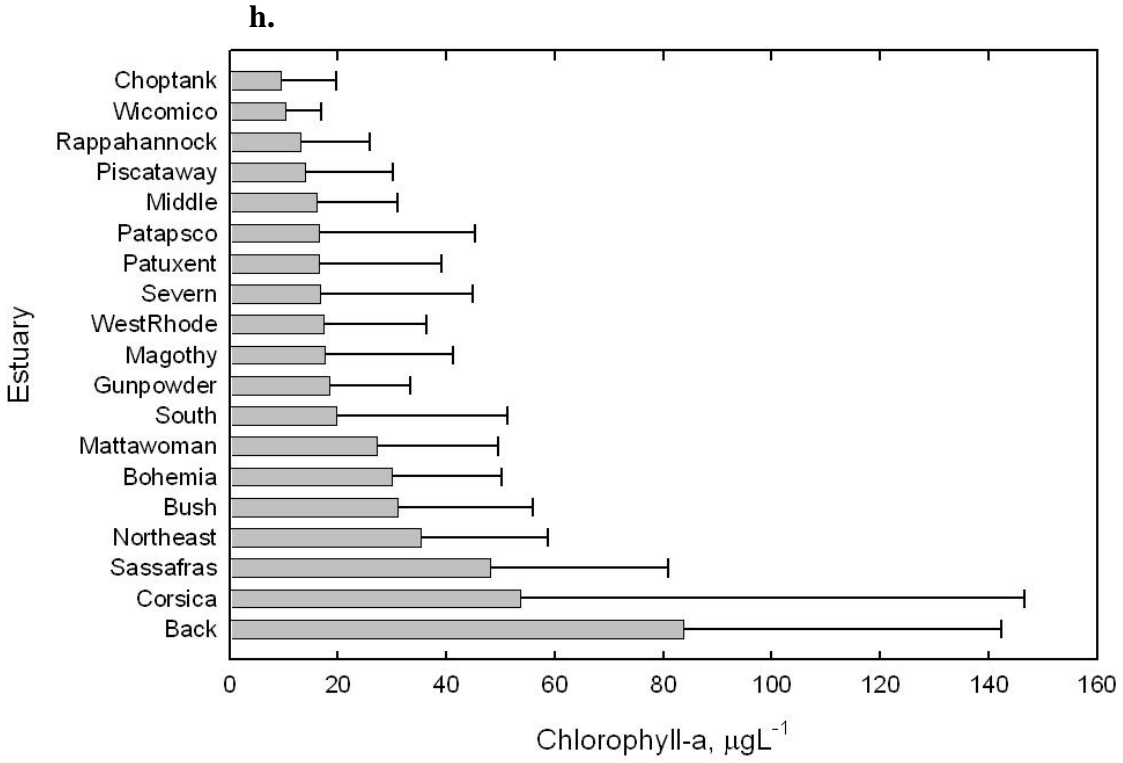












2-6 Relationships Between Nutrient Loads and Water Quality Conditions

The time-series data set organized for this work offers a huge potential for analysis. In this phase of the EPC Program we have initiated this analysis process but have not exhausted all of the possibilities. Future work is warranted. What we have accomplished to date includes the following: 1) examined the data set (both long-term average and 20 year annual time series) for relationships between nutrient inputs (N and P) and nutrient concentrations in tributary systems following the earlier work of Boynton and Kemp (2000); and 2) examined the long-term average data set for relationships between chlorophyll-*a* and other variables, including both nutrient loads, in-situ water quality conditions (e.g., water clarity, nutrient concentrations), and morphometric aspects of these systems (e.g., shoreline length, water residence times, depth). In the latter effort we initiated the analysis using linear correlation analysis and regression analysis and then expanded the analysis to include multiple linear regression analysis. Several other analytical approaches are possible but we have not had the resources to pursue these yet.

2-6.1 Nutrient Loads and In-Situ Nutrient Concentrations

We begin this analysis by examining the long term average data for relationships between total nutrient loads (both point and diffuse combined) and in-situ nutrient concentrations (DIN and DIP). Previously, Boynton and Kemp (2000) found strong relationships for a much smaller group (5 sites) of Chesapeake Bay systems between TN and TP loads and TN and TP concentrations (and TN and TP mass). In this analysis we also found a strong relationship ($r^2 = 0.81$) between total TN load (point and diffuse sources; expressed on an areal basis) and DIN concentration in the 19 systems examined (Fig. 2-7a-b), including two estimates focused on Back River (pre and post WWTP upgrades). The relationship appears linear with a y-intercept of about 0.12 mg N L^{-1} ($8.6 \text{ }\mu\text{M}$). The relationship between loads and nutrient mass (i.e., concentration multiplied by average system depth) were still significant but not nearly as strong as those with nutrient concentration (Figure not shown). The reason for this is not currently clear. It might be that even stronger load and in-situ concentration (or mass) relationships would have emerged if TN concentration data had been available in our data set. This is an addition to the data set that should be pursued. The important issue here is that there is a clear signal between loads and nutrient concentration among a diverse set of Chesapeake Bay tributary systems.

The case for the same relationships relative to phosphorus appears more complex (Fig. 2-7b). In this case the TP load versus in-situ DIP concentration relationship did not appear to be linear but rather rose steeply to a plateau. The best fit for this relationship appeared to be a second order polynomial. Several sites (e.g., Back River, Piscataway Creek, Patapsco River and South River) exhibited higher DIP concentrations relative to loads than did other sites. A possible explanation for this is that these most of these systems had a strong point source component and point sources release very little particulate P; most of the discharge is as DIP and this dominates the input signature. As with TN load versus DIN concentration (as mass), we found a weaker TP load versus DIP mass relationship. However, with both N and P there were distinct signals relating loads to estuarine concentrations on a long-term (20 year annual average) basis.

2-6.2 Nutrient Loads and Chlorophyll-*a* Concentrations

The importance of chlorophyll-*a* status in the Bay and tributaries can hardly be over-emphasized. Kemp *et al.* (1997) used a mass balance

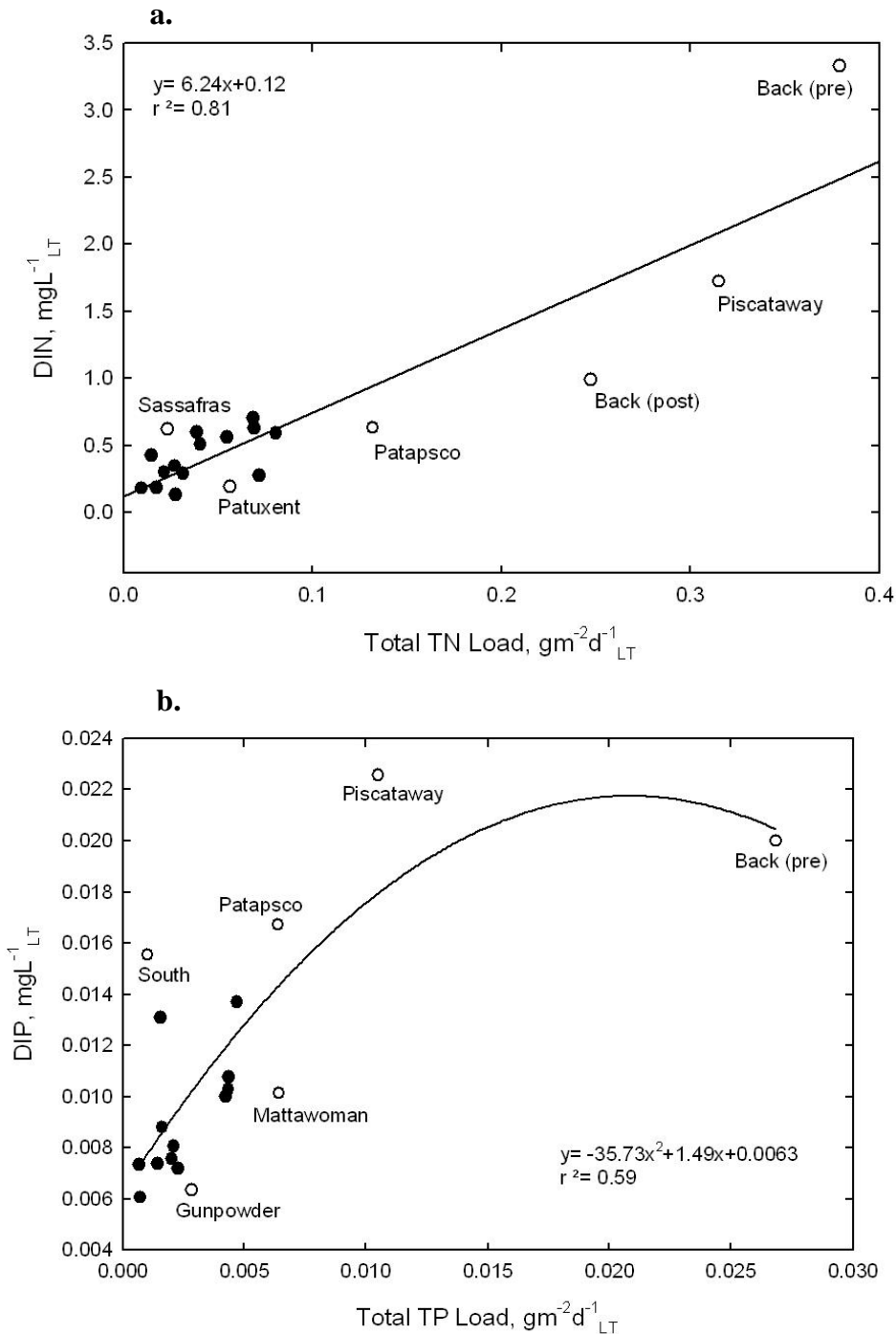


Figure 2-7 a-b. Scatter plots of 20 year average TN load versus 20 year average DIN concentration (a) and 20 year average TP load versus 20 year average DIP concentration (b) in tributary estuaries examined in this analysis. The solid line in (a) represents the best fit of the data based on a simple linear regression model and the curved line in (b) represents a polynomial fit of the P data . In both plots a selection of sites are identified. Back River sites “pre” and “post” indicate loads pre and post WWTP upgrades.

approach and found that phytoplanktonic production (indexed via chlorophyll-*a* concentration) was by far the largest source of labile organic matter in the Bay system and it is this labile organic matter that serves as the substrate for bacteria and other organism respiration which eventually leads to hypoxia and anoxia. A central management goal is to improve the DO status in the Bay region. Another pressing need is to establish quantitative links between nutrient loading rates, which are scheduled to be reduced under the TMDL program, and algal biomass (as indexed via chlorophyll-*a* concentration). Linkages such as this one are, of course, captured in some detail in the large water quality model developed for the Bay. However, this model has been mainly focused on the mainstem Bay and large tributary rivers. Our effort is a far simpler approach and seeks to develop statistical linkages between nutrient inputs and chlorophyll-*a* condition in a number of small Chesapeake Bay tributaries.

This statistical approach has been used before with some success. Vollenweider (1976) and others organized a vast data set from many temperate zone lakes and found they could reasonably predict ice-free season chlorophyll-*a* concentrations as a function of P loading, water residence time and a morphometric parameter (ratio of maximum depth to average depth). This relatively simple relationship was used by water quality managers to gauge expected water quality improvements relative to P load reductions. This sort of large-scale analysis has never been completed for estuarine systems but some limited analyses have been published. One of the earliest (Boynton *et al.*, 1982) reported a stronger relation to N loading than to P loading based on data from about a dozen estuarine systems but there was considerable residual variation in chlorophyll-*a* concentration not explained by TN loads. Later, Nixon *et al.* (1996), using a larger data set, also reported strong relationships between N loading and algal biomass for a group of plankton-dominated systems. More recently, Boynton and Kemp (2000) produced a version of a Vollenweider plot modified for estuarine systems (N load rather than P load was used and chlorophyll-*a* concentration was averaged over the full water column rather than just the surface layer). Boynton *et al.* (2013) organized data for five shallow Chesapeake Bay systems and found strong N-load – chlorophyll-*a* concentration relation when winter-spring N loads were used to forecast summer chlorophyll-*a* concentration. There have been some successes in developing simple but compelling statistical models of this important relationship. However, all of the above were characterized by small sample size and, for the most part, a single (or just several) year of data from each site.

In this analysis we organized a 20 year (1986-2005) record of water quality, physical characteristics, and nutrient load estimates for 19 relatively shallow and small tributary estuaries of Chesapeake Bay. One of the goals of this work was to explore this data set to see if understandable (i.e., readily explainable) relationships between nutrient loads from the land could be linked to algal biomass in these tributary systems.

We initiated this analysis by conducting a simple correlation analysis of the data set averaged for the 20 year analysis period (Table 2-4). We adopted this initial approach (using robust 20 year averages) based on work by Li *et al.* (2010) who reported that statistical measures explaining variability (e.g., *r* values) were generally quite low using monthly and seasonal-scale data, but more understandable and stronger at the multi-annual-scale. We were not able to examine the annual-scale data because of limited time to complete those analyses, but they are certainly worth exploring in the future. Several things are evident based on this initial correlation analysis.

Table 2-4. Results of Pearson Correlation Coefficient analysis (r) relating surface water chlorophyll-*a* concentration to a variety of variables. Asterisks indicate levels of significance (* = 5% level; ** = 1% level). All data are 20 year averages and variables in blue were included in the regression model.

variable number	r	variable name
1	0.44*	PS+NPS TN
2	0.44*	PS+NPS TP
3	0.41	DIN long term load avg.
4	0.46*	DIP long term load avg.
5	1.00**	Chlorophyll-a µg/L-1
6	0.69**	NH4 mg/L-1
7	0.41	NO3 mg/L-1
8	0.43	PO4 mg/L-1
9	-0.43	Salinity ppt
10	-0.50*	Secchi m
11	0.16	Temp °C
12	0.54*	DIN mg/L-1
13	0.17	N:P
14	-0.3	Basin Area
15	-0.33	Estuary Volume
16	-0.33	Estuary Surface Area
17	-0.15	Basin Area: Estuary Area
18	-0.1	Basin Area: Estuary Volume
19	-0.29	Estuary Average Depth
20	-0.25	Estuary Maximum Depth
21	-0.03	max depth: avg depth
22	-0.25	Estuary Mouth Length
23	-0.35	Smooth Shoreline Length
24	-0.18	Smooth Shoreline: Mouth
25	-0.35	Shoreline Length
26	-0.31	Shoreline: Mouth
27	-0.09	Tidal Prism Flushing Time (Tf)

First, not many of the 27 variables included in the analysis were significantly correlated with chlorophyll-*a* concentration. None of the morphometric variables exhibited significant correlations (variables 14-27; Table 2-4). However, 7 variables were significantly correlated with chlorophyll-*a* concentration (Table 2-4) and all of these had readily understandable relationships with chlorophyll-*a* concentration. Both N and P loads were significant as were ammonium and DIN concentration. Secchi disk depth exhibited a negative correlation, as expected, and suggests light limitation on chlorophyll-*a* production in some of the very turbid estuaries in this analysis (Figure 2-6g). The important variables related to chlorophyll-*a* concentration reflect the results of earlier work where investigators found both N and P limitation of phytoplankton growth (D'Elia *et al.*, 1986) and seasonal light limitation (Fisher *et al.*, 1999). In most of these systems TSS is responsible for a major portion of light attenuation.

Several results were also surprising. We had expected one or more of the morphometric variables to be correlated with chlorophyll-*a* concentration. For example, we might expect that the very shallow systems would sustain higher algal biomass than deeper systems because of a tighter coupling with sediment nutrient supplies. In addition, we expected flushing time to emerge as a strong explanatory variable just as it did in the lake synthesis conducted by Vollenweider (1976). The reason for this is not clear but we suspect the tidal prism method we used to compute annual-scale flushing time was just not sufficiently sensitive. Monthly time-scale estimates of flushing time for all the small tributaries of the Bay would be extremely useful for this and other water quality analyses.

Our next step in this analysis was to develop regression models linking water quality variables and nutrient loads to chlorophyll-*a* concentration. Many simple regression models were examined and several yielded suggestive results (Fig. 2-8a). When all 19 sites were considered there appeared to be a significant relationship between total TN load (averaged for the 20 year data record) and chlorophyll-*a* concentration averaged for the same time interval ($r^2 = 0.38$). However, very substantial variability remained. Examination of conditions at sites that strongly diverged from the general load-chlorophyll-*a* relationship suggested some explanations. For example, long-term water quality monitoring sites in the Sassafras and Corsica Rivers were located in the upper portions of these small estuaries where nutrient loads would be highest and water residence time longest, both of which would tend to promote algal biomass accumulation and subsequently lead to an overestimate of chlorophyll-*a* relative to loads. Conversely, there were two sites where chlorophyll-*a* concentration was depressed beyond expected (Patapsco and Piscataway). The monitoring sites in these systems were at middle or lower estuary locations and may be influenced by water quality and hydrodynamic conditions in the next larger system (Bay and Potomac River, respectively). We have no way of “correcting” these data for the effects of location or water residence time but we did develop a model where these sites were not included (Fig. 2-8b) and, as expected, the load – chlorophyll-*a* relationship improved a great deal. One of the lessons learned from this first stage analysis was that multiple factors need to be considered because there are considerable differences among the systems examined.

Our next step in this analysis was to develop multiple regression models in an effort to find stronger, and more complex, relationships between algal biomass and water quality and nutrient load conditions. One of the strongest results is shown in Fig. 2-9a where a linear multiple regression model used two of the strongest variables identified from the correlation analysis as predictor variables (NH_4 concentration and Secchi disk depth). The strength of the relationship improved considerably beyond the earlier models ($r^2 = 0.50$). However, the model over-predicted algal biomass in several tributaries (Piscataway, Patapsco and Gunpowder) and under-predicted biomass in several systems (Corsica and Sassafras). We have previously noted potential issues with several of these sites and those issues remain here. Nevertheless, the variables included in this model make biological sense and serve to link nutrient loads (via in-situ NH_4 concentration) and local water quality conditions (Secchi disk depth) to long-term average algal biomass levels.

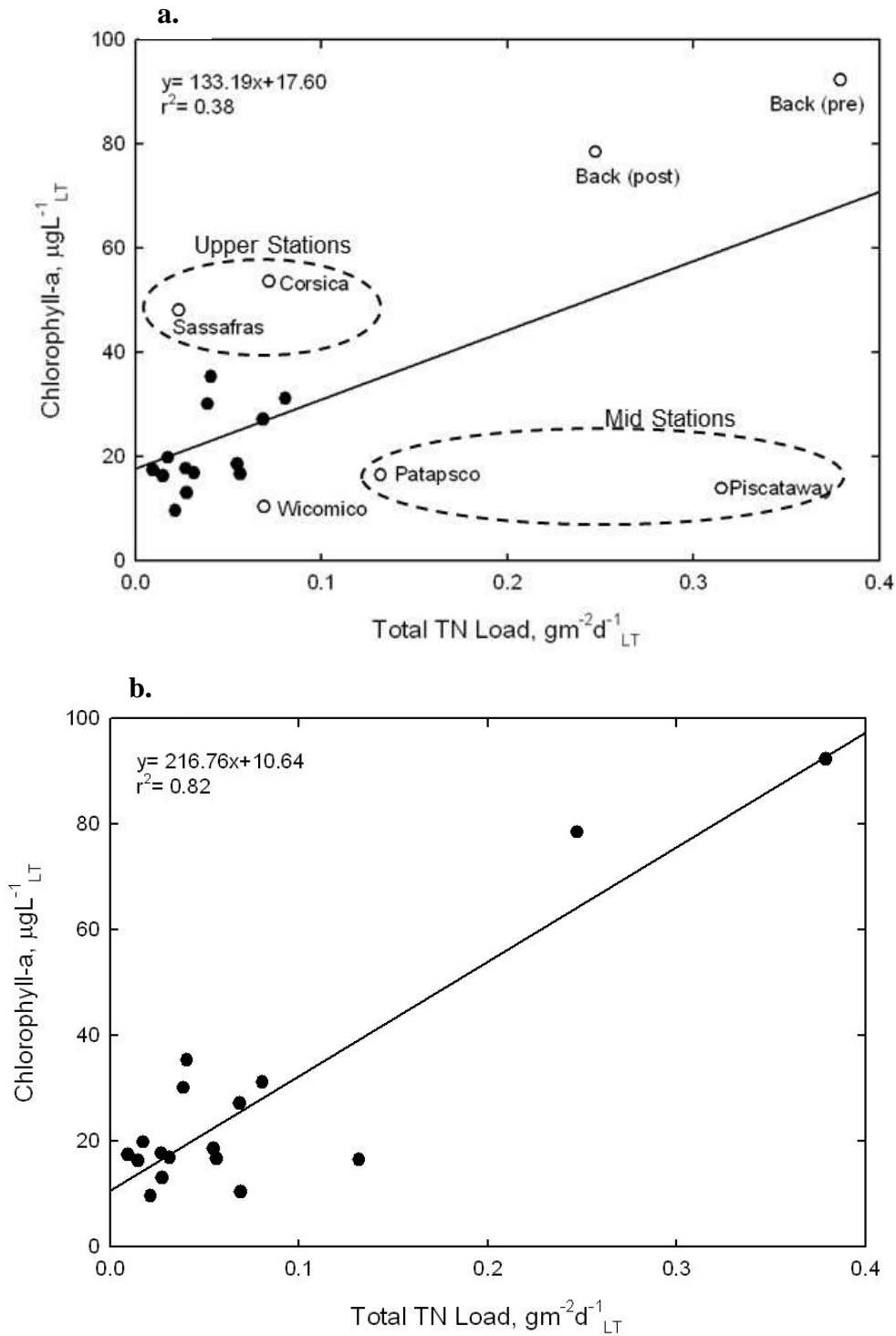


Figure 2-8 a-b. Scatter plots of TN load (both point and diffuse) versus surface water chlorophyll-*a* concentration from all 19 tributary systems considered in this analysis (a) and the same scatter plot with several systems removed. See text for details concerning deletion of some sites.

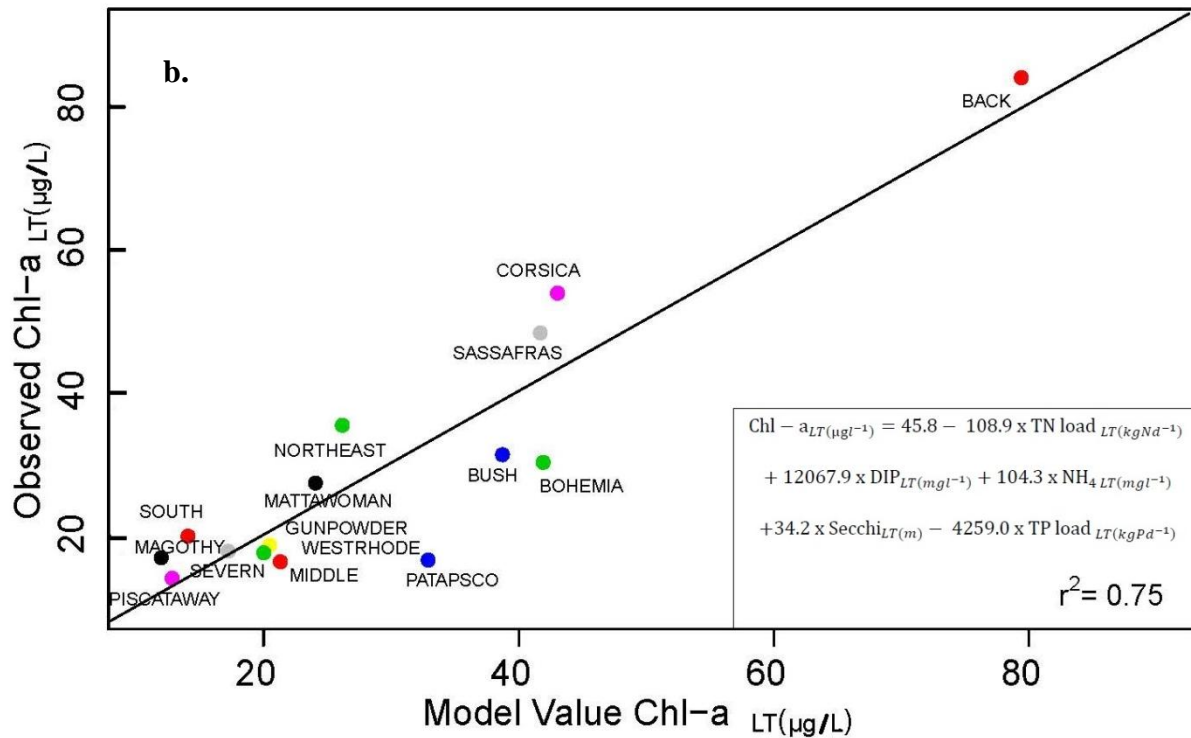
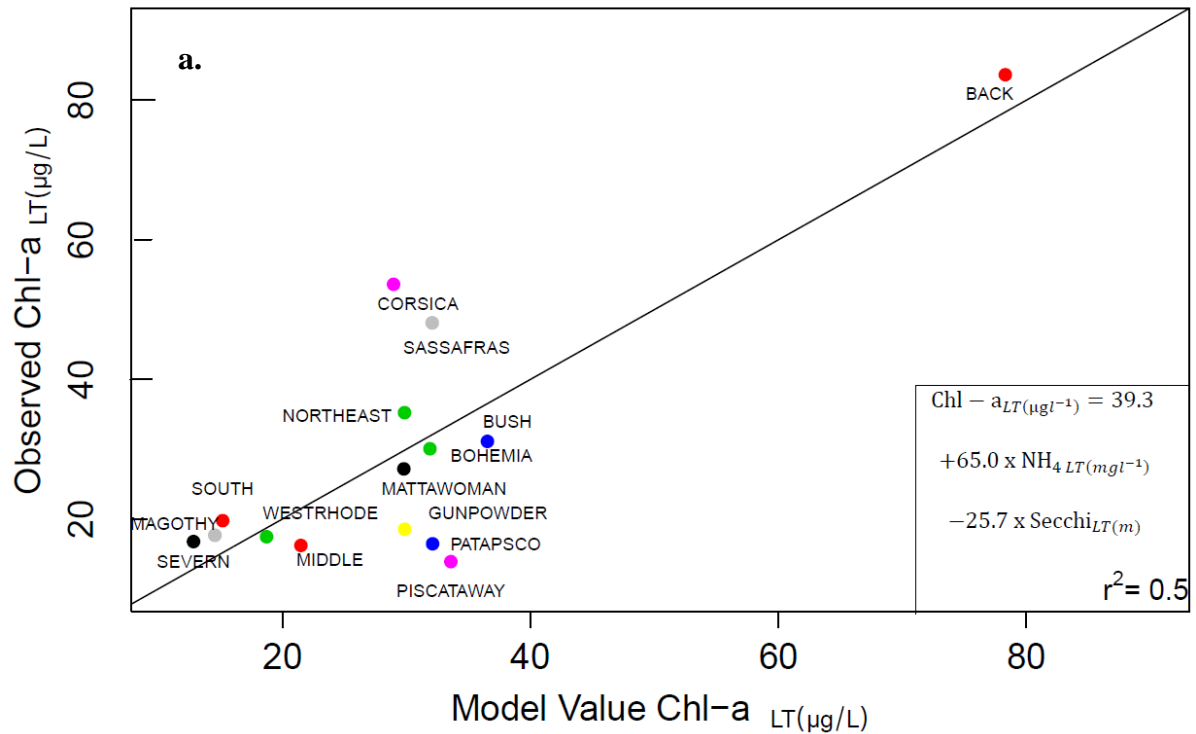


Figure 2-9 a-b. Results of two multiple regression models with both using 20 year averaged data from 19 tributary estuaries. The scatter plots in both (a) and (b) show observed chlorophyll-a versus the chlorophyll-a concentration predicted by the multiple regression models. The model in (a) uses just two independent variables while the model used in (b) used five independent variables. Tributaries predicted are labeled with their name. The multiple regression equations and r² values are provided.

We also explored the data set using a multiple regression approach described earlier in this report. In this case, a larger number of variables were selected on the basis that each significantly reduced the remaining variability in the model (Fig. 2-9b). In this case the r^2 value increased to 0.75, a substantial gain compared to the previous model. In this case independent variables included two nutrient load variables (TN and DIP loads), in-situ DIP and NH_4 concentration and Secchi disk depth. The strongly divergent predictions from the previous model were largely reduced except for the Patapsco River where the model still over-predicts chlorophyll-*a* concentration. Several additional points need to be made. First, this model may well be “over-parameterized” (i.e., too many independent variables included given the relatively small number of sites included in the analysis). Future work can address this issue by more closely examining the variable set used in the current model or by greatly increasing the number of observations by using the annual ($n = 380$ observations) data set, a task which fell beyond our time constraints in this effort. Second, there was a very large range in chlorophyll-*a* concentration among systems (~ 10 to $80 \mu\text{g L}^{-1}$). Despite this large range, the relationship appears to be quite linear and suggests a very large potential for algal biomass reduction associated with nutrient load reductions and water quality improvements.

2-7 Future Work and Other Related Issues

This work involved a very substantial effort in assembling a data set for these 19 tributary systems. It was especially challenging to obtain and verify nutrient inputs to these systems based on Chesapeake Bay Program land-use model results. As a result, we were not able to examine the larger, and possibly more useful, annual and seasonal-scale data sets. It would be worth investing in analysis of these data at some future date, especially since so much effort went into generating this data set. As specific examples of what yet needs to be done, we suggest the annual and seasonal-scale data be examined for both threshold responses and lag times relative to nutrient load changes (either due to management actions or wet/drought climate cycles). Earlier work (e.g., Testa *et al.*, 2008) has reported strong linkages between algal biomass or hypoxia during summer periods and winter-spring loads to estuaries.

We also need better estimates of water residence times for these small tributary systems. We used a tidal prism method as described by Wazniak *et al.* (2009) because it was easy to use and because we could obtain estimates from tributaries where there was no measurable salt (a salt gradient is needed for using box models to estimate water residence times). However, the tidal prism approach yields only one average estimate of water residence time yet we know from other work that this changes, sometimes dramatically, during the course of the year (Hagy *et al.*, 2000). The work of Hagy *et al.* (2000) concerning water residence time estimates needs to be implemented for all the small tributaries on seasonal or monthly time-scales. The importance of residence times seems clear and some think of water residence time as a “master variable” relative to such ecosystem scale processes as algal biomass accumulation and nutrient export dynamics (Nixon *et al.*, 1996).

This type of comparative analysis is an important adjunct to the more labor intensive and costly simulation modeling approaches used in many resource management programs. First, this approach can yield useful information quite rapidly. While we did not achieve all goals we had hoped for we did achieve some of those goals in less than one year of effort involving less than

one person-year of effort. Furthermore, the comparative approach makes clear the relative condition of many tributary systems and this is of interest to both resource managers and the public. Anyone can readily see how their system is doing relative to others. We recommend this parallel analysis approach continue.

Finally, we need to further assess the issue of monitoring station location in tributary systems and the degree to which these stations represent conditions in the full tributary system. For example, we located chlorophyll-*a* measurements (Fig. 2-10) made at three locations along the axis of the Back River estuary during summer 1997 (Boynton *et al.*, 1998).

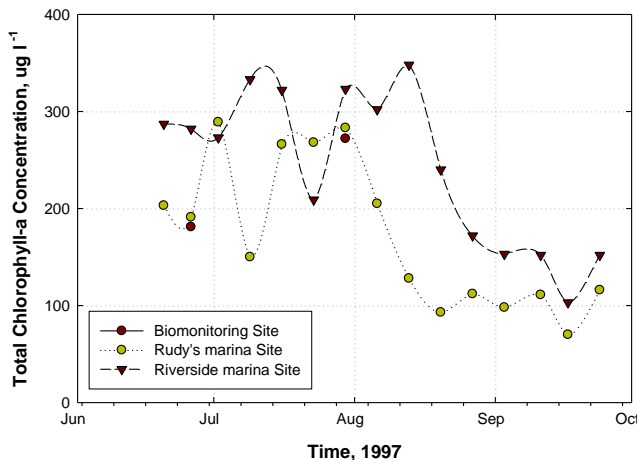


Figure 2-10. Time series plot of surface water chlorophyll-*a* concentrations collected from three sites in the Back River estuary during summer, 1997. Data were from the Chesapeake Bay Program data hub (water quality) and from Boynton *et al.* (1998).

One site was located on the north side of the upper Back River very close to the WWTP discharge while the other site was located nearer the junction of the Back River with upper Chesapeake Bay. The Biomonitoring site is located between these two sites. Several things are apparent in these data. First, there is often a very large difference between chlorophyll-*a* concentrations at the two sites. Concentrations were almost always lower at the site closer to the Bay. Finally, there were only 2 observations available from the Biomonitoring program during this time period and both were similar to those measured at the site closest to the Bay. These data suggest several things. First, the Biomonitoring data may better represent the “outer Back River” than the inner portion of the estuary most heavily impacted by WWTP discharges. Second, and of particular concern here, is that the Biomonitoring site may be mainly representative of the “outer Back River” but may, at times, be representative of the hyper-eutrophic inner estuary. For example, if routine sampling took place during the final stages of a strong ebb tide chlorophyll-*a* concentration at the Biomonitoring site might reflect conditions in the inner estuary while the last part of a strong flood tide might reflect chlorophyll-*a* conditions in the outer Back River or upper Chesapeake Bay. Some of the extreme variability exhibited in monthly chlorophyll-*a* measurements may be the result of a very strong chlorophyll-*a* gradient in this and other enriched systems. The issue of single station representativeness will not be easily solved and certainly has implications for comparative work such as presented here. One solution would be to examine Dataflow information and ask if these more detailed data could be used instead of traditional monitoring data in comparative studies or if Dataflow data could be used to adjust traditional monitoring data to more accurately represent average conditions at the whole estuary spatial scale.

2-8 References

Boynton, W. R., W. M. Kemp, and C. W. Keefe. 1982. A comparative analysis of nutrients and other factors influencing estuarine phytoplankton production, p. 69-90. In: V.S. Kennedy (ed.) *Estuarine Comparisons*. Academic Press, New York

Boynton, W. R., N. H. Burger, R. M. Stankelis, F. M. Rohland, J. D. Hagy III, J. M. Frank, L. L. Matteson and M. M. Weir. 1998. An environmental evaluation of Back River with selected data from Patapsco River. UMCES. Chesapeake Biological Laboratory Ref. No. [UMCES]CBL 98-112b.

Boynton, W. R. and W. M. Kemp. 2000. Influence of river flow and nutrient loading on selected ecosystem processes and properties in Chesapeake Bay. In *Estuarine Science: A synthetic approach to research and practice*, ed. J.E. Hobbie, 269-298. Washington, DC: Island Press.

Boynton, W. R., J. D. Hagy, J. C. Cornwell, W. M. Kemp, S. M. Greene, M. S. Owens, J. E. Baker, and R. K. Larsen. 2008. Nutrient budgets and management actions in the Patuxent River Estuary, Maryland. *Estuaries and Coasts* 31(4): 623-651.

Boynton, W.R. and W.M. Kemp. 2008. Nitrogen in Estuaries. In: Capone, D., D. A. Bronk, M. R. Mulholland and E. J. Carpenter (eds.), *Nitrogen in the Marine Environment* (Second Edition). Academic Press, p.809-866: 978-0-12-372522-6.

Boynton, W.R., J.M. Testa and W.M. Kemp. 2009. An Ecological Assessment of the Corsica River Estuary and Watershed Scientific Advice for Future Water Quality Management: Final Report to Maryland Department of Natural Resources. Ref. No. [UMCES]CBL 09-117. [UMCES Technical Series No. TS-587-09-CBL].

Boynton, W. R., C.L.S. Hodgkins, C.A. O'Leary, E.M. Bailey, A.R. Bayard, and L.A. Wainger. 2013. Multi-decade responses of a tidal creek system to nutrient load reductions: Mattawoman Creek, Maryland USA. *Estuaries and Coasts* (In Press)

Chesapeake Bay Watershed Model Land Use and Linkages to the Airshed and Estuarine Models. 2000. US EPA Chesapeake Bay Program, Annapolis, MD (<http://www.chesapeakebay.net>)

Chesapeake Bay Water Quality Monitoring Program. 2001. US EPA Chesapeake Bay Program, Annapolis, MD (<http://www.chesapeakebay.net>)

D'Elia, C. F., J. G. Sanders and W. R. Boynton. 1986. Nutrient enrichment studies in a coastal plain estuary: phytoplankton growth in large-scale continuous cultures. *Can. J. Fish.Aquat. Sci.* 43: 397-412.

D'Elia, C. F., W. R. Boynton and J. G. Sanders. 2003. A watershed perspective on nutrient enrichment, science, and policy in the Patuxent River, Maryland: 1960-2000. *Estuaries* 26(No. 2A): 171-185.

Department of Commerce (DOC), National Oceanic and Atmospheric Administration (NOAA). 1998. U.S. Estuarine Bathymetric Datasets, VA/MD (M130) Bathymetric Digital Elevation Model (30 meter resolution); <http://estuarinebathymetry.noaa.gov/>

ESRI (2012). ArcMap, ArcGIS Desktop, and ArcINFO Workstation 10, Environmental Science Research Institute. Redlands, California.

Fisher, T. R., A. B. Gustafson, K. Sellner, R. Lacuture, L. W. Haas, R. Magnien, R. Karrh and B. Michael. 1999. Spatial and temporal variation in resource limitation in Chesapeake Bay. *Mar. Biol.* 133:763-778.

Hagy, J. D., L. P. Sanford and W. R. Boynton. 2000. Estimation of net physical transport and hydraulic residence times for a coastal plain estuary using box models. *Estuaries Vol 23(3)*: 328-340.

Hirsch, Robert M., D. L. Moyer, and S. A. Archfield. 2010. Weighted Regressions on Time, Discharge, and Season (WRTDS), With an Application to Chesapeake Bay River Inputs. *Journal of the American Water Resources Association (JAWRA)* 1-24. DOI: 10.1111 / j.1752-1688.2010.00482.x

Kemp, W. M., E. M. Smith, M. Marvin-DiPasquale, and W. R. Boynton. 1997. Organic carbon balance and net ecosystem metabolism in Chesapeake Bay. *Marine ecology Progress Series* 150: 229-248.

Kemp, W. M. and W. R. Boynton. 2012. Synthesis in estuarine and coastal ecological research: What is it, why is it important, and how do we teach it? *Estuaries and Coasts Vol. 35(1)*: 1-22

Li, W. K. W., M. R. Lewis and W. G. Harrison. 2010. Multiscalarity of the nutrient-chlorophyll-*a* relationship in coastal phytoplankton. *Estuaries and Coasts*. 33:440-447.

Nixon, S.W. and fifteen others. 1996. The fate of nitrogen and phosphorus at the land-sea margin of the North Atlantic Ocean. *Biogeochemistry*. 35:141-180.

Parsons, T. R., M. Takahashi and B. Hargrave. 1984. *Biological Oceanographic Processes*. Pergamon Press, Oxford. 330 p.

Sarthou, G., K. R. Timmermans, S. Blain and P. Treguer. 2005. Growth physiology and fate of diatoms in the ocean: a review. *J. Sea Res.* 53: 25-42.

Shenk G.W., and L.C. Linker. In Press. Development and Application of the Phase 5 Chesapeake Watershed Model. *Journal of the American Water Resources Association*.

Testa, J. M., W. M. Kemp, W. R. Boynton and J. D. Hagy III. 2008. Long-term changes in water quality in the Patuxent River estuary: 1985 to 2003. *Estuaries and Coasts* 31(6): 1021-1037.

USEPA (U.S. Environmental Protection Agency). 2010. Chesapeake Bay Phase 5.3 Community Watershed Model EPA 903S10002 - CBP/TRS-303-10 U.S. Environmental Protection Agency, Chesapeake Bay Program Office, Annapolis MD. December 2010.

United States Geological Survey (USGS). 2012. Stream Flow Data. <http://waterdata.usgs.gov/md/nwis/sw>

USGS National Hydrography Dataset, 2009; <http://viewer.nationalmap.gov/viewer/>; <http://nhd.usgs.gov/>

Vollenweider, R. A. 1976. Advances in defining critical loading levels of phosphorus in lake eutrophication. *Memorie-Istituto Italiano de Idrobiologia* 33: 53-83.

Wazniak, T., W. Boicourt, and E. North. 2009. Residence Times of Small Chesapeake Bay Tributaries. Li, W. K. W., M. R. Lewis and W. G. Harrison. 2010. Multiscalarity of the nutrient-chlorophyll relationship in coastal phytoplankton. *Estuaries and Coasts*. 33:440-447.

Chapter 3

Linking ConMon and Dataflow© for Spatial Dissolved Oxygen Criteria Assessment

C.A. O'Leary, W.R. Boynton, E. Perry, A. Bayard and L. Wainger

CHAPTER 3	1
3-1 INTRODUCTION	1
3-2 EXPLORATORY DATA ANALYSIS	3
3-3 AMPLITUDE MODEL DEVELOPMENT AND ANALYSIS	6
3-4 RESULTS	8
3-4.1 STAGE ONE: TRIGONOMETRIC TIME SERIES	8
3-4.2 STAGE TWO: DO AMPLITUDE MODEL	10
3-4.3 STAGE THREE: DO AMPLITUDE MODEL VALIDATION	14
3-5 EXTENSION OF MODEL TO SPATIAL ASSESSMENT	17
3-6 DISCUSSION, IMPLICATIONS AND FUTURE	23
3-7 REFERENCES	27
3-8 APPENDIX	30

3-1 Introduction

Depletion of dissolved oxygen (DO) in coastal waters is a widespread phenomenon that impacts the structure and function of biological communities and impacts biogeochemical cycling of nutrients (Henrichs 1992; Wu *et al.*, 2003; Bishop *et al.*, 2006; Ludsin *et al.*, 2009; Prasad *et al.*, 2011). There are both physical and biological factors that contribute to seasonal reduction in DO concentration (Kemp *et al.*, 1992; Boynton and Kemp, 2000); however, the timing and extent of DO fluctuations varies on multiple time scales including hourly, daily, seasonal and inter-annual. If an organism is exposed to low DO for too long, it may become stressed (Wu *et al.*, 2003; Bishop *et al.*, 2006; Montagna and Froeschke, 2009). Despite the importance of DO and many organisms' sensitivity to hypoxic conditions, DO remains difficult to predict due to the many potential drivers of oxygen dynamics (Prasad *et al.*, 2011).

The Chesapeake Bay program adopted a hierarchy of DO criteria which are designed to protect aquatic resources. These criteria range from time scales of month to hours and depth ranges of surface to very deep waters. Criteria assessment relies on a bi-monthly to monthly sampling intensity at channel stations in the mainstem Bay and tributaries, which does not provide sufficient data for assessing the criteria for short time scales and is minimally adequate for assessing spatial variability. A partial solution to this problem was the development and use of supplemental ConMon and Dataflow© measurement technologies. There is nearly an eleven year record for many of these sites (over 95) in the Chesapeake Bay (EPC report Boynton *et al.*, 2012). These two monitoring programs each contribute in their own way to DO criteria assessment.

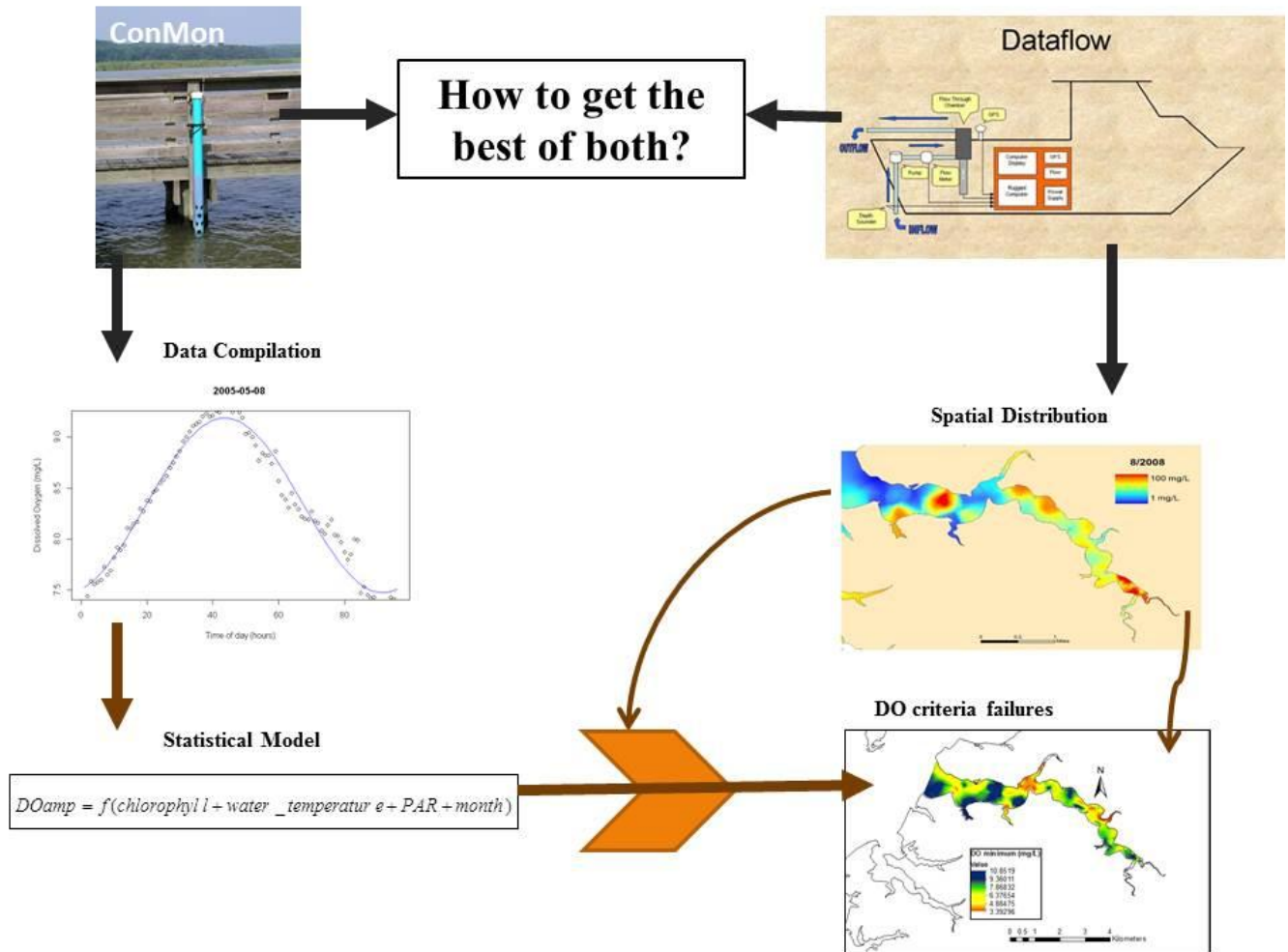
The ConMon monitoring program provides detailed time series of water quality information. These data offer some of the best information for understanding hourly to interannual dynamics of DO and other conditions (e.g., water clarity, temperature, pH and chlorophyll-*a*) relevant to

sustaining aquatic organisms. ConMon stations record high frequency (every 15 minutes for three years; generally from April – October of each year) data on nearshore shallow water DO and other measurements at fixed locations (date, time, water temperature, salinity, pH, turbidity, and chlorophyll-*a*). These data provide adequate information for water quality assessment of many tributaries in the Chesapeake Bay, and are especially relevant for shallow water (<2 m) assessments. Despite the temporal strength of ConMon, it is difficult to judge the spatial extent of surface water DO assessment at the scale of the whole estuary from the fixed ConMon sites. Extrapolating these data to the larger tributary area remains problematic.

In contrast, Dataflow© provides spatially-detailed data on the magnitude and fine-scale variability of water quality variables at the “whole estuary” scale. This technology is limited by infrequent measurement intensity; generally one measurement per month is collected. Water quality measurements are taken every 30-60 m, covering a tributary system within a few hours. These measurements are repeated monthly between April and October for three years at each tributary. Measurements are spatially intensive but lack in temporal coverage as it is restricted to monthly time intervals. In addition, Dataflow© cruises are typically conducted during the mid-day period (i.e., between 0900 and 1600 hours) when surface water DO concentrations are approaching, or at, maximum values. To assess the maximum potential of hypoxia stress to aquatic organisms, these values need to be adjusted to the daily minimum DO concentrations, which typically occur in the immediate post-dawn period. Hence, extrapolating these data across time remains problematic.

To summarize, we are faced with a space-time issue: despite the high frequency of ConMon temporal data, spatial extrapolation of these data is difficult and despite Dataflow© measurements having relatively intense spatial coverage, they lack sufficient temporal coverage.

This chapter presents results of a study to solve this space-time issue. A link between time and space in surface DO monitoring through the use of both Dataflow© and ConMon data is explored. Specifically, ConMon data were used to develop a statistical model of daily DO dynamics as a function of other variables. Because of the complexity of DO drivers, we sub-selected data for ‘biologically relevant’ days, for use in fitting the model. We define biologically relevant days as those with DO signals primarily driven by biological processes rather than physical processes. Once the model was developed, it was used to adjust Dataflow© spatial DO measurements to levels representative of daily DO minimum values (Fig. 3-1). Thus, spatial and temporal data were combined to better assess short-term surface water DO criteria. This is a preliminary report on the findings of this proof of concept investigation to provide a template with which to expand and improve upon the techniques reported here.



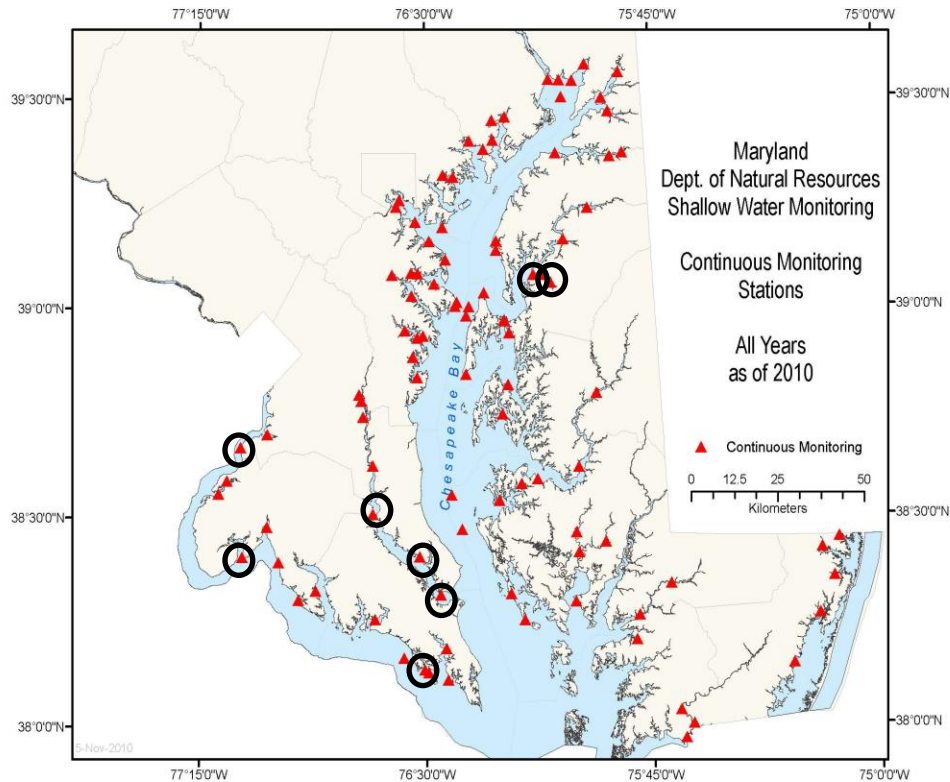


Figure 3-2. Locations of all MD ConMon sites for all years of deployment through 2010. Sites circled in black were used in analysis. Sites span a large eutrophication gradient.

ConMon data used in this exploratory analysis were accessed from the ‘Eyes on the Bay’ website (<http://mddnr.chesapeakebay.net/eyesonthebay/index.cfm>) maintained by the Maryland Department of Natural Resources (DNR). Data from locations noted above (Fig. 3-2) were used because of the eutrophication gradient present across sites (to generalize the analysis) and because ConMon and Dataflow© data collections overlapped during these years. For the purpose of this exercise, all depths were considered the same. Photosynthetically active radiation (PAR) data from Horn Point Laboratory in Cambridge, Maryland was used to estimate the effect of radiation on the daily DO cycle. In addition, these sites represent severe to moderate nutrient impacts on DO to allow for assessment of model robustness.

Data were found to have great variations in surface DO during short periods of time. For example, within 24 hours DO in the same location were seen to vary by as much as 15 mg/L (Fig. 3-3). This has large implications for DO criteria assessment as it indicates that the timescale used to estimate DO criteria failure is of importance. DO patterns were found to repeat seasonally: summer daily DO ranges were very large and winter DO ranges were very small (Fig. 3-5). In addition, the winter DO concentration was generally higher (Figs. 3-4, 3-5).

Sycamore Point July 1-10 2005

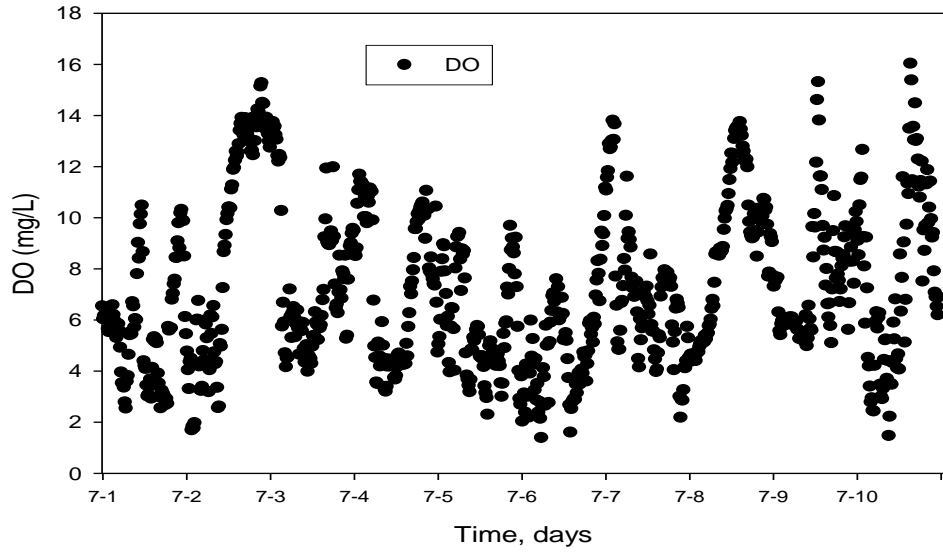


Figure 3-3. Surface dissolved oxygen (mg/L) data at Sycamore Point ConMon station from 1 July 2005 to 10 July 2005 showing large fluctuations in DO concentrations over a short time period (10 days).

Sycamore Point (Corsica) 2005-2008

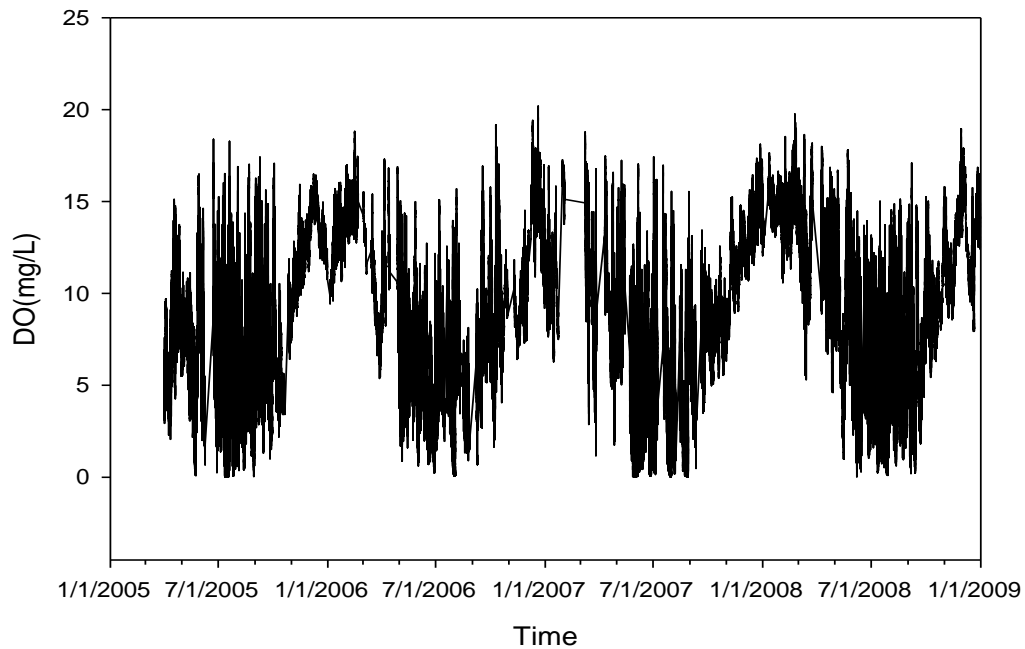


Figure 3-4. Surface dissolved oxygen (mg/L) data at Sycamore Point ConMon station from 1 January 2005 to 31 December 2009 showing seasonal-scale DO fluctuations.

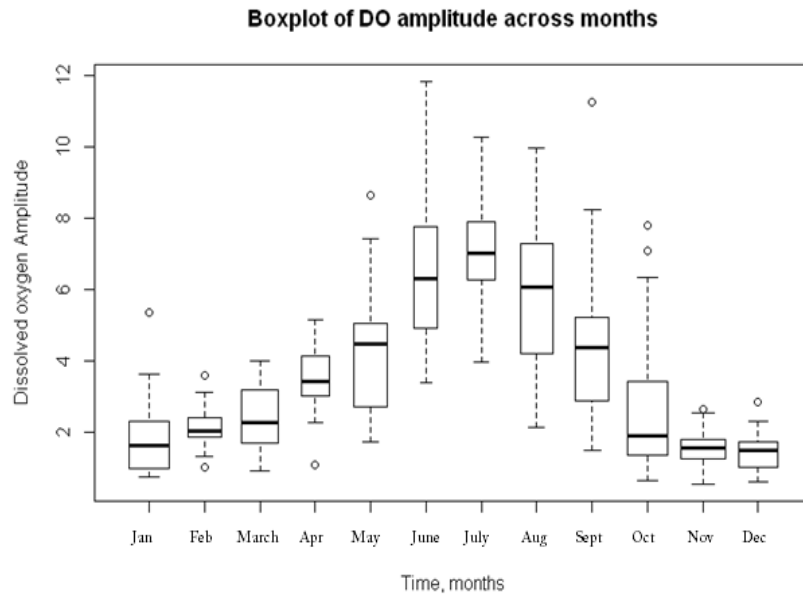


Figure 3-5. Box and Whisker Plot of DO amplitude by month from Sycamore Point station in the Corsica from 2003-2005. The dark horizontal lines represent monthly median DO amplitude. In this case DO amplitude is defined as the difference between maximum and minimum concentrations during a 24 hour period.

The relationship between the range of daily surface DO concentration and water quality variables was examined in order to estimate the daily variability of DO as a function of surface water quality properties. Variables examined included chlorophyll-*a* concentration, water temperature, turbidity, salinity, pH, and (PAR) at ConMon sites in three different tributaries (Fig. 3-2). These variables were chosen because of the role they play in DO dynamics on a short time scale, because they are indicators of primary production and respiration, and/or data availability.

3-3 Amplitude Model Development and Analysis

A strategy for combining the spatial information of Dataflow© and temporal information of ConMon data was initiated through the statistical exploration of ConMon data.

The statistical analysis initially used data from Sycamore Point in the Corsica River from January 2005 to December 2008. This station was selected due to its known high variability in dissolved oxygen and overlap with Dataflow© data collection in the Corsica (Boynton *et al.*, 2009). The 15-minute data were converted to Diel time, thus a ‘day’ was defined as 06:00A.M. on one calendar day to 05:59A.M. the following calendar day. Observations used in this analysis had complete data for all variables considered and contained at least 72 observations per day (Perry 2012). This data was used in first stage model development and all further model development.

Development of a statistical model of surface water DO dynamics based on ConMon data (fine temporal scale) was constructed in multiple stages:

The **first** stage was the application of a trigonometric time series model using Sine and Cosine functions of time scaled to have a 24 hour cycle. The combination of sine and cosine functions limits the range to positive numbers only and generates the theoretically expected relationship between DO and time within a biologically mediated system. This model was applied to each day of ConMon data to capture the possible DO range within a 24 hour time period. The dependent variable, DO amplitude in mg/L, was considered as a linear function of the independent variable, a transformed time series. This model equation took the following form:

$$DO_{it} = \mu_i + \beta_1 \sin\left(\frac{t * 2\pi}{24}\right) + \beta_2 \cos\left(\frac{t * 2\pi}{24}\right)$$

Where μ is the mean DO for the 24 hour period, β_1 and β_2 are regression coefficients, t is time of day and i is an ordinal index for day. The Sine and Cosine functions were parameterized so that the functions completed a cycle aligned with a 24 hour cycle. This trigonometric time series model provided the amplitude (i.e., range) of DO for every day that ConMon data were collected. Daily DO amplitude was computed as the difference between the model predicted minimum and maximum DO concentration in a 24 hour period:

$$\hat{a} = \sqrt{\hat{\beta}_1^2 + \hat{\beta}_2^2}$$

The trigonometric time series was then used to define diel cycles that resembled an expected biological diel cycle (i.e., DO increasing during daytime and decreasing during hours of darkness) from those DO cycles that resulted from more complex issues (e.g., tidal or wind-induced influences on DO dynamics) using the coefficient of determination (R^2) as a measure of fit (Murphy *et al.*, 2011). DO fluctuations that resembled a biologically mediated day ($R^2 \geq 0.7$) were kept for continued analysis as suggested by Perry (2012). The trigonometric time series model was later used as an exploratory tool for other ConMon stations to assess long-term, seasonal, and site-specific patterns in DO amplitude.

Model development continued into a **second** stage by developing a model that would estimate the DO amplitude, as estimated from the trigonometric time series, as a function of variables available in the ConMon data set. Equations tested were functions of all combinations of the listed variables: PAR, water temperature, salinity, turbidity, chlorophyll-*a*, and month. The idea was to use as few independent variables as possible to predict the diel variability in DO concentration (maintain model parsimony). All independent variables considered in the model were mean daily estimates.

Many different statistical models and methods of fitting were considered including linear model (LM), General Additive Model (GAM), Generalized Linear Model (GLM), Generalized Least Squares (GLS) with various correlation structures, Artificial Neural Network (ANN) and causal models. See Table 3-6 in the appendix for full descriptions of each model type tested. Significant variables were identified using stepwise selection. The variables were chosen using p-values and Akaike Information Criterion (AIC) and the best-fit model was selected using Anova, residual analysis and assumption tests such as Wilkes-Shapiro and Breusch-Pagan tests (Johnson 2004; Faraway 2006; Matthiopoulos 2011). The independent variables in the final model and amplitude estimating equations tested are presented in the results section.

Heteroskedasticity of the errors was assessed and addressed within the models using a maximum likelihood method of fit (Faraway 2006; Matthiopoulos 2011, Zuur *et al.*, 2009). In addition, the distribution and outliers of each variable were considered to determine whether any variables should be adjusted for the model to a logarithmic scale (Elgin Perry, pers. comm.). A log transformation of chlorophyll-*a* made the deviations from the model more symmetric and reduced the influence of outliers.

The **third** stage of model development was validation of the second-stage model. Model validation was done using ConMon station data from seven stations not including Sycamore Point. ConMon stations used were from the Corsica River, the Patuxent River, and the Potomac River. Data were first adjusted using the first stage trigonometric time series equation to maintain a 06:00 to 05:59 diel cycle. The resulting model predictions of daily DO amplitude were compared to DO amplitude calculated directly from these ConMon DO measurements. The difference between observed and predicted DO amplitude or bias was graphically assessed. Root mean square error was also assessed.

3-4 Results

3-4.1 Stage One: Trigonometric Time Series

The trigonometric time series revealed two main points about data collected at ConMon stations. The first is that the dissolved oxygen data were highly variable within a 24 hour period, ranging from nearly anoxic to highly super-saturated. The second point is that dissolved oxygen concentrations were extremely seasonal with high daily fluctuations occasionally reaching very low levels during summer and periods of low fluctuation and high levels of DO in winter. These patterns in variation from nearly hypoxic to super-saturated within these time periods were observed across all stations in all tributaries that were considered (Figs. 3-3, 3-4, 3-5).

Data exploration of the trigonometric time series led to the following results. Daily DO patterns were visually analyzed and a fit of $R^2=0.7$ was used as a filter criteria for model input. This R^2 was determined to be the cutoff value for the tradeoff between DO measurements resembling a biologically mediated DO curve while maintaining enough data to create a statistically meaningful model (Table 3-1). Visuals of typical diel DO cycles seen and their corresponding R^2 are reported to give an idea of the type of data that was included or excluded (Fig. 3-6). This step helped simplify the modeling process by keeping only biologically mediated processes. Data that likely included physical events, such as wind events or other water mass movements and daily fluctuations in PAR due to cloud cover, would make modeling too complex for the purpose of this exploratory exercise.

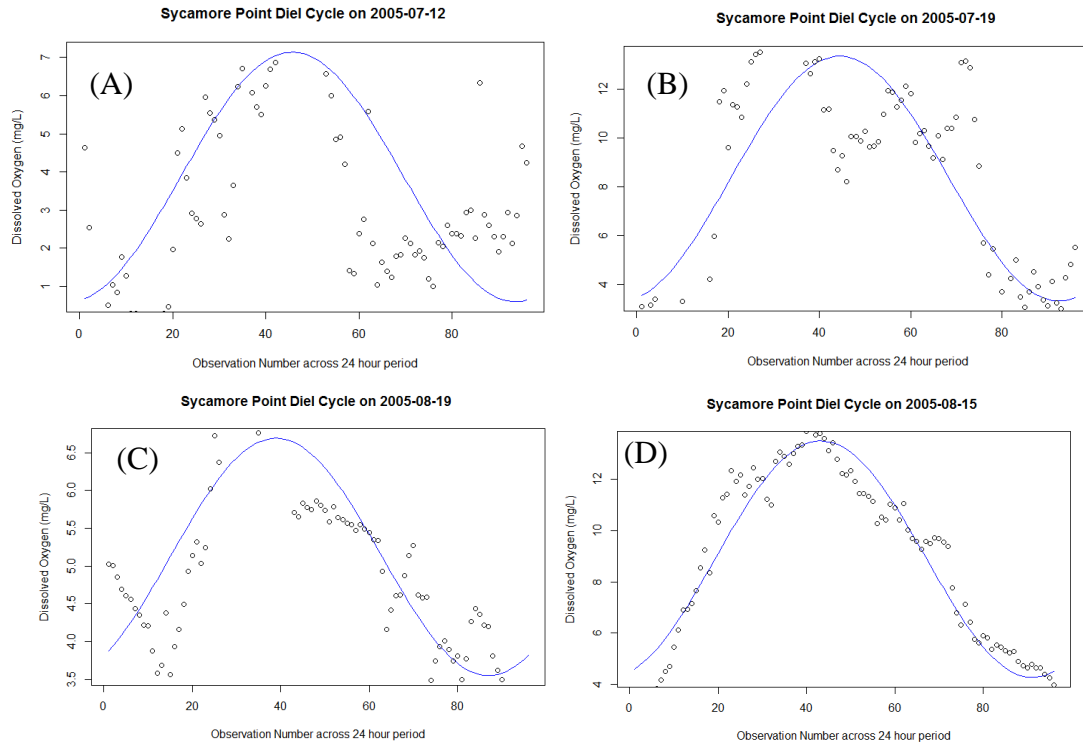


Figure 3-6. Examples of diel DO ConMon data plotted (black dots) with a trigonometric time series fit (blue line). The fits are (A) $R^2=0.5$, (B) $R^2=0.6$, and (C) $R^2=0.7$ and (D) $R^2=0.9$. An R^2 of 0.7 was used as the lower limit value for ConMon DO data that resembled an expected daily biological curve.

Table 3-1. Total number of observations from Sycamore Point 2003-2005 ConMon data that were considered for inclusion in model. One observation is equivalent to one full diel cycle.

R^2 value	Number of Observations	Percent of total observations
0.5	619	54%
0.6	492	43%
0.7	349	30%
0.8	171	15%
0.9	45	4%
Total observations	1150	100%

Amplitudes reported for the biologically relevant days followed the expected pattern: DO was highly variable within a 24 hour period and DO had a wide range in summer months and a smaller range in winter months. The trigonometric time series reinforced this pattern of seasonality across all tributaries analyzed (Fig. 3-7). The trigonometric time series also revealed that while the overall range in DO followed similar seasonal patterns, the scale at which the DO range occurred varied from season to season. Thus, we needed to verify that any model that predicted DO range captured this seasonal variation in scale. Variation in scale between sites was most likely due to local primary production and respiratory processes. The site differences for

primary production and respiration are most likely due to differences in nutrient loads and water residence time.

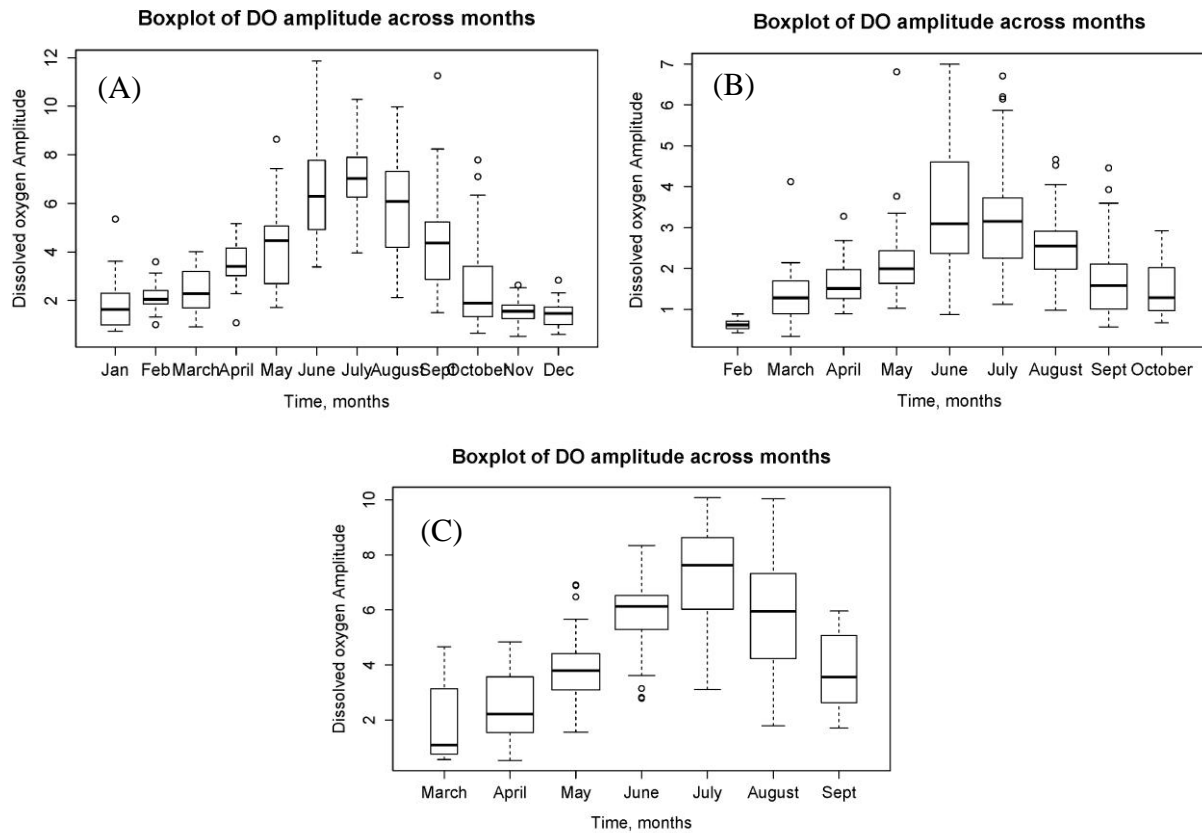


Figure 3-7. Time series boxplots of DO amplitude from (A) Sycamore Point (Corsica River) 2005-2008 and (B) CBL (Patuxent River) 2003-2005 and (C) Fenwick (Potomac) 2004-2008. Dark horizontal lines indicate median values. Boxes represent monthly amplitude inter-quartile range, revealing that winter months (October-April) had a much smaller daily range in DO values than summer months (May-August). Widths of boxes correspond to the frequency of data available for that month.

3-4.2 Stage Two: DO Amplitude Model

The model was created using the ConMon station Sycamore Point in the Corsica River. The current statistical model created indicates that $\log(\text{chlorophyll-}a)$, water temperature, month, and PAR are key factors in predicting daily DO range:

$$DOamp = f(\log(\text{chlorophyll} - a) + \text{water_temperature} + \text{PAR} + \text{month})$$

Model variables were consistent between sites and this bodes well for later use as a global model. To ensure that model selection and fit was accurate, a series of regression models were created and Akaike information criterion (AIC) values, residual plots, and assumption tests (such as Shapiro, Wilcox, Breusch-Pagan and Durbin-Watson) were compared to choose the best model (Figs. 3-8, 3-9).

It was determined that the DO amplitude data exhibit patterns of non-constant variance and correlation amongst residuals (Breusch-Pagan test $p=0.0002$; Durbin-Watson test $p=0.01$). The linear model using the least squares estimator assumes homogeneous variances and independent observations and was rejected because the data violated both of these assumptions. The GLM can accommodate some forms of heteroskedastic variance, but was rejected because the dependence among residuals indicated a violation of the independence assumption. GLS and GAM deal with both non-constant variance and correlation. It was established using added variable plots that the relationship between variables and amplitude was linear; therefore the complex spline function model of the GAM was not needed to model this simple linear relationship and the GAM was rejected in favor of the simpler linear model of GLS (Weisberg 1985). An ordinary linear model using least squares estimator alone did not account for the seasonal heterogeneity apparent within the model variables; therefore a GLS fit by maximum likelihood was used with a correlation structure based on month (Fig. 3-8).

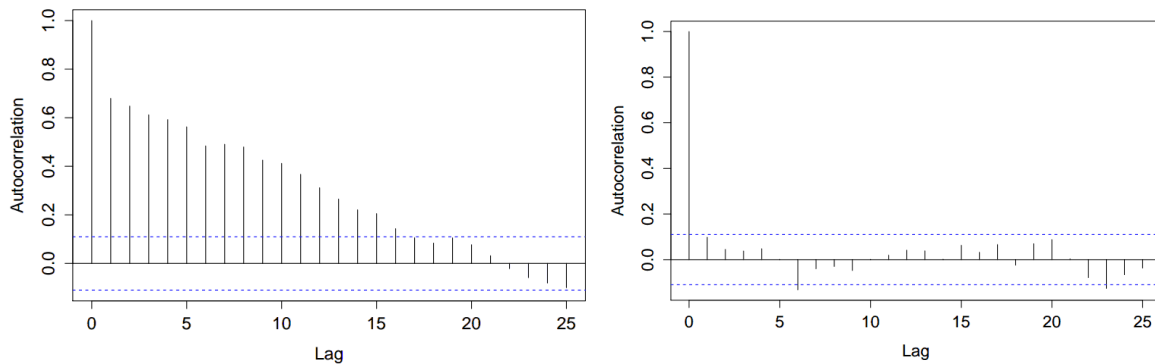


Figure 3-8. An autocorrelation function plot from the Sycamore Point ConMon station data (left) and final GLS model (right) selected. Both plots display the correlation between different time steps within the same variable. Values within the range of the dotted line do not have significant correlation. The vertical lines from the Corsica ConMon data in the left plot that extend far from zero indicate there was correlation amongst raw data points. The vertical lines from the GLS model right plot close to zero confirm that the correlation between time steps within the selected model was small.

Seasonal heterogeneity was observed in model residuals (Fig. 3-9). This issue was addressed using a correlation structure to account for the correlation between variables (Zuur *et al.*, 2009; Matthiopoulos 2011; Fox 2002) defined by an identity function based on month.

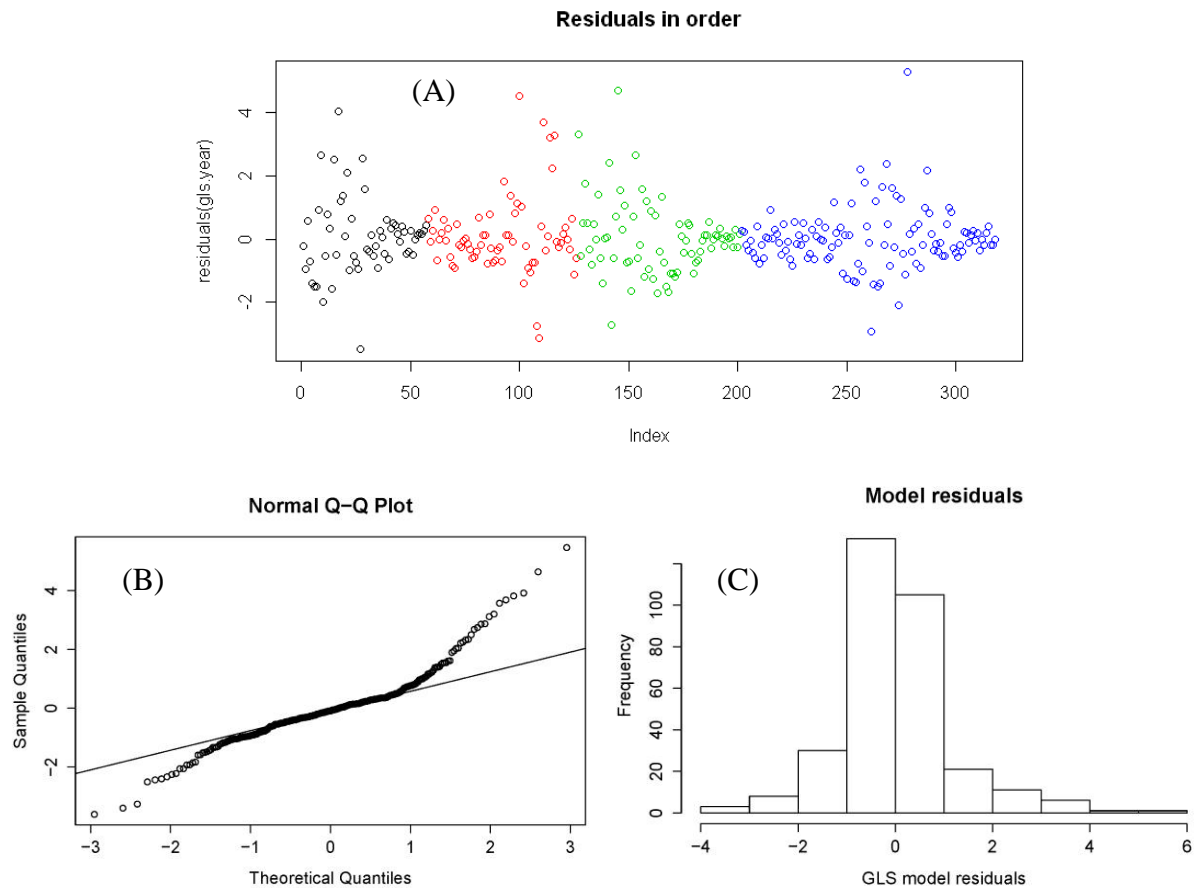


Figure 3-9. GLS model residuals after seasonal correction. In (A) each color corresponds to a year starting in January 2005 (black) and proceeding to December 2008 (blue). An obvious scatter of errors (i.e. greater variation from the model) was apparent in summer months while a smaller range was visible during winter months. The normal error spread was reported in the (B) Q-Q plot and (C) frequency of errors bar plot. Plots were used in evaluating the assumption tests Shapiro-Wilk (1965), Wilcox (1945), and Durbin-Watson (1950).

Anova tests revealed that PAR, log(chlorophyll-*a*), month, and water temperature were significant variables within the model (Table 3-2). Therefore, a suitable and simple GLS model using fit by maximum likelihood for the purpose of this exploratory exercise was selected with the following variables included: month, water temperature, log(chlorophyll-*a*), and PAR (Table 3-3). Coefficients of month successfully captured the seasonality of DO amplitude so the model remained an annual predictive tool.

Table 3-2. Analysis of Variance for Stage 2 DO Amplitude Model. Variables with their associated p-value that were kept according to associated p-values from Anova tests with the GLS model.

Coefficient	df	F-value	p-value
Month	11	63.019	<0.0001
Water Temperature	1	30.529	<0.0001
Log(Chlorophyll- <i>a</i>)	1	115.799	<0.0001
PAR	1	25.156	<0.0001

The model predicted DO patterns in amplitude well when compared to observed amplitudes. It successfully captured inter-annual and intra-annual patterns in DO range fluctuation (Fig. 3-10). It failed to capture the maximum DO amplitude, but this is an unresolved problem amongst all proposed DO models using classical statistics. This overestimation of DO minimum can be seen as a conservative estimate of the DO amplitude during summer months (Beck 1987; Borsuk *et al.*, 2001; Basant *et al.*, 2010; Prasad *et al.*, 2011)

Sycamore Point 2005–2008

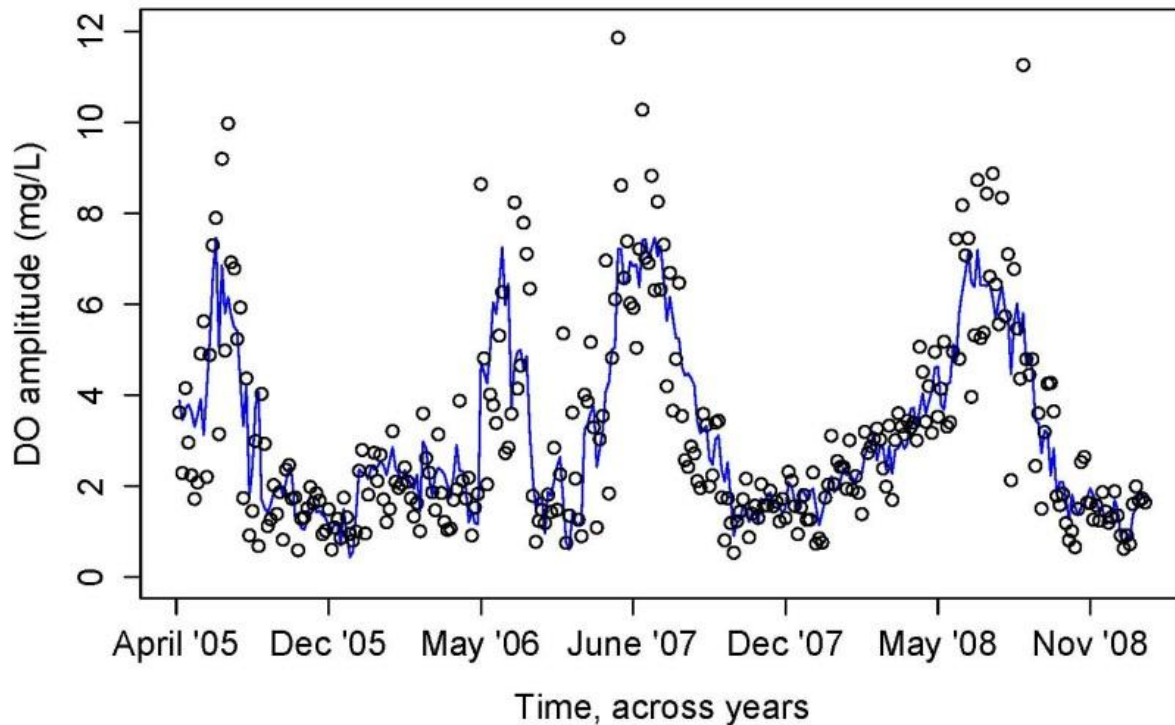


Figure 3-10. The results of the GLS model created from Sycamore Point (Corsica River) data from January 2005 to December 2008. The open black dots are DO amplitude from observed ConMon data and the blue line is predicted DO amplitude from the model.

Table 3-3. Coefficients for final DO Amplitude Model.

Parameter	Estimate	Std.err	t value	p-value
Jan	-2.00	0.340	-5.896	0.000
Feb	-.0520	0.200	-2.641	0.009
March	-0.420	0.224	-1.873	0.062
April	-0.330	0.316	-0.105	0.917
May	-0.410	0.463	0.893	0.372
June	1.680	0.700	2.402	0.017
July	2.030	0.511	3.984	0.000
August	1.310	0.567	2.304	0.022
Sept	0.700	0.471	1.486	0.138
October	-0.003	0.331	-0.009	0.992
November	-0.180	0.195	-0.947	0.344
December	-0.150	0.172	-0.890	0.374
Water temp	0.100	0.014	6.731	0.000
PAR	0.030	0.006	5.016	0.000
log(Chlorophyll-<i>a</i>)	1.70	0.156	10.916	0.000

Month was included as a factor variable to compensate for the heterogeneity within the data set. In addition, month was used rather than an all-encompassing seasonal variable to hopefully pick up on algal speciation or sedimentation events that would be missed by seasonal markers such as water temperature and PAR.

After estimating a model with seasonal effect, the most important variable was log(chlorophyll-*a*). This is consistent with other research which finds that large diel DO ranges are associated with large algal and macrophyte (SAV) communities (Seeley 1969; Sampou and Kemp 1994; Zimmerman and Canuel 2000). Note that the distribution of chlorophyll-*a* was highly skewed which was the motivation for using a log transformation of the chlorophyll-*a* data.

The next most important variable was daily mean water temperature. Water temperature has effects both on respiration (DO loss from the water column) and photosynthesis (DO gain in the water column). In addition, oxygen saturation levels in warmer water decrease but we suspect the effects of higher respiration and photosynthesis are sufficiently strong enough to result in a strong relationship in spite of being moderated by the effect of temperature on DO saturation.

Finally, the last variable to enter the model was PAR. Low values of sunlight were associated with lower amplitudes in the DO cycle. The DO diel range was sensitive to PAR due to insufficient light on cloudy days for photosynthesis to occur therefore suppressing DO range.

3-4.3 Stage Three: DO Amplitude Model Validation

Amplitude model predictions were verified using other ConMon station data compared to model output (Fig. 3-11). Model predictions captured seasonality patterns within years and between years accurately. Most stations and tributary DO amplitude were captured with good success. In a few instances maxima peaks were missed, as is the case with most current DO predictive

models. DO amplitude was significantly missed at Fenwick station in the Potomac (Fig. 3-11). Other stations in the Potomac, such as Blossom Point and Piney Point, had accurate model predictions. This could indicate that there are other driving forces at the Fenwick station that are not captured by this model and that an upstream/downstream water mass tracer variable should be considered.

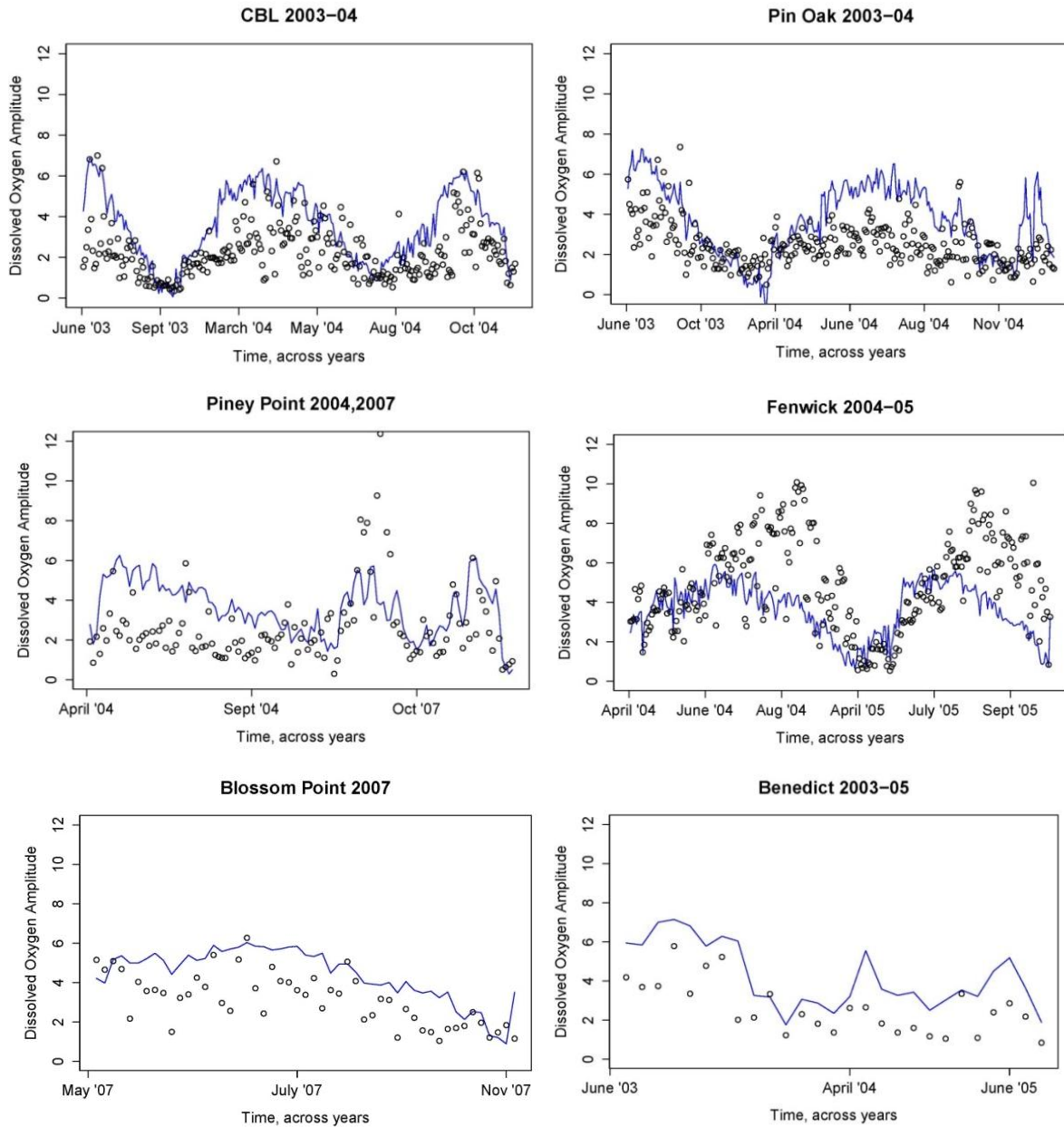


Figure 3-11. The DO amplitude prediction output of the GLS model from Chesapeake Bay tributaries. These include stations from the Patuxent, the Potomac, and the Corsica River. The open black dots are DO amplitude in mg/L calculated directly from observed ConMon data. The blue line is predicted DO amplitude in mg/L from the model.

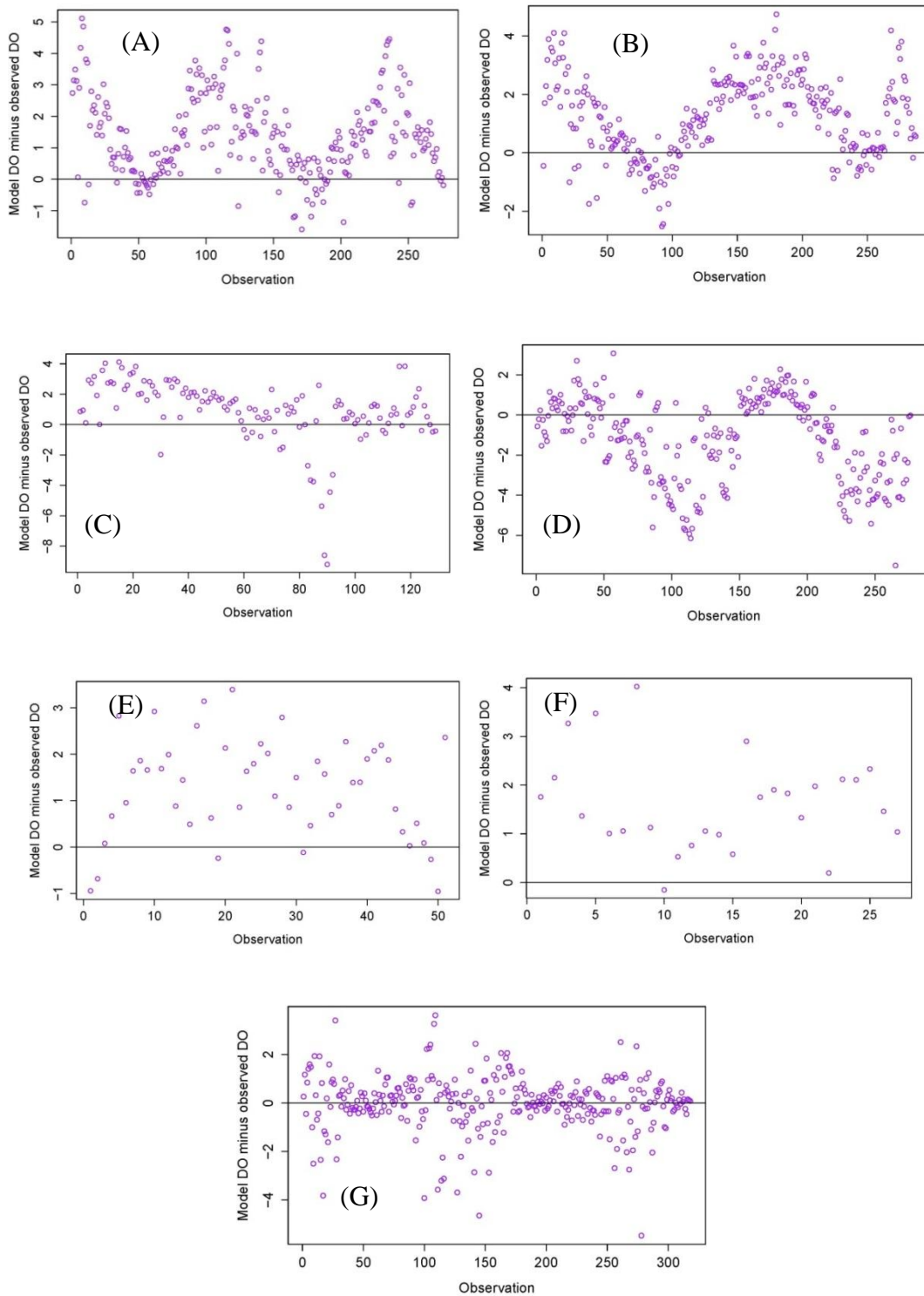


Figure 3-12. The difference between predicted DO amplitude and observed DO amplitude for each observation at (A) Chesapeake Biological Lab,(B) Pin Oak, (C) Piney Point, (D) Fenwick, (E) Blossom Point, (F) Benedict, (G) Sycamore Point in mg/L. The purple dots reflect the difference between predicted DO amplitude and observed DO amplitude.

The Stage 2 DO amplitude model’s ability to capture the peak DO amplitude was more important than capturing the DO amplitude’s trough because the purpose of the model was to accurately assess DO minimum. The peaks in a DO amplitude model will provide information on the widest possible range of DO for that day and therefore predict the lowest possible DO values. The model accurately predicted the peaks of the ConMon stations (Fig. 3-11). Therefore, overall model validation proved successful and the GLS amplitude model was sufficient to predict DO daily amplitude measurements across tributaries and years (Wang *et al.*, 2003; Naik and Manjapp, 2011). The model tended to overestimate DO range in the Patuxent River, underestimate DO range in the Potomac, and have little or no bias in DO range in the Corsica River (Fig. 3-12). However, the model does a relatively good job of capturing (Beck 1987, Chapra 1997) seasonal and daily patterns in DO amplitude fluctuation in the Corsica (Figs. 3-10, 3-11). Root mean square error of each validation test is provided for comparison of relative goodness of fit to other DO models produced in other studies (Table 3-4).

Table 3-4. Root mean square error of validation runs

Site (Tributary)	RMSE
Benedict (Patuxent)	1.89
CBL (Patuxent)	1.89
Pin Oak (Patuxent)	1.84
Piney Point (Potomac)	2.26
Blossom Point (Potomac)	1.65
Fenwick (Potomac)	2.43
Sycamore Point (Corsica)	1.15

3-5 Extension of Model to Spatial Assessment

The predictive ability of the model allowed for revisiting of the main purpose of the exercise: using the amplitude model to predict daily DO minimum across a tributary based on Dataflow© data.

The Stage Two DO amplitude model that was created predicted daily surface DO range. This DO range can be used to calculate DO minimum in one location (Fig. 3-13). The DO minimum can be extrapolated to a “whole estuary” scale by coupling the Stage Two DO amplitude model with spatially explicit Dataflow© data (Fig. 3-15). For each location that a Dataflow© measurement was taken the Stage Two DO amplitude model can be used to calculate a daily DO amplitude. This daily DO amplitude can then be used in each location to revert the Dataflow© DO measurement back to its daily minimum. The DO daily minimum is then extrapolated across the whole estuary surface. These steps are explained in further detail throughout the rest of this section. The end result is an assessment of areal DO compliance. In this “proof of concept” analysis we chose to focus on the Corsica River estuary for coupling the DO amplitude model with Dataflow© results. Details are provided in the following sections.

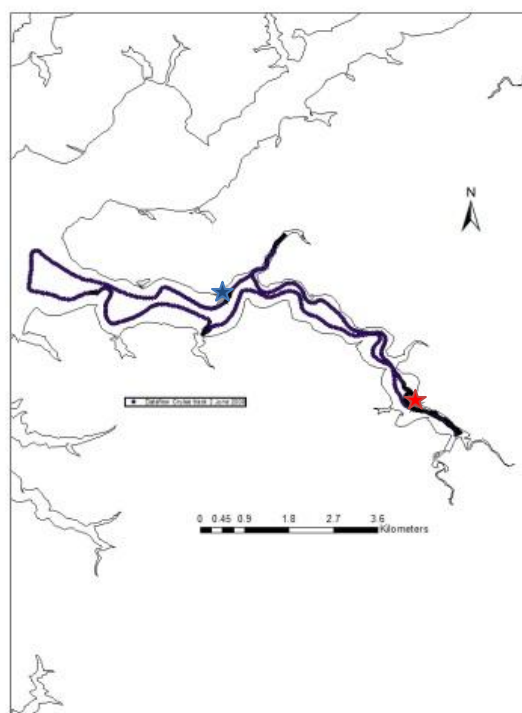


Figure 3-13. A Dataflow© cruise track on 2 June 2008 in the Corsica River. Each point contained all sensor data collected (time, date, DO, GPS location, water temperature, and chlorophyll-*a*). In this figure there were a total of 1001 observations collected. The red star indicates the position of Sycamore Point ConMon station and the blue star Possum Point ConMon station. These were the only ConMon stations in the Corsica River in 2008.

The first step to predict instantaneous spatial DO minimums from the statistical model was to determine the amount of the predicted DO amplitude to subtract from the Dataflow© measured DO. This was done using site specific averages of ConMon measured DO across multiple years (Fig. 3-14). The DO measures for one ConMon station were averaged across multiple years and seasons. The ConMon station chosen was the station that was being extrapolated spatially, so in this case it was Sycamore Point from the Corsica River. The averages were computed within bins defined by integer values of hour. For example, all DO data points between the hours of 13:00 and 14:00 for one ConMon station were averaged. All resulting hourly averages were plotted using a linear equation $y=mx+b$ to be able to assess the change in dissolved oxygen per hour. This linear equation is referred to as the ‘megacurve’ for the remainder of the paper. The independent variable (x) is DO in mg/L that were averaged from the ConMon Station and the dependent variable (y) is time across the twenty-four hour diel cycle period the DO measurements were taken as defined in pervious sections. The same was done for each tributary during summer months (June-August) across multiple years. This slope (i.e. change in DO across time) was used to calculate the expected DO percent increase per hour in the tributary of interest. This curve also provided a quantitative assessment of the time of day of the expected daily DO minimum and maximum, providing a template to determine at what point on the diel DO cycle the Dataflow© cruise data were collected.

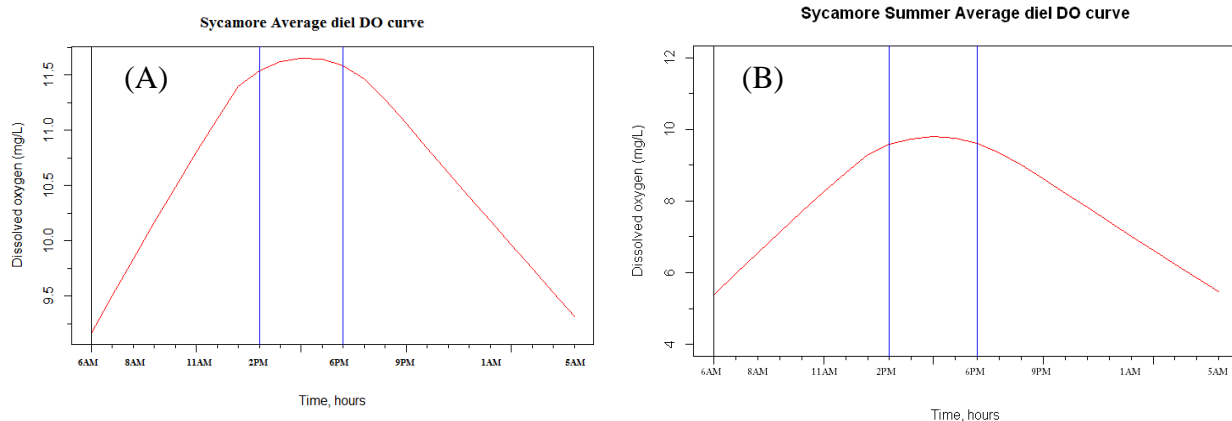


Figure 3-14. Daily expected DO curves in the Corsica River. These curves provide an estimate for the time of day (intercept) for DO minimum as well as a calculation of the expected percent increase of DO per hour (slope). Slope equations were used to calculate the percent hourly increase based on the predicted model DO amplitude and then used to adjust the measured Dataflow© DO back to the daily minimum. Vertical lines at 6AM indicate daily minimum and vertical lines at 2PM and 6PM indicate time range during which maximum DO occurred.

This ‘megacurve’ was used to determine what amount of the DO amplitude should be subtracted from the Dataflow© measurement to reach the DO minimum for that day. The slope of the curve was used to calculate the expected hourly percent increase of DO and the expected time of day that minimum DO occurred. The percent increase per hour was then calculated from the predicted amplitude from the model. This value was then subtracted from the Dataflow© DO measurement based on time of day to calculate DO minimum. For example, a Dataflow© DO measurement of 12 mg/L collected at 2PM with a percent hourly DO change of 1 mg/L would have 8 mg/L subtracted from the Dataflow© measurement to calculate the daily DO minimum. Should the Dataflow© cruise occur after the daily maximum time of day, the percent hourly change is used to add DO back to the maximum based on the time of day. The new maximum value is then subtracted to obtain the 06:00A.M. minimum value. The 06:00 A.M. value was selected as it was the time of day of DO minimum for the expected DO curve.

These calculated DO minimums were input into an ArcGIS map to assess spatial patterns and time-trends concurrently (Fig. 3-15). The Dataflow© observations (Fig. 3-13) were interpolated across the space of the Corsica River to have estimates of the DO minimum across the whole river (Fig. 3-15). Kriging (ESRI 2001) was used to create this continuous map of DO daily minimums. The Geostatistical toolbox available within ArcMap (ESRI 2010) was used. This tool uses patterns of spatial covariance to fit a statistical model to each cruise to achieve the following: (1) capture how the data varies in space and (2) establish weights on observations that minimized estimation variance. In this type of interpolation, the closest observations were given the largest weight when estimating un-sampled points (Fortin and Dale, 2005; Webster and Oliver, 2007). In addition, tributaries were split up using a quadrant during interpolation to also ensure weights were drawn from multiple compass directions rather than simply proximity. The Corsica, for example, was split into a quadrant system to develop these weights and points within 25 pixels in all directions of the Dataflow© cruise and were used for estimation. The quadrant in the Corsica was oriented in the standard NE, SE, SW, and SE directions (Wainger and Bayard,

EPC report 2012; Murphy *et al.*, 2010). This allowed for computation requirements to remain low while still creating a more accurate portrait of the daily DO minimums spatially.

Each color in the DO minimum map corresponds to the level that the daily DO minimum has met DO criteria (Fig. 3-15). In this case, red is serious failure and dark blue is no failure. This map achieved two goals: (1) presenting the minimum DO criteria across this tributary and (2) presenting the DO criteria in an obvious manner.

The maps were used to calculate area coverage of DO minimums each day (Table 3-5). This was done using the Spatial Analyst tools available in the Arc toolbox (ESRI 2010). All areas where DO criteria were not met within the estuary boundary were converted to square meters to enumerate the total coverage of DO criteria failure.

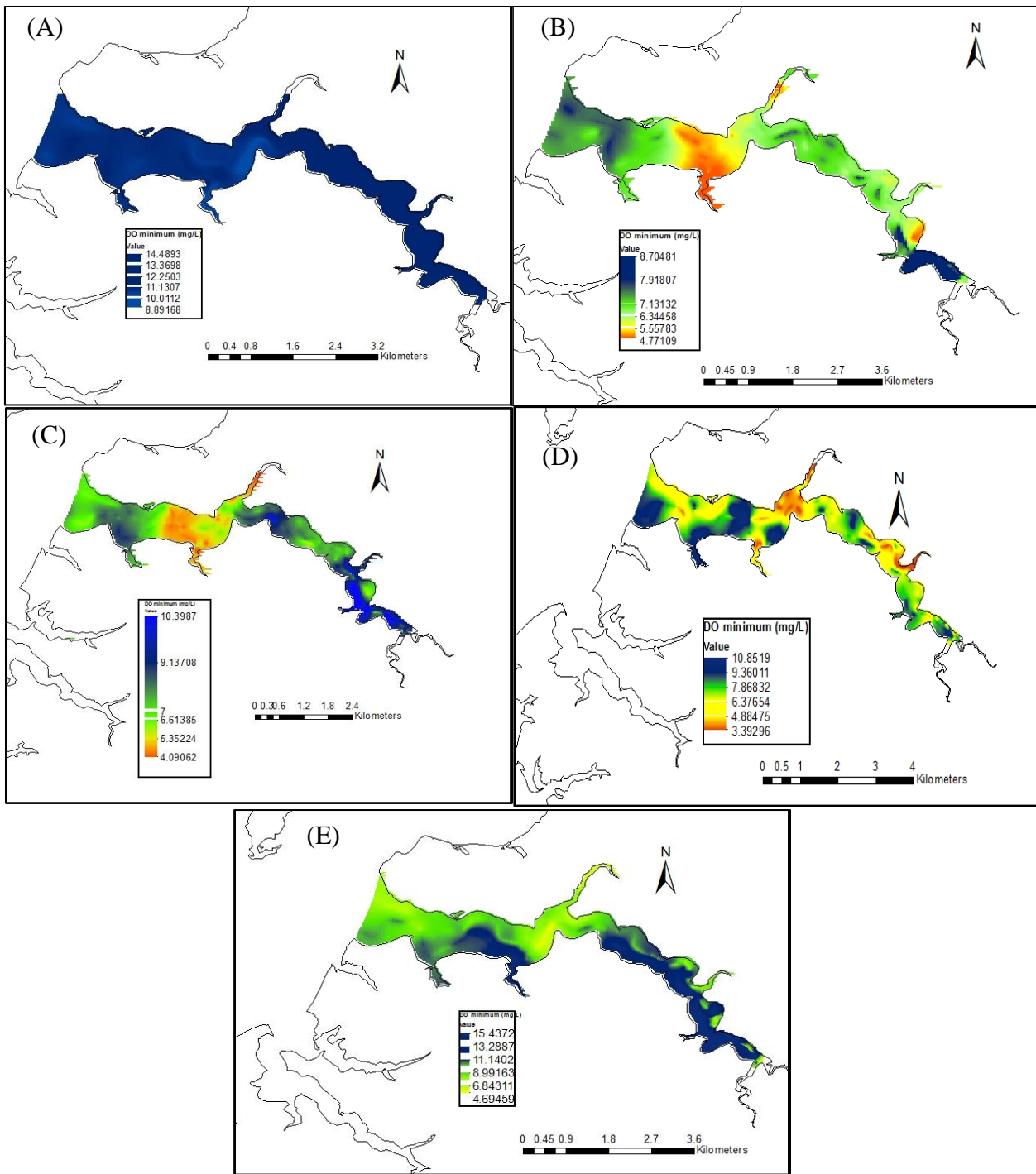


Figure 3-15. Map of the Corsica River on (A) 1 May 2008, (B) 2 June 2008, (C) 16 July 2008, (D) 4 August 2008 and (E) 8 September 2008 with interpolated daily DO minimum values (mg/L) from the Dataflow© data across the entire tributary.

The percent area of the tributary that passed the DO criteria established by the U.S. Environmental Protection Agency (EPA) was evaluated for each day that Dataflow© data were interpolated (Table 3-5). In early spring, the daily DO average was above 8 mg/L. In July, August, and September the majority of the Corsica DO daily minimum was between 5 mg/L and

8 mg/L, often closer to the lower end of that range. In addition, more values less than 5mg/L occurred in summer months with the majority of those values just above 3.2 mg/L. This provided insight into the seasonal changes of DO daily minimum not captured with spatial data alone but captured with the adjustment back to the DO minimum using the predicted amplitude from the model.

Table 3-5. Percent area coverage of each DO criteria in the Corsica River after data interpolation for daily DO minimum value. The range in which the highest percentage of DO values occurred for that day are highlighted in purple.

DO Criteria	1 May 2008	2 June 2008	16 July 2008	4 Aug 2008	8 Sept 2008
<3.2 mg/L	0%	0%	0%	0%	0%
<5 mg/L	0%	1%	0.4%	1.8%	0.1%
5-8 mg/L	6.3%	0.5%	80.3%	76.2%	61.8%
>8 mg/L	93.7%	98.5%	19.3%	22.1%	38.1%

Comparisons between July and August Dataflow© measured DO and calculated daily DO minimum make it apparent that there are distinct differences between measured DO and the actual DO minimum when traced back to the lowest point on the daily DO curve (Fig. 3-16). In addition, the locations of the lowest value DO minimum in the Corsica reveal that it is occurring in different places than the available ConMon data (upriver from where Sycamore Point is located and downriver from Possum Point; Fig. 3-13).

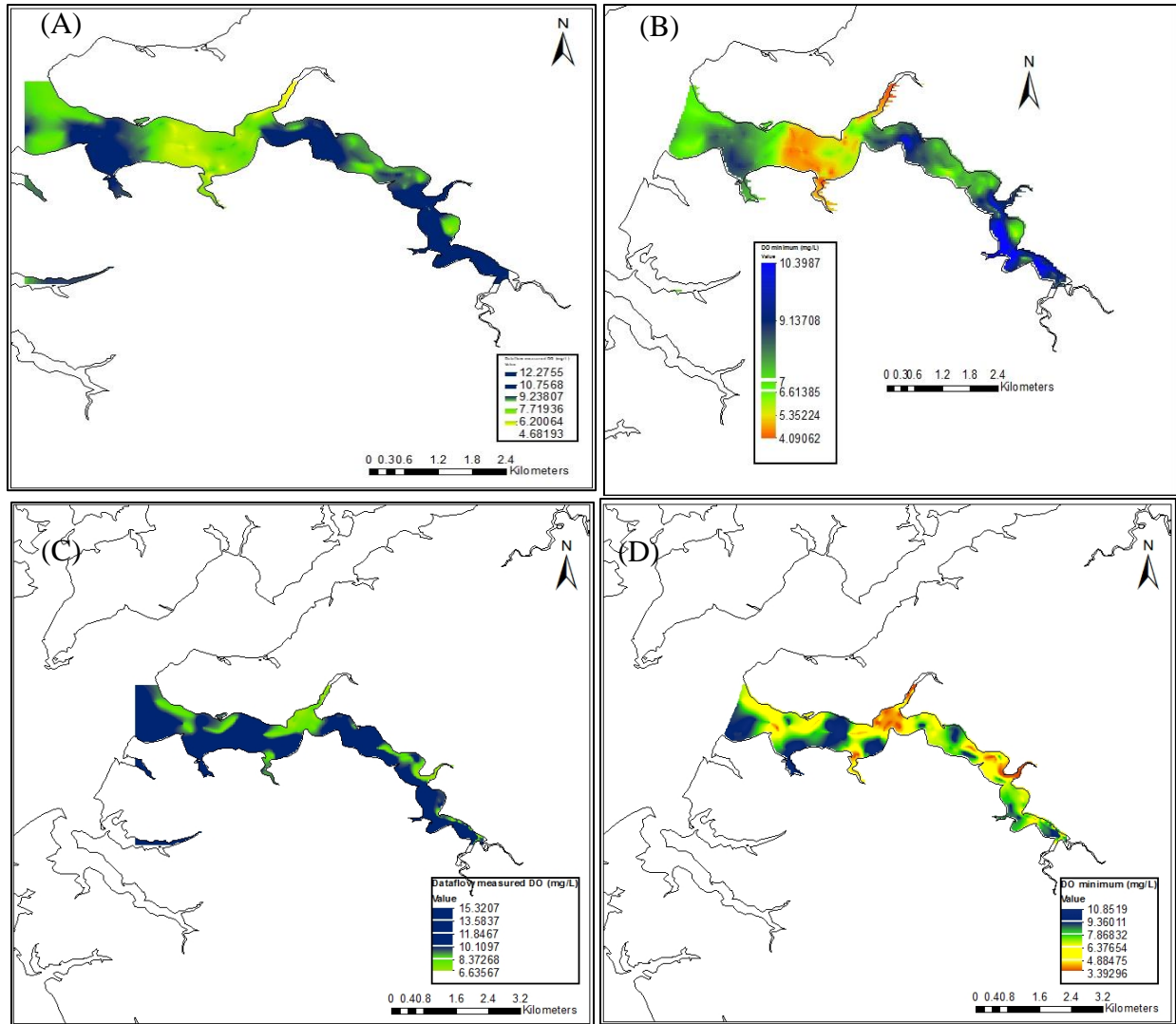


Figure 3-16. Comparison between (A) Dataflow© measured DO on 16 July 2008, (B) calculated DO minimum on 16 July 2008, (C) Dataflow© measured DO on 4 August 2008 and (D) calculated DO minimum on 4 August 2008.

3-6 Discussion, Implications and Future

The results generated by the linear regression GLS model presented in section 3-5 and its ability to predict spatial DO minimum in the Corsica lead to the conclusion that the integration of spatial and temporal data is feasible, necessary and useful as a local and eventually global prediction tool for assessing DO criteria in shallow surface waters. The variability in spatial DO levels (depicted in Fig. 3-16) stresses the importance of assessing all locations in a tributary. Some locations are more hypoxic than others and missing these low DO areas by excluding spatial DO data can have serious repercussions for any organism that is particularly sensitive to hypoxic conditions.

Diel-scale DO variability was evident depending on the day and month that the Dataflow© cruise was made, justifying the need for this adjustment of Dataflow© measurements back to a daily minimum. Comparisons between July and August Dataflow© measured DO and calculated daily DO minimum make a particularly compelling case for emphasizing the importance of this model in management decisions regarding DO criteria assessments. The fact that in both cases values below 5 mg/L became more frequent when DO was calculated back to a daily minimum was highly relevant to scientists examining full ecosystem dynamics and to management that is looking to resolve human and ecosystem dynamics. Even though the model tends to over or underestimate the range of DO for the day, the calculated DO minimum successfully represents the daily DO patterns and is a more accurate representation of DO minimum than the Dataflow© measurements which are generally conducted near the zenith of the diel DO cycle. The results of this model emphasize the point that it would be misleading to carry out DO criteria assessment on an instantaneous and 1-day mean level using only Dataflow© measurements. In addition, the locations of the lowest value DO minimum in the Corsica reveal that it is not occurring at the locations of the available ConMon data (upriver from where Sycamore Point is located and downriver from Possum Point; Fig. 3-13). This also supports the idea that ConMon data cannot be used alone for accurate assessment of DO minimum as the lowest DO values are occurring in places other than ConMon location sites.

The point of this modeling exercise was to build a relationship between DO range and causative variables first to then later go back and refine methods. There are some aspects of model development that should be improved upon to reduce associated error and increase prediction accuracy to make further extension of this model successful.

The main issue with the DO minimum calculation is the under and over estimation of daily DO amplitude based on the tributary assessed (Figs. 3-9, 3-12). This is currently an issue for all known globally proposed modeling systems, such as the Regional Ocean Modeling System (ROMS) used for the Chesapeake Bay Program (Borsuk *et al.*, 2001; Prasad *et al.*, 2011). For the purpose of this proof of concept model, the underestimation of DO amplitude scale was accepted because this results in a more conservative estimate for daily DO minimum. This decision was a trade-off that is currently debated among statisticians. In a more location specific model, lower precision occurs because each system has its own parameter values and is based on less information (Borsuk *et al.*, 2011). However, in a global model parameters may lack site specific processes in the interpretation phase of the model.

Another source of error is the exclusion of DO data collected on days that appear to be dominated by physical rather than biological processes. This exclusion occurred in Stage one when data was filtered for the Step Two DO amplitude model. We excluded these days to simplify the modeling process. In this exercise, a preliminary attempt to include physically dominated DO days was made by using salinity as a marker to track water masses movement throughout a tributary. This was done because the relationship between DO and salinity in the Corsica was found to be inversely proportional and the salinity traces that occurred were happening on time scales too short to be explained by tidal advection of different water masses past the ConMon sensors. It was therefore assumed that the movement of DO was not advective. This tool remains instructive, however, as the prediction of DO is necessary in the management

of the Chesapeake Bay ecosystem and many of the biological mechanisms that forecast DO remain to be fully understood (Prasad *et al.*, 2011).

A final source of error is in the extrapolation of Dataflow© DO data back to a daily DO minimum. When extrapolating the Dataflow© data back to the daily minimum, Dataflow© input parameters for the DO amplitude model use both biologically and physically driven days. There is no current way to determine the difference between those DO cycles in the Dataflow© data. The development of Bayesian prior probability distributions may help to deal with this issue (Borsuk *et al.*, 2001; Albert 2009; Basant *et al.*, 2010). Prior probability distributions are developed by basing the probability distribution on previously collected data and knowledge about the area of interest. In this case, model distribution could be built around the differences in biologically and physically driven days due to the expert knowledge and data sets around expected trigonometric DO curves.

One last point regarding the models used in this exercise is about the depth of the sensors used for data collection of water quality variables. In future studies, the depth of sensors should be maintained at uniform depths. Our impression is that this model missed low values and this is potentially due to the different depths of sensors that collected ConMon data versus Dataflow© data. Near surface water tends to be affected by air-water diffusion and has more light available for photosynthesis. Therefore, near surface water is more apt to have higher values of DO because of phytoplankton photosynthesis. Deeper waters, on the other hand, have lower DO values because of light limited photosynthesis and proximity to bottom using oxygen. This aspect in combination with different physical characteristics of watersheds can lead to a larger margin of error than is acceptable. In the case of this study, the tool developed to segregate days where the DO profile was driven by physical rather than biological processes often eliminated ConMon days with extremely low DO values. Therefore, for the purpose of this study the depth of sensors was not considered.

Despite all of these errors, the model and spatial interpolation remain instructive tools for diel DO amplitude and DO minimum prediction and the model can be used for DO spatiotemporal assessment. The Chesapeake Bay is a complex system and models that include physical processes in the Chesapeake Bay would be ideal and should be incorporated at the next stage of development in temporal and spatial data integration. The biggest task at hand remains defining the physical processes parameters within a model to reduce prediction error. There are many routes that model development could proceed to improve upon the methods used here. One such route is this idea of salinity as a tracer for physical processes. It could be included in model development through the use of causal models to follow these non-tidal and wind events.

Another modification would be to incorporate physical processes in a biological model like the one constructed in this study by incorporating Bayesian methods in the trigonometric time series transformation (Borsuk *et al.*, 2001; Greene *et al.*, 2009; Basant *et al.*, 2010). This would allow for the development of a DO amplitude coefficient that responds to priors such as water temperature, for example, to distinguish between physical events and biological events. The Bayesian method could be utilized to detect weak diel cycles that are related to phytoplankton bloom changes or some other phenomena. In addition, it could be used in a hierarchical manner

to transform use of this simple model to a more general global model and then elaborate further with site-specific responses to physical processes.

This model and map provide DO criteria assessment at time intervals that the Bay program does not yet assess on this spatial scale. The integration of spatial and temporal data equips scientists and managers with a more accurate representation of dissolved oxygen daily fluctuation and provides a way to determine the actual daily DO minimum across a tributary such as the Corsica. This removes limiting factors of water quality studies such as survey effort that is limited to certain times and locations. This will better inform management of the entire system response at the appropriate time scale.

The possibility remains for a broader application of this model using a combination of ConMon and Dataflow© information to depict habitat suitability with even more accuracy. The first extension of this model should be to capture the DO minimum values that are poorly estimated in some locations, whether it is by an extension of parameters or change in statistical technique from Classical to Bayesian as discussed previously. The next extension of the current model should then be to obtain DO minimums to assess instantaneous and 24 hour DO criteria across all Chesapeake tributaries at seasons and times of interest. Finally, the last task that remains to fully utilize this modeling approach is to use aerial remote sensing in combination with ConMon data to use this model in places where no Dataflow© data are available. In addition to these extensions, the magnitude of diel amplitude could be developed as an indicator of an impaired water body.

3-7 References

Albert, Jim. Bayesian Computation with R. New York, NY: Springer-Verlag New York, 2009.

Basant, N., Gupta., S., Malik, A., and Singh, K.P. 2010. Linear and nonlinear modeling for simultaneous prediction of dissolved oxygen and biochemical oxygen demand of the surface water – A case study. *Chemometrics and Intelligent Laboratory Systems*, 172-180.

Beck, M.B. 1987. Water quality modeling: a review of the analysis of uncertainty. *Water Resour. Res.* 23, 1393-1442.

Bishop, M. J., Powers, S. P., Porter, H. J., & Peterson, C. H. 2006. Benthic biological effects of seasonal hypoxia in a eutrophic estuary predate rapid coastal development. *Estuarine, Coastal and Shelf Science*, 70(3), 415-422.

Borsuk, M. E., Higdon, D., Stow, C. A., & Reckhow, K. H. (2001). A Bayesian hierarchical model to predict benthic oxygen demand from organic matter loading in estuaries and coastal zones. *Ecological Modelling*, 143(3), 165-181.

Boynton, W.R. and W.M. Kemp. 2000. Influence of river flow and nutrient loading on selected ecosystem processes: a synthesis of Chesapeake Bay data. pp. 269-298, In: Hobbie, J. (Ed.), A Blueprint for Estuarine Synthesis. Beckman Center, Univ. of California at Irvine, CA. [UMCES Contribution No. 3224-CBL].

Boynton, W. R., Testa, J. M., Kemp, W. M., Cornwell, J. C., Palinkas, C. M., Brooks, M. T., & Bailey, E. M. 2009. An ecological assessment of the Corsica River estuary and watershed: scientific advice for future water quality management. University of Maryland Center for Environmental Science.

Boynton, W.R., E.M. Bailey, L.A. Wainger, M.A.C. Ceballos, K.V. Wood, W.M. Kemp, J.M. Testa, M.T. Brooks, J.C. Cornwell, M.S. Owens, and C. Palinkas. Ecosystem Processes Component (EPC). Maryland Chesapeake Bay Water Quality Monitoring Program, Level 1 report No. 25 Jul. 1984—Sept. 2008. Ref. No. [UMCES] CBL 08-080. [UMCES Technical Series No. TS- 565-08].

Boynton, W.R., L.A. Wainger, E.M. Bailey, and M.A.C. Ceballos. Ecosystem Processes Component (EPC). Maryland Chesapeake Bay Water Quality Monitoring Program, Level 1 report No. 26 Jul. 1984—December 2008. Ref. No. [UMCES] CBL 09-082. [UMCES Technical Series No. TS- 583-09].

Boynton, W.R., L.A. Wainger, E.M. Bailey, A.R. Bayard, C.L. Sperling and M.A.C. Ceballos. Ecosystem Processes Component (EPC). Maryland Chesapeake Bay Water Quality Monitoring Program, Level 1 report No. 29 Jul. 1984—Dec. 2011. Ref. No. [UMCES] CBL 12-020. [UMCES Technical Series No. TS- 637-12].

Chapra, S.C. 1997. Surface Water-Quality Modeling. Boston, MA: McGraw-Hill.

Faraway, Julian James. Extending the linear model with R: generalized linear, mixed effects and nonparametric regression models. Boca Raton: Chapman & Hall/CRC, 2006.

Fortin, Marie, and Mark R. T. Dale. Spatial analysis: a guide for ecologists. Cambridge, N.Y.: Cambridge University Press, 2005.

Fox, John. An R and S-Plus companion to applied regression. Thousand Oaks, Calif.: Sage Publications, 2002.

Greene, R. M., Lehrter, J. C., & III, J. D. H. 2009. Multiple regression models for hindcasting and forecasting midsummer hypoxia in the Gulf of Mexico. *Ecological applications*, 19(5), 1161-1175.

Henrichs, S. M. 1992. Early diagenesis of organic matter in marine sediments: progress and perplexity. *Marine Chemistry*, 39(1), 119-149.

Johnson, J. B., & Omland, K. S. 2004. Model selection in ecology and evolution. *Trends in ecology & evolution*, 19(2), 101-108.

Kemp, W.M., P.A. Sampou, J. Garber, J. Tuttle, and W.R. Boynton. 1992. Seasonal depletion of oxygen from bottom waters of Chesapeake Bay: roles of benthic and planktonic respiration and physical exchange processes. *Marine Ecology Progress Series*, 85,:137-152.

Ludsin, S. A., Zhang, X., Brandt, S. B., Roman, M. R., Boicourt, W. C., Mason, D. M., & Costantini, M. 2009. Hypoxia-avoidance by planktivorous fish in Chesapeake Bay: implications for food web interactions and fish recruitment. *Journal of Experimental Marine Biology and Ecology*, 381, S121-S131.

Matthiopoulos, Jason. How to be a quantitative ecologist the 'A to R' of green mathematics and statistics. Chichester, West Sussex, U.K.: Wiley, 2011.

Montagna, P. A., & Froeschke, J. 2009. Long-term biological effects of coastal hypoxia in Corpus Christi Bay, Texas, USA. *Journal of Experimental Marine Biology and Ecology*, 381, S21-S30.

Murphy, R. R., Curriero, F. C., & Ball, W. P. 2010. Comparison of spatial interpolation methods for water quality evaluation in the Chesapeake Bay. *Journal of Environmental Engineering*, 136(2), 160-171.

Murphy, R. R., Kemp, W. M., & Ball, W. P. 2011. Long-term trends in Chesapeake Bay seasonal hypoxia, stratification, and nutrient loading. *Estuaries and coasts*, 34(6), 1293-1309.

Naik, V. K., & Manjapp, S. 2011. Prediction of Dissolved Oxygen through Mathematical Modeling. *Int. J. Environ. Res*, 4(1), 153-160.

Perry, E. 2012. Adjustment of Dissolved Oxygen Observations for Diel Cycles in Maryland Coastal Bays. Maryland Department of Natural Resources report.

Prasad, M. B. K., Long, W., Zhang, X., Wood, R. J., & Murtugudde, R. 2011. Predicting dissolved oxygen in the Chesapeake Bay: applications and implications. *Aquatic sciences*, 73(3), 437-451.

Sampou, P. and W.M. Kemp. 1994. Factors regulating plankton community respiration in Chesapeake Bay. *Mar. Ecol. Prog. Ser.* 110, 249-258.

Seeley C.M. 1969. The diurnal curve in estimates of primary productivity. *Chesapeake Science* 10, 322–326.

Wang, H., Yuan, J. and Herskin J. 2003. Modeling of Dissolved Oxygen concentration in Sonderup River in Denmark. *Environmental Informatics Archives*, 1, 254-260.

Webster, R., and M. A. Oliver. Geostatistics for environmental scientists. 2nd ed. Chichester: Wiley.2007.

Weisberg, S. Applied Linear Regression, Second Edition, John Wiley & Sons, Inc. 1985.

Wu, R. S., Zhou, B. S., Randall, D. J., Woo, N. Y., & Lam, P. K. 2003. Aquatic hypoxia is an endocrine disruptor and impairs fish reproduction. *Environmental science & technology*, 37(6), 1137-1141.

Zimmerman, A. R., & Canuel, E. A. 2000. A geochemical record of eutrophication and anoxia in Chesapeake Bay sediments: anthropogenic influence on organic matter composition. *Marine Chemistry*, 69(1), 117-137.

Zuur, Alain F. Mixed effects models and extensions in ecology with R. New York: Springer, 2009.

3-8 Appendix

Table 3-6. Descriptions of each type of model tested to predict DO amplitude.

Regression Model type	Description
Linear model (LM)	A model with linear parameters using an ordinary least squares estimator for model parameters
Generalized linear model (GLM)	Same as linear model but specific error distribution and link function for the linear predictor and maximum likelihood estimation.
Generalized least squares (GLS)	Way of estimating the parameters of a linear model when variances of observations are unequal (heteroscedasticity) and there is correlation between observations
General Additive Model (GAM)	Blends properties of GLM with non-parametric additive models. Assume that the mean of the dependent variable depends on an additive predictor through a nonlinear link function. Permit the response probability distribution to be any member of the exponential family of distributions. Specifies a distribution and a link function.
Artificial Neural Network (ANN)	Nonlinear model based on structure and function of biological neural networks; uses Bayesian fit methods and the model can change or learn based on input and output
Causal Model	Assigns causal links between variables

Chapter 4

Role of Late Winter-Spring Wind Influencing Summer Hypoxia in Chesapeake Bay

Younjoo J. Lee, Walter R. Boynton, Ming Li, and Yun Li

4-1	INTRODUCTION	1
4-2	DATA AND METHODS	3
4-2.1	DISSOLVED OXYGEN (DO) AND HYPOXIC VOLUME	3
4-2.2	DENSITY STRATIFICATION, CHLOROPHYLL-A, AND RIVER FLOW	4
4-2.3	WIND, SEA-LEVEL PRESSURE (SLP), AND CLIMATE INDICES	5
4-2.4	ANALYTICAL METHODS	5
4-2.5	HYDRODYNAMIC OCEAN MODEL	6
4-3	RESULTS	6
4-3.1	SELF-ORGANIZING MAP (SOM) ANALYSIS OF DISSOLVED OXYGEN (DO)	6
4-3.2	RELATIONSHIP BETWEEN HYPOXIC VOLUME AND ENVIRONMENTAL VARIABLES	7
4-3.3	MULTIPLE REGRESSION ANALYSIS AND EFFECTS OF LATE WINTER-SPRING WIND	9
4-4	EMPIRICAL ORTHOGONAL FUNCTION (EOF) ANALYSIS OF SEA-LEVEL PRESSURE (SLP)	13
4-5	WIND DIFFERENCE BETWEEN 2000 AND 2003	15
4-6	RESIDUAL FLOW FIELDS FROM HYDRODYNAMIC SIMULATION	16
4-7	DISCUSSION	18
4-8	SUMMARY	21
4-9	REFERENCES	22

4-1 Introduction

The variability of dissolved oxygen (DO) in coastal water is caused by complex interactions between physical transport and biogeochemical production-consumption of oxygen in the water column and sediments. DO often becomes low (hypoxic) or depleted (anoxic) when the rate of supply is less than the rate of consumption. Hypoxic conditions in estuaries have been exacerbated by anthropogenic activities including coastal eutrophication and coastal hypoxia has been increasing in severity, frequency, and duration in many areas of the world (Diaz and Rosenberg, 1995 and 2008). There have been numerous efforts to mitigate hypoxia by reducing nutrient loading rates into estuaries (USEPA, 2010). Despite some reduction of nitrogen loads from point and diffuse sources, severe hypoxic and anoxic events continue to occur, often to a degree lesser or greater than expected from observed relationships based only on nutrient loading rates (Hagy *et al.*, 2004; Lee and Lwiza, 2008a).

It has been suggested that DO depletion results primarily from increased stratification in the water column which inhibits the supply of DO across the pycnocline to the bottom layer (Officer *et al.*, 1984; Seliger *et al.*, 1985) where particulate organic carbon sinks after the spring bloom and is decomposed during summer (Testa and Kemp, 2008). However, Malone *et al.* (1986) suggested that wind-driven oscillation of the pycnocline could provide a mechanism for transporting nutrients and DO onto the shallow flanks of Chesapeake Bay. Sanford *et al.* (1990)

also noted that the large variability of DO was associated with lateral oscillation of the pycnocline due to the longitudinal wind in the bay. O'Donnell *et al.* (2008) and Wilson *et al.* (2008) showed that wind-induced straining of the density field described by Scully *et al.* (2005) plays a dominant role in controlling summer hypoxia through the variations of vertical mixing and ventilation of bottom waters in Long Island Sound. Scully (2010b) also demonstrated that the extent of hypoxia in Chesapeake Bay is strongly modulated by the interactions between vertical mixing over shoal areas and lateral circulation associated with summer wind. More recently, Murphy *et al.* (2011) suggested that the variability of summer hypoxia in Chesapeake Bay was associated with large-scale climate forcing over the last six decades, possibly due to the shifts in prevailing summer wind directions (Scully, 2010a). Scully (2010a) found a significant positive relationship between observed summer hypoxia in the bay and the previous winter North Atlantic Oscillation (NAO) index, which has largely been in a positive phase since 1980 (Hurrell, 1995). This correlation is likely due to more frequent westerly wind (Scully, 2010b) and higher river discharge (Whitney, 2010) and thus summer stratification was enhanced during the positive NAO periods on a decadal time-scale.

However, a large-scale (basin to global-scale) climate index has limitations when it is linked to local climate (Stenseth *et al.*, 2003). For example, the NAO was not found to influence stream flow in the eastern United States (U.S.) (Tootle *et al.*, 2005). Chesapeake Bay is considered to be one of the estuaries where large-scale ocean-atmospheric forcing fails to explain variability since it is strongly influenced by the surrounding watershed (Kimmel *et al.*, 2009). Miller and Harding (2007) demonstrated that the interannual variability of spring phytoplankton biomass was highly responsive to the frequency and type of winter weather patterns prevailing over the watershed area. Miller *et al.* (2006) reported that winter synoptic climatology largely accounted for springtime freshwater flow, varied threefold over the last 52 years, and was related to phytoplankton biomass (Harding and Perry, 1997), zooplankton abundance (Kimmel and Roman, 2004), juvenile anadromous fish recruitment (North and Houde, 2003), and DO conditions (Schubel and Pritchard, 1985; Boicourt, 1992; Hagy *et al.*, 2004). There is growing evidence that climate forcing plays a strong role in recent changes in Chesapeake Bay, but the link between winter-spring (January-May) climate and summer (June-August) hypoxia has not been well established yet, especially a role of late winter-spring (February-April) wind in controlling summer hypoxia. We hypothesized that wind during the spring bloom period may affect the transport or deposition of phytoplankton biomass, the primary organic carbon pool, ultimately responsible for consuming DO during summer.

The purpose of this paper is to improve understanding of the relationship between winter-spring climate variability and its influence on summer hypoxia in Chesapeake Bay, and thus assist further in the development of a predictive tool to forecast the hypoxic volume of the bay. To reach this goal, a comprehensive analysis was performed using water quality monitoring data to identify the characteristics of DO and re-evaluate the relationship between summer hypoxia and possible causative factors. This paper (1) describes the dominant temporal and spatial patterns of summer DO in the mainstem bay using 23 years of observational data from the Chesapeake Bay Program, (2) examines the relationship between seasonal hypoxia and winter-spring processes, (e.g., freshwater flow, nitrogen loading, phytoplankton biomass, and wind with climate variability), (3) predicts summer hypoxic volume based on winter-spring conditions, and (4)

addresses how summer hypoxia can be influenced by the variability of late winter-spring wind based on results obtained from a hydrodynamic ocean model

4-2 Data and Methods

4-2.1 Dissolved oxygen (DO) and hypoxic volume

The Chesapeake Bay Program has monitored water quality in Chesapeake Bay and tributary systems since 1984. The analysis in this study was based on the data collected between 1985 and 2007 at 39 stations in the mainstem of the bay (MD and VA stations) including temperature, salinity, chlorophyll-*a*, and DO in the water column (Fig. 4-1a). These data can be downloaded from a website (<http://www.chesapeakebay.net/data/>). Field survey cruises were conducted monthly or bimonthly (during summer) to sample water quality data including hydrographic and biogeochemical properties. Assuming data collected in each survey cruise could provide a spatial snapshot of measured parameters, we interpolated DO fields based on the cruises that were completed within 5 day periods with a minimum of 28 sampling stations throughout the mainstem of the bay during May-September. The sampling cruises that were completed over a period of more than 6 days due to sampling irregularities (11 out of 195 total field surveys) were excluded from the analysis. Thus, survey data were available for 5 to 6 cruises in most of the summers. DO vertical profiles were interpolated to one meter depth intervals from the surface to the bottom at each station, and then DO fields were horizontally interpolated from the surface to 20 m depth at every one meter. The water column deeper than 20 m was assumed to have the same DO concentration as at 20 m since DO values changed little with depth below 20 m in the observational data. The interpolation was based on the Data Interpolating Variational Analysis (DIVA) software package available at a website (<http://www.seadatanet.org/Standards-Software/Software/DIVA>). Thus, in each valid survey cruise, the observations were interpolated onto a grid with 1 km and 1 m horizontal and vertical spacing, respectively, which is based on the bathymetric information from the NOAA/National Geophysical Data Center Coastal Relief Model (<http://www.ngdc.noaa.gov/mgg/coastal/crm.html>). Hypoxic volume was calculated in each cruise by integrating the volume of interpolated grid cells where DO was below a critical DO threshold (e.g., 2, 3, or 5 mg L⁻¹) and then temporally averaged each year during summer (May- September) season. In this study, we focused on hypoxia defined as DO concentration less than 2 mg L⁻¹ because of its severe impacts on habitat quality (Eby and Crowder, 2002) and sediment nutrient biogeochemistry (Kemp *et al.*, 2005).

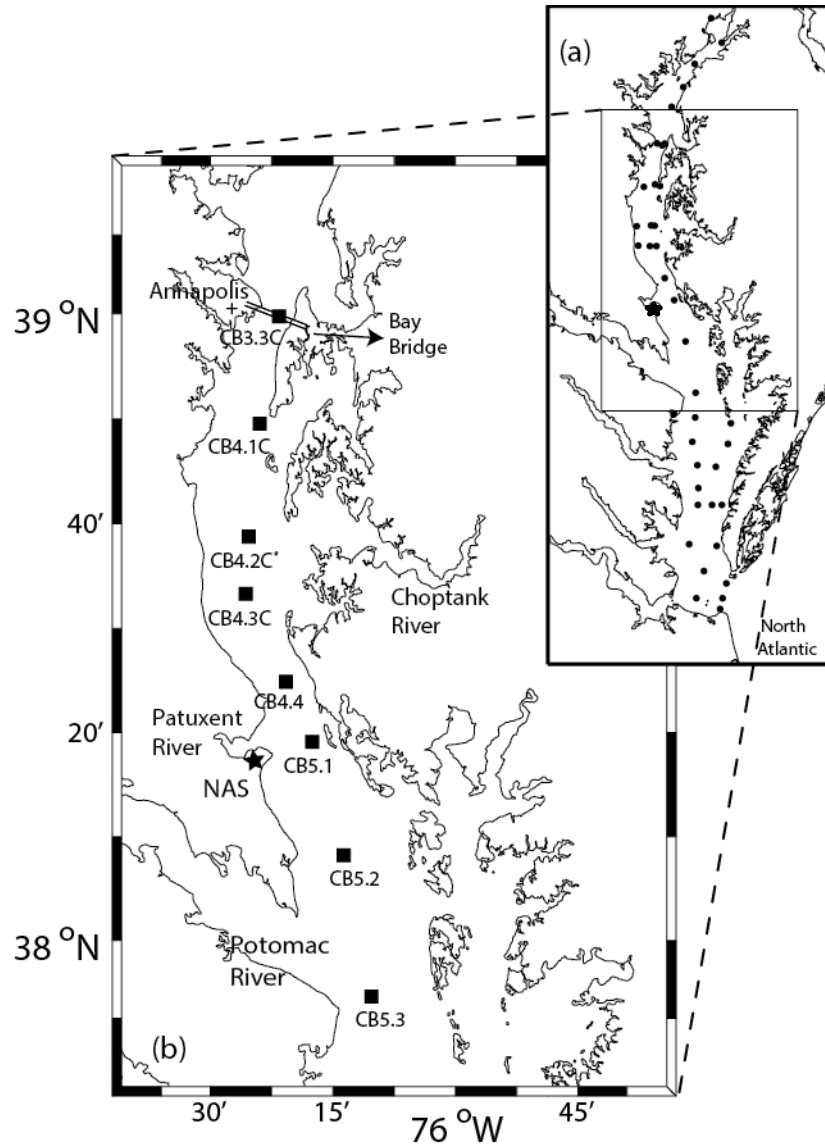


Fig. 4-1. (a) The Chesapeake Bay Program water quality monitoring stations (●) in the mainstem of Chesapeake Bay and (b) the mid-bay section of the bay (square markers indicate the mid-bay stations along the deep channel). The Naval Air Station Patuxent River (NAS) is the location (★) where wind speed and direction were measured.

4-2.2 Density stratification, chlorophyll-*a*, and river flow

Summer hypoxia is shown to be driven by various factors such as density stratification, chlorophyll-*a* concentration, freshwater flow, nutrient loading, and wind condition associated with climate variability. Summer density stratification is related to vertical mixing and thus DO supply below the pycnocline. The Brunt–Väisälä frequency (N^2) was calculated for each station using temperature and salinity (e.g., Pond and Pickard, 1983) to determine the strength of the pycnocline that is mainly controlled by the winter-spring Susquehanna River flow (Hagy, 2002). Since the accumulation of phytoplankton biomass during spring is the principle source of organic matter fueling summer oxygen depletion in the bay (Malone, 1992), measured near-bottom

(within ~2 m off the bottom) chlorophyll-*a* concentration was used as a proxy for phytoplankton biomass produced during the spring bloom period (February-April). Maximum N^2 , water column temperature, and near-bottom chlorophyll-*a* concentration were spatially averaged for the monitoring stations in the mid-bay region as shown in Figure 4-1b. The Susquehanna River discharge is the largest single source (45% of the total riverine freshwater input) to the bay (Lee and Lwiza, 2008b) and it was considered a good estimate of freshwater flow and total nitrogen (TN) loading (Hagy *et al.*, 2004). Both monthly flow and TN loading from the Susquehanna River were retrieved from the U.S. Geological Survey website (<http://waterdata.usgs.gov/nwis>; station ID 01578310).

4-2.3 Wind, sea-level pressure (SLP), and climate indices

Since the dynamics of DO in estuaries are influenced by wind-driven processes (e.g., O'Donnell *et al.*, 2008; Scully, 2010b), wind data were examined from winter to summer seasons. Hourly measurements of wind speed and direction were obtained from the Naval Air Station (NAS) near the mouth of the Patuxent River, a centrally located position in the Chesapeake Bay region (Fig. 4-1b). The wind data were decomposed into two components, including zonal (easterly-westerly; cross-bay) and meridional (northerly-southerly; along-bay) wind velocity ($m\ s^{-1}$) and then averaged by month. To evaluate the influence of winds from different directions on summer hypoxia, the components of wind velocity were computed in various directions by rotating the wind vector from -20 to 60 degrees from the east (0 degrees). Due to the significant role of climate variability in estuarine processes (e.g., Miller and Harding, 2007), monthly sea-level pressure (SLP) from the NCEP/NCAR reanalysis datasets was also investigated for the eastern U.S. bounded by 25-50°N latitude and 65-100°W longitude with 2.5×2.5 degree resolution. The SLP data were acquired from Physical Research Division, the NOAA Earth System Research Laboratory (<http://www.esrl.noaa.gov/psd/data/gridded/data.ncep.reanalysis.html>) and empirical orthogonal function (EOF) analysis was applied to classify spatial climate patterns and extract temporal variability of winter-spring SLP anomalies derived by subtracting monthly climatology. Then, leading EOF modes were compared with the local wind components from the NAS, the North Atlantic Oscillation (NAO), the Niño 1+2 index (sea surface temperature in the region of eastern tropical Pacific bounded by 0-10°S latitude and 80-90°W longitude), and the Bermuda High index (BHI). In this study, the NAO and Niño 1+2 indices were retrieved from the NOAA Climate Prediction Center (http://www.cpc.ncep.noaa.gov/products/monitoring_and_data/oadata.shtml). The BHI was calculated as the pressure difference between Bermuda (32.5°N, 65°W) and New Orleans (30°N, 90°W), Louisiana (Katz *et al.*, 2003) based on the monthly SLP data.

4-2.4 Analytical methods

EOF analysis is a statistical technique used to extract information from large datasets by identifying spatial and temporal structures of variability within a given field in terms of orthogonal functions. The covariance matrix of the data field is decomposed into a set of eigenvalues and eigenvectors. Each eigenvector can be regarded as a spatial pattern, and the eigenvector is projected on to the original field to obtain a principle component time series in

order to see how a given spatial pattern evolves with time (Venegas *et al.*, 1997). Usually, the first few orthogonal functions explain most of the variance and may then be linked to possible dynamical mechanisms (Emery and Thomson, 1997). More detailed description of EOF analysis can be found in Bretherton *et al.* (1992) and Wallace *et al.* (1992).

Summer DO conditions along the axis of the bay were characterized using a self-organizing map (SOM), which is an artificial neural network based on unsupervised learning (Kohonen, 2001). It is an effective tool in extracting patterns from large data sets that may exhibit nonlinear features. SOM analysis has been widely used in various fields of studies (Kaski *et al.*, 1998; Oja *et al.*, 2002) including oceanography (i.e., Richardson *et al.*, 2003; Liu and Weisberg, 2005; Lee and Lwiza, 2008a). Time-dependent patterns in DO were extracted and frequencies of occurrence were quantified using a software package SOM Toolbox 2.0 for Matlab with [3×3] map grid (Vensanto *et al.*, 2000), and the software can be obtained from the Helsinki University of Technology, Finland (<http://www.cis.hut.fi/projects/somtoolbox>).

4-2.5 Hydrodynamic ocean model

The Regional Ocean Modeling System (ROMS) developed for Chesapeake Bay (Li *et al.*, 2007; Li and Zhong, 2009) was used to examine how wind influences residual currents between the years 2000 (moderate hypoxia; 5.6 km³) and 2003 (severe hypoxia; 9.0 km³) with moderate Susquehanna River discharge (1570 and 1700 m³ s⁻¹, respectively) during January-May in both years. The model has an open connection to the Mid-Atlantic Bight and included eight major tributary systems in the bay (i.e., Susquehanna, Patapsco, Patuxent, Potomac, Rappahannock, York, James, and Choptank Rivers). The curvilinear model grid contained 120 by 80 cells with 20 stretched σ -levels in the vertical. The model was forced by observed wind at five weather stations in the bay area, freshwater inflows from eight major rivers based on the USGS daily values, and sea surface temperature (SST) measured by the Chesapeake Bay Program. In the simulation, the vertical eddy viscosity and diffusivity were computed using the k-kl turbulence closure scheme (Warner *et al.*, 2005) with the background diffusivity and viscosity set at 10⁻⁵ m² s⁻¹ (Li *et al.*, 2005). The open boundary conditions include tides specified using the Oregon State University global inverse tidal model of TPXO7, non-tidal sea level fluctuations acquired from a NOAA tidal station at Duck, North Carolina (http://tidesandcurrents.noaa.gov/station_info.shtml?stn=8651370+Duck,+NC), and climatological temperature and salinity extracted from the World Ocean Atlas (<http://www.nodc.noaa.gov/OC5/indprod.html>). The surface elevation and barotropic velocity were prescribed using Chapman and Flather conditions (Flather, 1976; Chapman, 1985). An Orlandi-type radiation boundary condition was applied to baroclinic velocity (Orlandi, 1976). The salinity and temperature fluxes across the open boundary were simulated with a combination of radiation condition and nudging with a relaxation time scale of 1-day (Marchesiello *et al.*, 2001).

4-3 Results

4-3.1 Self-organizing map (SOM) analysis of dissolved oxygen (DO)

To examine how the vertical distribution of DO along the bay axis evolves during summer months, the SOM analysis was applied on the interpolated fields of cruise surveys along the main channel of the bay between May and September (Fig. 4-2). In general, hypoxia ($\text{DO} < 2\text{mg L}^{-1}$) starts near Annapolis, Maryland in May (Fig. 4-2a). Hypoxic condition intensifies in June as hypoxic water expands both vertically and horizontally, and maximum hypoxic volume is attained during July (Fig. 4-2b). Although there is some weakening in stratification during August, hypoxia still persists in the mid-bay area between Annapolis and the mouth of the Potomac River (Fig. 4-2c). As density stratification weakens significantly in September, hypoxic volume is greatly reduced (Fig. 4-2d). By the end of October, hypoxia usually disappears, which is associated with destruction of the strong summer pycnocline (not shown).

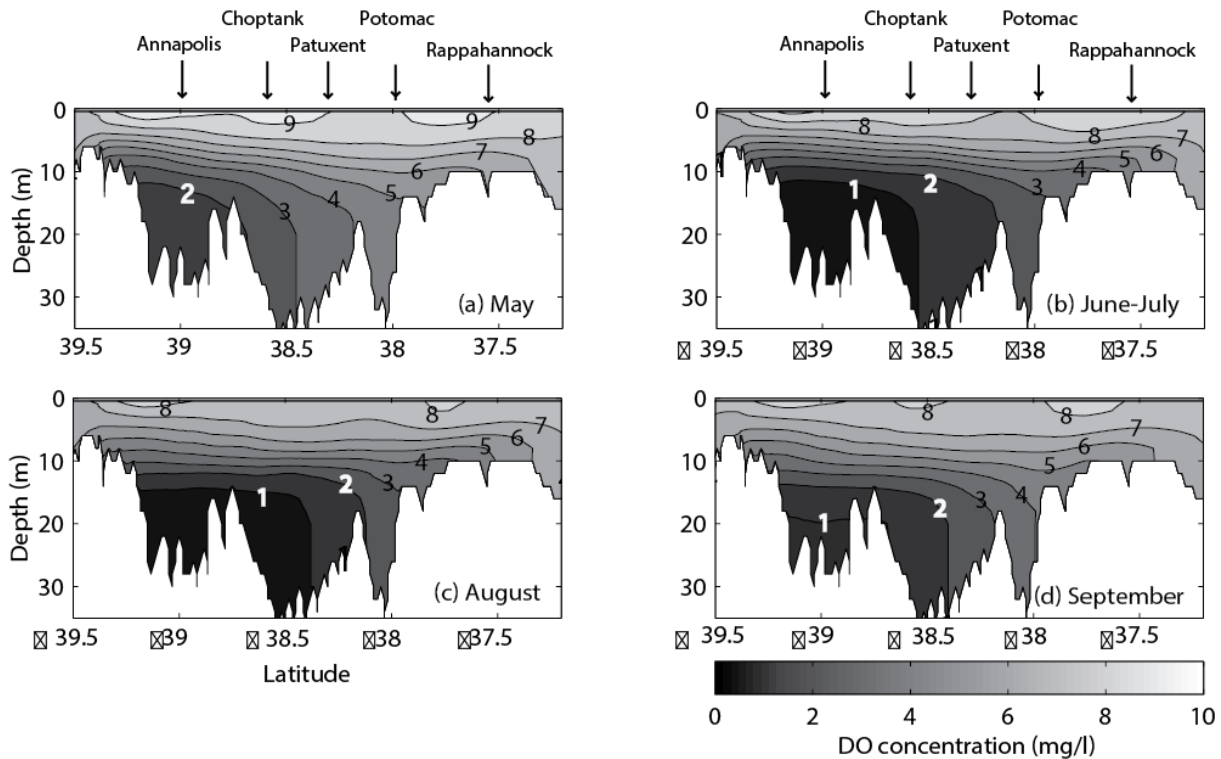


Fig. 4-2. The most frequently observed dissolved oxygen (DO) patterns during 1985-2007 using self-organizing map (SOM) based on the data acquired from the Chesapeake Bay Program water quality database (<http://www.chesapeakebay.net/data/>). The locations along the axis of the Bay where major tributaries enter are marked by arrows in the top panels. The numbers written on contour lines indicates DO concentration (mg L^{-1}).

4-3.2 Relationship between hypoxic volume and environmental variables

We found, as have others, that summer (June-August) hypoxia in the bay is generally coupled with the development of a strong pycnocline ($r=0.70$, $p<0.01$; Fig. 4-3). Years with high (low) spring discharge tend to produce stronger (weaker) stratification during summer. However, the amount of freshwater was not always strongly related to seasonal hypoxia, especially in the years with wet winter-spring conditions (e.g., 1994 and 1996 in Fig. 4-3). In contrast, large hypoxic

volumes ($> 7.0 \text{ km}^3$) were observed in 4 out of 7 years when winter-spring (January-May) river discharge was moderate or less than average ($1300\sim 1700 \text{ m}^3 \text{ sec}^{-1}$; 1986, 1987, 1989, and 2003 in Fig. 4-3). Table 4-1 indicates that the nutrient-laden freshwater from the land not only contributes to stratification in the water column but also enhances phytoplankton growth in the bay. The interannual variability of summer hypoxia is correlated with the winter-spring river discharge ($r=0.60$, $p<0.01$) and TN loading ($r=0.59$, $p<0.01$) from the Susquehanna River as well as the near-bottom chlorophyll-*a* concentration ($r=0.42$, $p<0.05$) during the spring bloom periods. However, hypoxia exhibited no significant relationship to summer winds. We also examined nitrogen and phosphorus concentrations from the Susquehanna River, but no significant correlation with summer hypoxic volume emerged (not shown).

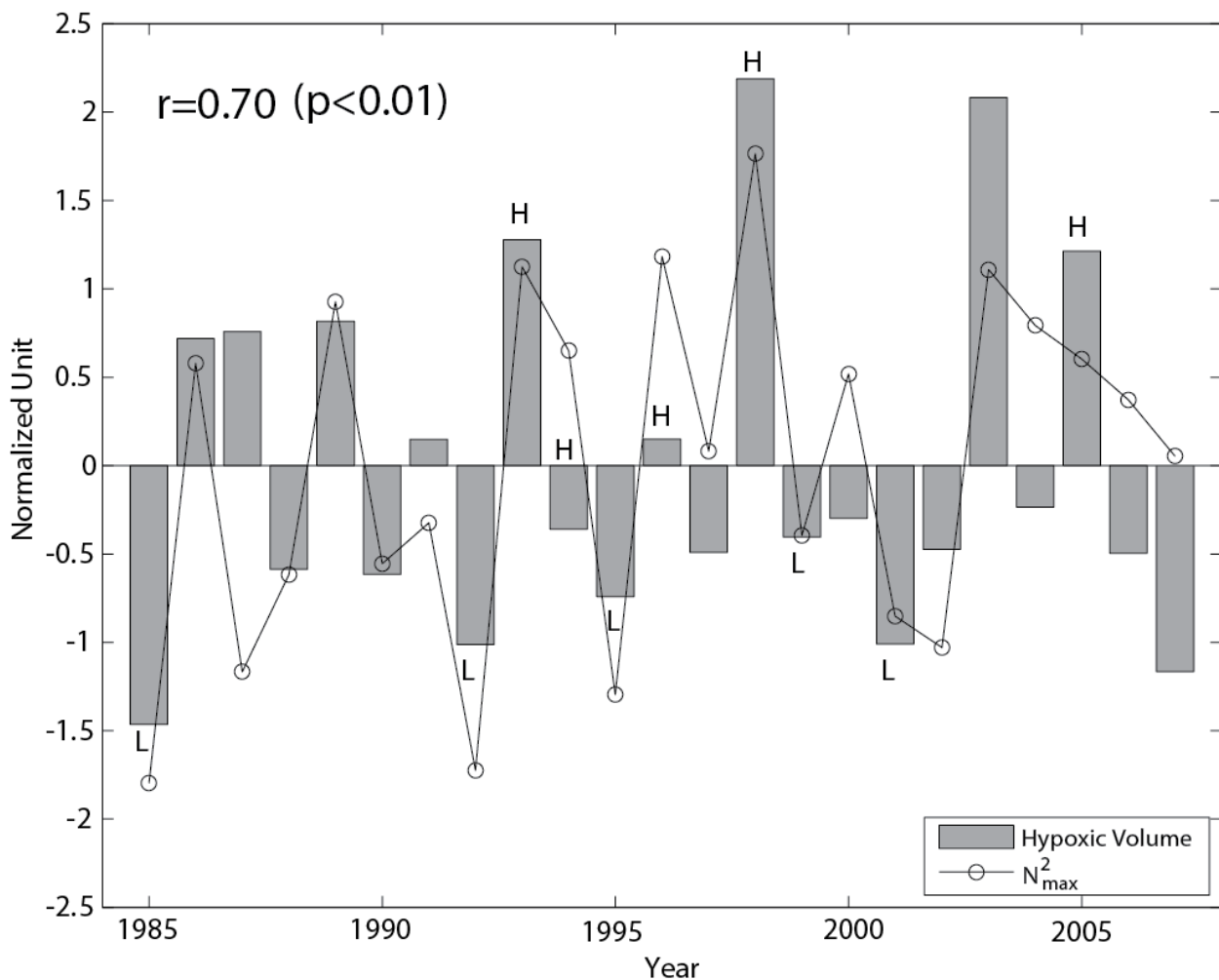


Fig. 4-3. Mean summer (June-August) hypoxic volume and maximum density stratification (N^2_{\max}) in the mid-bay region (see Fig. 4-1b) during 1985-2007. Each time series is normalized by subtracting its mean value and dividing the difference by its standard deviation. H indicates a year with high winter-spring (January-May) discharge (greater than $2000 \text{ m}^3 \text{ s}^{-1}$) and L indicates a year with low winter-spring discharge (less than $1250 \text{ m}^3 \text{ s}^{-1}$) from the Susquehanna River. The correlation coefficient (r) is shown in the upper-left.

Table 4-1. Summary of correlation coefficients (r) between mean summer (June-August) hypoxic volume (km^3), winter-spring (January-May) freshwater discharge ($\text{m}^3 \text{s}^{-1}$) and total nitrogen (TN) loading (kg day^{-1}) from the Susquehanna River, near-bottom chlorophyll- a concentration (Chla, $\mu\text{g L}^{-1}$) in the mid-bay region during the spring bloom period (February-April), summer maximum density stratification (N^2_{max} , $\text{rad}^2 \text{sec}^{-2}$) in the mid-bay, and summer zonal (east-west) and meridional (north-south) wind velocity (m s^{-1}). Significant relationships ($p < 0.05$) are indicated in bold numbers.

	Hypoxic volume	River discharge	TN loading	Chla	N^2_{max}	Zonal wind	Meridional wind
Hypoxic volume		0.60	0.59	0.42	0.70	0.06	-0.13
River discharge			0.95	0.44	0.80	0.14	0.20
TN loading				0.48	0.70	0.17	0.30
Chlorophyll- a					0.35	0.19	0.07
N^2_{max}						0.20	-0.16
Zonal wind							0.44
Meridional wind							

4-3.3 Multiple regression analysis and effects of late winter-spring wind

In order to model summer hypoxia using a linear regression method, TN loading was eliminated and summer stratification and river discharge were mutually excluded since the major factors influencing hypoxia are intercorrelated with each other as shown in Table 4-1 (i.e., river discharge, TN loading, bottom chlorophyll- a , and summer stratification). Hence, two regression models became available for estimating hypoxic volume during summer. One model is based on two independent variables (summer stratification and spring near-bottom chlorophyll- a concentration) and another model is dependent on one variable (winter-spring river discharge). Both models produced significant results but the relationship with observed hypoxic volume was relatively weak (Fig. 4-4a and 4-4b). We further explored the residuals from these regression models to enhance the relationship by adding other factors one at a time. We found that the regression residuals as well as summer hypoxia had a significant relationship with the late winter-spring (February-April) zonal (easterly-westerly; cross-bay) wind velocity (m s^{-1}), which was not intercorrelated with any other variables listed in Table 4-1. Considering winds from different directions, the northeasterly-southwesterly (NE-SW) wind exhibited the strongest correlation coefficient with summer hypoxic volume in Chesapeake Bay ($r = -0.71$; $p < 0.01$; Table 4-2). This relationship indicates that the severe hypoxic events having volume greater than 7.0 km^3 coincided with frequent northeasterly winds whereas the mild to moderate hypoxia is associated with frequent southwesterly winds.

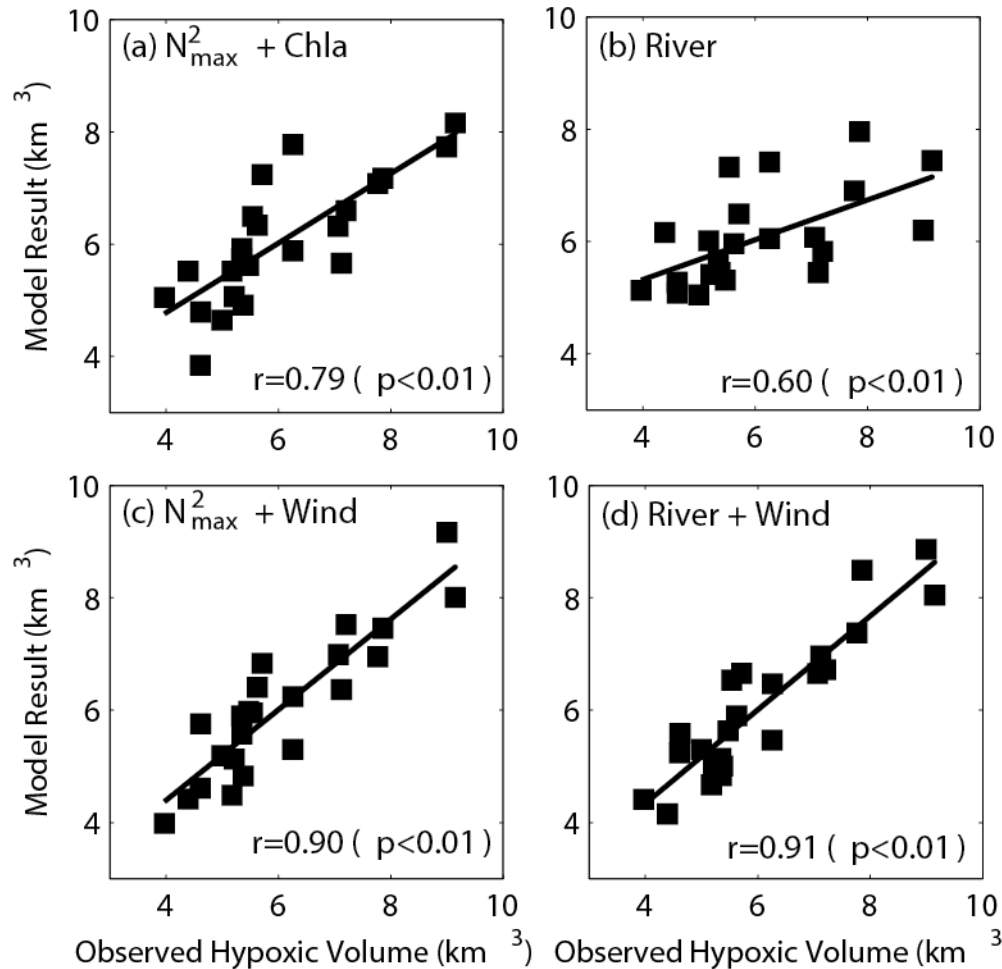


Fig. 4-4. Results from application of several multiple linear regression models. Observed mean summer hypoxic volume (km^3) represents the June-August period in the years 1985-2007 as a dependent variable on the x-axis and the modeled values are plotted on the y-axis. Independent variables are (a) mean summer (June-August) maximum density stratification (N_{max}^2 , $\text{rad}^2 \text{ s}^{-2}$) and spring (February-April) bottom chlorophyll-*a* concentration (Chla, $\mu\text{g L}^{-1}$) in the mid-bay, (b) mean winter-spring (January-May) freshwater flow (River, $\text{m}^3 \text{ s}^{-1}$) from the Susquehanna River, (c) mean summer maximum density stratification and late winter-spring (February-April) northeasterly-southwesterly wind velocity (Wind, m s^{-1}), and (d) mean winter-spring freshwater flow and late winter-spring northeasterly-southwesterly wind velocity. The solid lines indicate the least-square fit from linear regression models and the correlation coefficients (r) are shown in the lower-right of each panel.

Table 4-2. Correlation coefficient (*r*) between mean summer (June-August) hypoxic volume (km³) and late winter-spring (February-April) zonal (easterly-westerly) wind velocity (m s⁻¹; no rotation, 0 degrees). The mean zonal wind is rotated by changing a wind vector polar angle from -20 to 60 degrees to maximize correlation with summer hypoxic volume. Thus, the northeasterly-southwesterly wind, rotated counterclockwise by 30 degrees from the east, was used for the analysis of this study. 0 degrees indicates east and north is 90 degrees.

Wind vector polar angle (degrees) from the east	Hypoxic volume (km ³)
60	-0.59 (<i>p</i> <0.01)
50	-0.65 (<i>p</i> <0.01)
40	-0.69 (<i>p</i> <0.01)
30	-0.71 (<i>p</i> <0.01)
20	-0.71 (<i>p</i> <0.01)
10	-0.70 (<i>p</i> <0.01)
0	-0.67 (<i>p</i> <0.01)
-10	-0.62 (<i>p</i> <0.01)
-20	-0.57 (<i>p</i> <0.01)

By adding the NE-SW wind velocity component during late winter-spring, the results from the several regression models (Fig. 4-4a and 4-4b) were greatly improved. The correlation coefficient (r) between the model and observations became 0.90 ($p < 0.01$) and 0.91 ($p < 0.01$), respectively (Fig. 4-4c and 4-4d). Figure 4-4c shows that the model consists of two independent variables (wind and stratification) because a stepwise regression eliminated the near-bottom chlorophyll- a concentration when the late winter-spring wind was included in the regression model from Figure 4-4a. Since we could reasonably estimate the magnitude of summer hypoxia using winter-spring conditions (NE-SW wind and river discharge), we tested how the regression model (Fig. 4-4d) performed in forecasting summer hypoxia. After the regression model was produced using the first half of the Chesapeake Bay Program data set (1985-1995), summer hypoxia was predicted using the rest of the data set (1996-2007). Observed and predicted hypoxia were plotted together in a scatter diagram (Fig. 4-5) and data clustered around a slope of 1.0 (diagonal line), showing good agreement between the model and observations ($r = 0.91$; $p < 0.01$). The mean difference between observation and predictions was 0.10 km^3 indicating that the prediction error of summer hypoxia was not very biased. The root-mean-square error (RMSE) was 0.64 km^3 . The largest model-data misfit occurred in 1998 and 2001 when the river flow was the highest ($2360 \text{ m}^3 \text{ s}^{-1}$) and the lowest ($1100 \text{ m}^3 \text{ s}^{-1}$), respectively during the predicted years (1996-2007).

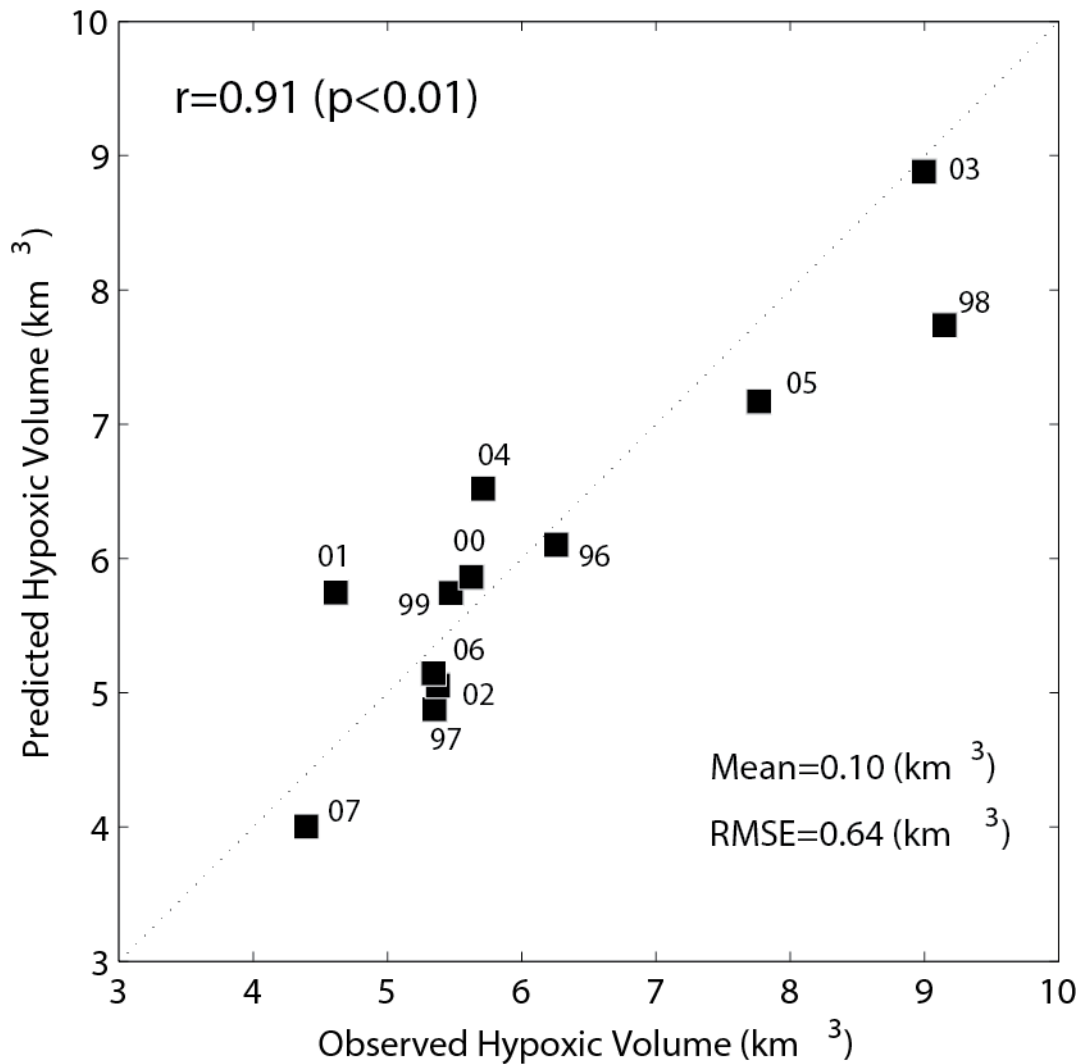


Fig. 4- 5. Relationship between the observed and predicted summer hypoxic volume (km^3) using a multiple linear regression model from Fig. 4-4d with two independent variables: mean winter-spring (January-May) freshwater flow (River, $\text{m}^3 \text{s}^{-1}$) from the Susquehanna River and late winter-spring (February-April) northeasterly-southwesterly wind velocity (Wind, m s^{-1}) from the Naval Air Station Patuxent River (see Fig. 4-1b). The regression model ($\text{Hypoxia}_{\text{predicted}} = 0.00142 \cdot \text{River} - 1.99 \cdot \text{Wind} + 3.94$) was derived from the data between 1985 and 1995 and then the model was verified with the observed hypoxic volume representing the June-August period in the years of 1996-2007. The mean and root-mean-square error (RMSE) between the observed and predicted are shown in the lower-right. The dotted lines indicate a slope of 1.0, and the correlation coefficient (r) is shown in the upper-left.

4-4 Empirical orthogonal function (EOF) analysis of sea-level pressure (SLP)

Although the regression analysis was based on local wind conditions from a weather station, the observed wind pattern may have resulted from climate variability over larger areas. This suggested that we should determine the connection between local wind and larger-scale climate by analyzing SLP to extract the spatial pattern and temporal variability for the eastern U.S. The

first EOF mode of the monthly SLP anomaly (February-April; 1985 to 2007) accounted for 61% of the total variance and the spatial pattern exhibited lower amplitude in the northern U.S. and higher amplitude centered on the southeastern U.S. (Fig. 4-6a). The first mode was significantly correlated with the February-April NAO index ($r=0.61$, $p<0.01$; Fig 4-6b). The second EOF mode explained 15% of the total variance and showed a spatial pattern of north-south oscillation (Fig. 4-6c) which may promote the observed variability of late winter-spring zonal wind. The second mode exhibited the teleconnection (a linkage between weather patterns at large distances) with El Niño/Southern Oscillation (ENSO) since it was correlated with the February-April Niño 1+2 index ($r=-0.61$, $p<0.01$; Fig. 4-6d). The third EOF mode showed an east-west oscillation with 11% of the explained variance (Fig. 4-6e), which may be related to the variability of meridional wind. We found that the third mode was significantly correlated with the February-April BHI ($r=0.60$, $p<0.01$; Fig. 4-6f). Among the first three EOF modes, the late winter-spring NE-SW wind from the NAS was statistically correlated to the principle component time series of the second mode ($r=0.73$, $p<0.01$), but the wind showed no significant relationship with the Niño 1+2 index. Different months during December-May and modes from EOF analysis in SLP anomalies were also considered, and the second EOF mode of the February-April SLP anomaly produced the strongest relationship with the late winter-spring wind.

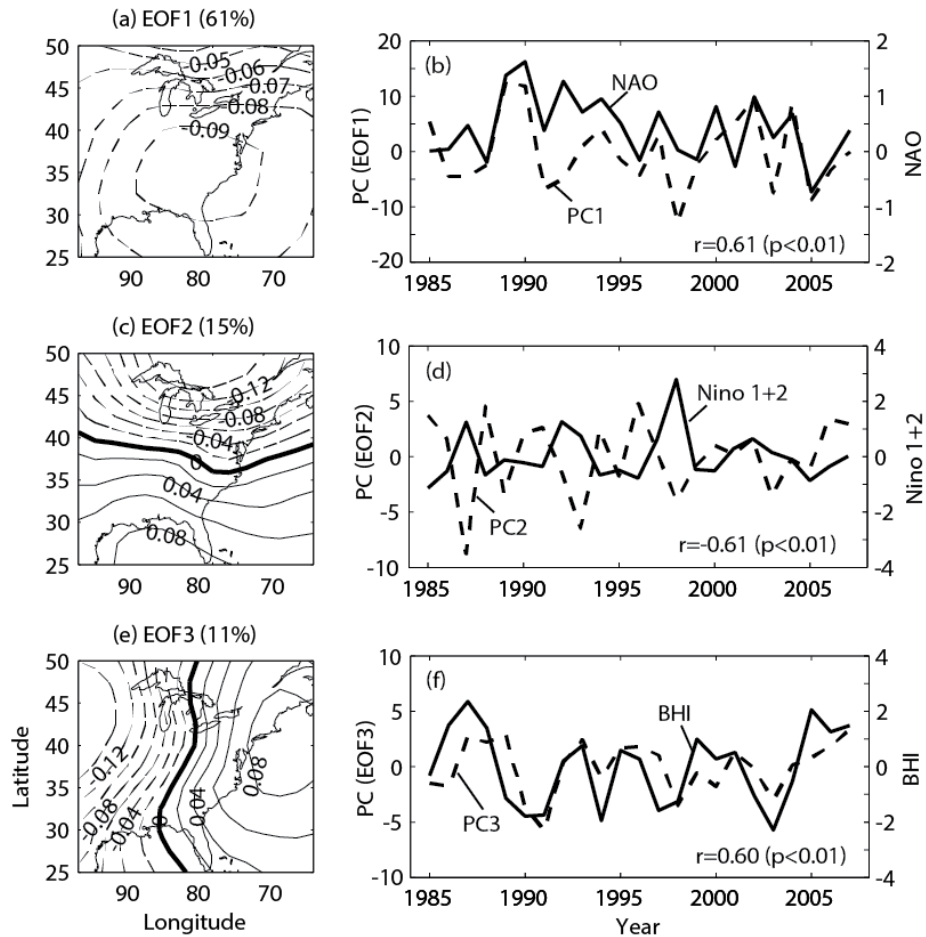


Fig. 4-6. Panels (a), (c), and (e) are the spatial patterns of the first three modes from an empirical orthogonal function (EOF) analysis that is based on sea-level pressure (SLP) anomalies during the late winter-spring (February-April) in the eastern United States (1985-2007). A percentage of the total variance explained is shown on the top of each panel. The solid contour lines are positive values while the dashed lines correspond to negative values with a contour interval of 0.01 in the panel (a) and 0.02 in the panels (c) and (e). The principle component time series (PC) of each EOF mode is compared with (b) the North Atlantic Oscillation (NAO) index, (d) the Niño 1+2 sea surface temperature (SST) anomaly index, and (f) the Bermuda High index (BHI) during February-April. The correlation coefficients (r) are shown in the lower-right in each panel.

4-5 Wind difference between 2000 and 2003

Prior to running a numerical model, we analyzed how late winter-spring wind was different between two years. Wind speed was similarly distributed between 2000 and 2003 with a mean value of 4.7 m s^{-1} (Fig. 4-7a and 4-7b). However, differences in wind direction were notable between the two years, especially for northeasterly and southwesterly winds (Fig. 4-7c and 4-7d) which were found to be related to summer hypoxia (Table 4-2). There were more frequent observations of northeasterly wind during 2003 than 2000 whereas southwesterly winds were more prevalent during 2000 compared to 2003. During the years when northeasterly winds in late winter-spring were frequently observed, summer hypoxia in the bay was severe (i.e., 1986, 1989, 1998, and 2003).

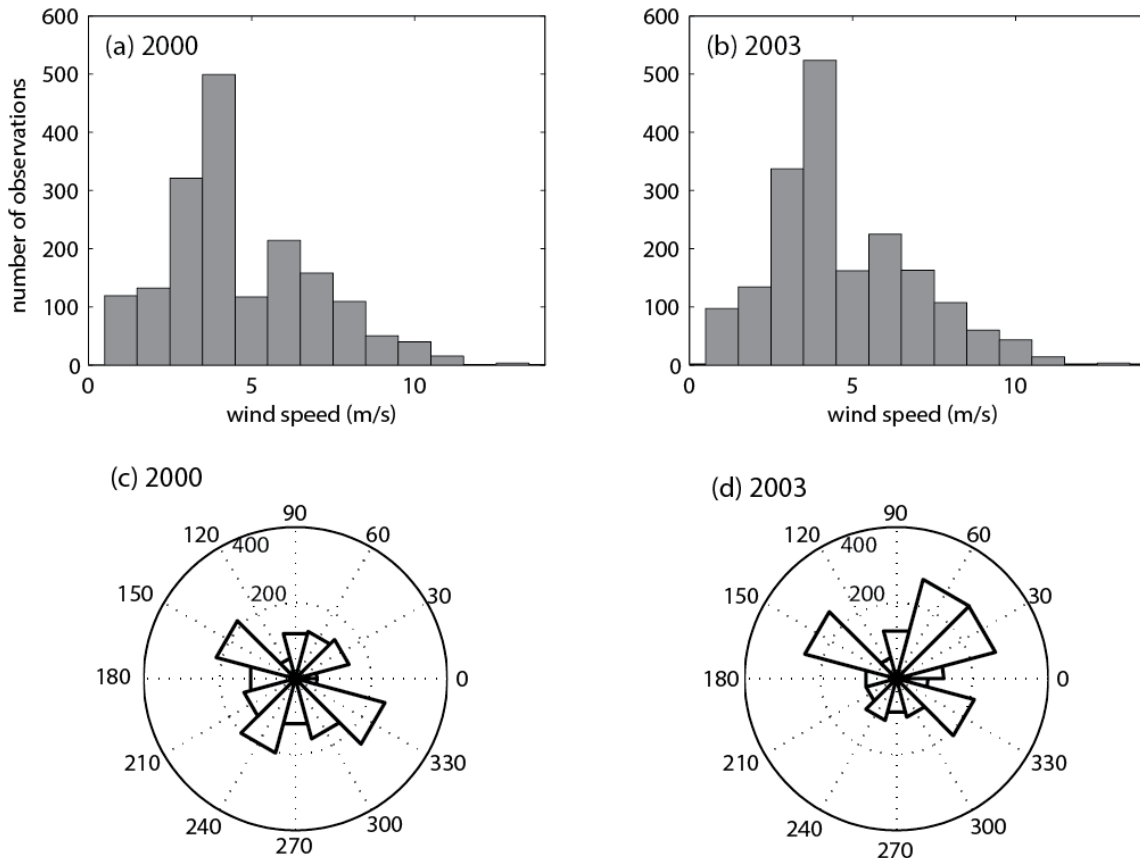


Fig. 4-7. Comparison of wind speed (m s^{-1}) and direction (degrees) for the years 2000 and 2003 during February-April. Panels (a) and (b) are histograms for wind speed and panels (c) and (d) are wind rose plots indicating wind direction where wind is coming from.

4-6 Residual flow fields from hydrodynamic simulation

We used the ROMS model output to investigate how residual flow fields were different between the two years by subtracting the late winter-spring (February-April) residual flow of 2003 from 2000. In this analysis, for example, down-estuary direction indicates either relatively stronger down-estuary flow or weaker up-estuary flow in 2000 compared to 2003. Figure 4-8 shows residual currents during the spring bloom period (February-April) in the mid-bay region. There was a tendency of strong south-eastward flows, especially over the western flank in the bottom residual currents while there was no evident pattern over the eastern side of the bay in 2000 relative to 2003 (Fig. 4-8a). In contrast, the difference in the surface residual currents had the opposite characteristics; a tendency of up-estuary direction in 2000 relative to 2003 (Fig. 4-8b). The difference in cross-sectional residual flows was also examined near the mouth of the Potomac River (see Fig. 4-8a). Figure 4-9a illustrates the velocity field normal to the section (along-channel flow) and shows that there was a down-estuary tendency of residual flows in 2000 compared to 2003, especially over the deep channel and the near-bottom layer of the western flank. On the other hand, the up-estuary tendency of the surface flow is more dominant in 2000 than 2003 over both sides of the shoals. For the cross-channel (lateral) flows, there was a

tendency for eastern shoreward flows located between the surface and 5 m depth, whereas there was a tendency for western shoreward flows below 5 m in 2000 relative to 2003 (Fig. 4-9b).

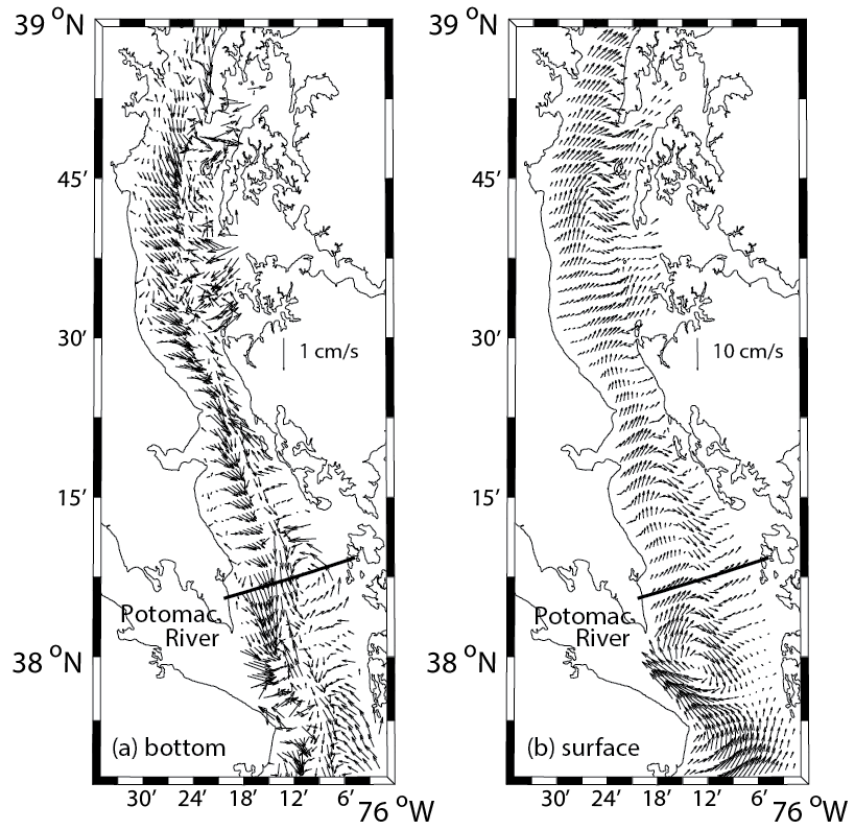


Fig. 4-8. Differences in the late winter-spring (February-April) residual currents between the years 2000 and 2003 at (a) the bottom and (b) the surface. The solid line in the panel (a) indicates the mid-bay cross-section shown in Fig. 4-9.

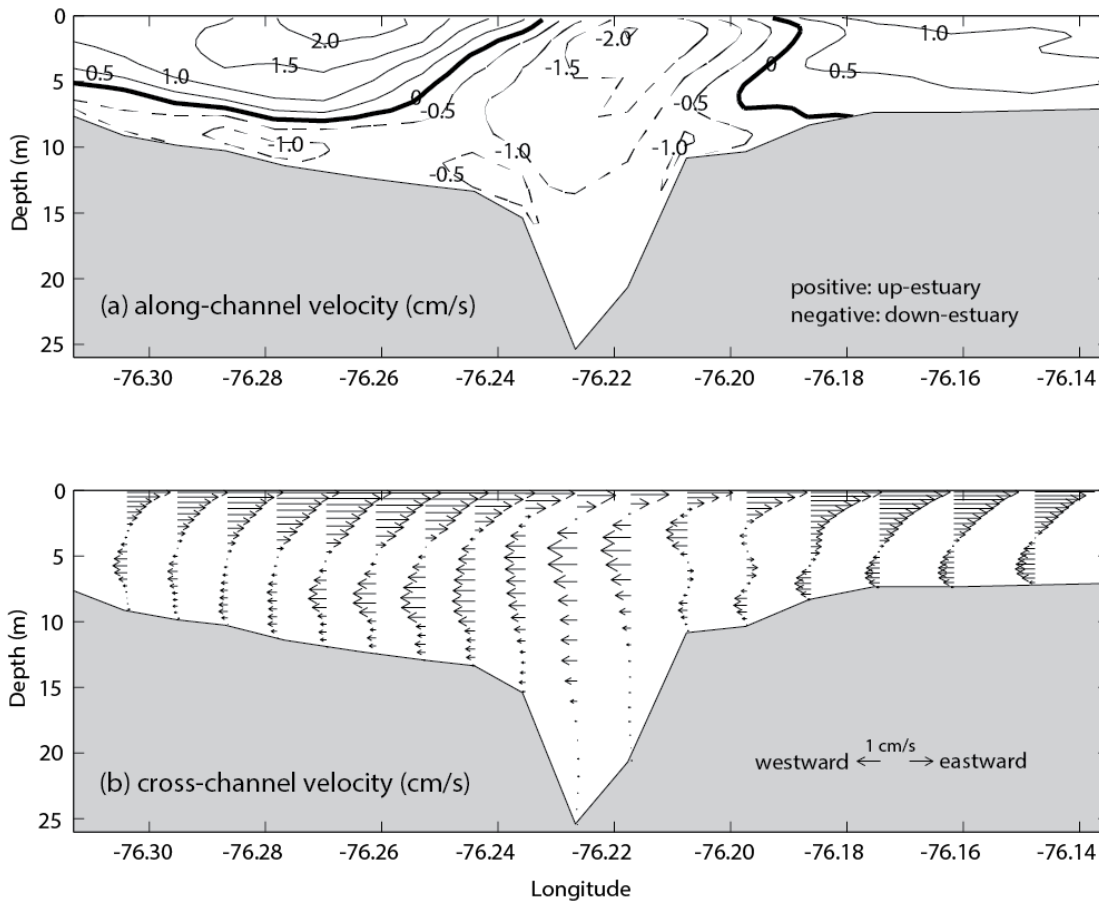


Fig. 4-9. Differences in the late winter-spring (February-April) residual currents between the years 2000 and 2003 at the mid-bay cross-section indicated in Fig. 4-8a. Panel (a) is an along-channel velocity field normal to the section. The solid contour lines are positive values (up-estuary direction) while the dashed lines correspond to negative values (down-estuary direction) with a contour interval of 0.5 cm s^{-1} . Panel (b) is a cross-channel velocity field parallel to the section.

4-7 Discussion

Winter-spring river flows affect major processes involved in seasonal hypoxia as previous studies have shown (Table 4-1). We found that the TN loading due to the winter-spring freshwater input influences the spring near-bottom chlorophyll-*a* concentration along the deep channel which is correlated with summer hypoxia. However, this relationship does not hold for the chlorophyll-*a* concentration at the surface as well as at the stations over the shallow shoals. Testa and Kemp (2008) suggested that a large fraction of labile organic matter sinking from shoal surface water is transported laterally to the deep channel and then respired later at the sediment-water interface as temperature increases (Cowan *et al.*, 1996). The SOM analysis revealed that hypoxia was mostly initiated at the bottom near Annapolis, Maryland (Fig. 4-2a), where the bathymetry deepens sharply, in May and occasionally in April (e.g., 1985, 1991 and 1994). Hypoxic conditions became severe with the development of a strong pycnocline in June-August because of the inhibition of vertical transport of DO into the bottom layer. However, unlike in the mid-bay, the relationship between hypoxia and stratification is not well defined in

the lower-bay. This is likely due to its shallower depth, stronger tidal mixing, and horizontal advection of normoxic deep water from the adjacent coastal ocean.

This study showed that the amount of winter-spring freshwater discharge and the intensity of summer stratification accounted for 36% and 49% of the interannual variability in summer hypoxia, respectively. After adding the late winter-spring NE-SW wind in the analysis, the regression models were significantly improved (Fig. 4-4c and 4-4d), suggesting a possible role for wind in transport and distribution of organic matter during the spring bloom period. The analysis showed that summer wind was not correlated with the interannual variability of hypoxic volume in more recent years (1985-2007; Table 4-1) although Scully (2010a) demonstrated that summer hypoxia was related to the duration of summer wind based on data spanning the period from 1950 to 2007 (58-year period). There was a summer wind shift during the early 1980s from southeasterly to westerly winds and this was correlated with a jump in hypoxic volumes that occurred with no increases in nutrient loading rates. Scully (2010b) emphasized a potential role of southerly wind in ventilating hypoxic water during summer. That study found that summer winds from the south were found to be the most effective at supplying oxygen to hypoxic regions whereas winds from the west were least effective. Hence, decadal variability of hypoxic volume in the bay is possibly due to changes in summertime wind directions associated with large-scale climate forcing such as the NAO.

Our analysis focused on the interannual variability of climate influencing summer hypoxia due to its effects on several physical processes in Chesapeake Bay, including wind and river discharge. When the late winter-spring NE-SW wind in the regression analyses (Fig. 4-4c and 4-4d) was replaced by the second EOF mode of the February-April SLP anomaly, the relationships between the modeled and observed hypoxic volume remained significant ($r=0.87$, $p<0.01$ and $r=0.79$, $p<0.01$, respectively). This suggests that processes involved in the interannual variability of hypoxia are influenced by the winter-spring process that is teleconnected with the El Niño events over the eastern U.S. (e.g., Meehl *et al.*, 2007). The late winter-spring wind in the Chesapeake Bay region was not significantly correlated with the variability of the Niño 1+2 index (eastern Pacific SST anomaly) but rather influenced by the SLP anomaly associated with the ENSO (the second EOF mode). We also found that the January-April temperature in the mid-bay was related to the winter (December-February) BHI ($r=-0.58$, $p<0.01$) as well as the third EOF mode of the winter SLP anomaly ($r=0.63$, $p<0.01$) albeit no eminent trend in temperature variability. Hence, it is possible that temperature warming in winter-spring with climate change increases bacterial production resulting in higher oxygen demand and lower oxygen solubility in the water column (Najjar *et al.*, 2000). This may affect the total oxygen budget during spring time and stimulate earlier onset of seasonal hypoxia. Temperature change in estuaries also plays a role in ecological processes such as the timing of phytoplankton bloom (e.g., Kronkamp and Engeland, 2010) and the magnitude of phytoplankton biomass accumulation (e.g., Oviatt *et al.*, 2002). Thus, alteration of organic carbon flow may impact not only higher trophic levels but also the dynamics of DO in the water column and sediment.

Summer stratification is most likely affected by climate variability via its influence on precipitation over the watershed region. We found that the second EOF mode of winter (December-February) SLP was significantly correlated with winter-spring (January-May) river flow ($r=0.54$, $p<0.01$) as well as TN load ($r=0.52$, $p<0.05$). In previous studies, estuarine

ecosystems respond strongly to interannual variability of freshwater flow (Schubel and Pritchard, 1986; Kimmerer, 2002) and the magnitude of spring discharge from the Susquehanna River is associated with winter weather patterns transiting the eastern U.S. (Miller *et al.*, 2006). Winter climate patterns also appear to explain the position, extent, and magnitude of the spring bloom in Chesapeake Bay (Miller and Harding, 2007). For example, years dominated by dry winter patterns result in lower chlorophyll-*a* biomass with its peak towards the upper-bay region whereas years with wet winter patterns are associated with higher chlorophyll-*a* in the mid-bay region (Kimmel *et al.*, 2009). Hence, it is possible that vertical export of organic carbon to the bottom water is enhanced during wet winters, resulting in elevated biological oxygen demand and thus hypoxia in the mid-bay. What was worrisome with this argument is that there are years with warm and wet (cool and dry) winters which do not coincide with severe (or less severe) hypoxic conditions (i.e., cool/dry winter but severe hypoxia observed in 1989 and warm/wet winter but mild hypoxia in 1990 and 1996).

As we hypothesized, climate variability may also affect the distribution of phytoplankton biomass depending on the patterns of the late winter-spring wind during the spring bloom period. The hydrodynamic ocean model was applied to assess the importance of wind direction during February-April and provided evidence for the transport of phytoplankton biomass within the bay. The analysis of residual flow fields indicated that more organic matter could be transported to the lower bay and the shallow western shoals in 2000 than 2003 during the spring bloom period. These findings are consistent with previous modeling studies reporting that up-estuary wind tends to produce surface up-estuary flows over shoals and down-estuary flow over a deep channel and vice versa (Wong, 1985; Guo and Valle-Levinson, 2008; Li and Li, 2011). Frequent southwesterly winds during 2000 were favorable for transport of organic matter to the lower-bay where seasonal hypoxia is not prevalent for the reasons indicated earlier. In contrast, years with frequent northeasterly wind tend to be associated with larger volume of hypoxia since organic carbon is most likely retained in the deep channel. In addition, lateral circulation response to northeasterly wind may have contributed to the accumulation of phytoplankton biomass in the deep channel transported from the shallow western flank. This physical phenomenon is consistent with observations suggesting that wind-driven forcing may play a role in lateral exchange through lateral upwelling and downwelling (Malone *et al.*, 1986; Sanford *et al.*, 1990) as well as results from a modeling study (Li and Li, 2012). Hence, our study suggests that a large fraction of bloom produced organic matter could be transported laterally into the deep channel as well as retained in the mid-bay due to enhanced gravitational circulation with northeasterly wind. For example, severe hypoxia occurred in 2003 when northeasterly wind was dominant while the winter-spring Susquehanna River flow was moderate. This mechanism may be the key to understanding hypoxia and modeling biogeochemical cycles in Chesapeake Bay.

Although the regression model does not specifically identify the mechanistic links between winter-spring conditions and summer hypoxia, it can be used as a practical tool to forecast summer hypoxia based on those winter-spring conditions that were the most important variables in the analysis (Fig. 4-4d). The predictive model tracks observations very well (Fig. 4-5), and the relationship is still very significant without the need for summer stratification data. The results from the analysis indicate that processes involved in summer hypoxia are largely controlled by winter-spring processes, but it is difficult to assess the relative contribution of individual factors from the regression analysis due to multicollinearity. Although the late winter-spring wind is

most likely to affect the transport of organic matter, it remains certain that nitrogen loads to the bay have to be lowered to adequately reduce the organic carbon pool that ultimately fuels processes creating hypoxic conditions. This study has shown that processes involved in the dynamics of DO are more complicated than previously thought and that they interact with the interannual variability of climate. Future research efforts need to focus on the redistribution of phytoplankton biomass in the water column and to conduct surveys capturing those processes at timescales on the order of days. Then, we can determine dominant mechanisms in the DO dynamics based on different scenarios of climate change and nutrient loading rates using a numerical modeling approach.

4-8 Summary

Summer hypoxia in Chesapeake Bay results from the interaction between the physical supply of DO and biological production/consumption of phytoplankton biomass. Hypoxic volume is largely modulated by the strength of the pycnocline and the amount of nutrients input that are associated with the variability of winter-spring discharge from the watershed. This study emphasized the role of climate variability in winter-spring processes influencing summer hypoxia in the bay. We found that the late winter-spring (February-April) wind plays a crucial role in the dynamics of DO via the transport of organic matter produced in shallow shoals into the deep channel possibly due to lateral advection and enhanced gravitational circulation. Thus, in years with frequent northeasterly (southwesterly) wind during late winter-spring, the summer hypoxia in the bay was severe (moderate). In addition, the late winter-spring wind was significantly correlated with the second EOF mode of the winter (December-February) SLP anomaly that is teleconnected with the El Niño events. Based on a step-wise regression method, we successfully predicted summer average hypoxic volume using two independent variables from the winter-spring period, i.e., river flow and wind condition.

4-9 References

- Boicourt, W. C. 1992. Influence of circulation processes on dissolved oxygen in the Chesapeake Bay, in *Oxygen Dynamics in Chesapeake Bay: A Synthesis of Research*, edited by D. Smith, M. Leffler, and G. Mackiernan, 5-59, University of Maryland Sea Grant. College Park, Maryland.
- Bretherton, C. S., C. Smith, and J. M. Wallace. 1992. An intercomparison of methods for finding coupled patterns in climate data. *Journal of Climate* 5: 541-560.
- Chapman, D.C. 1985. Numerical treatment of cross-shelf open boundaries in a barotropic coastal ocean model. *Journal of Physical Oceanography* 15: 1060-1075.
- Cowan, J.L.W., J.R. Pennock, and W.R. Boynton. 1996. Seasonal and interannual patterns of sediment-water nutrient and oxygen fluxes in Mobile Bay, Alabama (USA): regulating factors and ecological significance. *Marine Ecological Progress Series* 141: 229-245.
- Diaz, R. J. and R. Rosenberg. 1995. Marine benthic hypoxia: A review of its ecological effects and the behavioural responses of benthic macrofauna. *Oceanography and Marine Biology: an Annual Review* 33: 245-303.
- Diaz, R. J., and R. Rosenberg, 2008: Spreading dead zones and consequences for marine ecosystems. *Science* 321: 926–929.
- Eby, A. E. and L. B. Crowder. 2002. Hypoxia-based habitat compression in the Neuse River Estuary: context-dependent shifts in behavioral avoidance thresholds. *Canadian Journal of Fisheries and Aquatic Sciences* 59: 952-965
- Emery, W. J. and R. E. Thomson. 2001. *Data Analysis Methods in Physical Oceanography*, 2nd ed. Elsevier, New York.
- Flather, R.A. 1976. A tidal model of the northwest European continental shelf. *Memoires de la Societe Royale de Sciences de Liege* 6: 141-164.
- Guo, X. and A. Valle-Levinson. 2008. Wind effects on the lateral structure of density-driven circulation in Chesapeake Bay. *Continental Shelf Research* 28: 2450-2471.
- Hagy, J. D. 2002. Eutrophication, hypoxia and trophic transfer efficiency in Chesapeake Bay. Ph.D. dissertation, University of Maryland, College Park, MD
- Hagy, J. D., W. R. Boynton, C. W. Keefe, and K. V. Wood. 2004. Hypoxia in Chesapeake Bay, 1950-2001: Long-term Change in Relation to Nutrient Loading and River Flow. *Estuaries* 27(4): 634-658.
- Harding, L. W., Jr., and E. S. Perry. 1997. Long-term increases of phytoplankton biomass in Chesapeake Bay, 1950 – 1994. *Marine Ecology Progress Series* 157: 39-52.

- Hurrell, J. W. 1995. Decadal trends in the North Atlantic Oscillation: Regional temperature and precipitation. *Science* 269: 676-679.
- Kaski, S., J. Kangas, and T. Kohonen. 1998. Bibliography of self-organizing map (SOM) papers: 1981-1997. *Neural Computing Surveys* 1: 102-350.
- Katz, R. W., M. B. Parlange, and C. Tebaldi. 2003. Stochastic modeling of the effects of large-scale circulation on daily weather in the southeastern U.S. *Climate Change* 60: 189-216.
- Kemp, W. M., W. R. Boynton, J. E. Adolf, D. F. Boesch, W. C. Boicourt, G. Brush, J. C. Cornwell, T. R. Fisher, P. M. Glibert, J. D. Hagy, L. W. Harding, E. D. Houde, D. G. Kimmel, W. D. Miller, R. I. E. Newell, M. R. Roman, E. M. Smith, and J. C. Stevenson. 2005. Eutrophication of Chesapeake Bay: historical trends and ecological interactions. *Marine Ecology Progress Series* 303: 1-29.
- Kimmel, D. G., W. D. Miller, L. W. Harding, Jr., E. D. Houde, and M. R. Roman. 2009. Estuarine Ecosystem Response Captured Using a Synoptic Climatology. *Estuaries and Coasts* 32: 403-409.
- Kimmel, D. G., and M. R. Roman. 2004. Long-term trends in mesozooplankton abundance in Chesapeake Bay, USA: Influence of freshwater input. *Marine Ecology Progress Series* 267: 71-83.
- Kimmerer, W.J. 2002. Effects of freshwater flow on abundance of estuarine organisms: physical effects or trophic linkage? *Marine Ecology Progress Series* 243: 39-55.
- Kohonen, T. 2001. *Self-Organizing Maps*, 3rd ed. Springer-Verlag, New York.
- Kromkamp, J. C. and T. V. Engeland. 2010. Changes in phytoplankton biomass in the Western Scheldt estuary during the period 1978-2006. *Estuaries and Coasts* 33: 270-285. doi:10.1007/s12237-009-9215-3.
- Lee, Y. J. and K. M. M. Lwiza. 2008a. Characteristics of bottom dissolved oxygen in Long Island Sound, New York. *Estuarine Coastal and Shelf Science* 76: 187-200.
- Lee, Y. J. and K. M. M. Lwiza. 2008b. Factors driving bottom salinity variability in the Chesapeake Bay. *Continental Shelf Research* 28: 1352-1362.
- Li, M., L. Sanford, and S. Y. Chao. 2005. Effects of time dependence in unstratified tidal boundary layers: Results from large eddy simulations. *Estuarine Coastal and Shelf Science* 62(1-2): 193-204.
- Li, M. and Y. Li. 2011. Effects of winds on stratification and circulation in a partially mixed estuary. *Journal of Geophysical Research* 116: C12012. doi:10.1029/2010JC006893.

- Li, Y., and M. Li. 2012. Wind-Driven Lateral Circulation in a Stratified Estuary and its Effects on the Along-Channel Flow, *Journal of Geophysical Research* 117: C09005. doi: 10.1029/2011JC007829.
- Li, M. and L. J. Zhong. 2009. Flood-ebb and spring-neap variations of mixing, stratification and circulation in Chesapeake Bay. *Continental Shelf Research* 29(1): 4-14.
- Li, M., L. Zhong, W. C. Boicourt, S. L. Zhang, and D. L. Zhang. 2007. Hurricane-induced destratification and restratification in a partially-mixed estuary. *Journal of Marine Research* 65(2): 169-192.
- Liu, Y. and R. H. Weisberg. 2005. Patterns of ocean current variability on the West Florida Shelf using the self-organizing map. *Journal of Geophysical Research* 110: C06003. doi: 10.1029/2004JC002786.
- Malone, T.C. 1992. Effects of water column processes on dissolved oxygen: Nutrients, plankton and zooplankton. In: Smith, D., M. Leffler and G. Mackiernana (eds.). *Oxygen Dynamics in Chesapeake Bay: A Synthesis of Research*. University of Maryland Sea Grant College Publications, College Park, Maryland. pp 61-112.
- Malone, T. C., W. M. Kemp, H. W. Ducklow, W. R. Boynton, and J. H. Tuttle, 1986: Lateral variation in the production and fate of phytoplankton in a partially stratified estuary. *Marine Ecology Progress Series* 32: 149–160.
- Marchesiello, P., J. McWilliams, and A. Shchepetkin. 2001. Open boundary conditions for long-term integration of regional oceanic models. *Ocean Modelling* 3(1): 20. doi: 10.1016/S1463-5003(00)00013-5.
- Meehl, G. A., C. Tebaldi, H. Teng, and T. C. Peterson. 2007. Current and future U.S. weather extremes and El Niño. *Geophysical Research Letter* 34: L20704. doi:10.1029/2007GL031027.
- Miller, W. D. and L. W. Harding, Jr. 2007. Climate forcing of the spring bloom in Chesapeake Bay. *Marine Ecology Progress series* 331: 11-22.
- Miller, W. D., D. G. Kimmel, and L. W. Harding. 2006. Predicting spring discharge of the Susquehanna River from a winter synoptic climatology for the eastern United States. *Water Resources Research* 42: W05414. doi:10.1029/2005WR004270.
- Murphy, R.R., W.M. Kemp, W.P. Ball. 2011. Long-term Trends in Chesapeake Bay Seasonal Hypoxia, Stratification, and Nutrient Loading. *Estuaries and Coasts* 34: 1293-1309.
- Najjar, R.G., H.A. Walker, P.J. Anderson, E.J. Barron, R.J. Bord, J.R. Gibson, V.S. Kennedy, C.G. Knight, J.P. Megonigal, R.E. O'Connor, C.D. Polsky, N.P. Psuty, B.A. Richards, L.G. Sorenson, E.M. Steele, and R.S. Swanson. 2000. The potential impacts of climate change on the mid-Atlantic coastal region. *Climate Research* 14: 219-233.

- North, E. W., and E. D. Houde. 2003. Linking ETM physics, zooplankton prey, and fish early-life histories to striped bass *Morone saxatilis* and white perch *M. Americana* recruitment. *Marine Ecology Progress Series* 260: 219-236.
- O'Donnell, J., H. G. Dam, W. F. Bohlem, W. Fitzgerald, P. S. Gay, A. E. Houk, D. C. Cohen, and M. M. Howard-Strobel. 2008. Intermittent ventilation in the hypoxic zone of western Long Island Sound during the summer of 2004. *Journal of Geophysical Research* 113: C09025. doi:10.1029/2007JC004716.
- Officer, C. B., R. B. Biggs, J. L. Taft, L. E. Cronin, M. A. Tyler, and W. R. Boynton. 1984. Chesapeake Bay anoxia: Origin, development, and significance. *Science* 223: 22-27.
- Oja, M., S. Kaski, and T. Kohonen. 2002. Bibliography of self-organizing map (SOM) papers: 1998-2001 addendum. *Neural Computing Surveys* 3: 1-156.
- Orlanski, I. 1976. A simple boundary condition for unbounded hyperbolic flows. *Journal of Computational Physics* 21(3): 251-269.
- Oviatt, C., A. Keller, and L. Reed. 2002. Annual Primary Production in Narragansett Bay with no Bay-Wide Winter-Spring Phytoplankton Bloom. *Estuarine, Coastal and Shelf Science* 54: 1013-1026.
- Pond, S. and G. L. Pickard. 1983. *Introductory Dynamical Oceanography*, 2nd ed. Pergamon Press, Oxford, England.
- Richardson, A.J., C. Risien, and F. A. Shillington. 2003. Using self-organizing maps to identify patterns in satellite imagery. *Progress in Oceanography* 59: 223-239.
- Sanford, L. P., K. G. Sellner, and D. L. Breitburg. 1990. Covariability of dissolved oxygen with physical processes in the summertime Chesapeake Bay. *Journal of Marine Research* 48: 567-590.
- Schubel, J. R., and D. W. Pritchard. 1986. Response of upper Chesapeake Bay to variations in discharge of the Susquehanna River. *Estuaries* 9: 236-249.
- Scully, M. E. 2010a. The Importance of Climate Variability to Wind-Driven Modulation of Hypoxia in Chesapeake Bay. *Journal of Physical Oceanography* 40: 1435-1440.
- Scully, M. E. 2010b. Wind Modulation of Dissolved Oxygen in Chesapeake Bay. *Estuaries and Coasts* 33: 1164-1175.
- Scully, M.E., C.T. Friedrichs, and J.M. Brubaker. 2005. Control of estuarine stratification and mixing by wind-induced straining of the estuarine density field. *Estuaries* 28:321-326.
- Seliger, H. H., J. A. Boggs, and W. H. Biggley. 1985. Catastrophic Anoxia in the Chesapeake Bay in 1984. *Science* 228(4695): 70-73

Stenseth, N. C., G. Ottersen, J. W. Hurrell, A. Mysterud, M. Lima, K.-S. Chan, N. G. Yoccoz, and B. Adlandsvik. 2003. Studying climate effects on ecology through the use of climate indices: The North Atlantic Oscillation, El Niño Southern Oscillation and beyond. *Proceedings of the Royal Society of London B* 270: 2087–2096.

Testa, J.M. and W.M. Kemp. 2008. Variability of biogeochemical processes and physical transport in a partially stratified estuary: a box-modeling analysis. *Marine Ecology Progress Series* 356:63-79.

Tootle, G.A., T.C. Piechota, and A. Singh. 2005. Coupled oceanic-atmospheric variability and U.S. streamflow. *Water Resources Research* 41: W12408. doi:10.1029/2005WR004381.

USEPA (U.S. Environmental Protection Agency). 2010. Chesapeake Bay Total Maximum Daily Load for Nitrogen, Phosphorus and Sediment. U.S. Environmental Protection Agency, Washington, DC.

Venegas, S. A., L. A. Mysak, and D. N. Straub. 1997. Atmosphere-Ocean Coupled Variability in the South Atlantic. *Journal of Climate* 10: 2904-2920.

Vesanto, J. J. Himberg, E. Alhoniemi, J. Parhankangas. 2000. Self-Organizing Map (SOM) Toolbox for Matlab 5. In Technical Report A57, Helsinki University of Technology. Helsinki, Finland.

Wallace, J.M., C. Smith, and C.S. Bretherton. 1992. Singular value decomposition of wintertime sea surface temperature and 500-mb height anomalies. *Journal of Climate* 5: 561-576.

Warner, J. C., W. R. Geyer, and J. A. Lerczak. 2005. Numerical modeling of an estuary: A comprehensive skill assessment. *Journal of Geophysical Research* 110: C05001. doi: 10.1029/2004JC002691.

Whitney, M. M. 2010. A study on river discharge and salinity variability in the Middle Atlantic Bight and Long Island Sound. *Continental Shelf Research* 30: 305-318.

Wilson, R. E., R. L. Swanson, and H. A. Crowley. 2008. Perspectives on long-term variations in hypoxic conditions in western Long Island Sound. *Journal of Geophysical Research* 113: C12011. doi:10.1029/2007JC004693.

Wong, K-C. 1994. On the nature of transverse variability in a coastal plain estuary. *Journal of Geophysical Research* 99: 14209-14222.

Chapter 5

Multi-decade responses of a tidal creek system to nutrient load reductions: Mattawoman Creek, Maryland USA

W.R. Boynton, C.L.S. Hodgkins, C.A. O'Leary, E.M. Bailey, A.R. Bayard, and L.A. Wainger

5-1	INTRODUCTION	1
5-2	MATTAWOMAN CREEK WATERSHED AND ESTUARY	2
5-3	DATA SOURCES AND ANALYTICAL APPROACHES	4
5-4	RESULTS AND DISCUSSION	8
5-4.1	CURRENT AND HISTORICAL NUTRIENT SOURCES	8
5-4.2	NUTRIENT EXCHANGES WITH THE POTOMAC	12
5-4.3	WATER QUALITY PATTERNS AND TRENDS	13
5-4.4	COMMUNITY PRODUCTION	16
5-4.5	SAV IN MATTAWOMAN CREEK	18
5-4.6	NITROGEN BUDGET FOR MATTAWOMAN CREEK	21
5-4.7	NUTRIENT CAUSE-EFFECT CHAINS	23
5-5	SUMMARY AND FUTURE INVESTIGATIONS	25
5-6	REFERENCES	28

5-1 Introduction

Understanding the causes and consequences of eutrophication in lagoons, bays, estuaries and near-coastal waters has been the focus of much research during the last five to six decades, starting perhaps in the USA with the work of Ryther (1954) on Moriches Bay, NY where duck wastes were linked to intense algal blooms, a reduction in oyster production and aesthetic impacts. Since that beginning our understanding of eutrophication now includes a useful definition (Nixon 1995), general conceptual models (Cloern 2001), more specific models of shallow (Nixon *et al.*, 2001) and river dominated (Kemp *et al.*, 2005) systems, reviews of nitrogen (N) versus phosphorus (P) limitation (Rabalais 2002; Howarth and Marino 2006; Smith *et al.*, 2006; Paerl 2009) and consideration of thresholds (Conley *et al.*, 2009) and other feedback processes that can exacerbate or suppress eutrophication (Kemp *et al.*, 2005; Conley *et al.*, 2007; Gruber and Kemp 2010).

During the past decade, there has been a growing interest in estuarine science and water quality management communities for improved understanding of ecosystem responses to nutrient load reductions or, in the terms of Nixon (2009), the oligotrophication of these systems. This represents a change in focus but is understandable because large amounts of public funds are being devoted to restoration efforts. Interest in oligotrophication has stimulated thinking, speculation and synthesis on the likely responses of these important resources to reduced nutrient loading rates. For example, Duarte *et al.* (2009) reviewed responses of several systems and found convoluted trajectories that failed to return to pre-eutrophication conditions. Kemp *et al.* (2009) examined response trajectories related to hypoxia reduction in 24 coastal ecosystems and found

about half displayed remediation trajectories that mirrored the degradation trajectory while the remainder displayed complex patterns similar to those reported by Duarte *et al.* (2009). Studies of ecosystem responses to load reductions in Chesapeake Bay and elsewhere are relatively rare. Available sources indicate a variety of responses including no or limited response (Conley *et al.*, 2002; Kronvang *et al.*, 2005; Boynton *et al.*, 2009), gradual improvement (Jeppesen *et al.*, 2005; Murphy *et al.*, 2011), rapid responses (Rask *et al.*, 1999), delayed algal biomass reduction (Yamamoto 2003; Boynton *et al.*, 2011) and several threshold-like responses involving SAV communities (Johansson 2002; Orth *et al.*, 2010; Ruhl and Rubicki 2010). Given the large financial costs associated with restoration programs in the Chesapeake and elsewhere it is important to develop a better understanding of system responses to these actions.

This analysis focuses on Mattawoman Creek, an oligohaline/tidal freshwater tributary of the upper Potomac River estuary. This site was selected for analysis for several reasons. First, between the 1970s and mid 1990s, this system was very eutrophic, having large algal blooms and lacking submerged aquatic vegetation (SAV). A major reduction of point source nutrient loads was achieved during the early 1990s. Second, this system has been the focus of study and interest by federal, state, and local volunteer organizations interested in preserving and improving habitat quality in the face of growing development. Hence, there is a diverse and long-term data set available for examination. Finally, this system is connected via tidal exchanges with the upper Potomac estuary. While nutrient load reductions have been achieved in the upper Potomac estuary, loads remain high and nutrient concentrations in the Potomac adjacent to Mattawoman Creek are higher than those within the creek. Thus, it is likely Mattawoman Creek receives nutrient loads from the local watershed, atmosphere and the adjacent tidal Potomac. Understanding the influence of downstream waters (tidal Potomac in this case) on upstream waters receiving management actions is of particular interest to the management community.

The focus of this analysis concerns water quality (chlorophyll-*a* and nutrient concentrations and water clarity) and habitat conditions (SAV communities) in Mattawoman Creek. We examine how these features have responded to past and current management actions and speculate how the creek may respond to future land use and nutrient load alterations. Specifically, we summarize information concerning nutrient loading rates from the surrounding basin, the atmosphere and the adjacent Potomac River for several time periods and compare these with other estuarine systems. We then examine time series data sets of water quality and habitat condition, largely from 1986 – 2010. Using both local information and literature sources a nitrogen budget was developed which placed nutrient sources and sinks in perspective, an exercise useful for future nutrient management decisions. Finally, we develop a “cause-effect” chain relating nutrient loads to algal biomass, water clarity and SAV community status using a comparative approach wherein data from other small, shallow, estuarine systems are combined in order to develop robust relationships among variables and test the generality of results (Kemp and Boynton 2012).

5-2 Mattawoman Creek Watershed and Estuary

The Mattawoman Creek watershed encompasses 245 km² of land, 7.4 km² of open tidal waters and 2.5 km² of wetlands; intertidal area is very small (Fig. 5-1). The watershed to estuarine surface area ratio is about 33, a value higher than 60% of USA estuarine systems, and much

higher than the full Chesapeake Bay system which as a ratio of 14 (Bricker *et al.*, 1999). The significance of this ratio (often called a dilution ratio) is a qualitative index of the potential influence of adjacent land on receiving waters. The high ratio for Mattawoman Creek indicates an elevated potential for pollution effects from the watershed. The shallow nature of this system further exacerbates this effect because there is not much water to dilute the effects of land-derived nutrients, sediments or other pollutants.

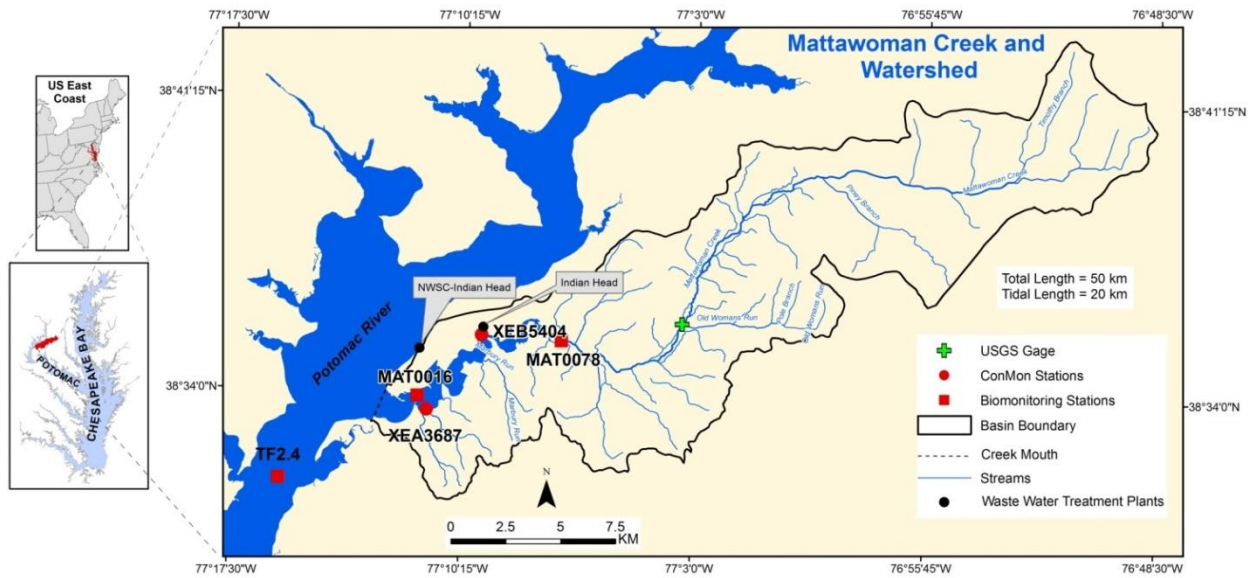


Figure 5-1. A map of Mattawoman Creek and watershed showing locations of stream network, water quality sampling sites, location of USGS flow gage and the cross-section of the creek mouth (dashed line) where net nutrient fluxes were estimated. The NWSC-Indian Head WWTP facility discharges into the Potomac and the Indian Head facility was upgraded with new nutrient removal technologies several times. Insets show the location of Chesapeake Bay on the east coast of the USA and the location of Mattawoman Creek on the Potomac River estuary.

The dominant land use in Mattawoman Creek basin in 2010 was forested lands (54%); agricultural land uses accounted for 9.3% of watershed land uses (Table 5-1). Urban, suburban and other developed land uses occupied 35% of the basin land area. Between 1973 and 2010 urban lands increased by about a factor of three (12% to 35%) and agricultural and forested lands both decreased. Changes in barren land and wetlands have been very small. Estimates of impervious surfaces in the watershed increased linearly from less than 2% in 1950 to 5% by mid 1980 (MDNR 2012, MDP 2012). The rate of change of impervious surface cover increased during the mid 1980s and by 2010 was just over 10%. As a rule of thumb, small basins with impervious cover greater than 10% often have impaired waterways (Schueler 1994; Allan 2004; Holland *et al.*, 2004).

Table 5-1. A summary of land use / land cover in the Mattawoman Creek watershed for three time periods (1973, 2002 and 2010). Areas are in hectares (ha) and numbers in the second column represent percent of cover by category for each time period. Data are from Maryland Department of Planning (2012).

Land Use/ Land Cover Type	1973		2002		2010	
	HA	%	HA	%	HA	%
Agriculture	3,951	16.2	2,901	11.9	2,280	9.3
Barren	0	0	48	0.2	243	1.0
Forest	17,193	70.4	14,477	59.2	13,142	53.8
Urban	3,053	12.5	6,672	27.3	8,447	34.6
Water	69	0.3	88	0.4	87	0.4
Wetlands	184	0.6	263	1.1	252	1.0
TOTAL AREA	24,450	100	24,449	100	24,451	100

Mattawoman Creek is typical in size and volume to many of the small tributaries of Chesapeake Bay and the Potomac River estuary (Cronin and Pritchard 1975). Mattawoman Creek is about 50 km in total length; the lower 20 km are tidal (Fig. 5-1). The upper portion of the tidal estuary is narrow and meandering (25-100 m wide) and turbid. The lower portion of the creek is much wider (1-3 km), deeper (mean depth ~ 1.5 m), clearer, and vertically well-mixed most of the time. The surface area and volume of the tidal estuary is $7.4 \times 10^6 \text{ m}^2$ and $10 \times 10^6 \text{ m}^3$, respectively. SAV are currently a prominent feature of this system covering about 3.5 km^2 of estuarine bottom area in 2010 (~47% of creek surface area).

5-3 Data Sources and Analytical Approaches

All data used in this analysis are listed in Table 5-2. Concise descriptions of variables, information regarding sampling sites, period of the data record, measurement frequency and analytical technique used are also provided, as are references to data sets and more detailed descriptions of methodologies. All water quality data were averaged to a monthly or annual basis even though some data were available on a bi-weekly basis. Differences between surface and bottom water concentrations were examined; differences were negligible at all sites during all seasons so surface water samples were used in this analysis.

Table 5-2. A summary of the types of data used in this analysis, sampling locations, period of data record, measurement frequency, analytical methods used and data sources. Additional details are contained in the text.

Data Types	Location or Sampling Sites	Period of Record	Measurement Frequency	Approach/Technique	Data Sources/Technique Details
System-Scale Data					
Land uses	full watershed; 6 land covers	1973, 2002, 2010	selected years	Aerial photos; GIS	Maryland Dept Planning (2012)
Impervious surfaces	full watershed	1950 - 2010	mainly annual	Aerial photos; GIS	Maryland Dept Planning (2012)
Creek dimensions	NA	1975	NA	bathymetric surveys	Cronin and Pritchard 1975
Freshwater input	one; see Fig. 1	2005 - 2011	daily	USGS gauge site	USGS (2011)
Nutrient loads					
measured	one; see Fig. 1	2005 - 2011	monthly average	USGS standard computation	USGS (2011)
model estimates	full watershed	1985, 2002, 2010	monthly average	Ches. Bay Prog. HSPF model	Shenk and Linker (In Press); Linker <i>et al.</i> , 2000
point source	several discharges	1986-2010	monthly average	grab samples	Ches. Bay Program (2011)
Atmos deposition	surface area of creek	1984 - 1999	annual	NADP and local data collection	Boynton <i>et al.</i> , 2008 (table 2)
Net nutrient exchange with Potomac River	mouth of creek; see Fig. 1	1991 - 2000	monthly average	Ches. Bay Prog. water quality model	Cerco <i>et al.</i> , 2010 and Linker (pers. comm.)
Water Quality Data					
Nutrient conc	3; see Fig. 1	1986-2011	1 or 2 per month	Standard chemical techniques	Ches. Bay Water Quality Monitoring Program (2012);
Chlorophyll- <i>a</i>	3; see Fig. 1	1986-2011	1 or 2 per month	"	Nutrient Analytical Services Lab (2012)
Secchi depth	3; see Fig. 1	1986-2011	1 or 2 per month	"	<u>As above for nutrients and chlorophyll-<i>a</i></u>
High frequency data	2; see Fig. 1	2004 - 2010	15 min; Apr - Oct	In-Situ Sondes; 1 m depth	Maryland Department of Natural Resources (2012)
Habitat Data					
SAV coverage	full creek area	1994 - 2010	annual	Aerial photographs; GIS	Virginia Institute of Marine Sciences (2011)
DO concentration					
monthly	2; see Fig. 1	1986-2011	1 or 2 per month	Sonde; water column profiles	Ches. Bay Water Quality Monitoring Program (2012)
high frequency	2; see Fig. 1	2004 - 2010	15 min; Apr - Oct	In-Situ Sondes; 1 m depth	Maryland Dept of Natural Resources (2012) ConMon Program
Nitrogen Rate Data					
	variety of shallow Ches	2005-2012	month-season	N ₂ -Argon technique	Greene (2005a,b); Boynton <i>et al.</i> (2009); Gao <i>et al.</i> (2012);

Bay sites				Cornwell (pers comm.)	
Denitrification					
Long-term N Burial	variety of shallow Ches Bay sites	1999-2005	annual	Pb-210 dating; PN analysis of sediment cores	Greene (2005a); Merrill (1999)
Sediment N Flux	variety of shallow Ches Bay sites	1986-2007	month-season	shipboard incubation of intact cores	Bailey <i>et al.</i> (2005); http://www.gonzo.cbl.umces.edu/data.htm

In addition to monthly water quality sampling, two high frequency monitoring sites (Maryland Dept. Natural Resources ConMon Program) were also established (Fig. 5-1) and these provided water quality measurements at 15 minute intervals from April-October from 2004 – 2010. Data collected included temperature, salinity, pH, water clarity (as NTUs), dissolved oxygen and chlorophyll-*a* concentration. High frequency water quality data (ConMon Program; Table 5-2) are ideal for computing rates of community production (photosynthesis) which is a basic property of all ecosystems. We adapted the Odum and Hoskin (1958) approach to computing community metabolism and adopted air-water dissolved oxygen flux corrections as suggested by Caffrey (2004). In brief, community production is inferred from the daytime increase in DO concentration. Community production rates are corrected for oxygen diffusion between the water and atmosphere which, in turn, is governed by water temperature and salinity effects on dissolved oxygen saturation in water.

The Phase 5.3 Chesapeake Bay Watershed Model is an application of the Hydrologic Simulation Program-Fortran (HSPF; Bicknell *et al.*, 2005; Linker *et al.*, 2008). The segmentation scheme divides the Chesapeake Bay watershed into more than 1,000 segments/subbasins (including Mattawoman Creek basin), uses 280 monitoring stations throughout the Bay watershed for calibration of hydrology and 200 monitoring stations to calibrate water quality. The model simulates on a one-hour time step and we used output on an annual basis. Nutrient input loads are from atmospheric deposition, fertilizers and manures and other smaller sources. Municipal and industrial wastewater treatment and discharging facilities and onsite wastewater treatment system (septic system) nitrogen, phosphorus, and sediment contributions are also included in the model (USEPA, 2010).

The Bay Water Quality Model combines a three-dimensional hydrologic transport model (CH3D) with a eutrophication model (CE-QUAL-ICM) to predict water quality conditions in the Bay resulting from changes in loads from the contributing basin areas. The hydrodynamic model computes transport using a three-dimensional grid framework (Cerco *et al.*, 2010). The hydrodynamic model was calibrated for the period 1991–2000 and verified against the large number of observed tidal elevations, currents, and densities available for the Bay. The eutrophication (water quality) model computes algal biomass, nutrient concentration, nutrient cycling rate, and DO concentration and other constituents and processes using a 15-minute time step (Cerco and Noel 2004). The model also incorporates a sediment diagenesis component which simulates the chemical and biological processes at the sediment-water interface (DiToro 2001). We used estimated net flux of N and P compounds across the mouth of Mattawoman Creek at monthly time scales for the period 1992 – 2000. Detailed documentation of the Chesapeake Bay Water Quality and Sediment Transport Model can be found at http://www.chesapeakebay.net/content/publications/cbp_26167.pdf.

We did not have local measurements of denitrification or long-term burial rates of particulate nitrogen (PN) and particulate phosphorus (PP). However, for the purposes of the preliminary nutrient budget that was developed, we used an average of denitrification values measured in similar shallow water, nitrate-rich tributaries of Chesapeake Bay that also had oxidized surface sediments likely to support active nitrification. Burial estimates were from similar environments

and we chose to use a value at the conservative end of Chesapeake Bay values currently available (Table 5-2).

For this analysis, we used the correlation and linear regression analysis package available in MatLab. Where appropriate, we manually examined various time scales (monthly, seasonal and annual; with and without lags) for exploring relationships between nutrient loading rates and water quality and habitat conditions.

5-4 Results and Discussion

5-4.1 Current and Historical Nutrient Sources

The USGS maintained a gauging station in the Mattawoman watershed from 2005-2011. This site monitored water, nutrient and sediment discharges from 59% of the basin land area. Water flow and TN and TP loads varied seasonally as well as inter-annually (Fig. 5-2). During 4 of the 6 years of record, flow and loads were highest during winter-spring and much lower during summer and fall, a pattern typical of other tributaries of the Chesapeake Bay (Boynton *et al.*, 2008). However, during the spring and fall of 2006 and fall of 2011 as tropical storms (Alberto, Ernesto and Irene, respectively) passed through the area, and flow and loads exhibited large but temporary increases. On an inter-annual basis, diffuse N loads varied by a factor of two (180-343 kg N day⁻¹) and P loads by just over a factor of two (23.5 to 49.7 kg P day⁻¹). This scale of inter-annual variability has been reported for other Chesapeake Bay systems (Hagy *et al.*, 2004). Direct inputs of N to tidal waters from groundwater were not directly evaluated. However, groundwater N inputs were included in the USGS estimates of loads from 59% of the drainage basin located above the gauge (Fig. 5-1). We prorated these loads to the entire basin and, because of this, we have included an estimate of groundwater inputs to the tidal portion of the basin.

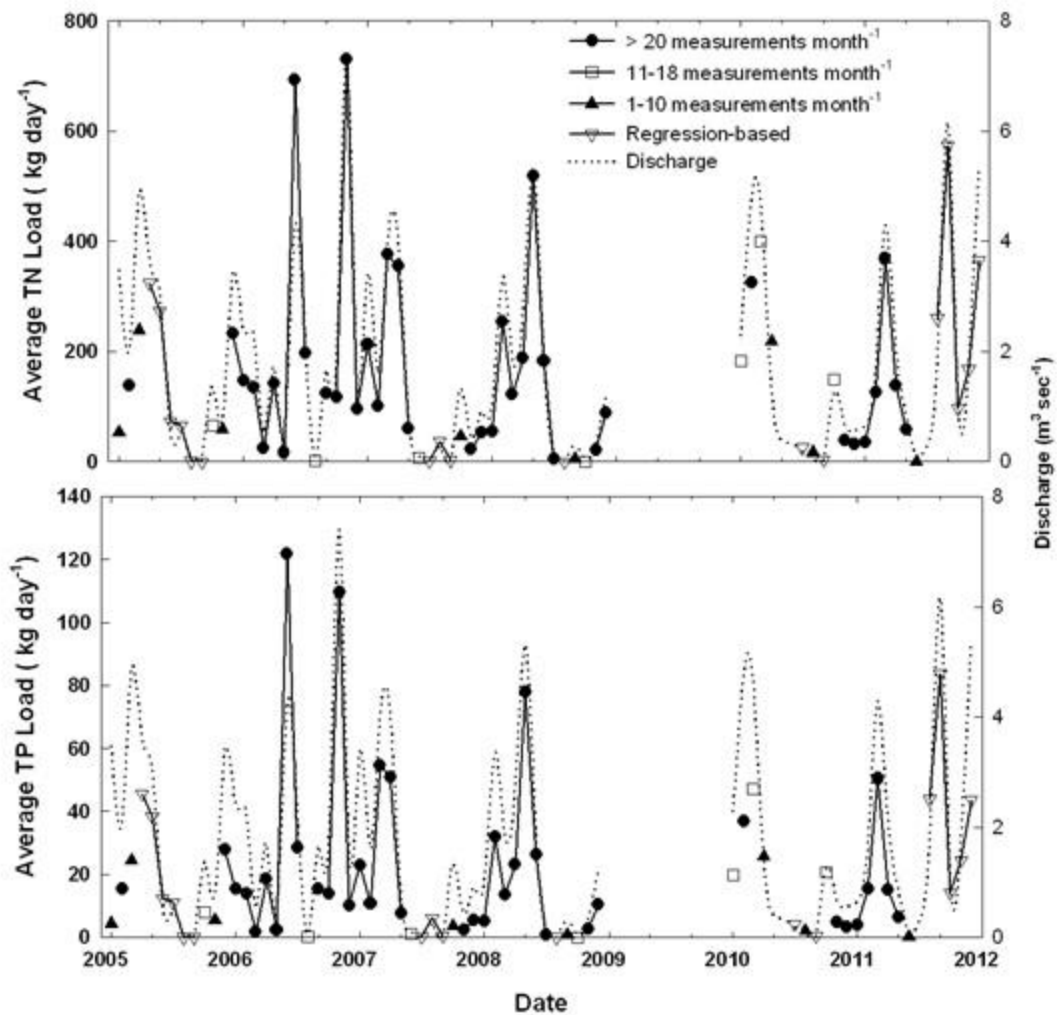


Figure 5-2. A time-series of TN, TP and water flows based on data collected at the USGS gauge on Mattawoman Creek (USGS 016558000; Fig. 5-1). There were some gaps in the load record and these were estimated using a linear flow-load relationship developed with these data. The intensity of measurements used to develop load estimates is also shown in the figure. Data were from the US Geological Survey (2011).

Diffuse source loads were also estimated based on the Chesapeake Bay Program land use model and those estimates (1985, 2002 and 2010) were similar to those derived from the USGS stream monitoring data and they served to extend temporal coverage of diffuse inputs to this system (Table 5-3). Based on both data sets it does not appear that diffuse loads have changed much between 1985 and the present time.

Table 5-3. Multiple estimates of annual diffuse source total nitrogen (TN) and total phosphorus (TP) loads to Mattawoman Creek. Direct atmospheric deposition of N to surface waters of the creek was included in the diffuse source estimates. TN and TP exchange with the Potomac River estuary are not included here, but are considered later. USGS data for the gauged portion of the watershed were scaled up to the full watershed using a linear ratio of gauged to non-gauged areas be comparable with data from the Chesapeake Bay Program model estimates (USGS 2011). Chesapeake Bay Program estimates were from G. Shenk (pers.comm.). Estimate of TN and TP loads from a pristine forested basin with no atmospheric deposition of N or P were based on basin area and used forest yield coefficients of 0.15 g N m⁻² yr⁻¹ and 0.004 g P m⁻² yr⁻¹ (Boynton *et al.*, 1995).

Data Source/Condition	Year	Annual Load (Kg N day ⁻¹)	TN	Annual Load (Kg P day ⁻¹)	TP	Reference
CBP landscape model estimates	1985	260		39.2		Linker <i>et al.</i> , 2000
	2002	251		33.0		and G.
	2010	233		26.1		Shenk ,(pers. Comm.)
USGS River Input Monitoring	2005	216		27.3		
	2006	343		49.7		
	2007	180		23.5		USGS (2011)
	2008	204		27.2		
	2009	No data		No data		
2010	204		24.1			
Pristine forested basin	Pre-European Settlement	100		2.7		Boynton <i>et al.</i> , 1995

The major change in landside nutrient input to Mattawoman Creek is related to point source reductions. During 1990 point source loads were about 360 kg N day⁻¹ and were a much larger source than diffuse loads. Point source loads declined very sharply to about 50 kg N day⁻¹ by 1995 and then decreased again beginning in 2000. Point source loads have been very low since then and now represent a small fraction of total nutrient load to the system.

Direct deposition of N to the surface waters of Mattawoman Creek represents another nutrient source. We used atmospheric deposition data from Boynton *et al.* (2008) that included all forms of N in both wet and dry deposition (0.81 mg N L⁻¹ as an annual average concentration). Given precipitation averages about 1 m year⁻¹, direct atmospheric deposition to surface waters of the creek contributed about 6000 kg N year⁻¹ or about 16 kg N day⁻¹ to the creek system. Thus, direct N deposition is a small component of the N budget for this system. However, rain (and dry deposition) falls on the full basin and all this rain contains N compounds. In the Chesapeake Bay basin, Fisher and Oppenheimer (1991) and more recently Castro *et al.* (2003) estimated that about 25% and 22%, respectively, of atmospheric N deposition to the landscape is exported to streams and estuarine waters. While direct measurements are not available for the Mattawoman basin, applying the most recent estimate of 22% suggests that about 120 kg N day⁻¹ would reach estuarine waters as a component of diffuse source loading, or about 49% of the total diffuse

source load. In this larger view, atmospheric deposition is a very important part of the N input signature for this system. If this estimate proves to be correct, continuing emphasis on decreasing atmospheric deposition of N is an important management objective and one where there has been progress on a regional scale during the last 20 years (Burns *et al.*, 2011).

One useful nutrient enrichment metric to consider is TN and TP loading rates to Mattawoman Creek compared with those of other estuarine ecosystems. To compare nutrient loading in this system to loading at other coastal and estuarine locations, we compiled N and P loading rates for many such systems and added Mattawoman Creek data for several time periods (Fig. 5-3). Several points are clear and include the following: 1) N and P loads prior to WWTP modifications were higher than at present but not, even prior to WWTP modifications, as high as they are in very heavily loaded systems; 2) there was a significant decline in N and P loading rates associated with WWTP modifications beginning in the early 1990s (TN and TP loads from all sources decreased by factors of factors of 1.9 and 2.4, respectively); 3) diffuse N and P loads exhibited considerable inter-annual variability related to wet and dry years (See Figure 5-2); 4) loading rate estimates from gauges and from models agreed quite well in this system; 5) loading rates for the completely forested watershed (with no atmospheric deposition) were about half what they are now during dry years and about four times lower than in recent wet years.

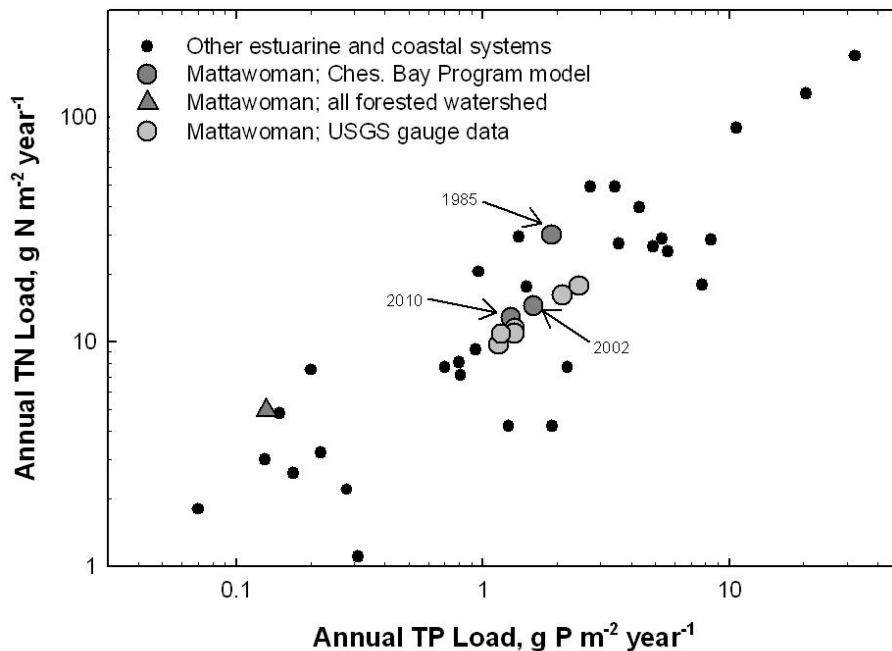


Figure 5-3. Scatter plot of annual TP versus TN loads for a variety of estuarine and coastal marine ecosystem (small gray circles; see Boynton *et al.*, 1995 for references for these sites). TP and TN loads for Mattawoman Creek were from several sources including the Chesapeake Bay Program land use model (1985, 2002 and 2010) and the USGS gauge data (2005-2011). An estimate of TN and TP loads from a fully forested pristine basin with no atmospheric deposition of N or P is also shown and was developed using forest yield coefficients of 0.15 g N m⁻² yr⁻¹ and 0.004 g P m⁻² yr⁻¹ (Boynton *et al.*, 1995).

5-4.2 Nutrient Exchanges with the Potomac

The final component of this evaluation of nutrient inputs to Mattawoman Creek concerned nutrient exchanges with the adjacent Potomac River estuary. These systems are connected via tidal water transport between the creek and Potomac River. These processes vary in magnitude on many time scales (hourly to inter-annual) and are also influenced by local and larger storm events.

In several previous studies of Chesapeake Bay tributaries we used salt and water box model results, coupled to nutrient concentrations, to estimate net nutrient flux into or out of these small estuarine systems (e.g., Hagy *et al.*, 2000; Boynton *et al.*, 2009; Boynton *et al.*, 2011). However, there is rarely any measurable salinity in Mattawoman Creek, rendering that approach impossible due to the lack of a conservative tracer. To estimate Potomac – Mattawoman nutrient exchange we obtained output from the Chesapeake Bay Program water quality model for net monthly N and P flux across the mouth of Mattawoman Creek for the period 1991-2000 (Cerco and Noel 2004). Model results indicated some DIN net transport from Mattawoman Creek to the Potomac during winter or spring and the opposite during summer-fall (Fig. 5-4). Averaged over all years the net DIN flux was about 102 kg N day⁻¹ directed into Mattawoman Creek from the Potomac River. We also had estimates of TN flux and the average multi-year flux was very small (0.4 kg N day⁻¹) and was directed from Mattawoman Creek to the Potomac River. Dissolved inorganic phosphorus (DIP) appeared to be exported from the creek during winter and imported from the Potomac during summer; the multi-year average was an export from the creek of 2.3 kg P day⁻¹ (Fig. 5-4). These results suggest Mattawoman Creek consumes DIN but exports little TN and seasonally imports or exports small amounts of DIP. The creek system acts as a sink for Potomac River N and both a small source and sink for Potomac river DIP.

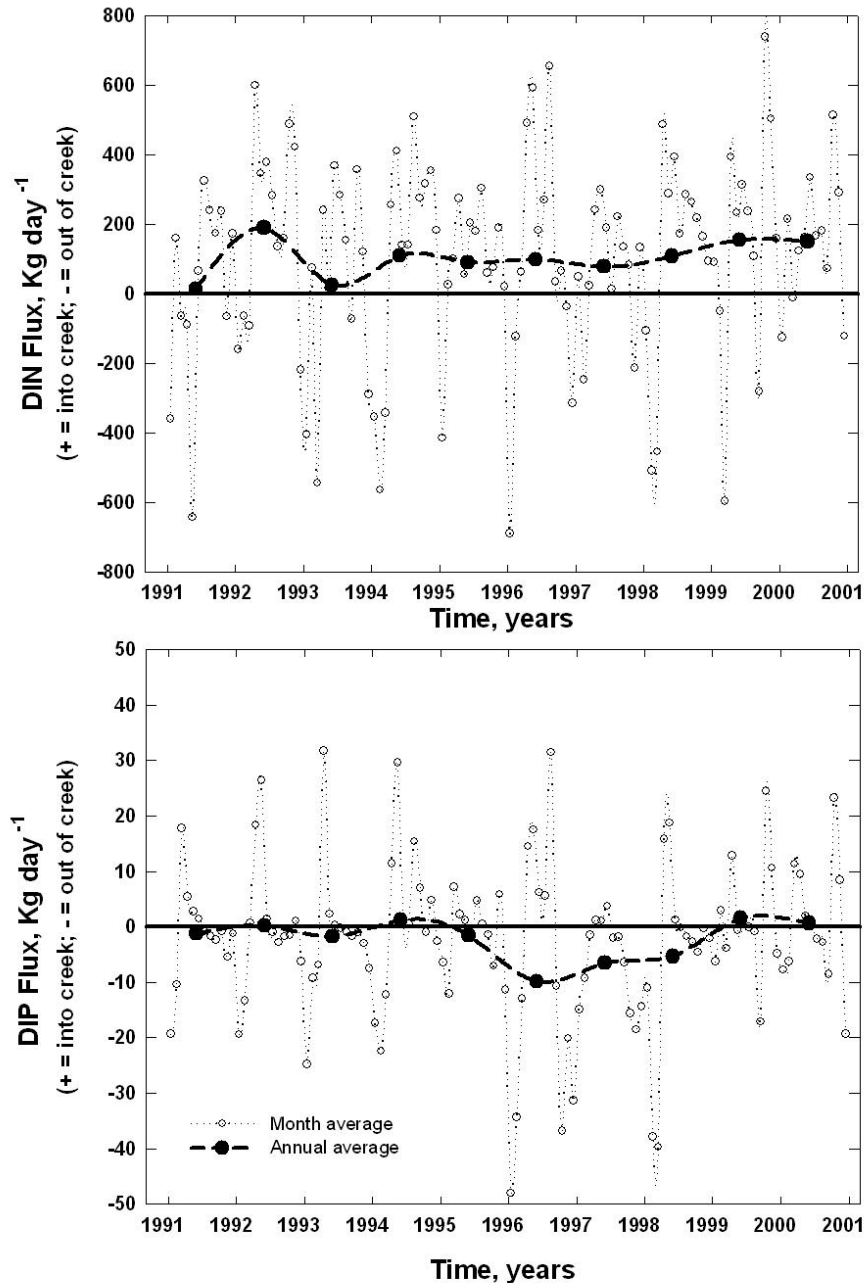


Figure 5-4. A time-series of monthly and annual net DIN and DIP exchanges between Mattawoman Creek and the Potomac River estuary for the period 1991 – 2001. The decade-long annual average exchange rates were 102 Kg N day⁻¹(into the creek) and -2.3 kg P day⁻¹ (out of the creek). These estimates were generated from the Chesapeake Bay Program water quality model (Cercio *et al.*, 2010; G. Shenk, pers.comm.).

5-4.3 Water Quality Patterns and Trends

Nutrient Concentrations: Nitrate plus nitrite (NO₂₃) and phosphate (PO₄) are essential plant nutrients, the excessive supply of which is often a root cause of estuarine eutrophication. Concentrations of NO₂₃ ranged from 0.003 to about 3 mg L⁻¹ and were uniformly higher at the

downstream site than at the upstream site throughout the period of record (Fig. 5-5). This sharply contrasts with most estuarine sites wherein nutrient concentrations decrease with distance from riverine (upstream) sources (Boynnton and Kemp 2008). In Mattawoman Creek, the higher NO_{23} concentrations at the downstream site likely reflect proximity to the Potomac River which has elevated NO_{23} and NH_4 concentrations for much of the year. Highest NO_{23} concentrations occurred during winter-spring, coincident with periods of high Potomac and local river flow. Concentrations were at times 2 orders of magnitude lower during the warm periods of the year coincident with rapid SAV and phytoplankton biomass accumulation and periods of the year when denitrification rates were also likely highest (Greene 2005b). During summer periods NO_{23} concentrations were frequently below N half-saturation (k_s) values for estuarine phytoplankton ($< 0.035 \text{ mg L}^{-1}$; Parsons *et al.*, 1984; Sarthou *et al.*, 2005) but the frequency of low values did not increase after WWTP modifications in 1996. NO_{23} concentrations at the downstream site and at the Potomac River site have decreased over time ($0.014 \text{ mg N L}^{-1} \text{ year}^{-1}$ and $0.03 \text{ mg N}^{-1} \text{ year}^{-1}$, respectively) possibly as a result of Potomac River and Mattawoman Creek WWTP modifications. No trends in NO_{23} concentration were evident at the upstream site. Ammonium concentrations were generally an order of magnitude lower than NO_{23} concentrations, were always higher in the Potomac than in Mattawoman Creek and did not exhibit strong temporal patterns at either sampling site in Mattawoman Creek (Fig. 5-5).

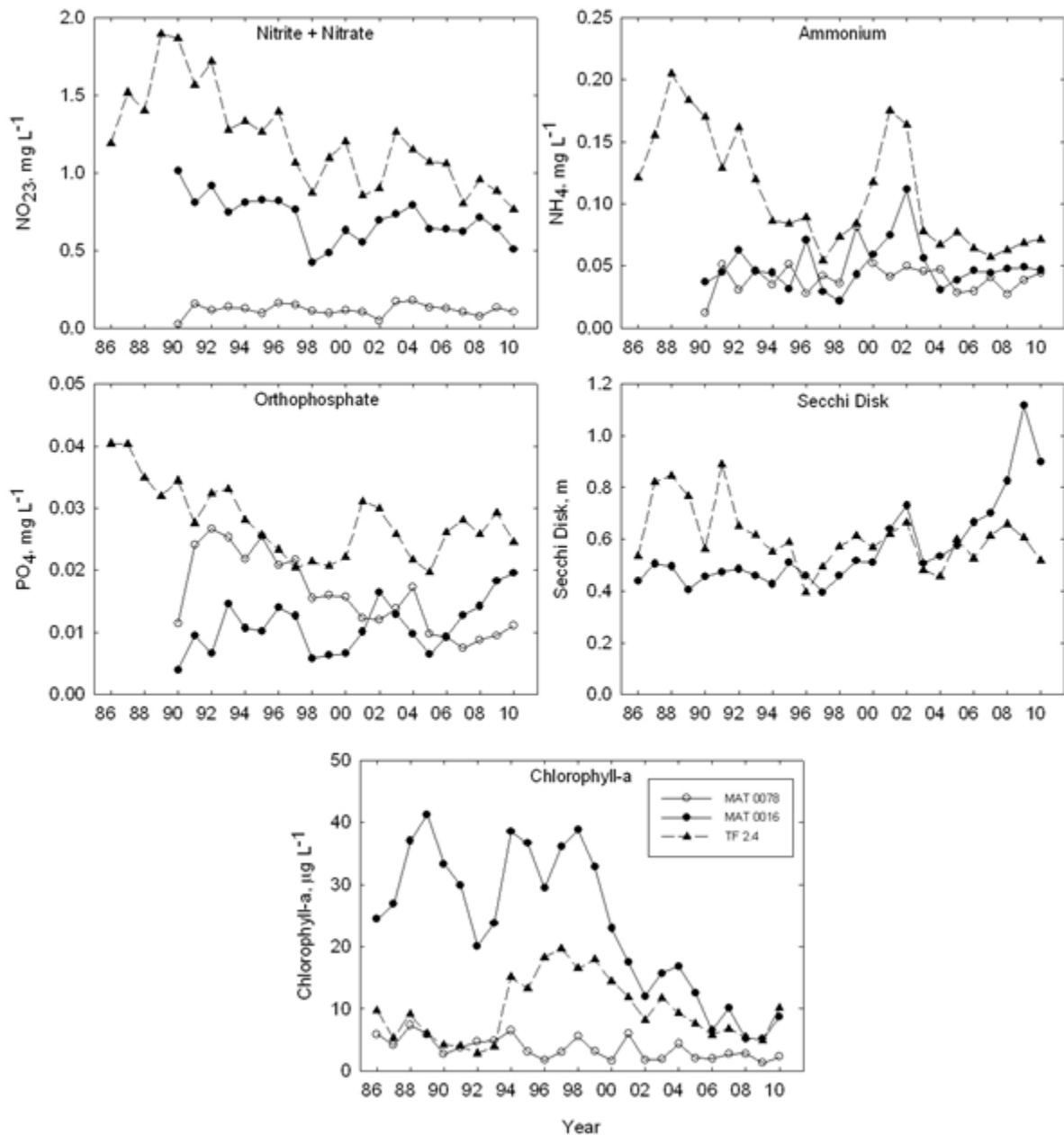


Figure 5-5. Annual average time-series data for water quality variables measured in surface waters at two sites in Mattawoman Creek (MAT 0078 and MAT0016) and one site in the adjacent Potomac River (TF2.4) for the period 1986 – 2010. Data are from Chesapeake Bay Water Quality Monitoring Program (2012).

The time-series of PO_4 concentrations in Mattawoman Creek indicate a complex pattern (Fig. 5-5). Concentrations ranged from 0.005 to 0.08 $mg L^{-1}$ at the upstream site and from about 0.002 to 0.06 $mg L^{-1}$ at the downstream site. These are typical values for a low salinity estuarine

ecosystem (Boynton and Kemp 2008). In this case, PO₄ concentrations were higher at the upstream site, as expected, during the early portion of the record (1991-2004) and then declined to levels lower than those at the downstream site. Since 2005 PO₄ concentrations at the downstream site have been increasing, possibly because of seasonal N limitation. TP concentrations were generally similar between upstream and downstream sites for the period of record and ranged from the level of detection (~0.01 mg L⁻¹) to about 0.3 mg L⁻¹. Highest TP values consistently occurred during the warmer portions of the year, a pattern frequently observed in shallow estuarine environments (Boynton and Kemp 2008), and caused by active sediment releases of P at a time of the year when autotrophic growth is limited by N.

Water Clarity: Secchi disk data are only available for the downstream station for the period 1986-2010 (Fig. 5-5). Measurements ranged from about 0.2 to 2.7 m. There was a clear trend in water clarity with values of about 0.5 m early in the record and then increasing sharply after 2004 to an annual average of about 1.1 m during 2009. Water clarity is a key issue regulating SAV community health. In the adjacent Potomac, Ruhl and Rybicki (2010) reported strong correlations between water clarity and SAV community density, coverage and species composition. At those sites, Secchi values in excess of 0.65 m were associated with bed expansion, increased plant density and a return of native species. The measurements reported here were made at sites along the main channel of Mattawoman creek rather than in SAV beds. It may be that these values underestimate water clarity in the SAV beds as shown by Gruber and Kemp (2010) based on detailed water clarity and other measurements inside and outside SAV beds in the mesohaline Chesapeake Bay. Conversely, measurements in the channel might also be higher than normal because SAV beds line much of the shoreline and tend to suppress shoreline erosion, sediment resuspension and efficiently trap sediments (Ward *et al.*, 1984).

Algal Biomass: Chlorophyll-*a* concentrations varied between 0.3 and 110 µg L⁻¹ at the downstream site and from 0.15 to 30 µg L⁻¹ at the upstream site (Fig. 5-5). Typical values at the downstream site were higher, at times an order of magnitude higher, than at the upstream site. It is likely that a combination of limited light and shorter water residence time both contributed to lower algal biomass at the upstream site. There did not appear to be any long-term trend in chlorophyll-*a* concentration at the upstream site. However, there were several distinctive temporal trends at the downstream site. Chlorophyll-*a* concentrations were generally high (annual average concentration 20-40 µg L⁻¹) from 1986-1998. Concentrations then steadily declined through 2010 to between 5 and 10 µg L⁻¹. The decline in algal biomass is likely caused by nutrient load reductions associated with WWTP operations both in Mattawoman Creek and the Potomac River. The general picture of water quality conditions that emerges from these data indicates an increase in water quality associated with changes in WWTP operations in both Mattawoman Creek and in the adjacent Potomac River. Water column pH (not shown), NO₂₃, PO₄, and chlorophyll-*a* concentration all declined and water clarity and SAV community metrics increased.

5-4.4 Community Production

We did not have high frequency water quality data for the period prior to WWTP load reductions so it was not possible to compare community production rates in the creek before and after load reductions. However, we did have estimates of community gross production (but not for total

community respiration) from a variety of shallow Chesapeake Bay sites. Community gross photosynthesis (Pg) rates in Mattawoman Creek ranged from about 2 to 11 g O₂ m⁻³ day⁻¹ (Fig. 5-6). Rates were lower during spring (Apr-May) and fall (Sep-Oct) and highest during Jun-Aug, particularly during July. Summer average rates were relatively low during 2004-2005, increased during 2006 and then declined through 2010. To place these in perspective we compared Pg rates for a variety of Chesapeake Bay systems ranging from very nutrient enriched to less enriched (Table 5-4). In general, rates were proportional to one index of enrichment (chlorophyll-*a* concentration; Pg = 5.8 + 0.15 chlorophyll-*a*; p<0.05; n=10; r²= 0.55) as Caffrey (2004) reported earlier. Rates in Mattawoman Creek tended to be low compared with rates measured in heavily enriched (e.g., upper Potomac and Corsica Rivers) ecosystems. These results are consistent with several observations: nutrient loading rates to Mattawoman Creek were sharply reduced during the time period when these measurements were made; nutrient and chlorophyll-*a* concentrations also decreased and SAV became abundant in Mattawoman Creek and such communities are not usually associated with heavily enriched systems (Latimer and Rego 2010; Orth *et al.*, 2010). Modest Pg rates support the idea that considerable oligotrophication of this system has occurred.

Table 5-4. A selection of community gross primary production rates from very enriched and less enriched Chesapeake Bay tributary sites. Since estimates of nutrient loads were not available for all sites for summer seasons (Jun – Aug) chlorophyll-*a* concentration was used as an indicator of nutrient enrichment. Details of the method for computing oxygen-based production are given in Hodgkins *et al.* (2012). Data for these estimates were from Maryland Department of Natural Resources (2012).

Nutrient		Summer Average	Summer
Enrichment	System or	Gross Primary Production	Average
Status	Location	g O₂ m⁻³ day⁻¹	Chlorophyll-<i>a</i>
Very Enriched	Bishopville (MD Cstl Bays)	17.0	70.2
	Turville Ck (MD Cstl Bays)	13.0	28.4
	Piscataway Ck (Upper Potomac)	16.0	28.8
	Upper Corsica River	12.3	45.7
	Back River	14.3	60.0
	Average	14.5	46.6
Less Enriched	St. Georges Ck (Lower Potomac)	7.3	5.9
	Stonington (Magothy)	7.5	23.5
	Mattawoman (Upper Potomac)	8.1	8.0
	Betterton Beach (Sassafras)	4.8	29.0
	Piney Pt (Lower Potomac)	5.0	10.3
	Average	6.5	15.3

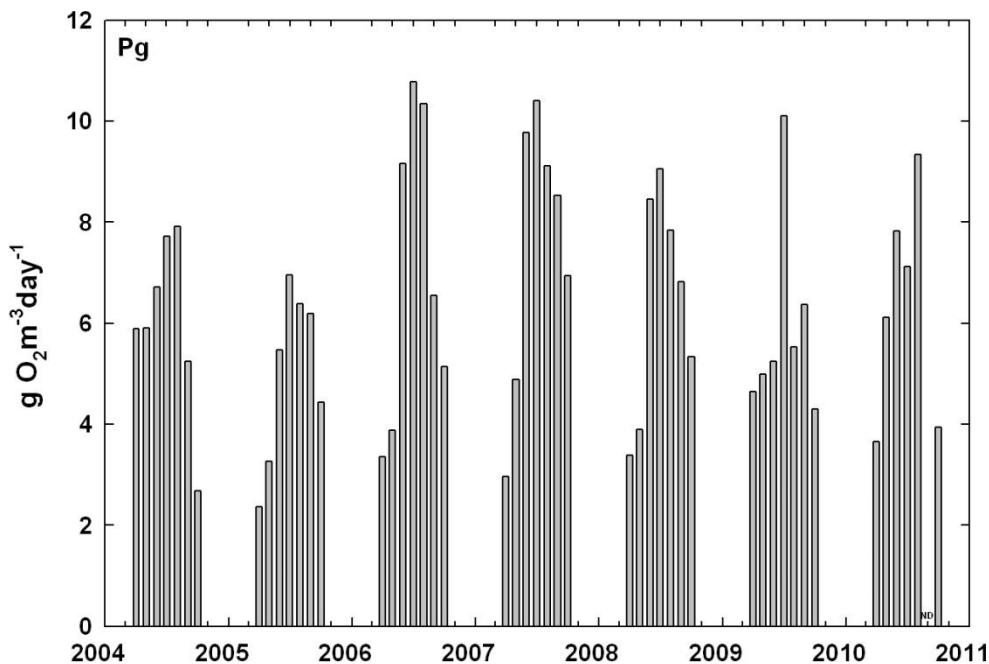


Figure 5-6. Mean monthly (Apr-Oct) estimates of community gross primary production (Pg; $\text{g O}_2 \text{ m}^{-3} \text{ day}^{-1}$) for the period 2004-2010. These estimates were generated following the technique of Odum and Hoskin (1958). Data used in these computations were from ConMon site XEA3687 in Mattawoman Creek (Figure 1). Data used in these computations are available at Maryland Department of Natural Resources (2012).

5-4.5 SAV in Mattawoman Creek

The resurgence of SAV in Mattawoman Creek represents one of a limited number of restoration successes in the Chesapeake Bay region (Orth *et al.*, 2010). It appears that substantial nutrient reductions from point sources within Mattawoman Creek and the mainstem Potomac initiated a cascade of events leading to water quality conditions supportive of SAV growth (Fig. 5-7). Before 1977 SAV were absent from the creek system. Beginning in 1989 SAV reappeared and covered a small percentage of creek bottom area (~5%) through 1997. After 1997 there was a very rapid increase in SAV coverage and beds were quite dense. By 2002 SAV beds covered about 40-50% of the surface area of the creek and have become an important component of this tributary system. The spatial pattern of SAV community recovery was also distinctive. Beginning in 1996 SAV appeared in the upper portions of the creek and began to extend downstream through 2000. By 2002 SAV had spread along both the north and south shores to the creek mouth. In more recent years (2005-2010) SAV has extended to deeper water along both

shores of the creek. This pattern of resurgence, beginning in the upstream areas of the creek, is similar to the pattern observed in other shallow, low salinity Chesapeake Bay tributaries (Boynton *et al.*, 2011). It may be that these areas are re-colonized first because they are proximal to seed and other vegetative propagules surviving in small streams of the watershed.

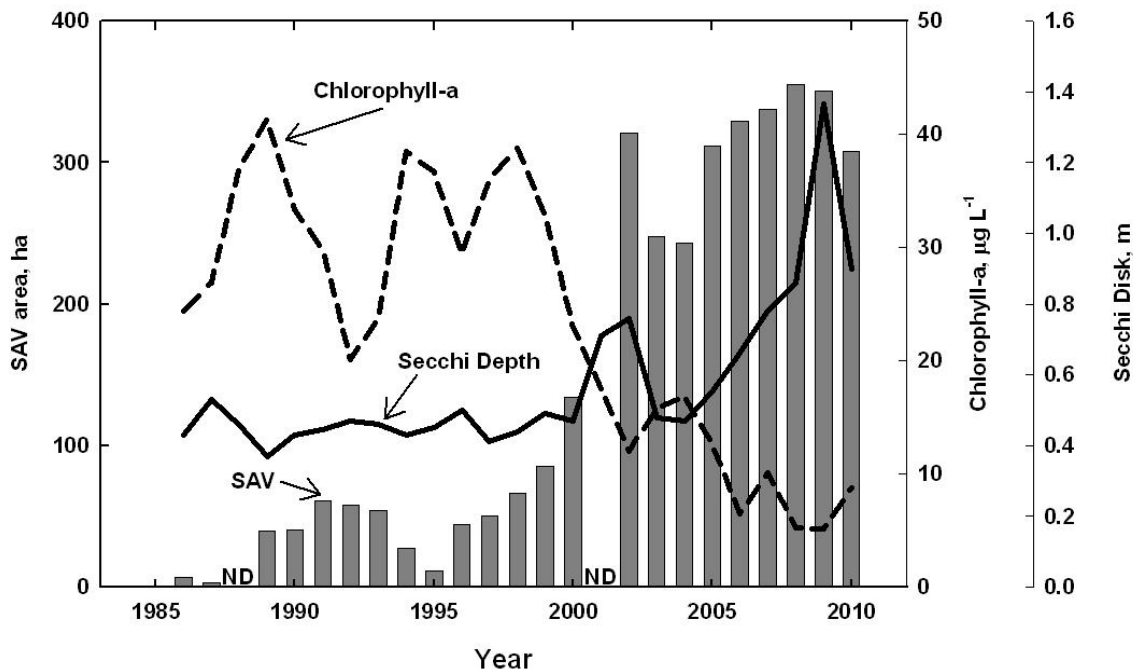


Figure 5-7. Annual summary of SAV coverage (ha), water clarity (Secchi Disk depth) and algal biomass (chlorophyll-*a* concentration) for the period 1986-2010 in Mattawoman Creek. Note the large change in SAV coverage and water clarity associated with the large decline in algal biomass. All data sources have been previously described.

The emerging understanding of SAV resurgence seems to be related to a chain of cause-effect events. It appears resurgence follows nutrient input reductions. In some cases, P seems to be the key element (e.g., Gunston Cove, a Potomac tributary; C. Jones, pers. comm.) and resurgence is preceded by a considerable lag period likely caused by the effects of excess P slowly purging from estuarine sediments. In other cases, there appears to be minimal lag and N seems to be the key element (e.g., upper Patuxent; Boynton *et al.*, 2011). Algal biomass declined and water clarity increased as nutrient inputs to Mattawoman Creek declined. We examined the Mattawoman data set for possible threshold responses relative to SAV resurgence (Fig. 5-8). The clearest of these appears to be related to water column chlorophyll-*a* concentration. When annual average chlorophyll-*a* concentration was in excess of about 18 µg L⁻¹, SAV coverage was either close to zero or minimal. In contrast, when chlorophyll-*a* concentration dropped below 18 µg L⁻¹ SAV coverage expanded very quickly; below this chlorophyll-*a* “threshold value” some other factor or factors apparently regulate inter-annual variability of SAV coverage. There was also some indication of threshold behavior related to water clarity where SAV coverage increased when Secchi disk depths exceeded about 0.5 m. Ruhl and Rybicki (2010) reported a similar

response in the adjacent tidal freshwater Potomac River although the “critical” Secchi disk depth was slightly higher (0.65 m). There now appear to be a number of cases in the Chesapeake system (in both small and large low salinity regions) where nutrient load reductions were followed by SAV resurgence and rapid bed expansion. It still remains uncertain what factors regulate lag times (when they occur) and under what conditions N or P load reductions might be the key element initiating the resurgence process.

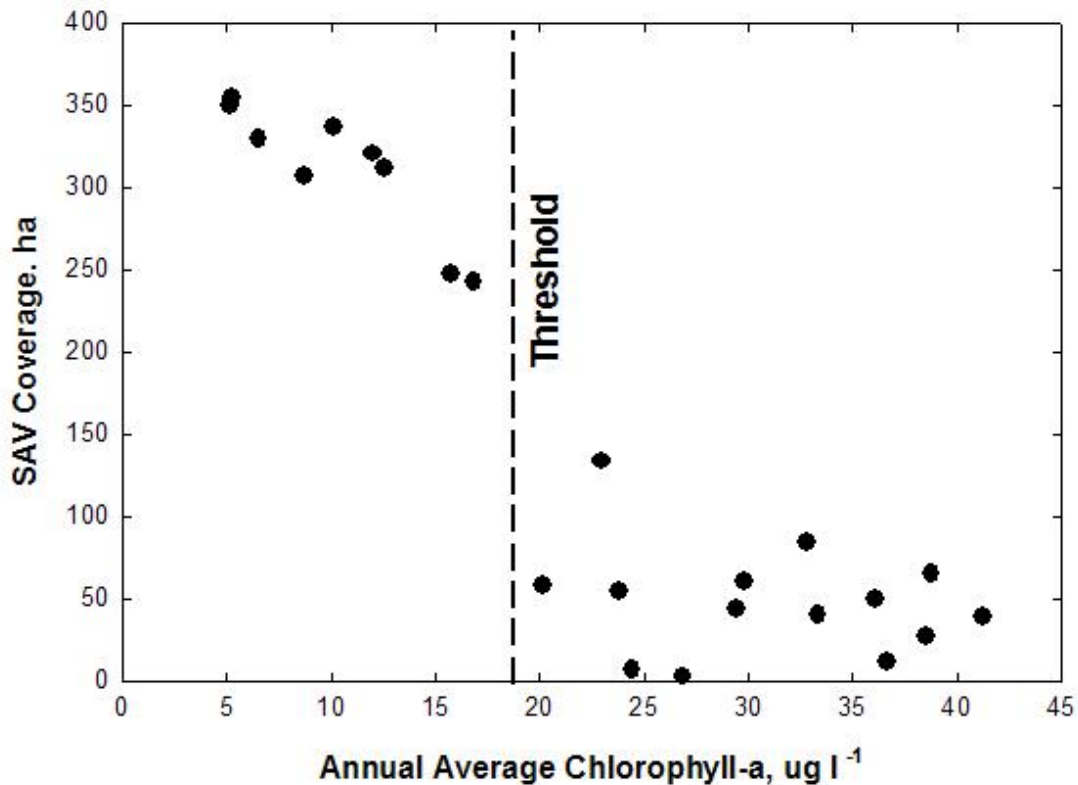


Figure 5-8. Scatter plots of average annual chlorophyll-*a* concentration versus SAV coverage for Mattawoman Creek. Data indicate a large change in SAV coverage associated with a chlorophyll-*a* threshold of about 18 $\mu\text{g L}^{-1}$ and Secchi Disk depth of about 0.5 m (not shown). Data sources have been previously noted.

A general understanding is emerging concerning relationships between nutrient loading rates and SAV community health (e.g., Kemp *et al.*, 2005). In general, it is thought that SAV communities are not competitive in environments having large nutrient loads (e.g., Valiela *et al.*, 1997). Orth *et al.* (2010) have shown that SAV resurgence in several areas of Chesapeake Bay was related to decreased N loading. In Mattawoman Creek, SAV were largely absent when N loading rates were in the range of 30 $\text{g N m}^{-2} \text{ yr}^{-1}$. When loading rates decreased to about 10-12 $\text{g N m}^{-2} \text{ yr}^{-1}$, SAV re-colonized the creek system. In addition, Latimer and Rego (2010) examined many SAV communities in southern New England for relationships to N loading rates and found SAV to be

healthy when loading rates were about $5 \text{ g N m}^{-2} \text{ yr}^{-1}$, less robust when loading rates were about $10 \text{ g N m}^{-2} \text{ yr}^{-1}$, and generally absent when loads exceeded this amount. Mattawoman Creek loads are in the upper portion of the range of “SAV-friendly” loads reported by Latimer and Rego (2010).

5-4.6 Nitrogen Budget for Mattawoman Creek

A nitrogen budget for Mattawoman Creek is provided in Figure 9; red circles indicate external N sources to the ecosystem, red arrows represent nitrogen inputs to and exports from the system, pink arrows represent estimated internal losses and gray arrows represent animal migrations that we did not attempt to quantify. In addition, water column, sediment and SAV N storages are indicated (but not evaluated) as are two internal nutrient pathways (sediment N re-cycling and net SAV N uptake). This annual time-scale budget assumes (1) completeness (i.e., there are no important missing terms in the budget) and (2) internal storages of N are not substantially changing from year to year. The attraction of a mass balance is as a quantitative framework against which we can test our understanding of system-scale nutrient dynamics (Boynton and Nixon 2012). If the budget balances (within reason) we conclude that all important processes were included and properly evaluated. However, if the budget does not balance then we know we have made an important error or neglected critical processes. Finally, reasonably balanced budgets allow us to separate large from small processes and this is an important step in choosing effective management actions.

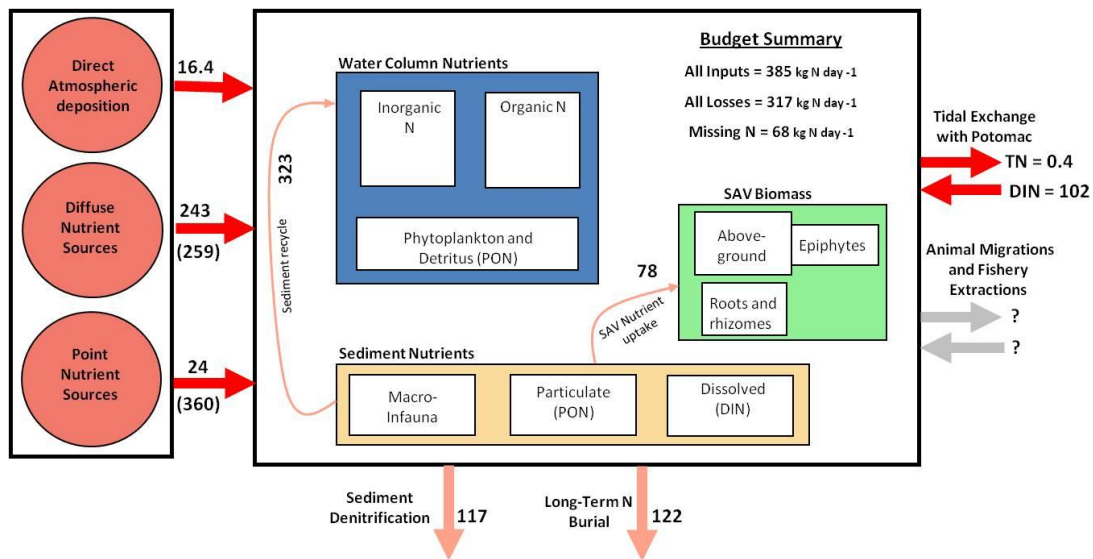


Figure 5-9. A schematic diagram of a nutrient budget (TN) model developed for Mattawoman Creek for the 2005-2010 time period. Nutrient sources are shown on the right (point, diffuse and atmospheric) and left (exchange with the Potomac River). Internal loss terms are shown at the bottom of the diagram (denitrification and long-term burial). One internal nutrient re-cycling process is also shown as is an estimate of growing season SAV N uptake. Internal stocks were not evaluated because data were not available. Bright arrows indicate data specific to Mattawoman Creek were used; light red arrows indicate data from the Chesapeake Bay region were used; gray arrows indicate no data were available and no estimate was attempted. The numbers in parentheses indicate diffuse and point source N loads prior to WWTP modifications.

External N inputs amounted to 385 kg N day⁻¹ and were dominated by diffuse sources (63%) followed by net inputs from the Potomac River (26%). Point sources and direct atmospheric deposition of N were small (6% and 4%, respectively). Prior to WWTP modifications, total N inputs were much larger (737 kg N day⁻¹) and point sources were the dominant source (47%). The two major internal losses include net denitrification and long-term burial of N (mainly particulate organic N) in the accreting sediments of the estuary. Unfortunately, there are no direct measurements of either of the major internal loss rates available for Mattawoman Creek. However, during the last decade there have been an increasing number of these measurements made in shallow estuarine systems and many of these measurements have been summarized by Greene (2005a and 2005b), Pina-Ochoa and Alvarez-Cobelas (2006) and Mullholland *et al.* (2008). To make preliminary estimates of net denitrification and long-term N burial we reviewed these values and other local values (Gao *et al.*, 2012 and Cornwell, pers.comm.) and used annual average rates of 47 $\mu\text{moles N m}^{-2} \text{ hr}^{-1}$ and 6.0 g N m⁻² yr⁻¹ for denitrification and long-term burial, respectively.

First, the proposed budget does not balance. TN inputs (385 kg N day⁻¹; including DIN inputs from the Potomac) are larger than estimated nitrogen losses (317 kg N day⁻¹) indicating that one or more major processes have not been adequately considered. One likely explanation for this is that we were not able to assign specific denitrification or nutrient burial rates to either the SAV or fringing tidal wetland communities. Direct measurements of these rates in tidal freshwater marshes of the Corsica River yielded rates three times the rates measured in open waters of the Corsica. If we adjusted Mattawoman internal loss rates so that N losses were higher in SAV and fringing tidal marsh communities, the budget readily balances. It may be worth supporting a measurement program to better quantify N losses in these communities. Boynton *et al.* (2008) found fringing tidal marshes to be a very large N and P sink in the tidal freshwater portions of the Patuxent River estuary. The second point is that diffuse sources are the most important nitrogen source. Efforts to further improve water quality will likely fail unless this term is considered and acted on; if this term increases because of changes in land use water quality will likely degrade. Third, the TN export/import term associated with exchanges with the Potomac River needs more examination. At present, model results indicate almost no net exchange of TN between the Potomac and Mattawoman Creek but also indicate a substantial input of DIN, almost all as NO₂₃, into the creek from the Potomac. This suggests that the creek acts as an N sink for the Potomac. During most of the year NO₂₃ concentration in the Potomac was higher than in the creek so the direction of net transport was largely consistent with model results presented earlier. Should nutrient concentrations in the Potomac increase further, or if remediation (and large SAV communities) further reduces N concentrations in Mattawoman Creek, the magnitude of DIN import to the creek could increase and the creek could become more nutrient enriched. DIN flux from large to smaller systems has already been documented for the Patuxent and Corsica estuaries (both Chesapeake Bay tributaries) in some summer and fall months (Boynton *et al.*, 2008). Finally, we were able to add a few internal nutrient-cycling terms to the budget analysis. Uptake of N from sediments and the water column by SAV serves as a seasonal-scale (i.e., SAV growing season; Apr-Oct) nutrient loss term as N is incorporated into plant tissue. We estimated this rate by using data from aerial SAV surveys (VIMS 2011), SAV biomass as suggested by Moore *et al.* (2000) and estimates of the % N content of SAV from a

variety of sources (e.g., Abbasi *et al.*, 1990, Yu *et al.*, 2010, Mukherjee *et al.*, 2008). The results indicate a modest seasonal-scale buffering of nutrients by the SAV community. It is likely that SAV nutrient buffering via enhanced denitrification and burial of PON, as indicated above, is considerably greater than the estimate we generated with available data from non-vegetated sediments. We also examined sediment flux data from many small tidal freshwater Chesapeake Bay tributaries (Bailey 2005) and estimated sediment NH₄ releases in Mattawoman Creek. These were substantial and were the largest single term in the budget. This result has been observed in other systems (Boynton *et al.*, 1995; Boynton and Kemp 2008) and indicates the importance of sediment nutrient sources in sustaining autotrophic production in shallow systems, especially during warmer months of the year when sediment processes are most active. However, we also know that sediment releases of NH₄ are sensitive to the supply of labile organic matter to the sediment surface (Cowan and Boynton 1996). The supply rate of such material likely decreased following large reductions in WWTP discharges and the magnitude of sediment nutrient releases probably also declined.

5-4.7 Nutrient Cause-Effect Chains

In many estuarine ecosystems, excessive nutrient loading is the primary cause of rapid algal growth and biomass accumulation and that seems to be the case in Mattawoman Creek. The relationship between nutrient loads from all sources and algal responses (chlorophyll-*a* concentration) is the starting point for the following analyses. Essentially, we attempted to link nutrient loading from drainage basins to estuarine chlorophyll-*a* concentration, and subsequently link algal stocks to summer water clarity. Linkages of key water quality variables to nutrient loads will allow for preliminary estimates of the magnitude of estuarine responses to future nutrient load reductions or increases. In developing these relationships, data from several shallow estuarine systems were used in a comparative analysis approach to increase the signal to noise ratio and to examine the robustness or generality of results (Kemp and Boynton 2012).

Many measurements of chlorophyll-*a* from several locations in Mattawoman Creek indicated elevated summer concentrations. Cold season algal blooms also occurred and likely deposited labile organic material onto sediments which are not decomposed until early-to-mid summer when elevated temperature stimulates sediment bacterial activity. Respiration of such material releases nutrients to the water column during summer and these nutrients, in addition to spring nutrient inputs, help stimulate the large summer blooms in the creek. The connection of winter-spring nutrient loads to summer blooms is well described in Chesapeake Bay and its tributaries and is also reflected in data for several shallow estuaries connected or adjacent to Chesapeake Bay region (Boynton *et al.*, 1995; Boynton and Kemp 2000) and elsewhere (Nixon 1988). Using a multi-system comparison of shallow, mildly to very eutrophic estuaries in the Chesapeake Bay region, winter-spring N loading and summer chlorophyll-*a* were found to be highly correlated, and data for Mattawoman Creek fit the general pattern (Fig. 5-10). The relationship appears to be linear and indicates the potential for large changes in chlorophyll-*a* in response to nitrogen load changes. Several annual observations were available for Mattawoman Creek including one set of observations from the 1985-1988 periods when nutrient loading rates were much higher and a set of more recent observations (2005-2010) collected when nutrient loading rates were much lower. Both data sets conformed to the general relationship. A factor of about four reduction of nutrient

loading rate resulted in about a factor of five reduction in chlorophyll-*a* concentration, suggesting this system is responsive to nutrient load changes.

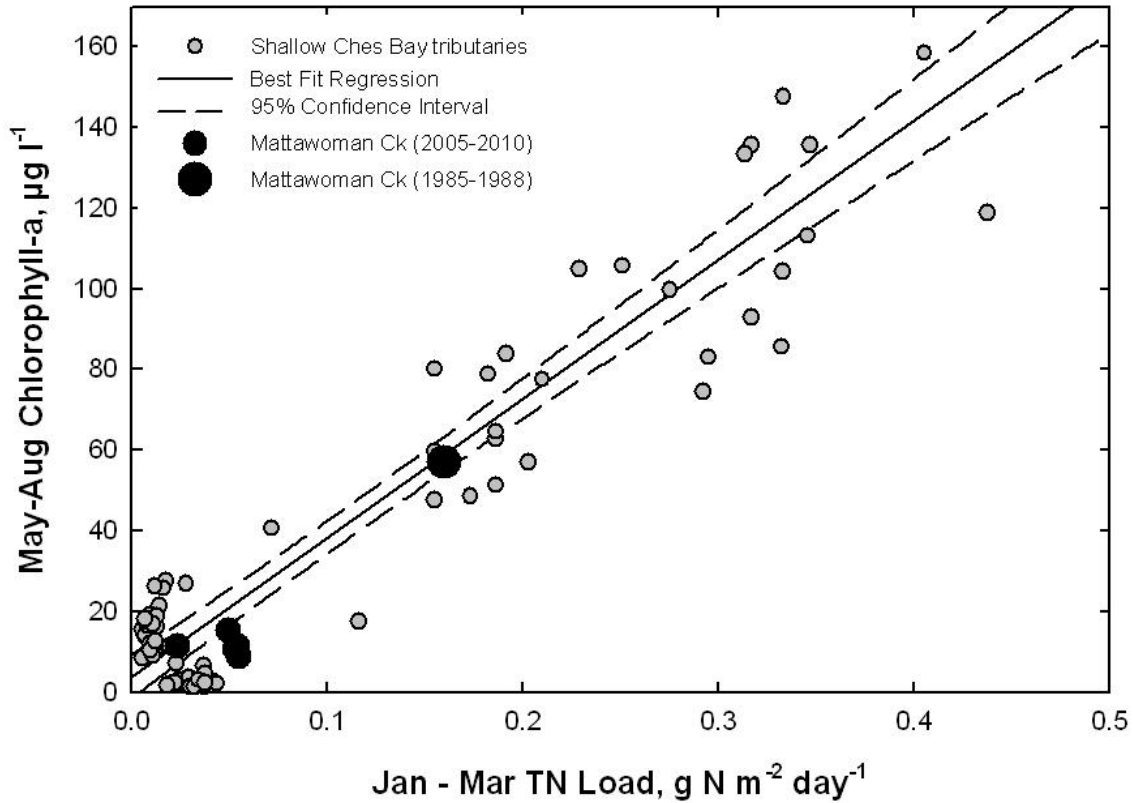


Figure 5-10. A scatter plot of winter-spring TN load versus chlorophyll-*a* concentration developed for Mattawoman creek and other shallow Chesapeake Bay tributaries. The large decrease in nitrogen loading was accompanied by a large reduction in chlorophyll-*a* concentration. Data for the other Chesapeake Bay systems was from Boynton *et al.* (2009).

Water clarity determines how much light is available for photosynthesis by phytoplankton in the water column and by SAV and benthic algae growing at the sediment surface. Water clarity is typically reduced in estuaries when the concentration of algae, sediments, colored dissolved materials and other particles increases in the water column, and that was the case in Mattawoman Creek during earlier years. Secchi disk measurements revealed distinct patterns in water clarity, the main ones being that depths varied seasonally during any one year (not shown) and water clarity has improved since 2000 (Fig. 5-5). Using Secchi disk data, we estimated the water depth to which 1% of surface light penetrated (minimum light needed for benthic diatom growth). Growth of these algae on the sediment surface can reduce nutrient flux from sediments to the water column and also suppress sediment re-suspension. It is clear that prior to 2000, 1% light reached depths of about 1.1m while during more recent years, Secchi depths increased and the 1% light depth increased to 3 m, considerably greater than the average depth of the creek.

Correlations between Secchi depth and both chlorophyll-*a* and total suspended solids (TSS) indicated that both contributed to light attenuation in the creek, but chlorophyll-*a* in this case was more strongly correlated with water clarity ($r^2 = 0.80$, $p < 0.01$) and this, in turn, suggested that reductions in chlorophyll-*a* via nutrient load reductions would result in increased water clarity. To continue examination of the cause-effect chain described earlier, chlorophyll-*a* and Secchi depth data from Mattawoman Creek and from several other small tributary rivers were combined in a comparative analysis and a strong relationship was again observed (Fig. 5-11). SAV were absent from this system when Secchi depths were less than 0.5 m or when chlorophyll-*a* concentrations were greater than about $18 \mu\text{g L}^{-1}$.

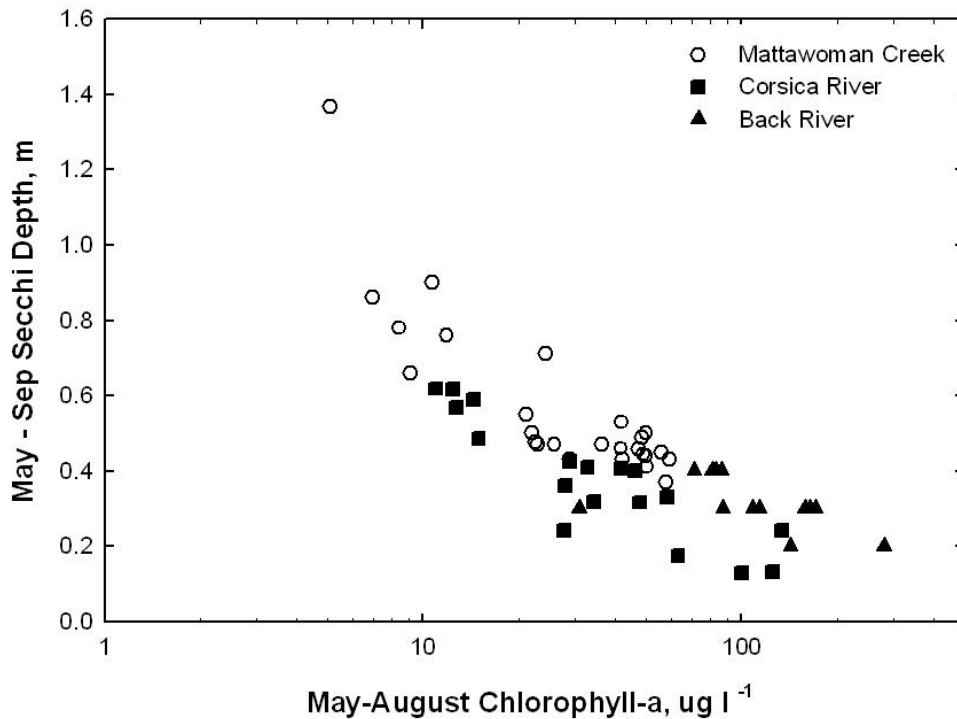


Figure 5-11. A scatter plot of chlorophyll-*a* versus Secchi disk depth developed for Mattawoman Creek and two other shallow Chesapeake Bay systems. Data for the other shallow systems were from Boynton *et al.* (2009) and Mattawoman Creek data were from the Chesapeake Bay Water Quality Monitoring Program (2012).

5-5 Summary and Future Investigations

Substantial point source nutrient (N and P) reductions in the system resulted in large reductions in algal biomass, large increases in SAV coverage and density and modest increases in water clarity. Initial responses to nutrient load reductions occurred relatively quickly (1-4 years) but more “steady-state” conditions took longer to emerge. For example, N and P load reductions

were initiated during 1991 and were largely completed by 1995; algal chlorophyll began declining during 1999 but did not reach low and stable levels until 2006, 11 years after input reductions were complete. A similar, but shorter, response pattern was evident with SAV wherein bed expansion started the year after load reductions were completed but did not reach a higher and more stable condition until 2003. Thus, system responses ranged from annual to decadal depending on the component being considered, a finding similar to those reported by Borja *et al.* (2010). We suggest that researchers clearly indicate the temporal sequence of nutrient load reductions as this clearly has implications for determining response lag times.

Duarte *et al.* (2009) considered the notion that appropriate nutrient load reductions would return impaired ecosystems to their original or baseline condition. In their evaluation of four systems they found complex restoration trajectories and each system failed to return to an earlier reference condition. This is depressing news for those charged with restoration and responsibility for the expenditure of public funds. In the case of Mattawoman Creek, we can make several observations relevant to the Duarte *et al.* (2009) results. While we do not have a reference condition with which to compare the current status of the creek, we do know several things. SAV were abundant in the upper Potomac, including Mattawoman and other small tributaries, prior to 1940 (Carter *et al.*, 1994). After that time, water quality and habitat conditions seriously deteriorated through the early 1970s; huge algal blooms were common, DO concentrations declined and SAV were largely absent (Jaworski *et al.*, 2007). We found a few chlorophyll-*a* measurements for Mattawoman Creek from the 1970s exceeding 100 $\mu\text{g L}^{-1}$ and aerial photographs indicated SAV were absent. Thus, there is qualitative information suggesting an earlier state of clearer water, low algal stocks and abundant SAV followed by a 40 year period of poor water and habitat quality. The current condition in Mattawoman Creek tends to resemble the pre-1940s condition with clearer water, a vibrant SAV community (with invasive species included), relatively low algal stocks and a “world-class” largemouth bass fishery. Mattawoman Creek may not have returned to a baseline condition (*Neverland* in Duarte’s terms) but, from the point of view of water quality managers and those who recreate in this system, it is vastly improved and it seems reasonable to call this a successful restoration. Similar results have been reported for Tampa Bay (Greening and Janicki 2006), and multiple SAV sites in Chesapeake Bay (Orth *et al.*, 2010).

The nutrient budget did not balance and that might be grounds for not reporting results. However, imperfect budgets can still be very useful thinking and organizational tools. First, nutrient input data were available and these indicated the current importance of diffuse sources and the large role atmospheric deposition plays in this load component. Without a budget framework these conclusions would not have been evident. In addition, use of water quality model results indicated nitrogen was imported from the Potomac to Mattawoman Creek, constituting another source. The budget framework allowed us to conclude this source represented about 25% of the annual N load. We often think of nutrient loads coming from the surrounding basin, atmospheric deposition and point sources but this observation indicates downstream sources can be important as well. A similar result has been reported for the Patuxent River estuary (Boynton *et al.*, 2008). Water quality managers need to know if enrichment problems are caused by local, downstream or some combination of both sources. We also considered why the budget did not balance and where the missing N sinks might be located. Work by others in Chesapeake Bay have indicated elevated denitrification rates in fringing

wetlands, oyster reefs and SAV communities (Gao *et al.*, 2012; Boynton *et al.*, 2008; Greene 2005a). Our estimates indicate even slightly elevated rates would lead to a balanced N budget.

5-6 References

- Abbasi, S.A., P.C. Nipanay, and G.D. Schaumberg. 1990. Bioenergy potential of eight common aquatic weeds. *Biological Wastes* 34: 359-366.
- Allan, J. D. 2004. Landscapes and Riverscapes: The influence of land use on stream ecosystems. *Ann. Rev. Ecol. Evol. Syst.* 35: 257-284.
- Bailey, E. 2005. Measurements of nutrient and oxygen fluxes in estuarine and coastal marine sediments: Literature review and data report, Technical Report Series Ref. No. [UMCES]CBL 05-091. University of Maryland Center for Environmental Science, Chesapeake Biological Laboratory, Solomons, MD, 36pp. <http://www.gonzo.cbl.umces.edu>.
- Bicknell, B.R., J.C. Imhoff, J.L. Kittle Jr., T.H. Jobes, and A.S. Donigian Jr. 2005. Hydrological Simulation Program—FORTRAN. User's Manual for Release 12.2. U.S. Environmental Protection Agency Ecosystem Research Division, Athens, GA, and U.S. Geological Survey, Office of Surface Water, Reston, VA.
- Borja, A., D. M. Dauer, M. Elliott, and C. A. Simenstad. 2010. Medium-and long-term recovery of estuarine and coastal ecosystems: patterns, rates and restoration effectiveness. *Estuaries and Coasts* 33: 1249-1260.
- Boynton, W. R., J. H. Garber, R. Summers and W. M. Kemp. 1995. Inputs, transformations, and transport of nitrogen and phosphorus in Chesapeake Bay and selected tributaries. *Estuaries* 18: 285-314.
- Boynton, W. R. and W. M. Kemp. 2000. Influence of river flow and nutrient loading on selected ecosystem processes and properties in Chesapeake Bay. In *Estuarine Science: A synthetic approach to research and practice*, ed. J.E. Hobbie, 269-298. Washington, DC: Island Press.
- Boynton, W.R. and W.M. Kemp. 2008. Nitrogen in Estuaries. In: Capone, D., D. A. Bronk, M. R. Mulholland and E. J. Carpenter (eds.), *Nitrogen in the Marine Environment* (Second Edition). Academic Press, p.809-866: 978-0-12-372522-6.
- Boynton, W. R., J. D. Hagy, J. C. Cornwell, W. M. Kemp, S. M. Greene, M. S. Owens, J. E. Baker, and R. K. Larsen. 2008. Nutrient budgets and management actions in the Patuxent River Estuary, Maryland. *Estuaries and Coasts* 31(4): 623-651.
- Boynton, W.R., J.M. Testa and W.M. Kemp. 2009. An Ecological Assessment of the Corsica River Estuary and Watershed Scientific Advice for Future Water Quality Management: Final Report to Maryland Department of Natural Resources. Ref. No. [UMCES]CBL 09-117. [UMCES Technical Series No. TS-587-09-CBL].
- Boynton, W.R., L.A. Wainger, E.M. Bailey, A.R. Bayard, C.L. Sperling and M.A.C.Ceballos. 2011. Ecosystem Processes Component (EPC). Maryland Chesapeake Bay Water Quality

Monitoring Program, Level 1 report No. 28. Jul. 1984 -- Dec. 2010. Ref. No. [UMCES] CBL 11-024. [UMCES Technical Series No. TS-620-11-CBL].

Boynton, W.R., L.A. Wainger, E.M. Bailey, A.R. Bayard, C.L.S. Hodgkins and M.A.C. Ceballos. 2012. Ecosystem Processes Component (EPC). Maryland Chesapeake Bay Water Quality Monitoring Program, Level 1 report No. 29. Jul. 1984 -- Dec. 2011. Ref. No. [UMCES]CBL 12-020.[UMCES Technical Series No. TS-637-12-CBL].

Boynton, W. R. and S. W. Nixon. 2012. Budget Analyses of Estuarine Ecosystems, Chapter 17, pp 443-464; In: John Day *et al* (eds). *Estuarine Ecology*. Wiley-Blackwell, New Jersey.

Bricker, S. B., C. G. Clement, D. E. Pirhalla, S. P. Orlando, and D. R. G. Farrow. 1999. National Estuarine Eutrophication Assessment: effects of nutrient enrichment in the nation's estuaries. NOAA, National Ocean Science, Centers for Coastal Ocean Science, Silver Spring, MD.

Burns, D.A., Lynch, J.A., Cosby, B.J., Fenn, M.E., Baron, J.S., US EPA Clean Air Markets Div. 2011. *National Acid Precipitation Assessment Program Report to Congress 2011: An Integrated Assessment*, National Science and Technology Council, Washington, DC, 114 p.

Caffrey, J. M. 2004. Factors controlling net ecosystem metabolism in U. S. estuaries. *Estuaries* 27(1): 90-101.

Carter, V., N. B. Rybicki, J. M. Landwehr, and M Turtora. 1994. Role of weather and water quality in population dynamics of submersed macrophytes in the tidal Potomac River. *Estuaries* 17(2): 417-426.

Castro, M. S., C. T. Driscoll, T. E. Jordan, W. G. Reay, and W. R. Boynton. 2003. Sources of nitrogen to estuaries In the United States. *Estuaries* 26(3): 803-814.

Cerco, C.F. and M.R. Noel. 2004. *The 2002 Chesapeake Bay Eutrophication Model*. EPA 903 04-004. U.S. Environmental Protection Agency, Chesapeake Bay Program Office, Annapolis, MD.

Cerco, C., S.C. Kim, and M.R. Noel. 2010. The 2010 Chesapeake Bay Eutrophication Model. A Report to the US Environmental Protection Agency and to the US Army Corps of Engineer Baltimore District. US Army Engineer Research and Development Center, Vicksburg, MD. (also http://www.chesapeakebay.net/content/publications/cbp_26167.pdf).

Chesapeake Bay Program. 2011. Point source loading database. US EPA Chesapeake Bay Program, Annapolis, MD (<http://www.chesapeakebay.net>)

Chesapeake Bay Water Quality Monitoring Program. 2012. US EPA Chesapeake Bay Program, Annapolis, MD (<http://www.chesapeakebay.net>)

Cloern, J. E. 2001. Our evolving conceptual model of the coastal eutrophication problem. *Mar. Ecol. Prog. Ser.* 210: 223-253.

- Conley, D. J., S. Markager, J. Andersen, T. Ellermann, and L. M. Svendsen. 2002. Coastal eutrophication and the Danish National Aquatic Monitoring and Assessment Program. *Estuaries* 25: 848-861.
- Conley, D. J., J. Carstensen, G. Ertebjerg, P. B. Christensen, T. Dalsgaard, J. L. S. Hansen and A. B. Josefson. 2007. Long-term changes and impacts of hypoxia in Danish coastal waters. *Ecol. Applications* 17(5) Supplement: S165-S184.
- Conley, D. J., J. Carstensen, R. Vaquer-Sunyer and C. M. Duarte. 2009. Ecosystem thresholds with hypoxia. *Hydrobiologia* 629: 21-29.
- Cowan, J. L. W. and W. R. Boynton. 1996. Sediment-water oxygen and nutrient exchanges along the longitudinal axis of Chesapeake Bay: Seasonal patterns, controlling factors and ecological significance. *Estuaries* 19 (3): 562-580.
- Cronin, W.B. and D.W. Pritchard. 1975. Additional Statistics on the Dimensions of the Chesapeake Bay and its Tributaries: Cross-section Widths and Segment Volumes Per Meter Depth. Special Report 42. Chesapeake Bay Institute, The Johns Hopkins University. Reference 75-3. Baltimore, MD
- DiToro, D. M. 2001. *Sediment Flux Modeling*. Wiley-Interscience, NY. 624pp.
- Duarte, C. M., D. J. Conley, J. Carstensen, and Maria Sanchez-Camacho. 2009. *Estuaries and Coasts* 32: 29-36.
- Fisher, D. and M. Oppenheimer. 1991. Atmospheric nitrogen deposition and the Chesapeake Bay estuary. *Ambio* 20(3): 102-108.
- Gao, Y., J. C. Cornwell, D. K. Stoecker, and M. S. Owens. 2012. Effects of cyanobacterial-driven pH increases on sediment nutrient fluxes and coupled nitrification-denitrification in a shallow freshwater estuary. *Biogeosciences* 9: 2697-2710.
- Greene, S. 2005a. Tidal freshwater and oligohaline marshes as nutrient sinks in the Patuxent River estuary, Maryland. MS Thesis, University of Maryland, College Park, MD
- Greene, S. 2005b. Measurements of denitrification in aquatic ecosystems; Literature review and data report. Technical Report Series Ref. No. [UMCES]CBL 05-094. University of Maryland Center for Environmental Science, Solomons, MD
- Greening, H. and A. Janicki. 2006. Toward reversal of eutrophic conditions in a subtropical estuary: Water quality and seagrass response to nitrogen reductions in Tampa Bay, Florida, USA. *Environ. Mgmt.* 38: 163-178.
- Gruber, R. K. and W. M. Kemp. 2010. Feedback effects in a coastal canopy-forming submersed plant bed. *Limnol. Oceanogr.* 55(6): 2285-2298.

Hagy, J. D., L. P. Sanford and W. R. Boynton. 2000. Estimation of net physical transport and hydraulic residence times for a coastal plain estuary using box models. *Estuaries* 23(3): 328-340.

Hagy, J. D., W. R. Boynton, C. W. Keefe and K. V. Wood. 2004. Hypoxia in Chesapeake Bay, 1950-2001: Long-term change in relation to nutrient loading and river flow. *Estuaries* 27(4): 634-658.

Hodgkins, C.L.S., W.R. Boynton, E.M. Bailey, and M.A.C. Ceballos. 2012. Community Metabolism as an Indicator of Water Quality Impairment and Restoration. Ecosystem Processes Component (EPC). Maryland Chesapeake Bay Water Quality Monitoring Program, Level 1 report No. 29. Jul. 1984-Dec. 2012. Ref. No. [UMCES] CBL 12-020. [UMCES Technical Series No. TS-637-12-CBL].

Holland, A. F., D. M. Sanger, C. P. Gawle, S. B. Lerberg, M. S. Santiago, G. H. M. Riekerk, L. E. Zimmerman, and G. I. Scott. 2004. Linkages between tidal creek ecosystems and the landscape and demographic attributes of their wetlands. *J. Exp. Mar. Biol. Ecol.* 298: 151-178.

Howarth, R. W. and R. Marino. 2006. Nitrogen as the limiting nutrient for eutrophication in coastal marine ecosystems: Evolving views over three decades. *Limnol. Oceanogr.* 51 (1, part2): 364-376.

Jaworski, N. J., W. Romano, C. Buchanan, and C. Jaworski. 2007. The Potomac River Basin and its Estuary: Landscape Loadings and Water Quality Trends, 1895-2005. Potomac Integrative Analysis Online Collection at www.potomacriver.org.

Jeppesen, E. and 30 others. 2005. Lake responses to reduced nutrient loading: an analysis of contemporary long-term data from 35 case studies. *Freshw. Biol.* 50: 1747-1771.

Johansson, J.O.R. 2002. Historical overview of Tampa Bay water quality and seagrass issues and trends, p. 1-10. In Greening, H.S. (ed.), Proceedings, Seagrass Management, It's Not Just Nutrients! Symposium held August 22-24, 2000, St. Petersburg, FL. Tampa Bay Estuary Program. 246 p.

Kemp, W.M., W.R. Boynton, J.E. Adolf, D.F. Boesch, W.C. Boicourt, G. Brush, J.C. Cornwell, T.R. Fisher, P.M. Glibert, J.D. Hagy, L.W. Harding, E.D. Houde, D.G. Kimmel, W.D. Miller, R.I.E. Newell, M.R. Roman, E.M. Smith and J.C. Stevenson. 2005. Eutrophication of Chesapeake Bay: historical trends and ecological interactions. *Mar. Ecol. Prog. Ser.* 303:1-29.

Kemp, W. M., J. M. Testa, D. J. Conley, D. Gilbert, and J. D. Hagy. 2009. Temporal responses of coastal hypoxia to nutrient loading and physical controls. *Biogeosciences* 6: 2985-3008.

Kemp, W. M. and W. R. Boynton. 2012. Synthesis in estuarine and coastal ecological research: What is it, why is it important, and how do we teach it? *Estuaries and Coasts* Vol. 35(1): 1-22.

- Kronvang, B., K. Jeppesen, D. J. Conley, M. Sondergaard, S. E. Larsen, N. B. Ovesen, and J. carstensen. 2005. Nutrient pressures and ecological responses to nutrient loading reductions in Danish streams, lakes and coastal waters. *J. Hydrol.* 304: 274-288.
- Linker, L.C., G.W. Shenk, P. Wang, R. Batiuk, 2008. Chapter 3: Integration of Modeling, Research, and Monitoring in the Chesapeake Bay Program in Management of Water Quality and Irrigation Techniques, Editors: Jose Albiac and Ariel Dinar, Earthscan. London, UK.
- Linker, L.C., G.W. Shenk, R.L. Dennis, and J.S. Sweeney. 2000. Cross-Media Models of the Chesapeake Bay Watershed and Airshed. *Water Quality and Ecosystem Modeling* 1(1-4):91-122.
- Latimer, J. S. and S. A. Rego. 2010. Empirical relationship between eelgrass extent and predicted watershed-derived nitrogen loading for shallow New England estuaries. *Estuarine, Coastal and Shelf Science.* 90: 231-240.
- Maryland Department of Natural Resources. 2012. Eyes on the Bay (www.eyesonthebay.gov)
- Maryland Department of Planning. 2012. Land Uses in Maryland (www.mdp.state.md.us and www.mdp.state.md.us/OurWork/landuse.shtml)
- Merrill, J. Z. 1999. Tidal freshwater marshes as nutrient sinks: particulate nutrient burial and denitrification. MS Thesis, University of Maryland, College Park, MD
- Moore, K.A., D.J. Wilcox and R.J. Orth. 2000. Analysis and abundance of submersed aquatic vegetation communities in the Chesapeake Bay. *Estuaries* 23(1): 115-127.
- Mukherjee, B., D. Mukherjee, and M. Nivedita. 2008. Modeling carbon and nutrient cycling in a simulated pond system at Ranchi. *Ecological Modelling* 213(3-4): 437-448.
- Mullholland *et al.* 2008. Stream denitrification across biomes and its response to anthropogenic nitrate loading. *Nature* 452: 202-206
- Murphy, R. R., W. M. Kemp and W. P. Ball. 2011. Long-term trends in Chesapeake Bay seasonal hypoxia, stratification, and nutrient loading. *Estuaries and Coasts* 34: 1293-1309.
- Nutrient Analytical Services Laboratory, Chesapeake Biological Laboratory. 2012. <http://nasl.cbl.umces.edu>
- Nixon, S. W. 1988. Physical energy inputs and the comparative ecology of lake and marine ecosystems. *Limnol. Oceanogr.* 33: 1005-1025
- Nixon, S. W. 1995. Coastal marine eutrophication: A definition, social causes, and future concerns. *Ophelia* 41: 199-219.

- Nixon, S., B. Buckley, S. Granger and J. Bintz. 2001. Responses of very shallow marine ecosystems to nutrient enrichment. *Human and Ecological Risk Assessment* 7(5): 1457-1481.
- Nixon, S. W. 2009. Eutrophication and the macroscope. *Hydrobiologia* 629: 5-19.
- Odum, H. T. and C. M. Hoskin. 1958. Comparative studies on the metabolism of marine waters. *Publ. Inst. Mar. Sci., Univ. Texas* 5: 16-46.
- Orth, R. J., M.R. Williams, S.R. Marion, D.J. Wilcox, T.J.B. Carruthers, K. A. Moore, W.M. Kemp, W.C. Dennison, N. Rybicki, P. Bergstrom, R. A. Batiuk. 2010. Long-term trends in submersed aquatic vegetation (SAV) in Chesapeake Bay, USA, related to water quality. *Estuaries and Coasts* 33: 1144-1163.
- Paerl, H. W. 2009. Controlling eutrophication along the freshwater-marine continuum: Dual nutrient (N and P) reductions are essential. *Estuaries and Coasts* 32:593-601.
- Parsons, T. R., M. Takahashi and B. Hargrave. 1984. *Biological Oceanographic Processes*. Pergamon Press, Oxford. 330 p.
- Pina-Ochoa, E. and M. Alvarez-Cobelas. 2006. Denitrification in aquatic environments: a cross-system analysis. *Biogeochemistry* 81: 111-130.
- Rabalais, N. N. 2002. Nitrogen in aquatic ecosystems. *Ambio* 31(2): 102-112.
- Rask, N., S. E. Pedersen and M. H. Jensen. 1999. Response to lower nutrient discharges in the coastal waters around the island of Funen, Denmark. *Hydrobiologia* 393: 69-81.
- Ruhl, H. A. and N. B. Rybicki. 2010. Long-term reductions in anthropogenic nutrients link to improvements in Chesapeake Bay habitat. *PNAS.org/cgi/doi/10.1073/pnas.1003590107*.
- Ryther, J. H. 1954. The ecology of phytoplankton blooms in Moriches Bay and Great South Bay, Long Island, New York. Contribution No. 685. Woods Hole Oceanographic Institution, Woods Hole, MA pp. 198-207.
- Sarthou, G., K. R. Timmermans, S. Blain and P. Treguer. 2005. Growth physiology and fate of diatoms in the ocean: a review. *J. Sea Res.* 53: 25-42.
- Schueler, T. 1994. The importance of imperviousness. *Watershed Protection Techniques* 1(3): 100-111.
- Shenk G.W., and L.C. Linker. In Press. Development and Application of the Phase 5 Chesapeake Watershed Model. *Journal of the American Water Resources Association*.
- Smith, V. H., S. B. Joye and R. W. Howarth. 2006. Eutrophication of freshwater and marine ecosystems. *Limnol. Oceanogr.* 51(1, part 2): 351-355.

United States Environmental Protection Agency. 2010. Chesapeake Bay Total Maximum Daily Load for Nitrogen, Phosphorus and Sediment. U.S. Environmental Protection Agency Chesapeake Bay Program Office, Annapolis MD. (<http://www.chesapeake.gov>)

United States Geological Survey. 2011. Water data for the nation (<http://waterdata.usgs.gov/nwis> and <http://va.water.usgs.gov/chesbay/RIMP/dataretrieval.html>).

Valiela, I., J. McClelland, J. Hauxwell, P. J. Behr, D. Hersh, and K. Foreman. 1997. Macroalgal blooms in shallow estuaries: Controls and ecophysiological and ecosystem consequences. *Limnol. Oceanogr.* 42(5, part 2): 1105-1118.

Virginia Institute of Marine Science (VIMS). 2011. <http://web.vims.edu/bio/sav/>

Ward, L. G., W. M. Kemp and W. R. Boynton. 1984. The influence of waves and seagrass communities on suspended particulates in an estuarine embayment. *Mar. Geol.* 59: 85-103.

Yamamoto, T. 2003. The Seto Inland Sea: eutrophic or oligotrophic? *Marine Pollution Bulletin* 47: 37-42.

Yu, H., C. Ye, X. Song, and J. Liu. 2010. Comparative analysis of growth and physio-biochemical responses of *Hydrilla verticillata* to different sediments in freshwater microcosms. *Ecological Engineering* 36(10): 1285-1289.

Zimba, P.V., M.S. Hopson, and D.E. Colle. 1993. Elemental composition of five submersed aquatic plants collected from Lake Okeechobee, Florida. *J. Aquat. Plant Manage.* 31: 137-14.